NUMERICAL SOLUTIONS OF THE FLOW FIELD PRODUCED BY A PLANE SHOCK WAVE EMERGING INTO A CROSSFLOW

By

LYNN DOLAN TYLER

Bachelor of Science
University of Tulsa
Tulsa, Oklahoma
1961

Master of Science
Oklahoma State University
Stillwater, Oklahoma
1962

Submitted to the Faculty of the Graduate School of
the Oklahoma State University
in partial fulfillment of the requirements
for the degree of
DOCTOR OF PHILOSOPHY
May, 1965

NUMERICAL SOLUTIONS OF THE FLOW FIELD PRODUCED

BY A PLANE SHOCK WAVE EMERGING

INTO A CROSSFLOW

Thesis Aproved:

Glen W. Zumwalt

Thesis Adviser

Jerald D. Parker

Ladislaus J. Fila

O. H. Hamilton

[signature]

Dean of the Graduate School

PREFACE

The study of a plane shock wave emerging into both still and supersonic streams was completed as a part of the research contract sponsored by the Sandia Corporation, Albuquerque, New Mexico. This study was conducted to determine the possible conditions under which a shock tube-on-wind tunnel arrangement may be used experimentally to simulate a blast loading of a model. This dissertation considered the transient interaction of a shock wave and a supersonic crossflow. A companion dissertation by Mr. W. N. Jackomis considered the transient flow field resulting from a blast wave intercepting a stationary cone.

A number of investigations are presently being conducted by Ph.D. candidates at Oklahoma State University in various areas of blast wave interaction. Mr. W. F. Walker is concerned with establishing a numerical technique to represent a turbulent jet mixing region and also with the interaction of a blast wave and a jet mixing region. Mr. Rusi J. Damkevala is studying experimentally the interaction of a blast wave with free flight models. Mr. R. R. Eaton is to study the phenomena associated with a missile emerging from a blast sphere. These investigations, with present work, should help gain an understanding of the complex phenomenon of blast-body interactions.

The author wishes to express his appreciation to Dr. G. W. Zumwalt, Associate Professor at Oklahoma State University, for the help and advice given as my thesis adviser and for adding this advisement position to his already large workload.

A special expression of appreciation is given to Professor L. J. Fila for his patience and helpful suggestions on many of the problems which arose during the course of this analysis. Also, I extend my gratitude to my Ph.D. committee members, Dr. J. H. Boggs, Dr. J. D. Parker, and Dr. O. H. Hamilton for their instructive assistance.

Thanks is also given to the U. S. Government and its taxpayers for the award of a National Defense Education Act Fellowship which gave the much needed financial aid for my continued education. The assistance given by Sandia Corporation is greatly appreciated and especially the assistance of Mr. H. R. Vaughn for sponsoring this research project at Oklahoma State University and making available the Sandia Corporation's computer facilities. A special thanks is given to Mr. Jim Smith of Sandia Corporation for his voluntary help in running the computer programs. I am very grateful to Mrs. Lynn Bowles for her patience and skill in typing this manuscript, particularly the many difficult equations, and to Mr. Larry Lowcock for his genuine effort under the pressures of his school work in preparing the fine figures presented in the text. I feel also that my association with Mr. W. F. Walker and Mr. Glenn Lazalier has been very beneficial during the past few years.

Finally, because of the love and understanding given by my family, I wish to dedicate this thesis to my wife Janet and my children, Lynn, Jr., Pamela, and Tommy.

TABLE OF CONTENTS

Chapter | Page

LIST OF TABLES

LIST OF FIGURES

Figure Page

Figure | Page

Figure | Page

LIST OF PLATES

NOMENCLATURE

$A(x,y,t)$	coefficient for x "dissipative" term
$B(x,y,t)$	coefficient for y "dissipative" term
b	defined for Appendix G on page 151
$C(r,z,t)$	coefficient for z "dissipative" term
c	speed of sound
C_v	constant volume specific heat
C_p	constant pressure specific heat
$D(r,z,t)$	coefficient for r "dissipative" term
D	shock velocity in Appendix C
d	defined for Appendix G on page 151
e	fluid energy per unit volume
f	defined on page 37
F^x	defined on page 37
F^y	defined on page 37
F^r	defined on page 38
F^z	defined on page 38
h_1	net space increment
h	diagonal of net space
$\tilde{h}$	r direction unit vector
$\tilde{i}$	x direction unit vector
$\tilde{j}$	y direction unit vector
$\tilde{k}$	z direction unit vector
k	specific heat ratio

K	the quantity $\sqrt{2}\ h/\tau$, page 45
K_1	the quantity h_1/τ, page 45
L	characteristic length
ℓ	opening length on page 9 y or r net number on page 45
M	Mach number
m	x or z net number, page 45
N	number of net spaces along the characteristic length
n	time net number, page 45
$\tilde{n}$	unit normal
p	pressure
R	channel opening for still problem
r,z	cylindrical coordinates
T	temperature
t	time
U	shock velocity, page 5
u	x or z velocity component
$\tilde{V}$	velocity vector
v	y or r velocity component
W	channel opening for crossflow problems
w	opening width, page 9 $= \lvert\tilde{V}\rvert$, velocity modulus, page 46
x,y	cartesian coordinates
α	coefficient of the "dissipative" difference term, page 45
β	coefficient of the "dissipative" difference term, Appendix E
γ	volume

ϵ	internal energy
η	a parameter defined on page 56
θ	angle of incidence on page 5 angular coordinate on page 29 defined for Appendix E on page 144
θ_m	limiting angle of incidence for regular reflections
λ	local propagation velocity, page 39
ξ	quantity defined on page 142
ρ	density
σ	discontinuity surface on page 39 Courant number, page 46 surface in Appendix A
τ	time increment
Φ	"dissipative" difference term, page 45
φ	perturbation quantity, Appendix E
χ	angle between h and h_1
ψ	defined on page 38 defined for Appendix E on page 143
ω	stability constant, page 46

Superscripts

n	time plane number
1	field in front of a shock
2	field behind a shock
'	reflected shock on page 5 dimensional variable on page 55
"	Mach stem quantity, page 5

Subscripts

ℓ	y or r net point location
m	x or z net point location
o	initial value of σ
s'	defined for Appendix G on page 151
s''	defined for Appendix G on page 151
s	shock center condition
x	dimensionless quantity in front of shock, Appendix C condition in front of shock, Appendix G
y	dimensionless quantity behind shock, Appendix C condition behind shock, Appendix G

CHAPTER I

INTRODUCTION

In the past several years missiles containing explosive warheads have been designed as defensive weapons against aircraft and missiles. The energy release from an explosion has two primary destructive features: heat generation and a pressure wave. The hot gas region is confined to the air in the immediate vicinity of the explosion and is due to the sudden release of a large quantity of energy. The pressure disturbance (blast wave) also results from the release of energy, but spreads more rapidly to the surrounding atmosphere. This study is concerned with a method for testing the effects of a blast wave on a body at some location outside the region of the fire ball.

When a blast wave intersects a body, it may cause structural failures or flight path changes from excessive pressures or accelerations. The interaction of a blast wave with a body is a very complex phenomenon and has created a great deal of interest. Both analytical and experimental studies are necessary to determine the proper formulation of the methods of solution to this pehnomenon. Many of the analytical approaches are references in the literature survey (Chapter III). The experimental studies may be either full scale tests or model simulation. This study was conducted for a particular model simulation test model.

An experimental arrangement has been proposed by Pierce [1]* which uses both a shock tube and a high velocity wind tunnel for blast simulation. The shock tube is the blast-producing device and is mounted on the side of the wind tunnel (Figure 1). This appears, at first, to be a very promising means of simulating the interaction of a blast wave with a moving body (Plate I). However, the properties of the blast are not known after the blast has propagated into the high velocity crossflow. The blast is deformed by the crossflow and may not be uniform in strength or direction of propagation. Thus, the deformed blast could fail to represent properly the free-air blast. Therefore, some knowledge is needed of the interaction between a blast (shock) wave and a high velocity crossflow. The shock-crossflow interaction problem is the subject of this study.

The study was conducted on an analytical basis with qualitative experimental support. Two problems were considered: a shock emerging from a round or slit-like opening into a still medium, and the shock-crossflow for a slit-like opening. Both problems were solved by a finite difference scheme on a CDC** 3600 computer and supported by hydraulic analogy results.

---

*Numbers in brackets refer to references in the Bibliography.

**Control Data Corporation.

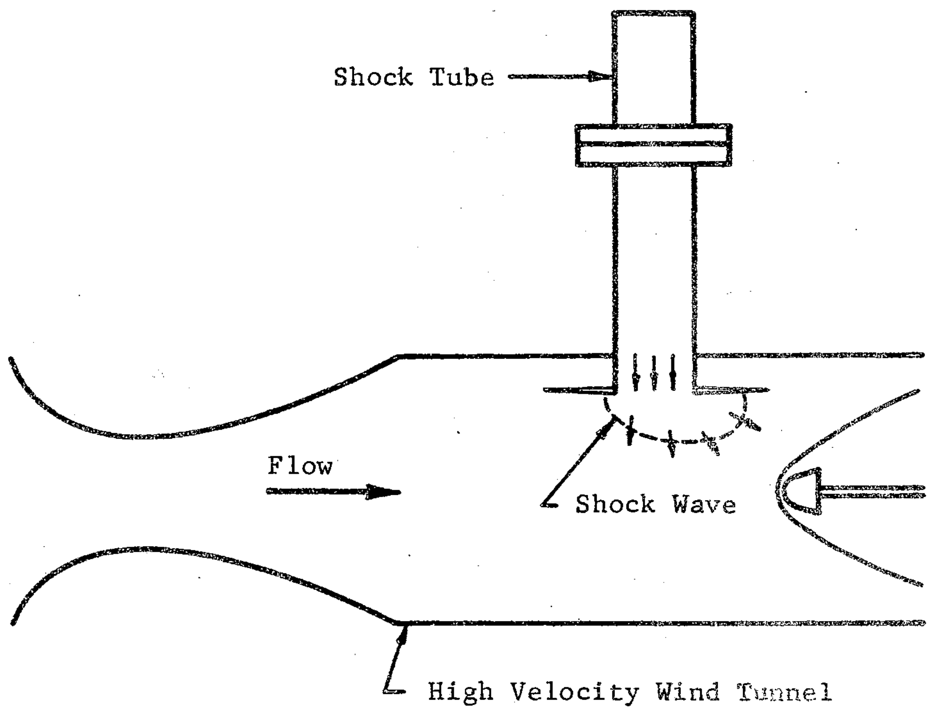

Figure 1. Shock Tube - Wind Tunnel Blast Experiment.

PLATE I

SCHLIEREN PHOTOGRAPHS OF A SHOCK TUBE FIRING
INTO A WIND TUNNEL

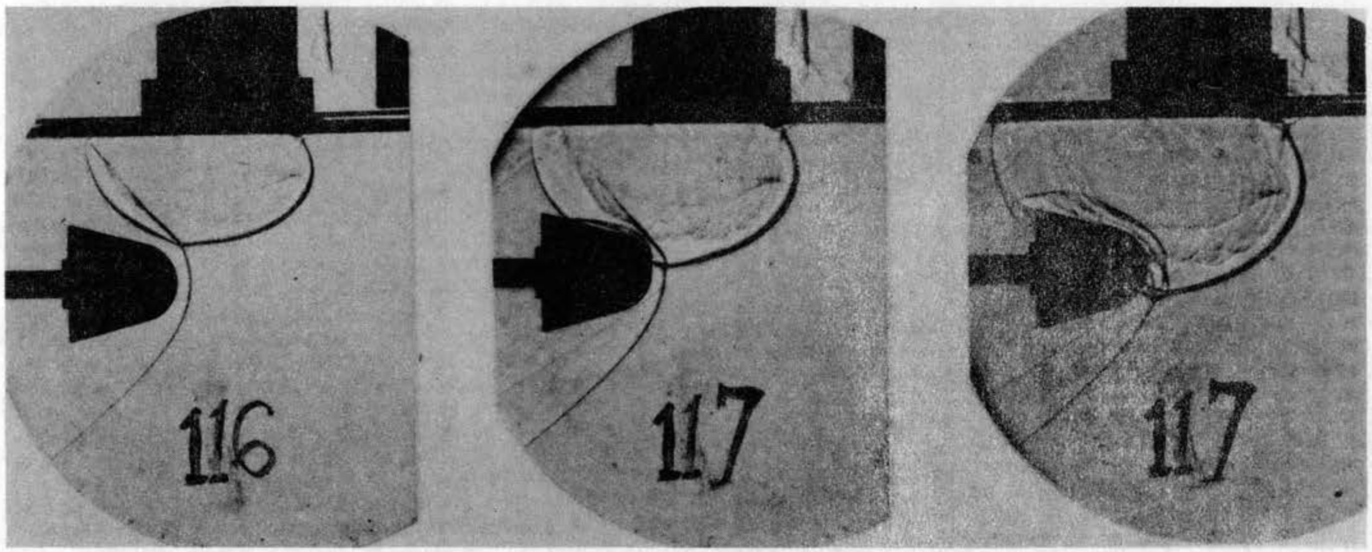

FREE STREAM MACH NO. 2.0
BLAST WAVE MACH NO. 2.9
30° CONE, NOSE RADIUS 1.1 INCHES

CHAPTER II

DESCRIPTION OF THE PHYSICAL PHENOMENA

General Shock Diffraction

Because the phenomenon of shock reflection and diffraction is complex, some physical definitions of general shock behavior are needed. Therefore, the concepts of shock reflection and diffraction are described below.

The oblique reflection of a shock occurs when the shock impinges on a body (or shock) at some arbitrary angle. Oblique reflections are divided into two basic types: regular reflection and Mach reflection. Regular reflection is the simplest shock configuration and is shown in Figure 2. A shock OA, with shock velocity U, strikes a boundary at a point O at an angle θ. The shock OB is the reflected wave, which moves away from the boundary at a shock velocity U'. A normal shock reflection (Figure 3) is a special case of regular reflection. For a given Mach number of the incident shock a maximum incidence angle, $\theta = \theta_m$, exists for which regular reflection may occur (Figure 4). For an angle θ greater than θ_m, shock reflection occurs as a Mach reflection (Figure 5). The incident shock OA has a velocity U and an angle $\theta > \theta_m$. A Mach stem OC is formed, which becomes perpendicular to the boundary. The Mach stem moves along the boundary while the reflected shock OB moves away from the boundary. The intersection of the shocks OA, OB, and OC at O is called the triple point. A contact discontinuity

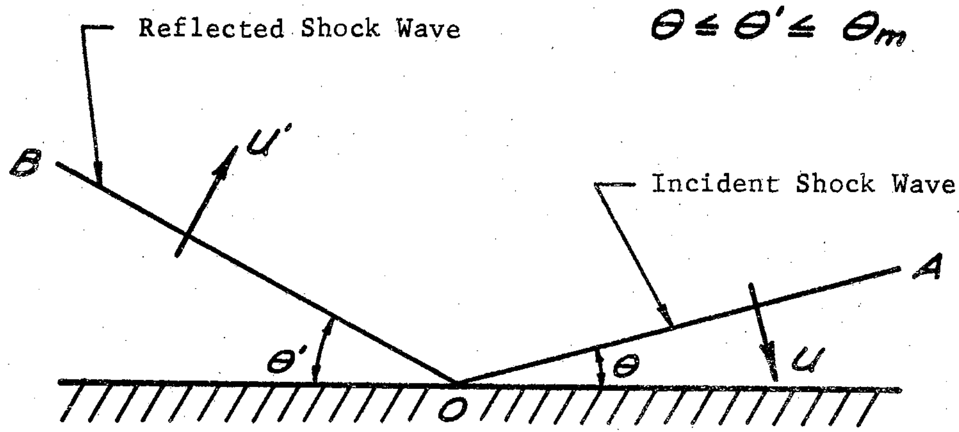

Figure 2. Regular Reflection.

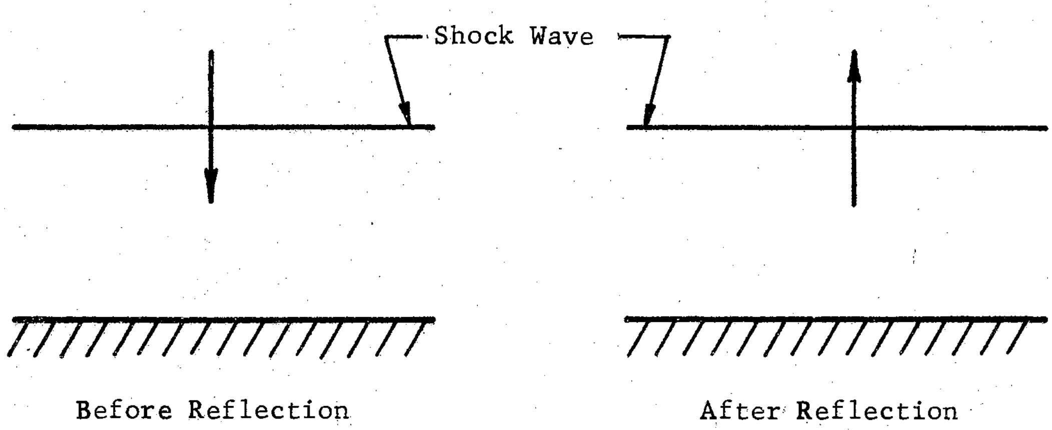

Figure 3. Normal Reflection.

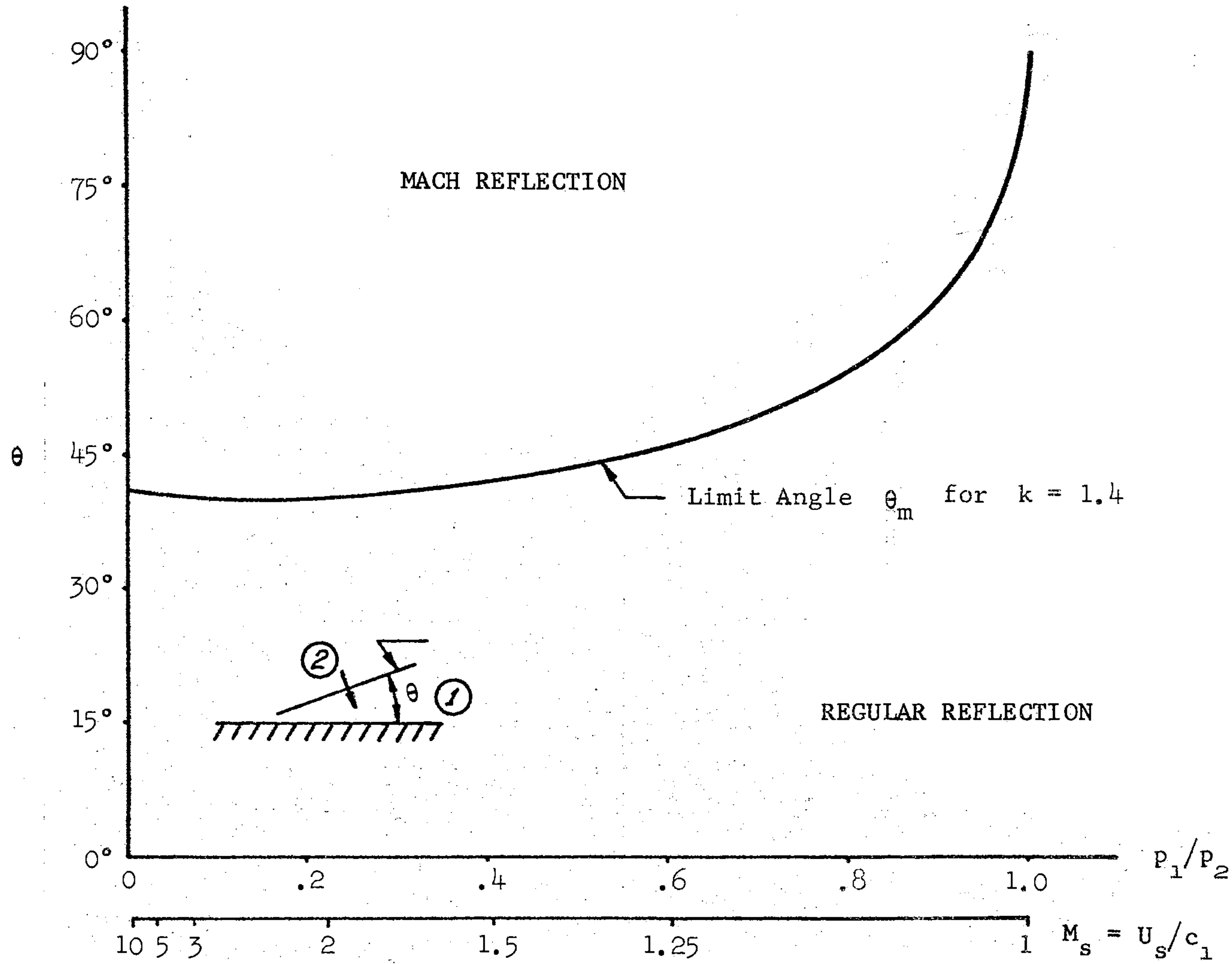

Figure 4. Limiting Conditions for Regular Reflection [2].

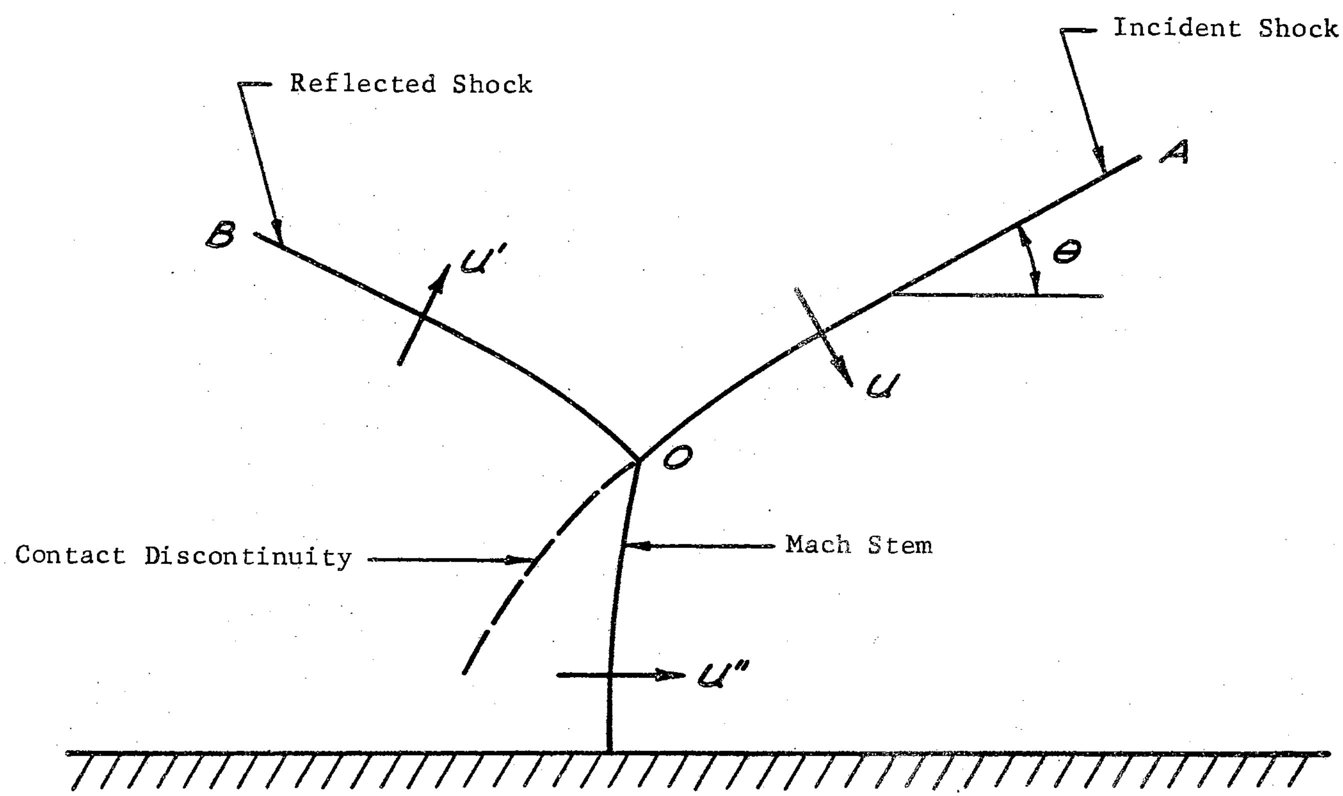

Figure 5. Mach Reflection.

is formed at 0 behind the shock system. This discontinuity is due to the difference in the entropy rise of the flow through the shocks OA and OB, and of the flow through the Mach stem OC. A plane shock encountering a concave corner (Figure 6) provides an example of a Mach reflection. In all cases of shock reflection the movement of the shock is confined or restricted in some manner. In each case, the wave is said to be diffracted (i.e., the shock shape is altered).

A shock may also be diffracted by allowing more freedom of movement. An example of this type diffraction is a plane shock encountering a convex corner (Figure 7). The corner 0 causes a disturbance to be propagated outward along the line OB after the shock passage. The disturbance causes the shock from A to B to be diffracted. The diffraction process occurs gradually as the shock BC moves downstream; therefore, the properties behind the diffracted shock are not uniform, and rotational flow exists even though there is a uniform field in front of the shock.

Propagation of a Plane Shock Wave Into a Still Medium

The first phase of this study pertains to the propagation of a shock from an opening in a plate into a still medium. Two openings are considered, circular and rectangular (Figure 8). For the rectangular opening, the length ℓ is assumed to be much larger than the width w, which allows the phenomenon to be essentially two-dimensional except close to the ends. The shock diffraction resulting from these two openings is qualitatively similar. The shock encounters a 90° convex corner at the edges of the opening and is symmetrically diffracted (Figure 9 - profile A). At some time later, the whole shock is

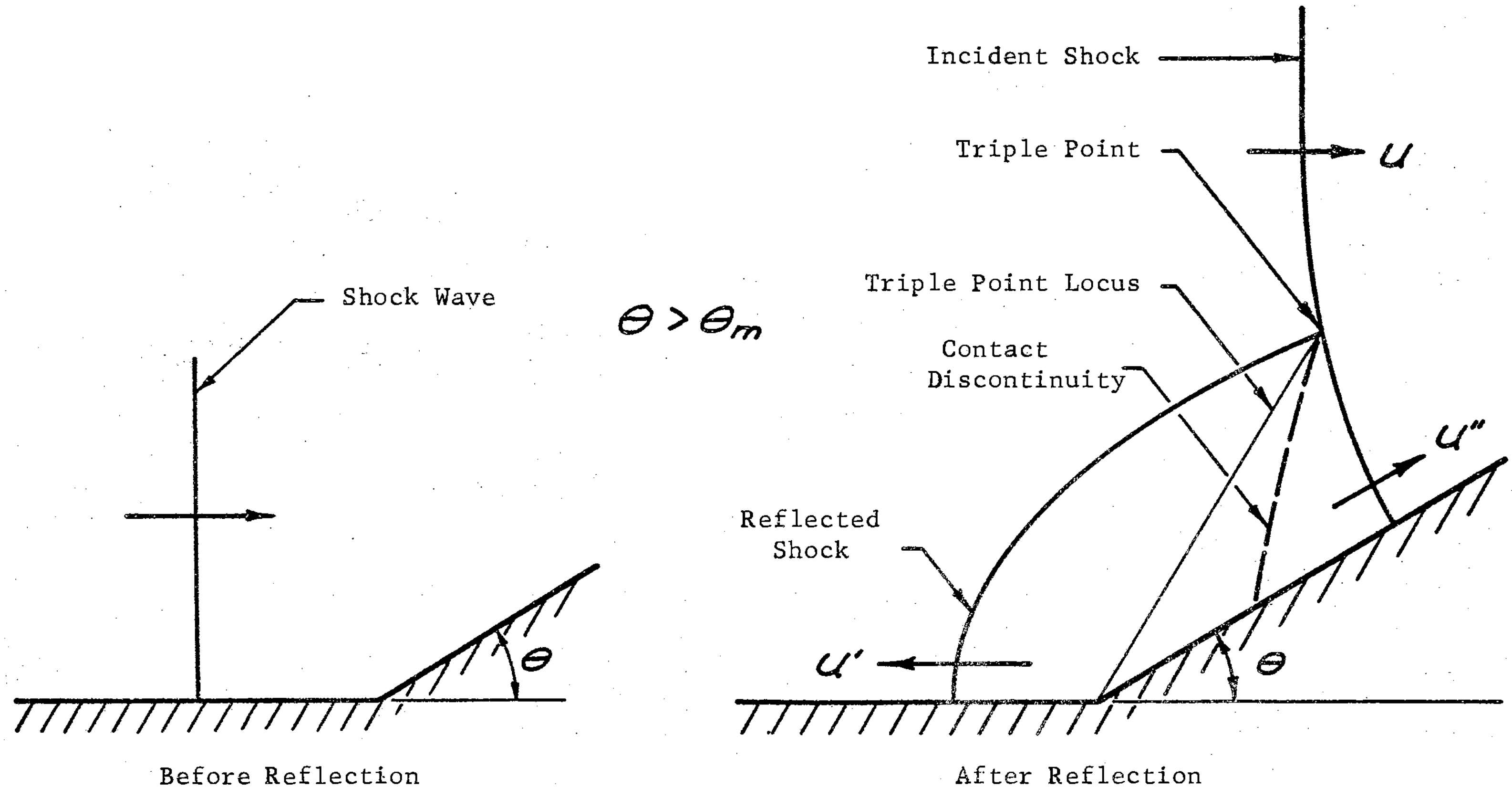

Figure 6. Wave Reflection at a Concave Corner.

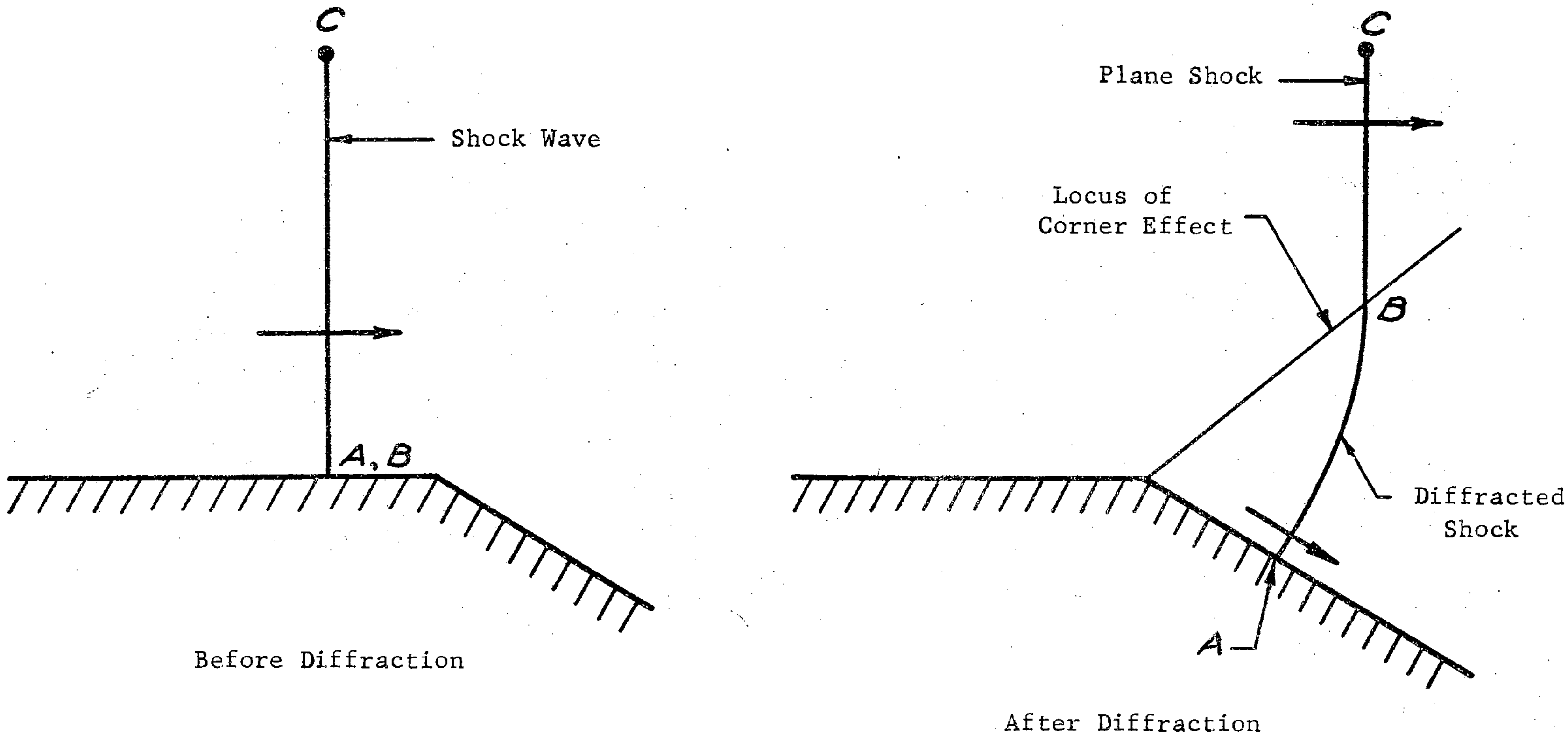

Figure 7. Wave Diffraction at a Convex Corner.

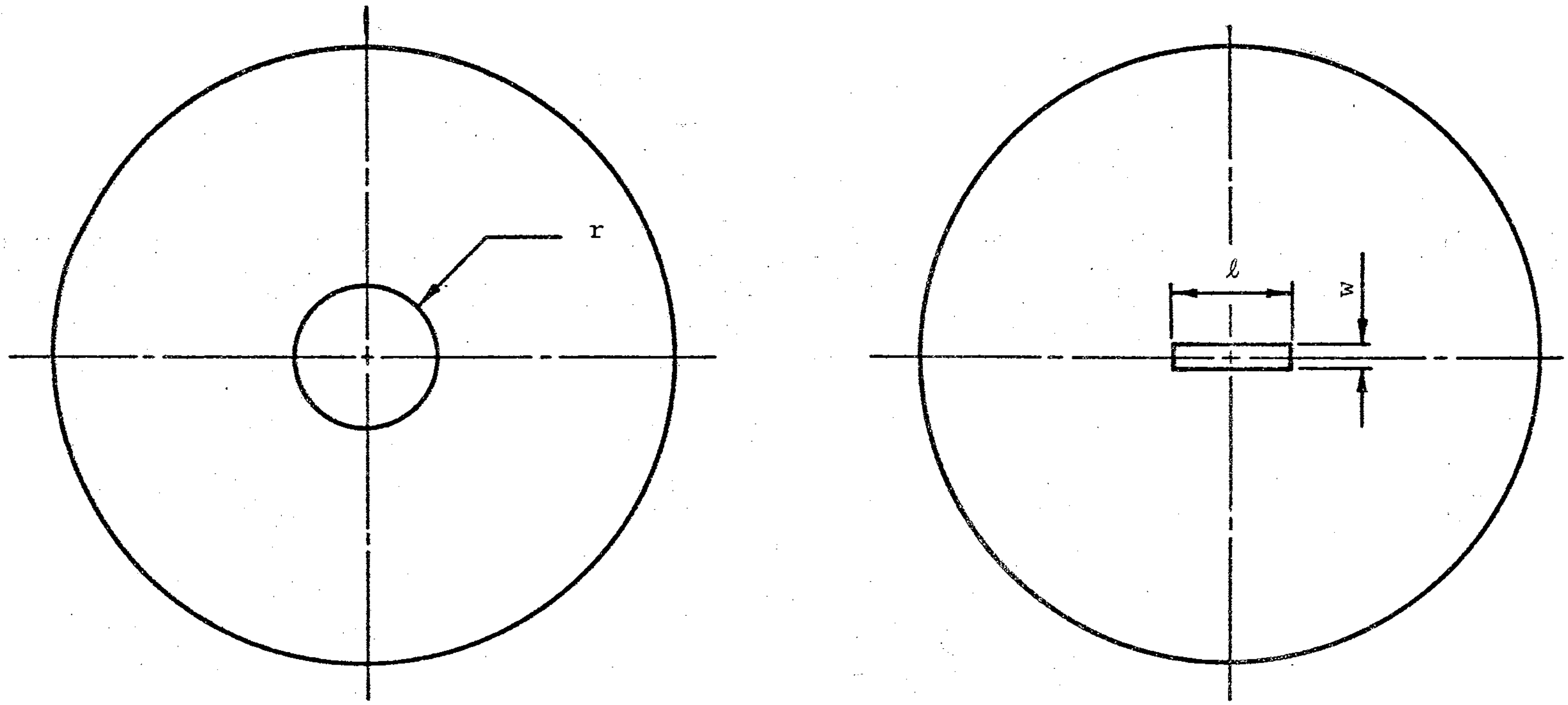

Circular

Rectangular

Figure 8. Geometries of Shock Tube Openings.

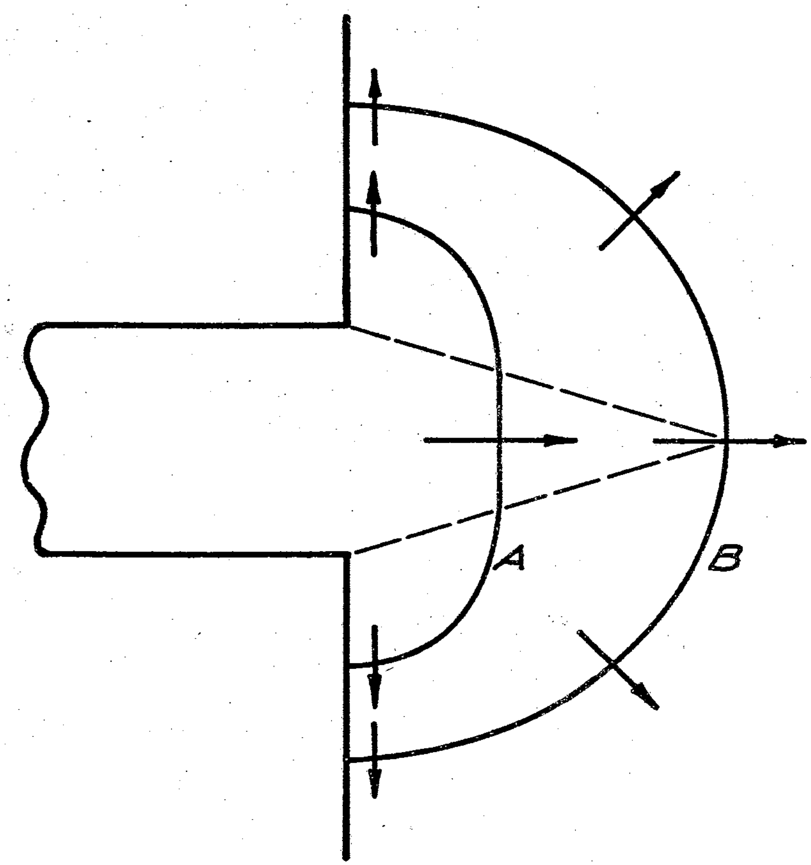

Figure 9. Shock Profile After Emerging From an Opening Into a Still Medium.

diffracted (Figure 9 - profile B); the disturbance is reflected; and the reflected disturbance is propagated outward along the shock. After a large number of disturbance reflections, the moving shock front approaches a cylindrical shape for the rectangular opening and a spherical shape for the circular opening.

Propagation of a Plane Shock Wave Into a Perpendicular High Velocity Crossflow

The shock-crossflow interaction was studied for a plane shock emerging from a rectangular opening. A large ℓ/w ratio (Figure 8) is assumed so the solution could be obtained in a plane. To gain insight into this phenomenon a preliminary water table study was made, leading to several observations.

As the shock emerges from the opening, a number of events occur; and the interaction may appear at some arbitrary time as shown in Figure 10. The portion of the shock labeled AB is moving into the stream and BC is a nearly stationary oblique shock which is formed because of the interaction of the two streams. A'B'C shows the shock position at some later time. At D the stream from the shock tube (2) and the crossflow field (1) meet to form a stagnation condition. As stream (2) emerges from the slit, it passes through an expansion region E and separates at F downstream of E. In some cases, where the total pressure of the crossflow is sufficiently greater than that of the fluid emerging from the slit, an internal shock appears at G.

This flow field can be seen to contain a number of quite complex phenomena. Analysis by resorting to shock-expansion theory appears hopeless, leading the investigators of such problems to numerical field solution methods.

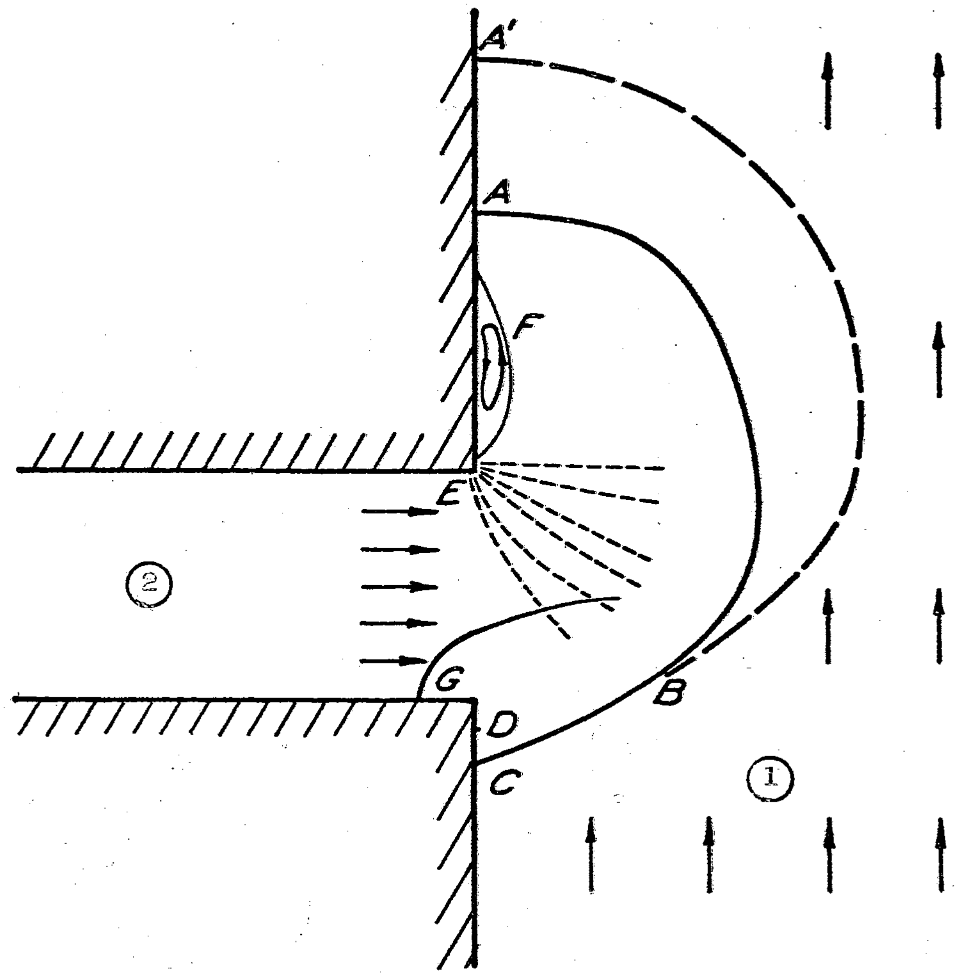

Figure 10. Shock-Crossflow Phenomenon at an Arbitrary Time.

CHAPTER III

LITERATURE SURVEY

Mathematical treatment of shock waves had been restricted to steady state phenomena up to the early 1940's when investigators became interested in the pressures produced by a shock wave colliding with an obstacle. The development of more powerful explosives was probably the primary reason for this interest. Most of the early investigations were done by linearizing the governing equations in some manner and using analytical techniques to obtain a solution. Finite difference schemes began to be developed for the nonlinear equations for shock propagation in the early 1950's, due to increased use of large digital computers. In recent years most investigations have employed a difference scheme to solve complex problems.

The literature has been divided into three categories for review. The literature on mathematical studies is divided into analytical and numerical investigations to compose two categories. The third category is the literature on the experimental studies of a shock tube firing into a high velocity wind tunnel. The discussion will follow chronological order.

Analytical Investigations

One of the first investigators of the principles of shock reflection and diffraction was John von Neumann [3]. Von Neumann conducted an experimental and theoretical study of head-on and oblique shock reflections from solid boundaries and observed that regular reflection gave way to a more complicated type reflection when the angle between shock and wall become large. This type of reflection is termed "Mach reflection". The phenomena of regular reflection, Mach reflection, and the "triple point" were described by von Neumann [3].

Lighthill gave an analytical solution for two problems, [4] and [5], that involved the reflection of a plane shock of arbitrary strength from a plane wall which had a sharp but small change in direction. The first paper gave the solution for a shock propagating parallel to the wall and the second paper perpendicular to the wall. The basic equations were linearized on the assumption that the small change in wall direction produced only small perturbations in the uniform flow behind the shock.

The diffraction of a shock at a convex corner was studied by Parks [6] and applied to a shock tube of diverging cross-section. An analysis similar to that used for nonstationary, one-dimensional, wave interaction problems was presented along with an experimental study.

Ting and Ludloff [7] considered the effect of a small lump on a blast which propagated along a flat surface. This problem is similar to Lighthill's problem [4], but a different technique was used to obtain the solution.

Chester used Lighthill's technique to solve three linearized problems. One paper [8] investigated the disturbance produced behind a plane shock that propagated through a channel in which the width possessed small variations. The shock strength was arbitrary and a relation was developed for the pressure change behind the shock along a channel variation. A second paper [9] extended Lighthill's work to consider the interaction of a shock wave with an infinite, yawed, thin wedge. Chester [10] extended his own work of the first paper to the propagation of a shock along a tube of arbitrary cross sectional shape but with small variations in the cross sectional area.

A theoretical study was conducted by Laporte [11] on the passage of a shock along a channel possessing a constriction or sudden area reduction. The purpose of the study was to present the diffraction theory for a shock encountering head-on a flat plate on which a regular array of perpendicular spikes or wedges was mounted.

In 1956, Whitham [12] presented a method to treat weak shock propagation problems of three independent variables. A large number of ray tubes was assumed to compose the flow field. For a single tube the energy was assumed to be conserved as a shock propagated along the tube. Geometrical acoustic theory was applied with the additional assumption that a shock wave moved at a speed appropriate to its local strength. A number of examples were given to demonstrate the use of the theory. The examples included unsymmetrical explosions and sonic boom problems.

Chester's work on shock propagation along a slowly varying channel was extended by Chisnell [13]. A first order relation between changes in area and in shock strength was developed in which reflected waves were neglected and the average shock strength was conserved along the channel.

Ting [14] considered the problem of the diffraction of a small disturbance caused by a convex right angle corner. The primary application for this work was wing-body interference.

Whitham [15] extended his previous work to give an approximate theory for two-dimensional problems of diffraction and stability of shock waves. The theory was based on the ray tube concept and on the relation for area and shock strength changes developed by Chisnell. Reflected waves were neglected and the average shock strength was assumed to be conserved along the tube. Disturbances to the flow were represented as wave propagating along the shock. This wave carried changes in shock angle and Mach number. Discontinuities of the disturbance wave were considered so that the shock could be diffracted on a way similar to the diffracted part of a Mach reflection. Whitham applied the theory to a number of diffraction problems.

In 1958, a paper [16] was presented by Whitham which referred to the work of Moeckel on the interaction of an oblique shock wave with a shear layer and to the work of Chester and Chisnell on the propagation of a shock down a nonuniform tube. Whitham obtained the same results as the above authors, but by a simpler method. The discussion by Whitham was mainly to gain a better understanding of the results given by his method.

Sternberg [17] gave a general discussion of the triple-point region of Mach reflections. An unsuccessful experimental attempt was made to define the angles between the shocks at the triple point. Also, a mathematical model was suggested which might be used to gain a better understanding of the problem.

In 1959, Whitham [18] extended his earlier work to apply his theory for shock propagation in three dimensions. An analogy between the presented theory and steady supersonic flow was found.

The diffraction of a shock wave by a small wedge-like deflection was treated by Bezhanov [19]. The method of solution of the problem made possible solution of more general physical conditions than Lighthill's approach to the problem. Solutions for the flow could be found when the wall deflected as a result of the oncoming shock and in the presence of unsteady disturbances ahead of the shock front which are generated by wall motion.

The diffraction of plane strong shocks by a cone, a cylinder, and a sphere was studied experimentally by Bryson and Gross [20]. Whitham's theory of shock diffraction was applied to the same physical models and gave very good results.

The diffraction problem of a plane weak shock wave by wall contours of arbitrary shapes was considered by Filippov [21]. A number of two-dimensional shapes were considered. The problems were solved in a linearized formulation and no consideration was given for nonlinear regions.

Smyrl [22] obtained a solution for the pressure field behind an arbitrary plane shock after the shock has encountered a thin airfoil moving at supersonic speed. The problem was linearized and a closed form solution resulted. Several examples were given to illustrate the effects of shock strength, airfoil speed, and yaw angle.

Whitham's method of diffraction of blasts by stationary bodies was applied by Miles [23] in 1963 to the problem of a blast diffracted by a thin supersonic wedge. Results by Whitham's method tended to the exact results for weak shocks but were unsatisfactory for strong shock.

A discussion and bibliography concerning reflection and diffraction of shock waves was presented by Pack [24]. A particularly good discussion of shock reflections is given.

Wolff [25] has presented a study of the head-on interception of a flying conical body with blast waves of various strengths. Two flight conditions were analyzed: a stationary body at sea level and a cone with a velocity of 19,000 ft./sec. at 40,000 feet altitude. The inviscid flow fields, shock-on-shock interaction phenomena, and non-equilibrium effects were determined. Some discussion was given for a body flying out of a blast. The analytical method employed was a co-ordinate transformation to make shock waves steady. Real-gas effects were included, and estimates of pressure distribution on the body as a function of time resulted.

Lee [26] discussed some aspects of the laboratory simulation of strong blast waves on flying projectiles by means of a shock tube discharging into a wind tunnel. Lee conjectured that for strong shocks (i.e., Mach number > 4) that the gas behind the shock from the shock tube projected from the tube as a column. He observed that if this were true the test time would be very short. Lee also discussed the use of the shock from a shock tube as a blast wave through which a hypervelocity model could be fired.

The majority of the analytical methods reviewed used some means of linearization to obtain solutions. The nonlinear shock diffraction methods were limited in that the flow field behind the shock was not defined. Therefore, there are no analytical procedures available to treat a complex nonlinear shock propagation problem.

Numerical Investigations

In 1950, a finite difference scheme was introduced by von Neumann and Richtmyer [27] in which a mathematical "viscosity" term was added to the Lagrangian equations. The "viscosity" term allowed a shock to be represented as a steep continuous gradient of properties, rather than a discontinuity. Using this representation the difference equations were written explicitly and the shock was treated as a steep gradient interior to the field and not as a discontinuity boundary. Requirements for defining the mathematical "dissipative" term were given and are presented in Chapter IV of this study.

Courant et. al. [28] presented a difference method for solving nonlinear hyperbolic equations in which the order of magnitude of the accuracy was the same as the order of magnitude of the net width. A scheme for curvilinear and rectangular nets was given. The sufficient condition given for convergence of the scheme was that the domain of dependence of any point in the net as given by the difference equations may not be less than the domain of dependence determined by the differential equation. Shock waves and other discontinuities were treated as boundaries.

In a report written by Lax [29] a very general discussion of mathematical conservation laws was given and a difference scheme was presented for shock propagation problems. By defining the time derivative as

$$\frac{\partial f}{\partial t} \simeq \frac{1}{\Delta t}\left(f_m^{n+1} - \frac{f_{m+1}^k + f_{m-1}^k}{2}\right)$$

Lax showed that a shock may be handled as a steep gradient, similar to the representation given by von Neumann and Richtmyer. By rearranging the terms of Lax's difference equation, it has been shown [30] that the equation could actually represent a differential equation in which a "dissipative" term had been added. One-dimensional problems were presented to compare the results of the scheme with those by classical moving shock theory.

Ludford et. al [31] presented a difference method using a "dissipative" term based on a viscosity law of physically proper form. However, to obtain reasonable results, unrealistically large values of the physical viscosity were used.

Lax presented in Reference 32 the work that had been done for the report discussed above. The paper was obviously required to be condensed, leaving out some details the report contained.

In 1955, Lax's difference scheme was extended to two-dimensions by Ludloff and Friedmann [33]. The problem of reflection and diffraction of strong shocks around corners of arbitrary angle was solved by an elliptic method and by a hyperbolic method (Lax's extended method). For the elliptic method conical coordinates were introduced and the basic equation became elliptic in nature. A difference approach was required to solve the equation and all discontinuities were treated as boundaries requiring an iterative procedure. The second method used was essentially Lax's technique for two dimensions in which the discontinuities were represented by steep gradients.

Ludloff and Friedmann [34] discussed the difference equation used in the hyperbolic method applied above and pointed out the general characteristics of the method for shock diffraction problems.

Lax's difference method was used by Payne [35] to solve the equation of motion for the cylindrically symmetric flow of a compressible gas. A converging cylindrical shock was found to increase in strength, in agreement with the relation obtained by Chisnell [13]. The presence of the "dissipative" term caused the pressure to remain finite at the axis and a reflected diverging shock was observed.

Godunov [36] presented a difference scheme which was similar to the methods of von Neumann and Richtmyer and of Lax. One-dimensional experimental problems were presented to illustrate the scheme.

A discussion of systems of conservation laws was given by Lax and Wendroff in Reference 37. Also, a new difference technique was presented in which an artificial "viscosity" was used. One-dimensional problems were used to demonstrate the results of the technique.

A difference method was presented by Rusanov [38] in 1960. This scheme also utilized a "dissipative" term to obtain solutions for shock diffraction caused by a number of different geometries. These geometries are shown in Figure 11 where the dashed lines represent the initial shock positions. Problem A involved a regular reflection and B involved a Mach reflection. Diffraction of a shock at a right convex corner is shown in C, and a head-on encounter of a shock with a right convex corner is shown in D. Geometries E and F are, respectively, a shock wave propagating from an annulus into a circular pipe and a shock propagating along a pipe into an annulus.

The "dissipative" difference method of von Neumann and Richtmyer was applied by Makino [39]. The scheme was used to obtain numerical calculations of the interaction of two spherical blast waves in air.

The Particle-in-Cell method of the Los Alamos Laboratory Computer Center was discussed by Harlow [40]. This method uses features of both Lagrangian and Eulerian meshes for compressible flow problems.

A report by Crocco [41] gave a new numerical approach for solving the Navier-Stokes equations. The technique was applied to a one-

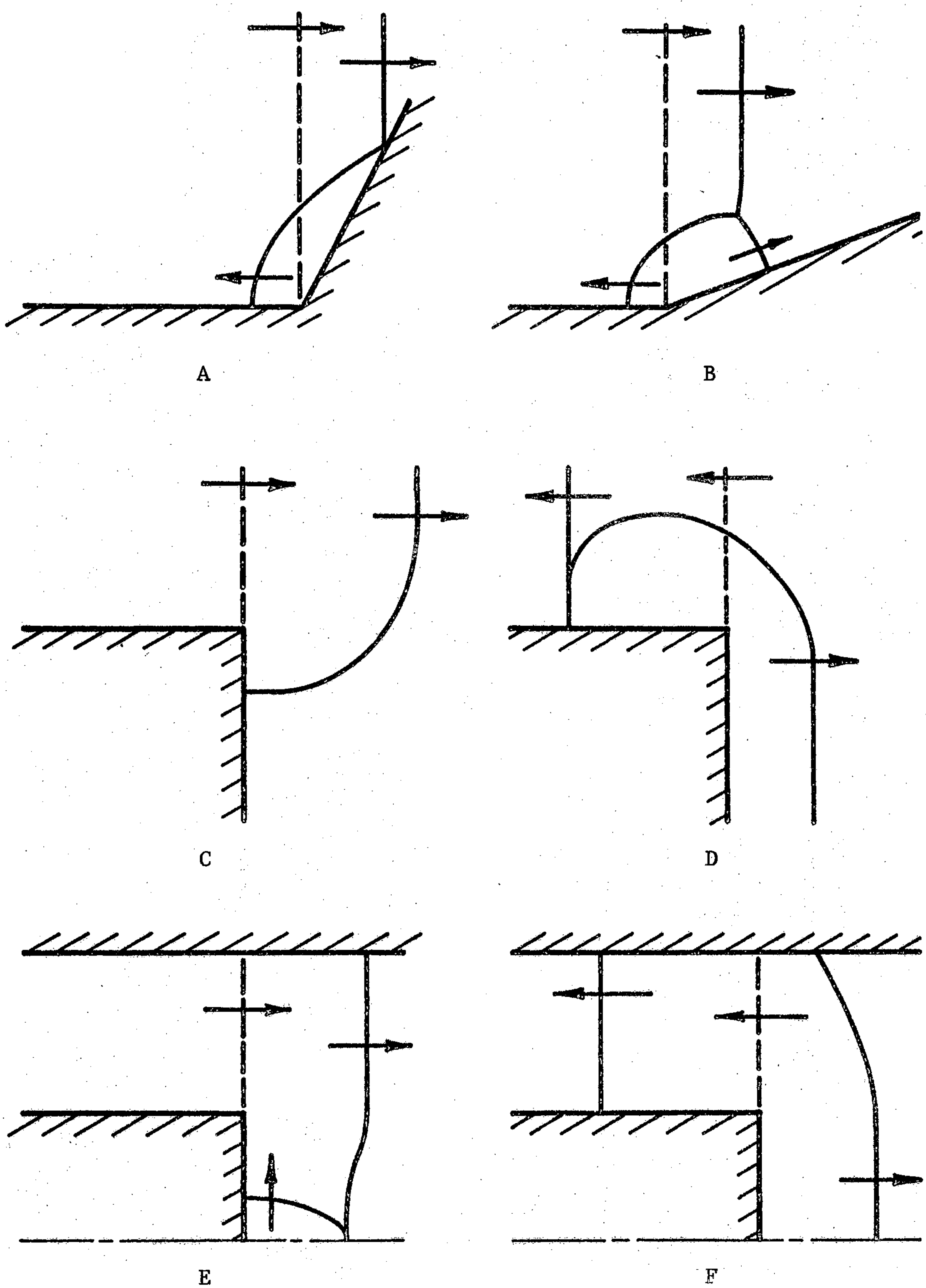

Figure 11. Shock Diffraction Problems Presented by Rusanov [38].

dimensional problem in which the unsteady equations were solved to obtain a steady state solution.

Burstein [42] applied the Lax-Wendroff method to obtain numerical results for oblique and Mach reflections in air. The Mach reflection calculations agreed with experimental photographic data obtained from wind-tunnel tests.

At the 1965 A.I.A.A. meeting, a two part paper was presented by Bohachevsky et. al. [43] in which Lax's [32] and Godunov's [36] methods were described and extended to include Lighthill's ideal dissociating diatomic gas model. In the first part of the paper, the two methods above were applied to plane flow about a rectangular body, axisymmetric flow about a flat faced cylinder, supersonic flow in the afterbody section of a cylindrical body, and axisymmetric flow about a sphere. The second part of the paper was devoted to a discussion on the development of techniques for computation of three-dimensional flow field. Also included in the second part of the paper were results for an Apollo-type body at an angle of attack in an ideal gas flow.

From the review of the above techniques and applications to shock propagation problems it appears that the only approach available to a complex nonlinear problem is a finite difference scheme of the types developed by Lax, Gudonov, and Rusonov.

Experimental Investigations

To date only three experimental studies on wind tunnel simulation of blast wave phenomena using a shock tube have appeared in the literature. The first work reported was by Pierce [1] in 1960. He had mounted a shock tube on the side of a wind tunnel with the driven end of the tube well into the flow field of the tunnel. A reflection plate was placed on the end of the tube to minimize the interference by the flow around the tube. Shadowgraph photographs of blast waves passing over a number of simple shaped models were studied for tunnel Mach number of 1.87. The initial blast wave Mach number was 2.38. Pierce concluded that local increases of pressure due to a blast acting on a body were several times the pressure behind the blast. He also observed that the duration of this high pressure was very short.

In 1964, a second experimental investigation was conducted by Bingham and Davidson [44] at Ohio State University. The wind tunnel was a hypersonic free-jet tunnel and was operated at Mach 7.3. Shock tubes were installed at angles of 30°, 60°, 90°, and 120° with respect to the tunnel centerline. The shock tube was a double diaphragm tube which was capable of generating shock velocities from 3,600 to 13,500 feet per second. Pressure measurements and Schlieren photographs were taken of the interaction of the bow shock of a hypersonic body with an obliquely moving shock wave. From this study it was concluded that this type of simulation of the interaction of a body shock wave and a moving shock was a feasible method.

The most recent study was reported by Merritt and Aronson [2] in January, 1965. Attempts were made to conduct a side-on blast study using a shock tube discharging into a Mach 5 flow. The shock tube extended into the stream and had a reflection plate on the end. The side-on study was abandoned because the complex wave patterns defied analysis, and no theoretical solution was available for comparison. The shock wave was highly curved and attenuated rapidly, and it was very difficult to get clear pictures at Mach 5. A study was then done for a head-on blast interaction. A small shock tube was mounted a short distance upstream of the throat of the tunnel nozzle and was discharged in a downstream direction. A Schlieren study was made for a hemisphere-cylinder and a wedge model. There was good agreement between the predicted and measured overpressures at the stagnation point of a blunt body and on the surface of a wedge.

From the literature presented, it may be seen that the blast simulation technique using a shock tube and wind tunnel possesses some difficult experimental problems. Even though these difficulties are present and the technique may not accurately simulate the blast problem, no better alternative has been presented. Merritt and Aronson have presented a technique for a special case (i.e., head-on interaction), but a technique must be developed to obtain a general side-on blast simulation. To date there has been no technique given to determine the variation of shock strength and direction of propagation along the shock.

CHAPTER IV

MATHEMATICAL ANALYSIS

Geometric Models

Plane Geometry - Still Medium

A shock emerging from a rectangular opening into a still medium spreads in a symmetrical manner about a plane which is perpendicular to the ends and includes the centerline A-A (Figure 12). For a large ℓ/w ratio, the shock shape is affected by the end wall only in the immediate vicinity of the end. Therefore, the model is taken as an infinite slit, allowing the problem to be formulated in two Cartesian dimensions, x and y, plus the time dimension, t. Since symmetry exists about a plane that includes A-A, any disturbance felt on this plane is reflected as if the plane were a wall. Thus, the center plane may be replaced by a wall (Figure 13). At all walls, a shock is considered to propagate in a direction parallel to the wall. The model may now be stated as the propagation of an initially plane shock from an opening, bounded on one side by a plane wall and on the other side by a $90°$ convex corner.

Axisymmetric Geometry - Still Medium

Symmetry exists about the centerline D-D (Figure 14) for a plane shock emerging from a circular opening. In cylindrical coordinates, the solution does not depend on the angular direction θ because of this symmetry. Therefore, an arbitrary r, z plane may be used to obtain the

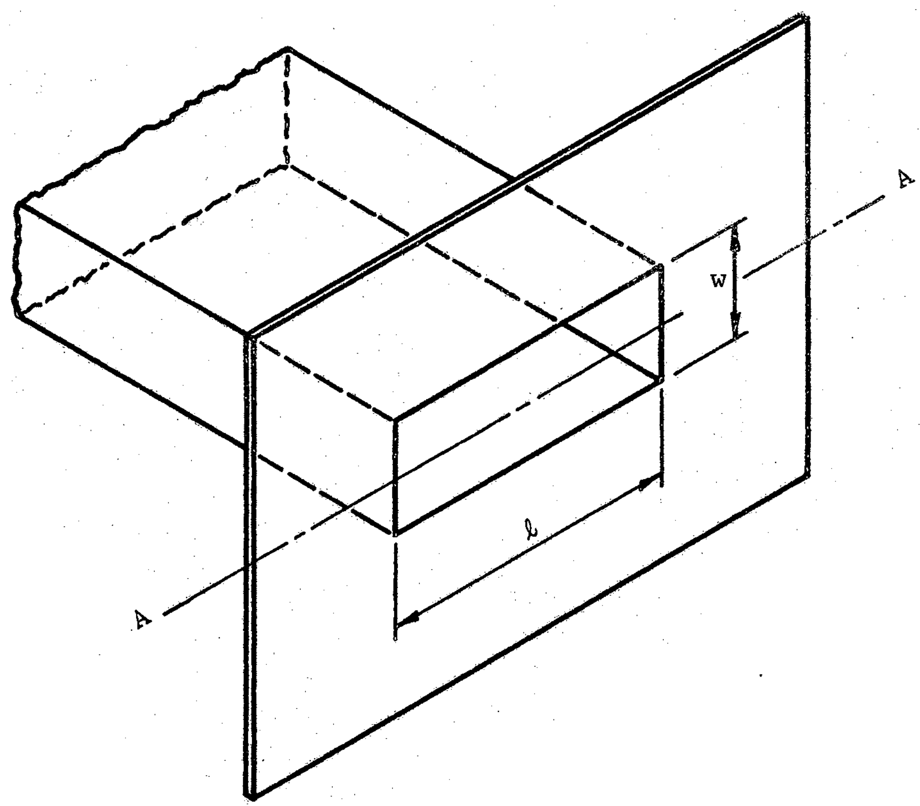

Figure 12. Geometry for a Rectangular Opening.

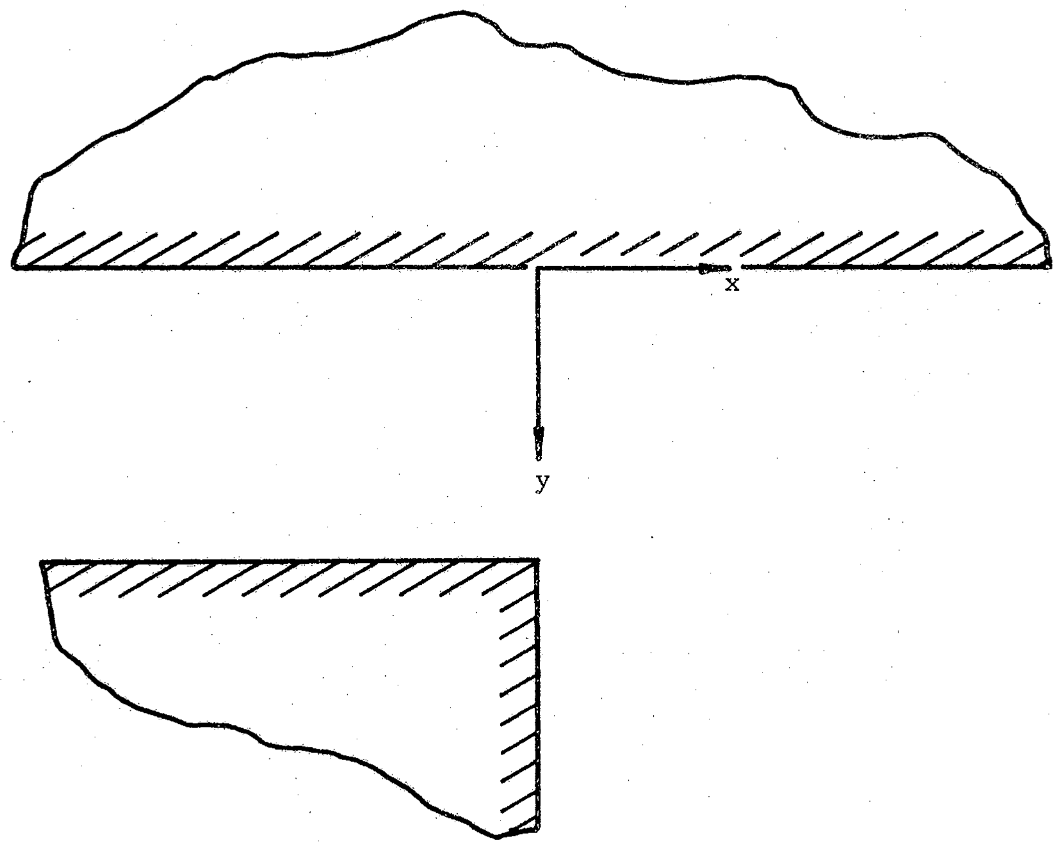

Figure 13. Geometric Model for Plane Geometry - Still Medium.

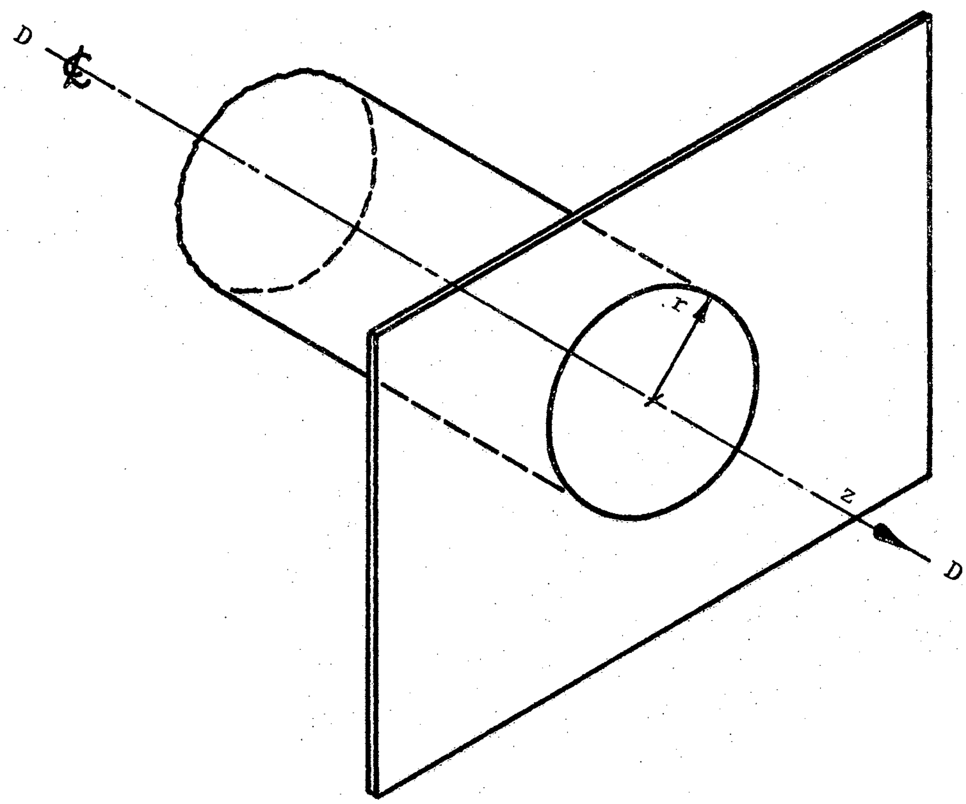

Figure 14. Geometric Model for a Circular Opening.

solution. For flow along the axis of symmetry, the gradients in the radial direction of pressure, density, and z-direction velocity must vanish. Also, the radial velocity must vanish at the axis due to the symmetry. As in the plane - still medium model, shocks are considered to propagate parallel to all walls.

Plane Geometry - Crossflowing Medium

The shock-crossflow interaction is considered for a plane shock propagating from a rectangular opening in a wall into a medium flowing parallel to the wall. If the ratio ℓ/w (Figure 12) is large, then, as in the plane - still medium model, the opening may be taken to be an infinite slit, which allows the problem to be formulated in the two Cartesian dimensions, x and y, and the time dimension t. Because the shock is distorted by the crossflow, no other symmetry exists. Therefore, the model is a plane shock emerging from an infinite slit (Figure 15) into a semi-infinite flowing field. As in the other models, shocks are considered to propagate parallel to the bounding walls.

Governing Equations

The conservation forms of the general flow equations are derived in Appendix A and are presented here. The fluid is assumed to be a gas, which is inviscid and ideal (i.e., the internal energy and enthalpy are functions of the absolute temperature, only). The general equations are:

Continuity,

$$\frac{\partial \rho}{\partial t} + \nabla \cdot (\rho \bar{V}) = 0 \; ; \qquad (1)$$

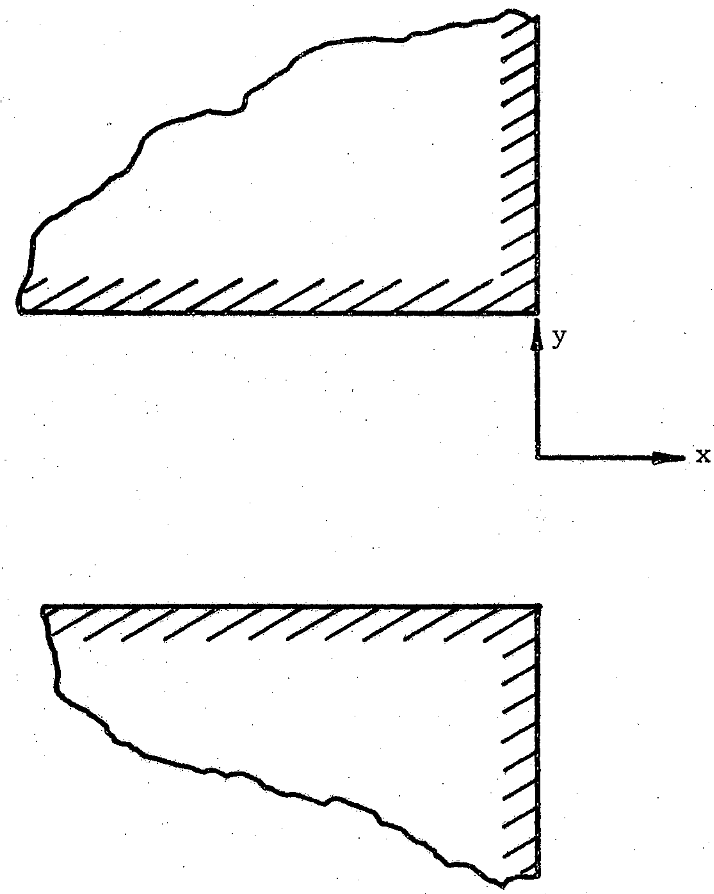

Figure 15. Geometric Model for the Shock-Crossflow Interaction (Plane Geometry).

Momentum,

$$\frac{\partial(\rho\bar{V})}{\partial t} + \nabla \cdot \rho[\bar{V}\bar{V}] + \nabla p = 0; \tag{2}$$

Energy,

$$\frac{\partial e}{\partial t} + \nabla \cdot [(e + p)\bar{V}] = 0; \tag{3}$$

where ρ = density,

p = pressure,

$\bar{V}$ = velocity vector,

e = fluid energy per unit volume

$= \dfrac{\rho|\bar{V}|^2}{2} + \dfrac{p}{k-1}$,

∇ = divergence vector operator.

The above equations are first order, quasi-linear, partial differential equations with dependent variables e, ρ, $\bar{V}$, and p. Equation (2) is a tensor equation which represents a system of equations for orthogonal momentum components. These equations are also said to be in conservation form (i.e., $\partial f/\partial t + \nabla \cdot \bar{F} = 0$). The properties of quasi-linear conservation equations are discussed in a later section of this chapter. The equations needed to describe the phenomena for the defined mathematical models are dependent on time and two space variables.

The equations which describe the phenomena in the still and cross-flow media plane models are given in Cartesian coordinates (x, y). The velocity and the divergence operator are defined respectively as

$$\bar{V} \equiv u\bar{i} + v\bar{j}$$

and

$$\nabla \equiv \bar{i}\frac{\partial}{\partial x} + \bar{j}\frac{\partial}{\partial y},$$

where $\bar{i}$ = x direction unit vector,

$\bar{j}$ = y direction unit vector,

u = x velocity component,

v = y velocity component.

The flow equations are then:

Continuity,

$$\frac{\partial \rho}{\partial t} + \frac{\partial(\rho u)}{\partial x} + \frac{\partial(\rho v)}{\partial y} = 0; \tag{4}$$

Momentum,

x-direction

$$\frac{\partial(\rho u)}{\partial t} + \frac{\partial}{\partial x}(\rho u^2 + p) + \frac{\partial}{\partial y}(\rho uv) = 0 \tag{5}$$

y-direction

$$\frac{\partial}{\partial t}(\rho v) + \frac{\partial}{\partial x}(\rho uv) + \frac{\partial}{\partial y}(\rho v^2 + p) = 0; \tag{6}$$

Energy,

$$\frac{\partial}{\partial t}(e) + \frac{\partial}{\partial x}[(e + p)u] + \frac{\partial}{\partial y}[(e + p)v] = 0. \tag{7}$$

The fluid energy is

$$e = \frac{\rho(u^2 + v^2)}{2} + \frac{p}{k - 1}. \tag{8}$$

The flow equations (4), (5), (6), and (7) may be written as a single equation:

$$\frac{\partial f}{\partial t} + \frac{\partial F^x}{\partial x} + \frac{\partial F^y}{\partial y} = 0, \tag{9}$$

where f, F^x, F^y are treated as four component vectors:

$$f = \begin{Bmatrix} \rho \\ \rho u \\ \rho v \\ e \end{Bmatrix} \; ; \qquad F^x = \begin{Bmatrix} \rho u \\ p + \rho u^2 \\ \rho uv \\ (e + p)u \end{Bmatrix} \; ; \qquad F^y = \begin{Bmatrix} \rho v \\ \rho uv \\ p + \rho v^2 \\ (e + p)v \end{Bmatrix} .$$

The equations for the axisymmetric, circular model are given in the cylindrical coordinates, z and r. The velocity and the divergence operator are defined respectively as

$$\bar{V} \equiv v\bar{h} + u\bar{k}$$

and

$$\nabla \cdot (\;) \equiv \bar{h}\left[\frac{\partial}{\partial r} + \frac{1}{r}(\;)\right] + \bar{k}\frac{\partial}{\partial z},$$

where $\bar{h}$ = r direction unit vector,

$\bar{k}$ = z direction unit vector,

u = z velocity component,

v = r velocity component.

The flow equations are now:

Continuity,

$$\frac{\partial}{\partial t}(\rho) + \frac{\partial}{\partial z}(\rho u) + \frac{\partial}{\partial r}(\rho v) + \frac{\rho v}{r} = 0; \tag{10}$$

Momentum,

z-direction

$$\frac{\partial}{\partial t}(\rho u) + \frac{\partial}{\partial z}(\rho u^2 + p) + \frac{\partial}{\partial r}(\rho uv) + \frac{\rho uv}{r} = 0 \tag{11}$$

r-direction

$$\frac{\partial}{\partial t}(\rho v) + \frac{\partial}{\partial z}(\rho uv) + \frac{\partial}{\partial r}(\rho v^2 + p) + \frac{\rho v^2}{r} = 0; \tag{12}$$

Energy,

$$\frac{\partial}{\partial t}(e) + \frac{\partial}{\partial z}[(e + p)u] + \frac{\partial}{\partial r}[(e + p)v] + \frac{v}{r}(e + p) = 0. \tag{13}$$

The fluid energy is

$$e = \frac{\rho(u^2 + v^2)}{2} + \frac{p}{k - 1}. \tag{14}$$

The flow equations (10), (11), (12), and (13) may be written as a single equation

$$\frac{\partial f}{\partial t} + \frac{\partial F^z}{\partial z} + \frac{\partial F^r}{\partial r} + \psi = 0 \tag{15}$$

by considering f, F^z, F^r, and ψ as four component vectors:

$$f = \begin{Bmatrix} \rho \\ \rho u \\ \rho v \\ e \end{Bmatrix}; \qquad F^z = \begin{Bmatrix} \rho u \\ \rho u^2 + p \\ \rho uv \\ (e + p)u \end{Bmatrix};$$

$$F^r = \begin{Bmatrix} \rho v \\ \rho uv \\ \rho v^2 + p \\ (e + p)v \end{Bmatrix}; \qquad \psi = \frac{v}{r} \begin{Bmatrix} \rho \\ \rho u \\ \rho v \\ e + p \end{Bmatrix}.$$

The dependent variables (ρ, u, v, e, p) of Equations (9) and (15) are made dimensionless with respect to some reference state, which for this study is the state in front of a moving shock wave. The non-dimensionalizing method, Appendix C, gives the static properties, ρ and p, in front of the shock a value of unity and behind the shock a value equal to the property ratio across a normal shock as given by a standard compressible flow table [45]. Velocities are non-dimensionalized with respect to the quantity $\sqrt{p/\rho}$ in front of the shock.

Mathematical Conservation Laws Applied to Gas Dynamics

The mathematical properties of conservation laws presented in this section are only those which pertain to nonlinear wave propagation in gas dynamics. For a general discussion of the mathematics of conservation laws, the reader is referred to the books, Non-Linear Wave Propagation by Jeffery and Taniuti [46] and Methods of Mathematical Physics, Volume II by Courant and Hilbert [47]. A discussion of the properties is given here with references for required proofs.

The differential form of a mathematical conservation law is expressed as

$$\frac{\partial f}{\partial t} + \nabla \cdot \bar{F} = 0 \qquad (16)$$

where f and $\bar{F}$ are not independent. Equation (16) is said to be in divergence form and expresses the divergence free character of the field $(f, \bar{F})$, (i.e., the divergence of the field vanishes).

If jump discontinuities of f and $\bar{F}$ are present across a surface σ, certain conditions must be satisfied to represent properly the discontinuity. The generalized Rankine-Hugoniot relation [46],

$$\lambda[f] = [\bar{F} \cdot \bar{n}], \qquad (17)$$

must be satisfied for the discontinuity surface σ. The brackets here denote changes in the quantities, f and $\bar{F}$, across the surface σ, and λ is the local velocity of propagation of σ, along the unit normal of σ, $\bar{n}$. In gas dynamics the conservation equations of the form of Equation (16) are statements of the conservation laws for mass, momentun, and energy, Equations (1), (2), and (3). The jump discontinuity σ is gas dynamics, described by the generalized Rankine-Hugoniot relation, Equation (17), is a shock wave where λ is the shock speed. For a stationary shock, the shock speed would be zero, which gives the more familiar Rankine-Hugoniot relation. One additional condition must be satisfied to determine a physically relevant state across a shock because the direction of the change of entropy must be defined. Therefore, the entropy condition (i.e., the second law of thermodynamics) must be satisfied to ensure the supersonic character of shocks.

The solutions for the conservation laws are of two types: genuine and weak. A genuine solution is a function which satisfies the differential equation and is Lipschitz continuous (i.e., a solution which is continuous and has a bounded first derivative). The concept of a weak solution (also called a generalized solution) allows the solution to be discontinuous. Therefore, the weak solution may possess jump discontinuities, such as the discontinuity surface σ mentioned above. The general theory of weak solutions has been discussed in mathematical journals [29], [37], [48], and [49]. It has been shown that a genuine solution is a special case of a weak solution; that is, a weak solution with continuous first derivatives is a genuine solution. The flow of a gas in a two-dimensional space R may serve as an example of the two types of solutions. Let a shock surface σ separate the region R into two subregions 1 and 2. The solution for region 1 is a genuine solution f_1 because the flow is uniform and possesses no discontinuities. Likewise, the solution f_2 for region 2 is a genuine solution. The generalized or weak solution of region R is formed by taking f_1 and f_2 together if the Rankine-Hugoniot relation, Equation (17), is satisfied across σ. A weak solution, as defined, is not unique because in physical phenomena certain quantities require a defined direction of change across discontinuity surfaces. Entropy is a quantity which must always increase across a shock discontinuity (the second law of thermodynamics). Therefore, the entropy condition must be satisfied by a weak solution before the solution may represent a physical shock problem.

A shock discontinuity is an irreversible process involving viscous and heat conduction effects while the conservation equations, (1), (2), and (3), are derived for an inviscid gas and describe reversible processes. A method of obtaining physically relevant weak solutions for the conservation equations, (1), (2), and (3), involving irreversible processes has been suggested by a number of mathematicians [27], [48], [50], [51], and [52]. The method is to introduce mathematical terms with small coefficients which are analogous to the "dissipative" terms of viscosity and heat conduction. It is then postulated that weak solutions for physical phenomena may be obtained from the limit of mathematical "dissipative" solutions as the coefficients of the "dissipative" terms tend to zero. Studies, [50] and [52], of the equation

$$\frac{\partial f}{\partial t} + \frac{\partial F(x, t, f)}{\partial x} = \lambda \frac{\partial^2 f}{\partial x^2}$$

have established that solutions of the equation with given initial conditions tend to a weak solution of

$$\frac{\partial f}{\partial t} + \frac{\partial F(x, t, f)}{\partial x} = 0 \qquad (18)$$

with the same initial conditions. Olejnik [52] has proved the existence of the weak solution for Equation (18) obtained by this method. In a study of continuous dependence of solutions upon their initial conditions, Douglis [53] rederived Olejnik's results as a special case. Olejnik also has given conditions for the use of nonlinear "dissipative" terms (i.e.,

$$\lambda \frac{\partial}{\partial x} \left[A(x, t) \frac{\partial f}{\partial x} \right]).$$

The use of nonlinear terms has also been suggested by Godunov [48], [51]. The addition of the "dissipative" terms causes the equation to be parabolic in nature. Therefore, the solution of the parabolic equation

$$\frac{\partial f}{\partial t} + \frac{\partial F(x, t, f)}{\partial x} = \lambda \frac{\partial}{\partial x}\left[A(x, t) \frac{\partial f}{\partial x} \right] \tag{19}$$

with the initial condition $f(x, o) = \phi(x)$, gives as a limit, for $\lambda \to 0$, the weak solution of the hyperbolic equation

$$\frac{\partial f}{\partial t} + \frac{\partial F(x, t, f)}{\partial x} = 0 . \tag{20}$$

When a system of equations in the form of Equation (19) is written for the conservation equations (1), (2), (3), a finite difference technique must be used to obtain a solution because of the nonlinear character of the equations. A number of different "dissipative" terms have been defined to represent moving shock waves [27], [36], [37], [38]. In numerical calculations the "dissipative" terms allow the shock to be smeared over a narrow region in which flow properties are represented as very steep continuous gradients. Von Neumann and Richtmyer [27], who were the first to apply the mathematical "dissipative" method to shock propagation, have given four requirements that must be met in defining a coefficient for the "dissipative" term:

1. The equations with "dissipative" terms must possess solutions without discontinuities.
2. The thickness of the shock must be of the same order as the length Δx used in numerical calculations, independent of the shock strength and of the condition of the flow into which the shock is propagating.

3. The effect of the "dissipative" terms must be negligible outside the shock region.

4. The Rankine-Hugoniot equations must be satisfied across the shock for a distance greater than the shock thickness.

It has been observed also that the addition of the "dissipative" terms has the effect of adding stability to the difference equation.

Difference Technique

The solutions of the conservation laws for the plane geometry, Equation (9), and axisymmetric geometry, Equation (15), are obtained by using the "dissipative" method previously described. The difference scheme of Rusanov [38] is developed below, including important details omitted in the original paper, for the nonlinear "dissipative" equation

$$\frac{\partial f}{\partial t} + \frac{\partial F^x}{\partial x} + \frac{\partial F^y}{\partial y} = \frac{\partial}{\partial x}\left[A(x,y,t)\,\frac{\partial f}{\partial x}\right] + \frac{\partial}{\partial y}\left[B(x,y,t)\,\frac{\partial f}{\partial y}\right] \qquad (21)$$

for plane geometries and

$$\frac{\partial f}{\partial t} + \frac{\partial F^z}{\partial z} + \frac{\partial F^r}{\partial r} + \psi = \frac{\partial}{\partial z}\left[C(z,r,t)\,\frac{\partial f}{\partial z}\right] + \frac{\partial}{\partial r}\left[D(z,r,t)\,\frac{\partial f}{\partial r}\right] \quad (22)$$

for axisymmetric geometries. The coefficients A, B, C, and D are determined by applying the Fourier stability technique to the difference equations for Equations (21) and (22).

The Equations (9) and (15) are written in the form of Equations (21) and (22), respectively; and, using a square net, the difference scheme for a general field point is derived in Appendix D. The square net (Figure 16) has steps $\Delta x = \Delta y = h_1$, $\Delta t = \tau$ in the (x,y,t) space. The coordinate of any quantity at a net intersection point is $(mh_1,$

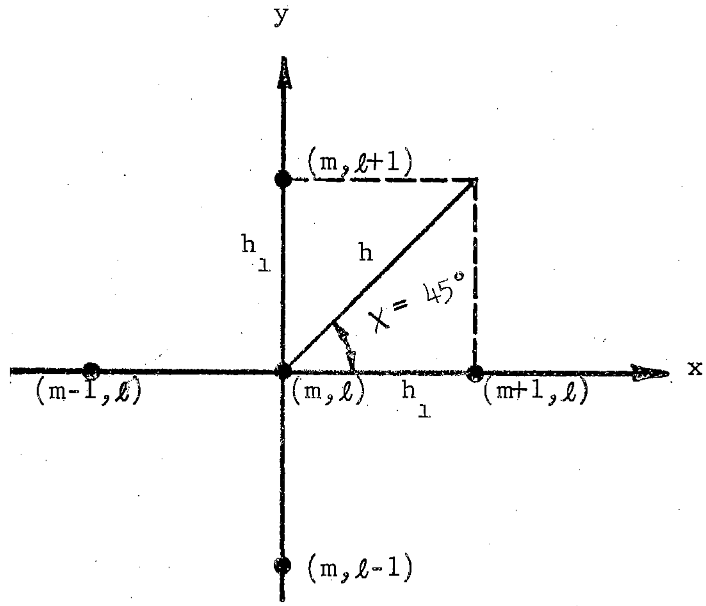

Figure 16. Net Point Nomenclature for Plane Geometry.

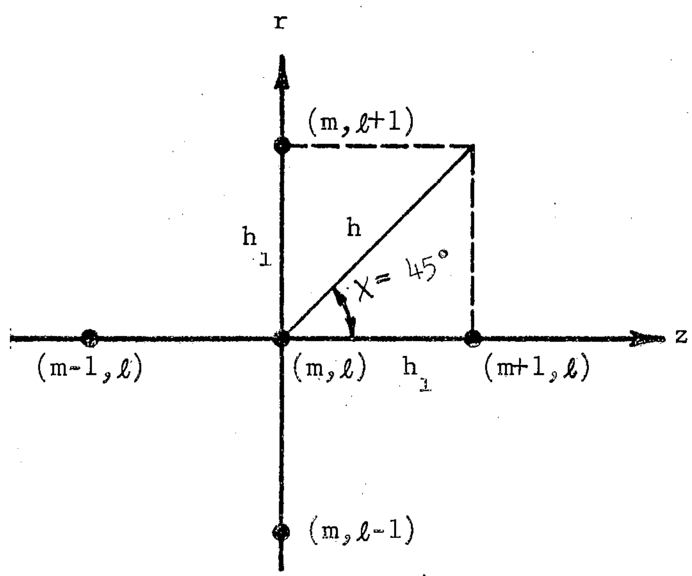

Figure 17. Net Point Nomenclature for Axisymmetric Geometry.

ℓh_1, $n\tau$) and a quantity a, at this point, is denoted by $a^n_{m,\ell}$. The increments h_1 and τ are related through the angle χ, which is between the diagonal h of a net and the x increment h_1 (Figure 16). These h_1 and τ relations are

$$K_1 \equiv \frac{\tau}{h_1} ; \qquad K = \frac{\sqrt{2}\,\tau}{h_1} ,$$

where $h_1 = h \cos \chi = h/\sqrt{2}$, for a square net;

$$\therefore \quad K = K_1 \sqrt{2} .$$

The difference equation corresponding to Equation (21) is

$$f^{n+1}_{m,\ell} = f^n_{m,\ell} - \frac{K_1}{2}\left[F^x_{m+1,\ell} - F^x_{m-1,\ell} + F^y_{m,\ell+1} - F^y_{m,\ell-1} \right]^n +$$

$$\frac{1}{2}\left[\Phi_{m+\frac{1}{2},\ell} - \Phi_{m-\frac{1}{2},\ell} + \Phi_{m,\ell+\frac{1}{2}} - \Phi_{m,\ell-\frac{1}{2}} \right] \tag{23}$$

where:

$$\Phi_{m+\frac{1}{2},\ell} = \alpha^n_{m+\frac{1}{2},\ell} \left(f^n_{m+1,\ell} - f^n_{m,\ell} \right),$$

$$\Phi_{m-\frac{1}{2},\ell} = \alpha^n_{m-\frac{1}{2},\ell} \left(f^n_{m,\ell} - f^n_{m-1,\ell} \right),$$

$$\alpha^n_{m+\frac{1}{2},\ell} \equiv \frac{\left(\alpha^n_{m+1,\ell} + \alpha^n_{m,\ell} \right)}{2} .$$

These definitions may be applied to the ℓ direction by interchanging the roles of m and ℓ. The relation for $\alpha^n_{m,\ell}$ is determined by the stability condition derived in Appendix E,

$$\alpha^n_{m,\ell} = \frac{\omega\, \sigma^n_{m,\ell}}{2}$$

where ω = constant

and $$\sigma^n_{m,\ell} = K(w + c)^n_{m,\ell} \qquad \text{(Courant Number).}$$

The condition required for the equation to be stable is

$$\left(\sigma^n_{m,\ell}\right)^2 \leq \omega\,\sigma^n_{m,\ell} \leq 1 ,$$

where

$$\sigma^n_{m,\ell} \leq 1 .$$

With $\sigma^n_o = \max\limits_{m,\ell} \sigma^n_{m,\ell}$, the stability condition gives the requirement for ω as

$$\sigma^n_o \leq \omega \leq \frac{1}{\sigma^n_o} \tag{24}$$

and

$$\sigma^n_o \leq 1 .$$

If σ^n_o is allowed to be a constant for all time planes, the value of K^n (and therefore of τ^n) may be determined from

$$K^n = \frac{\sigma^n_o}{\left[\max\,(w + c)_{m,\ell}\right]^n} .$$

Therefore, only the constants σ^n_o and ω, which satisfy condition (24), are needed to insure the stability of Equation (23) in a computer calculation.

The difference equation corresponding to Equation (22) for axial symmetry is

$$f^{n+1}_{m,\ell} = f^n_{m,\ell} - \frac{K_1}{2}\left[F^z_{m+1,\ell} - F^z_{m-1,\ell} + F^r_{m,\ell+1} - F^r_{m,\ell-1}\right]^n - \tau\,\psi^n_{m,\ell} +$$

$$\frac{1}{2}\left[\Phi_{m+\frac{1}{2},\ell} - \Phi_{m-\frac{1}{2},\ell} + \Phi_{m,\ell+\frac{1}{2}} - \Phi_{m,\ell-\frac{1}{2}}\right] \tag{25}$$

where the square net (Figure 17) has steps $\Delta r = \Delta z = h_1$, $\Delta t = \tau$ in the (r, z, t) space, and the coordinate of a net intersection point is $(mh_1, \ell h_1, n\tau)$. The definitions for Φ and K_1 in Equation (23) and condition (24) may be used for Equation (25).

The difference equations, Equations (23) and (25), are for net points which are interior to a flow field. The boundary difference equations for flow along a wall, which is parallel to either of the coordinate axes, are developed in Appendix F. Also derived in Appendix F is the difference equation for a net point on an axis of symmetry at $r = 0$. The plane boundary difference equation for a point (m, ℓ) on a wall parallel to the x axis is

$$f^{n+1}_{m,\ell} = f^{n}_{m,\ell} - \frac{K_1}{2}\left[F^{x}_{m+1,\ell} - F^{x}_{m-1,\ell} \right]^{n} \mp K_1 \left[F^{y}_{m,\ell\pm1} \right]^{n} +$$

$$\frac{1}{2}\left[\Phi_{m+\frac{1}{2},\ell} - \Phi_{m-\frac{1}{2},\ell} \right] \qquad (26)$$

where the upper and lower signs are, respectively, for flow above or below the wall. Only the first, second, and fourth components of $f^{n+1}_{m,\ell}$ are calculated by Equation (26). The third component $(\rho v)^{n+1}_{m,\ell}$ is zero from the boundary condition $v = 0$ at the wall. Similarly, for a wall parallel to the y axis, the equation is

$$f^{n+1}_{m,\ell} = f^{n}_{m,\ell} \mp K_1 \left[F^{x}_{m\pm1,\ell} \right]^{n} - \frac{K_1}{2}\left[F^{y}_{m,\ell+1} - F^{y}_{m,\ell-1} \right]^{n} +$$

$$\frac{1}{2}\left[\Phi_{m,\ell+\frac{1}{2}} - \Phi_{m,\ell-\frac{1}{2}} \right] \qquad (27)$$

gives the value of the first, third, and fourth components of $f^{n+1}_{m,\ell}$, where the upper and lower signs are, respectively, for flow to the right or left of the wall. The second component $(\rho u)^{n+1}_{m,\ell}$ is zero from the boundary condition. The axisymmetric boundary difference equations are

$$f^{n+1}_{m,\ell} = f^{n}_{m,\ell} - \frac{K_1}{2}\left[F^{z}_{m+1,\ell} - F^{z}_{m-1,\ell} \right]^{n} \mp K_1 \left[F^{r}_{m,\ell\pm 1} \right]^{n} - \tau \psi^{n}_{m,\ell}$$

$$+ \frac{1}{2}\left[\Phi_{m+\frac{1}{2},\ell} - \Phi_{m-\frac{1}{2},\ell} \right] \tag{28}$$

for a wall parallel to the z axis and

$$f^{n+1}_{m,\ell} = f^{n}_{m,\ell} \mp K_1 \left[F^{z}_{m\pm 1,\ell} \right]^{n} - \frac{K_1}{2}\left[F^{r}_{m+1,\ell} - F^{r}_{m-1,\ell} \right]^{n} - \tau \psi^{n}_{m,\ell}$$

$$+ \frac{1}{2}\left[\Phi_{m,\ell+\frac{1}{2}} - \Phi_{m,\ell-\frac{1}{2}} \right] \tag{29}$$

for a wall parallel to the r axis. The sign convention and $f^{n+1}_{m,\ell}$ component conditions for Equations (28) and (29) are, respectively, the same as for Equations (26) and (27). For a point on the axis of symmetry $r = 0$, the difference equation is

$$f^{n+1}_{m,o} = f^{n}_{m,o} - \frac{K_1}{2}\left[F^{z}_{m+1,o} - F^{z}_{m-1,o} \right]^{n} - K_2 \left[F^{r}_{m,1} \right]^{n} - \tau \hat{\psi}^{n}_{m,o}$$

$$+ \frac{1}{2}\left[\Phi_{m+\frac{1}{2},o} - \Phi_{m-\frac{1}{2},o} + 2\Phi_{m,\frac{1}{2}} \right] \tag{30}$$

where the quantity v/r in $\hat{\psi}^{n}_{m,o}$ is taken at the point $(m,1)$.

To solve a flow problem by a finite difference method, the defined field of the problem must be represented by a net of points at which the difference equations apply. Also, the solution obtained by a finite difference technique is an approximate solution and only approaches the true solution of the differential equation as the net point spacing approaches zero. These two facts, plus the condition that the shock thickness must be of the order of the net point spacing, require that a large number of points must be defined to represent the flow field. Therefore, shock propagation problems considered here, using the difference equations established above, must be programed for a high speed digital computer. A CDC 3600 computer was used for the programs presented in the following sections.

Application of the Difference Technique to Shock Propagation Into a Still Medium

For shock propagation into a still medium, a computer program was developed which gave solutions for both the plane and axisymmetric geometries. The sample net in Figure 18 will be used to explain the application of the difference equations to the two geometries.

Consider, first, the plane geometry. The points on the lines A, B, and C represent points along the boundary walls and all other points are interior field points. The walls A and B are parallel to the x axis and flow is in the x direction; therefore, the difference equation (26) is applied along these lines. Along the wall C, which is parallel to the y axis, the flow is in the y direction which requires the difference equation (27) to be used. The general field equation (23) is applied to all interior points.

The initial conditions for the field may be defined by considering the three regions of Figure 18. In Region 1 the field is uniform with a pressure p_1 and is said to be still (i.e., velocity is zero). The flow in Region 2 is uniform with a velocity u_2 in the positive x direction and a pressure p_2 greater than p_1. The Shock Region

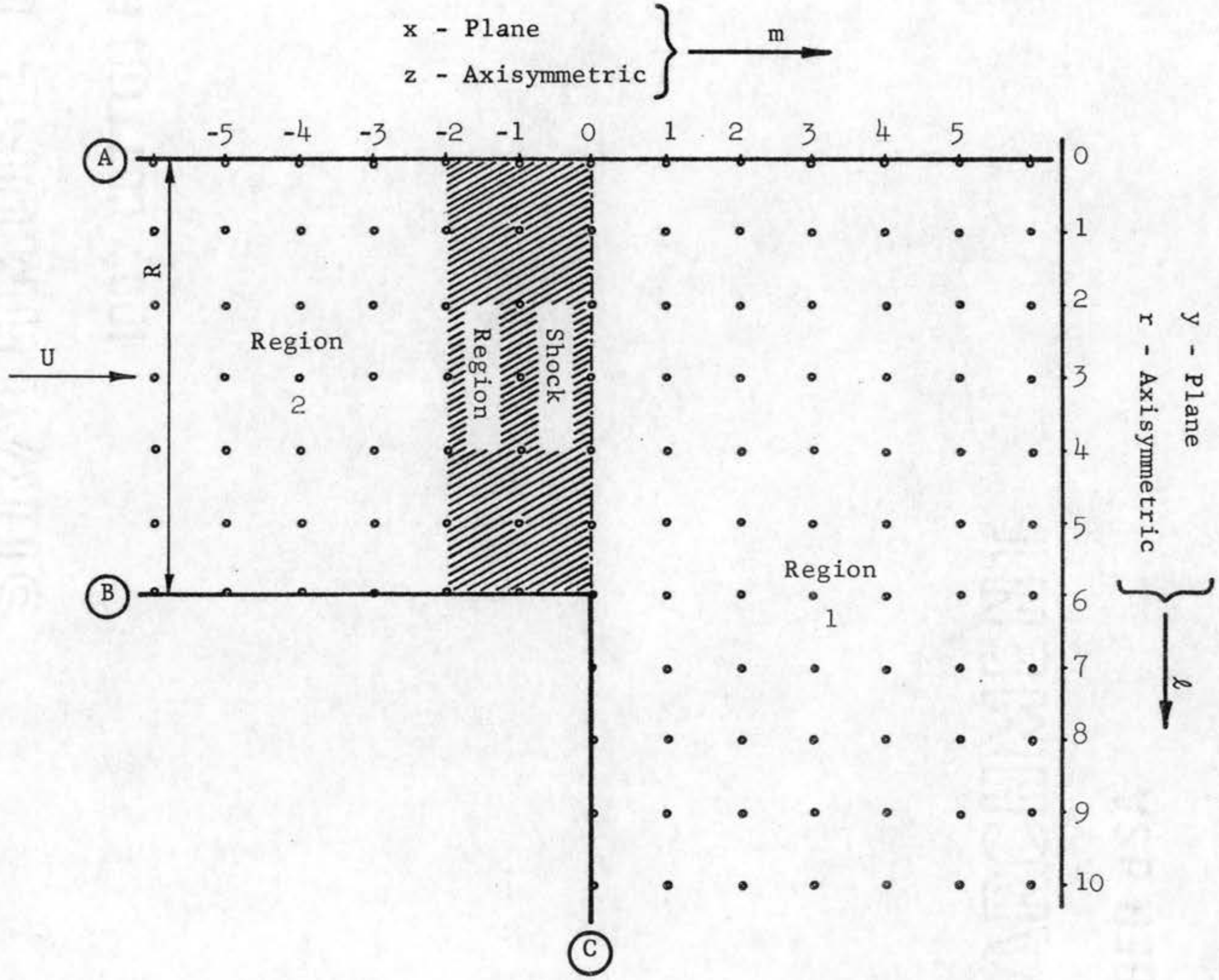

Figure 18. Sample Difference Net for Still Geometry Application.

divides Regions 1 and 2 and is the region in which a shock is defined. It has been observed that for an initial shock defined over one space interval (Figure 19) a small ripple disturbance is propagated away from the shock, similar to the disturbance shown by Lax and Wendroff [37] in Figure 20. The disturbance is formed because the initial conditions at these points do not satisfy the conservation equations. To eliminate this disturbance, a new method has been developed in which the shock is initially defined over two intervals. This is discussed in detail in Appendix G.

The axisymmetric geometry is now considered, using again Figure 18. The points on the A line represent an axis of symmetry at $r = 0$; therefore, the difference equation (30) is applied to these points. The points along the lines B and C represent walls which are, respectively, parallel to the z and r axis. The difference equations applied to these walls are Equation (28) for line B and Equation (29) along line C. The difference equation (25) for a point in an axisymmetric field is applied to all interior points.

The initial condition for the axisymmetric field, also, may be defined by considering the three regions of Figure 18. In Region 1, as in the plane geometry, the field is still and has a pressure p_1. The flow in Region 2 is uniform with a velocity u_2 in the positive x direction and a pressure p_2 greater than p_1. A shock, which propagates in x direction, is defined in the Shock Region by the same method used for the plane geometry shock. The computer program for the above application is discussed in Appendix H.

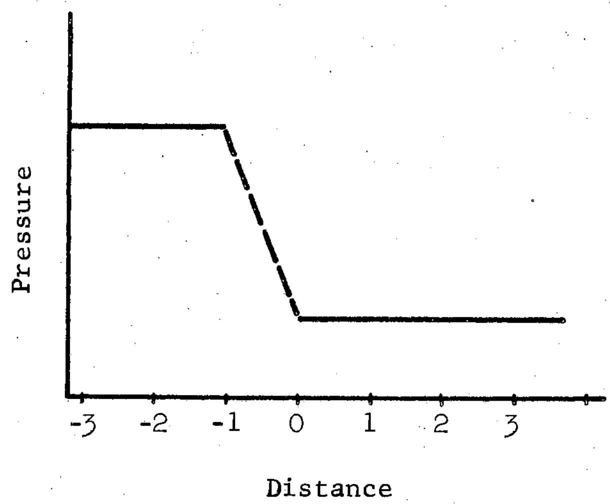

Figure 19. Initial Pressure Distribution for a Shock Defined Between Two Net Points.

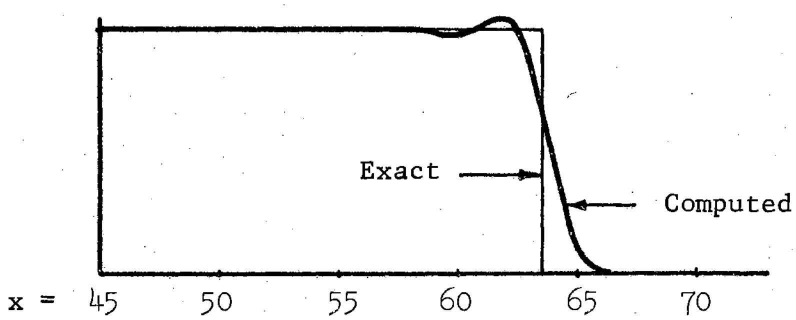

Figure 20. Shock Velocity Profile Showing a Small Ripple Disturbance [37].

Application of the Difference Technique to the Shock Propagation Into a Crossflowing Medium

To obtain solutions for the propagation of a shock into a perpendicular crossflow a computer program has been developed and is discussed in Appendix H. A sample net of points (Figure 21) is used to describe the application of the difference technique for the crossflow. The points on the lines A and B represent boundary walls which are parallel to the x axis and points along the lines C and D replace boundary walls that are parallel to the y axis. Flow is considered to be parallel to all of the boundary walls; therefore, the difference equations (26) and (27) are, respectively, applied to the lines A and B and to the lines C and D. The general field equation (23) for plane geometries is used at all interior points.

The initial conditions for the flow field are defined in three basic regions of the field. The flow in Region 1 is uniform with a pressure p_1 and velocity v_1 in the positive y direction. Region 2 is also a uniform flow field with a pressure p_2, greater than p_1, and a velocity u_2 in the positive x direction. The two uniform fields, Regions 1 and 2, are separated by a Shock Region in which a shock wave is defined. The shock propagates in a positive x direction and is defined, as stated before, over two net intervals to eliminate ripple disturbances on either side of the shock (Appendix G).

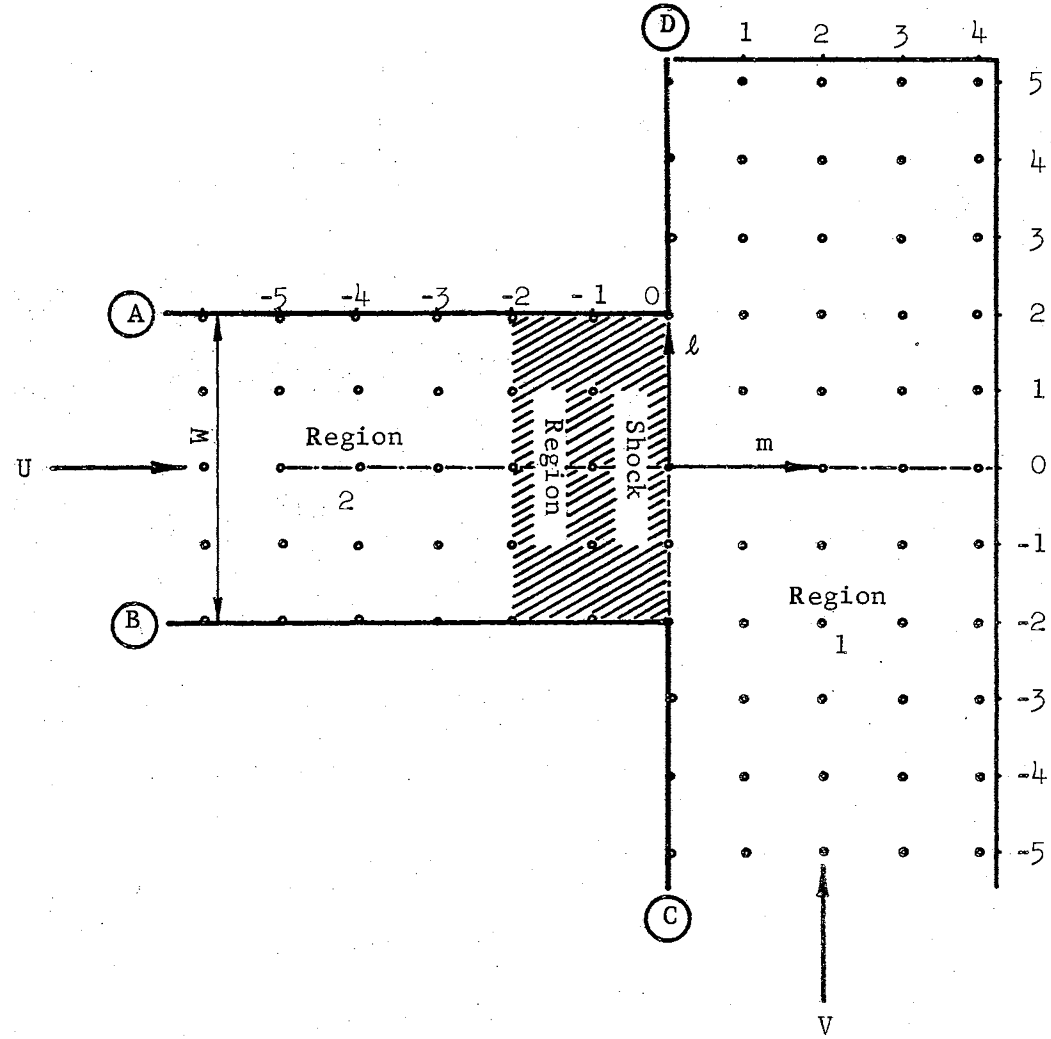

Figure 21. Sample Difference Net for Crossflow Geometry Application.

CHAPTER V

RESULTS FROM THE COMPUTED PROBLEMS

The results obtained from the computer programs are presented in the second and third sections of this chapter. In the first section a discussion is given on the procedure for obtaining dimensional values from the dimensionless results. The results of a shock propagating into a still medium, for both the plane and axisymmetric geometries, are presented in the second section. The final section contains the results for a shock propagating into a crossflowing medium.

Procedure for Obtaining Dimensional Quantities From Computer Results

All quantities used in the computer programs were made dimensionless by the method described in Appendix C. To have dimensional thermodynamic properties and velocities requires only that the nondimensionalizing technique be reversed (i.e., $p' = pp_1'$ and $u' = u\sqrt{p_1'/\rho_1'}$)*.

The time increment τ^n was not a constant but varied from time plane to time plane. The value of τ^n for a given time plane was computed by using the relation given on page 46

$$K^n = \frac{\sigma_o}{\left[\max\ (w + c)_{m,\ell}\right]^n}$$

---

*The prime denotes dimensional quantities and the subscript 1 refers to the initial condition in front of the shock.

where $$K^n = \frac{\tau^n \sqrt{2}}{h_1} .$$

The quantities σ_o and h_1 were chosen to be constant for all time intervals. Therefore, the values of τ^n depended on the maximum value of $(w + c)_{m,\ell}$ for each time plane n, requiring that K^n be computed for each time plane. The total dimensionless time was given by

$$t = \sum^{n} \tau^n$$

$$= \frac{h_1}{\sqrt{2}} \sum^{n} K^n$$

or

$$t = \frac{h_1}{\sqrt{2}} \sum^{n} \frac{\sigma_o}{\left[\max\ (w + c)_{m,\ell}\right]^n} .$$

To obtain a dimensional time from this relation requires that the velocity terms in the numerator be multiplied by the quantity $\sqrt{p_1{}'/\rho_1{}'}$, and that the net spacing h_1 be replaced by the ratio of the characteristic length to the number of net spacing along that length (i.e., L'/N). Using this information, dimensional time may be given as

$$t' = \frac{L' \sqrt{k}}{N\ c_1{}'\ \sqrt{2}} \sum^{n} \frac{\sigma_o}{\left[\max\ (w + c)_{m,\ell}\right]^n}$$

or

$$\eta = \frac{\sqrt{k}}{N \sqrt{2}} \sum^{n} K^n$$

where

$$\eta = \frac{t'\ c_1{}'}{L'} .$$

The parameter η is a dimensionless quantity which is used to designate the time for the results in the following sections.

Numerical Results of Shock Propagation Into a Still Medium

The results of a shock propagating into a still medium were obtained for both plane and axisymmetric geometries. Two sets of initial conditions were computed for the plane geometry and one set for the axisymmetric. The initial data are given in Table I. The results for the pressure ratio $p_2/p_1 = 4.0$* for the plane geometry were compared with results reported by Rusanov [38].

TABLE I

INITIAL CONDITIONS FOR STILL MEDIUM PROBLEMS

Properties	Plane Geometry		Axisymmetric Geometry
k	1.4	1.4	1.4
p_1	1.0	1.0	1.0
ρ_1	1.0	1.0	1.0
u_1	0.0	0.0	0.0
p_2	4.0	10.0	10.0
ρ_2	2.5	3.81	3.81
u_2	1.34	2.57	2.57
σ_o	0.50	0.50	0.50
ω	1.345	1.345	1.345

*Subscripted notation is defined in Figure 20 page 52 .

The characteristic length used to determine the η values was the initial length of the emerging shock, R (Figure 18), and the number of net spaces N was 29. The results from the initial conditions of Table I are given in Appendix A in the form of plots of the flow field with constant velocity modulus and constant pressure lines. Also given with each set of results is a plot of η versus Time Plane. The approximate shock location is denoted by a dashed line in the pressure and velocity figures. The shock location was taken as the location of the average pressure of a concentrated pressure region. A history of the approximate shock locations is given in Figures 22, 23, and 24, for the three initial shock conditions. Also plotted on these figures is a line along which a weak disturbance would theoretically propagate from the corner behind the shock. For a given shock position the shock properties begin to vary along the shock front from the disturbance line to the vertical wall, as would be expected. A water table (Plate II) which was equipped with a shock channel (Plate II) was used to obtain photographs of hydraulic wave forms. The wave forms in Plate III correspond to the initial pressure ratio of 10.0 for the plane geometry and compare well in shape and movement with the shock positions of Figure 23. The particle vector field for the three initial conditions are shown in Figures 25, 26, and 27 for a time when the shock has progressed approximately a distance R into region 1.

Numerical Results of Shock Propagation Into a Crossflowing Medium

Two sets of initial conditions were computed for the crossflow problems. In both sets of conditions the properties of the shock emerging into the flow were the same, but the crossflowing stream had Mach

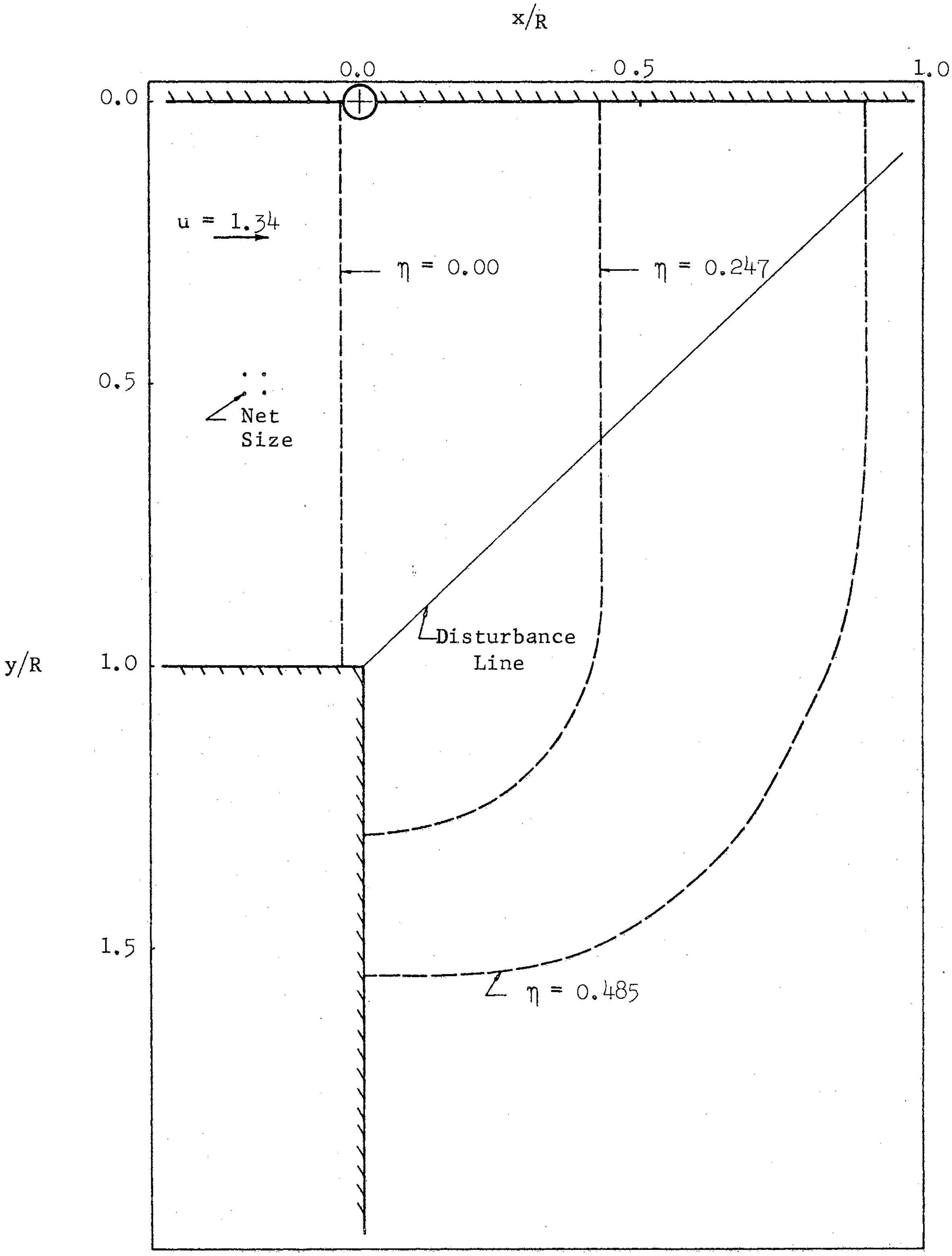

Figure 22. Shock Positions at Different Times in a Plane Geometry for the Still Propagation Problem. Initial Shock Pressure Ratio - 4.0.

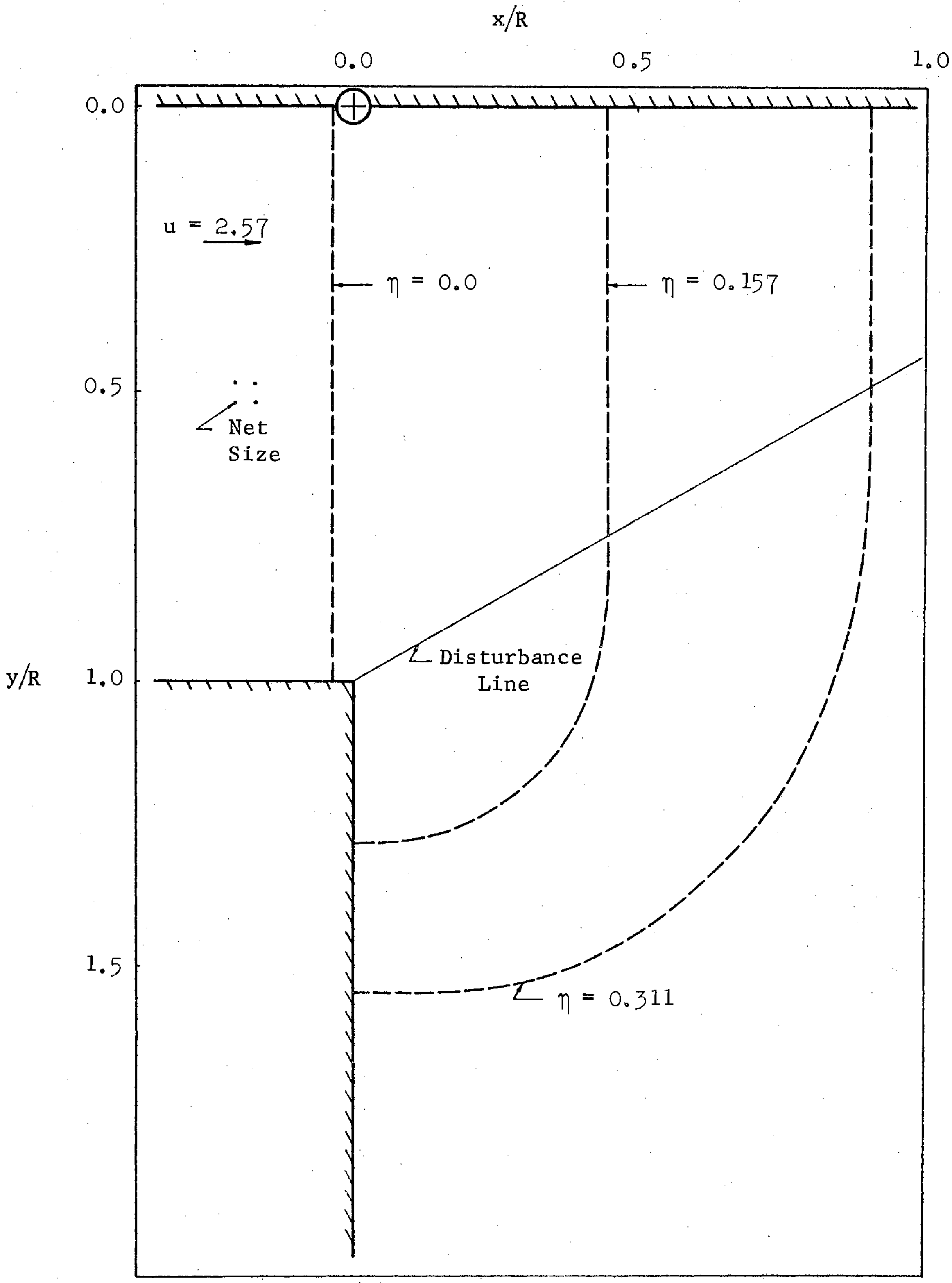

Figure 23. Shock Positions at Different Times in a Plane Geometry for the Still Propagation Problem. Initial Shock Pressure Ratio - 10.0.

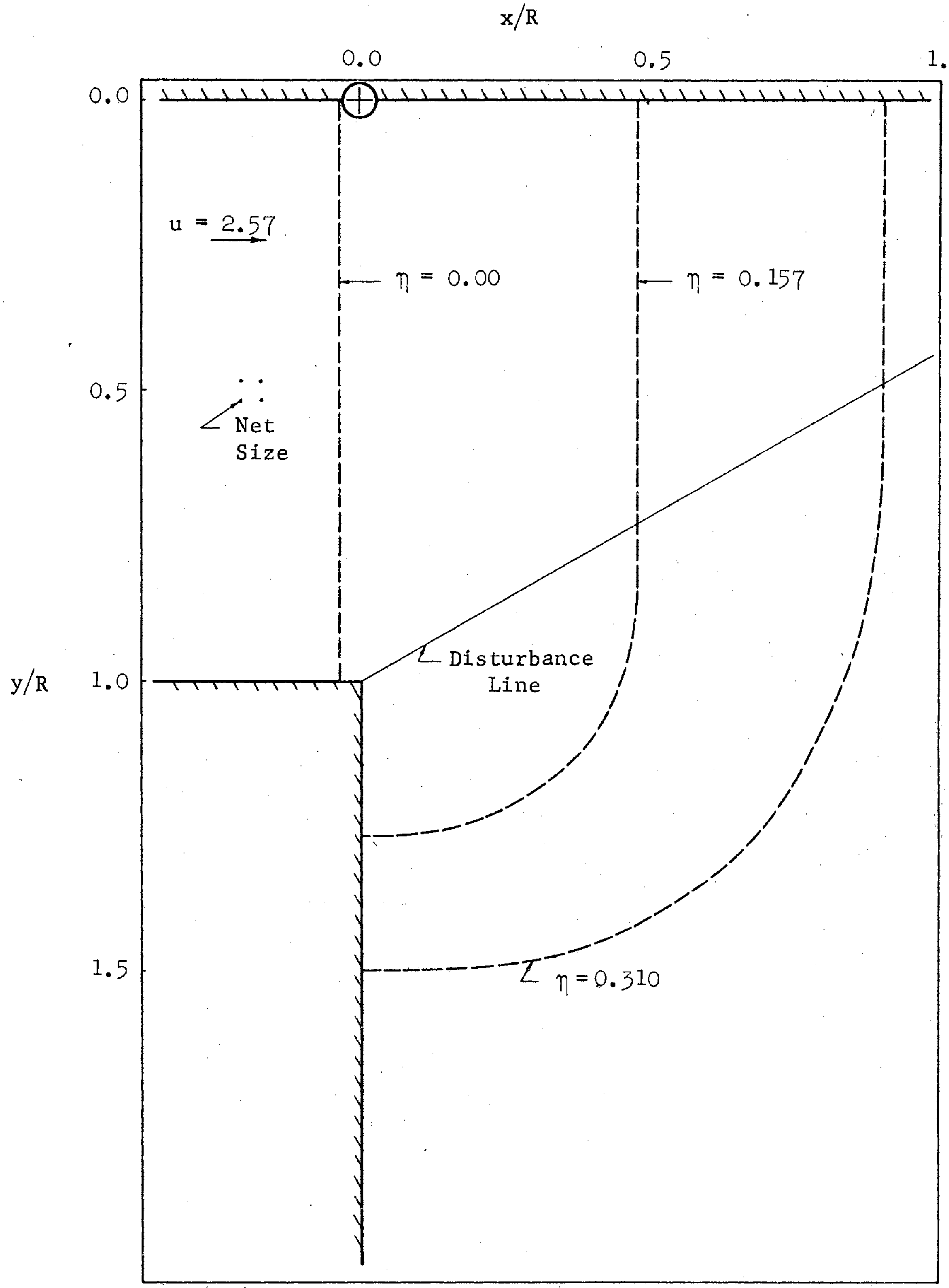

Figure 24. Shock Positions at Different Times in an Axisymmetric Geometry for the Still Propagation Problem. Initial Shock Pressure Ratio - 10.0.

PLATE II WATER TABLE - SHOCK CHANNEL ARRANGEMENT

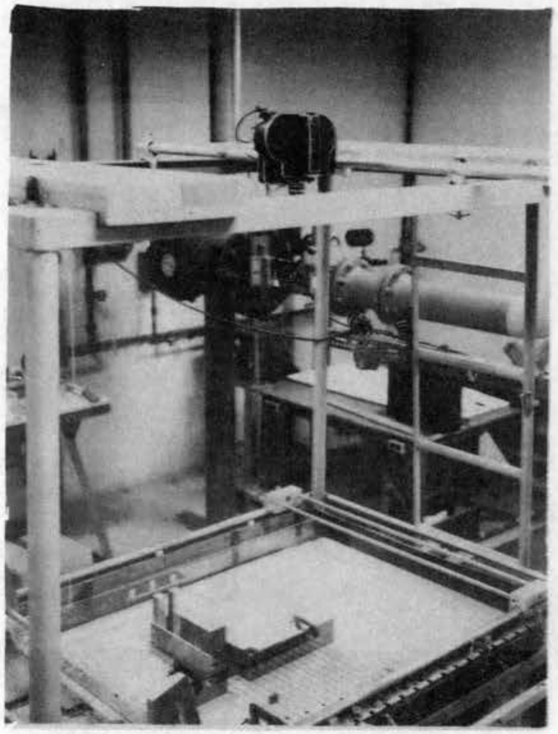

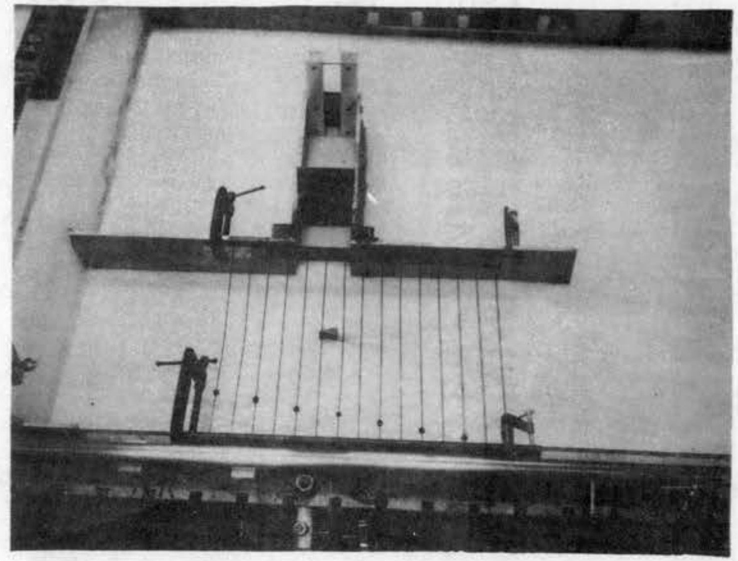

PLATE III

A HYDRAULIC BORE (CORRESPONDING TO A SHOCK PRESSURE RATIO
OF 10.0) EMERGING INTO A STILL MEDIUM
FROM A SHOCK CHANNEL

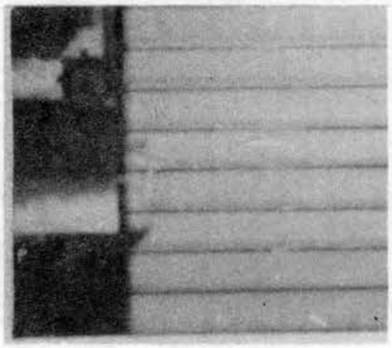

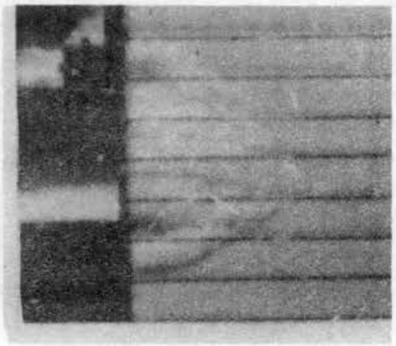

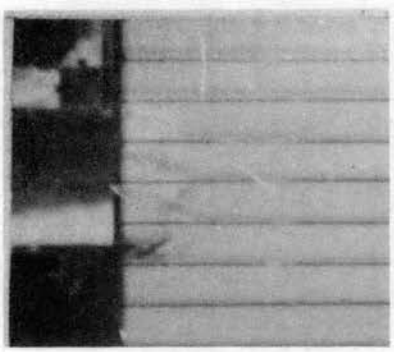

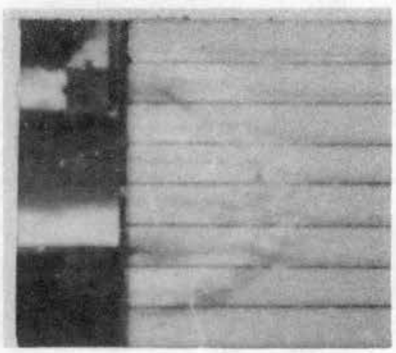

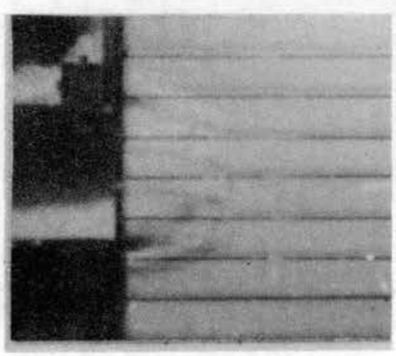

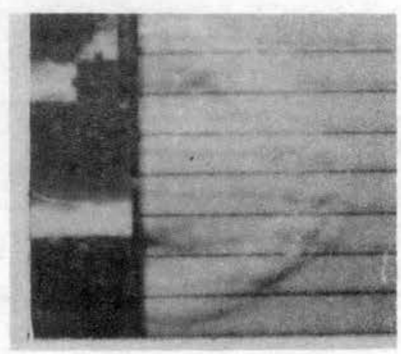

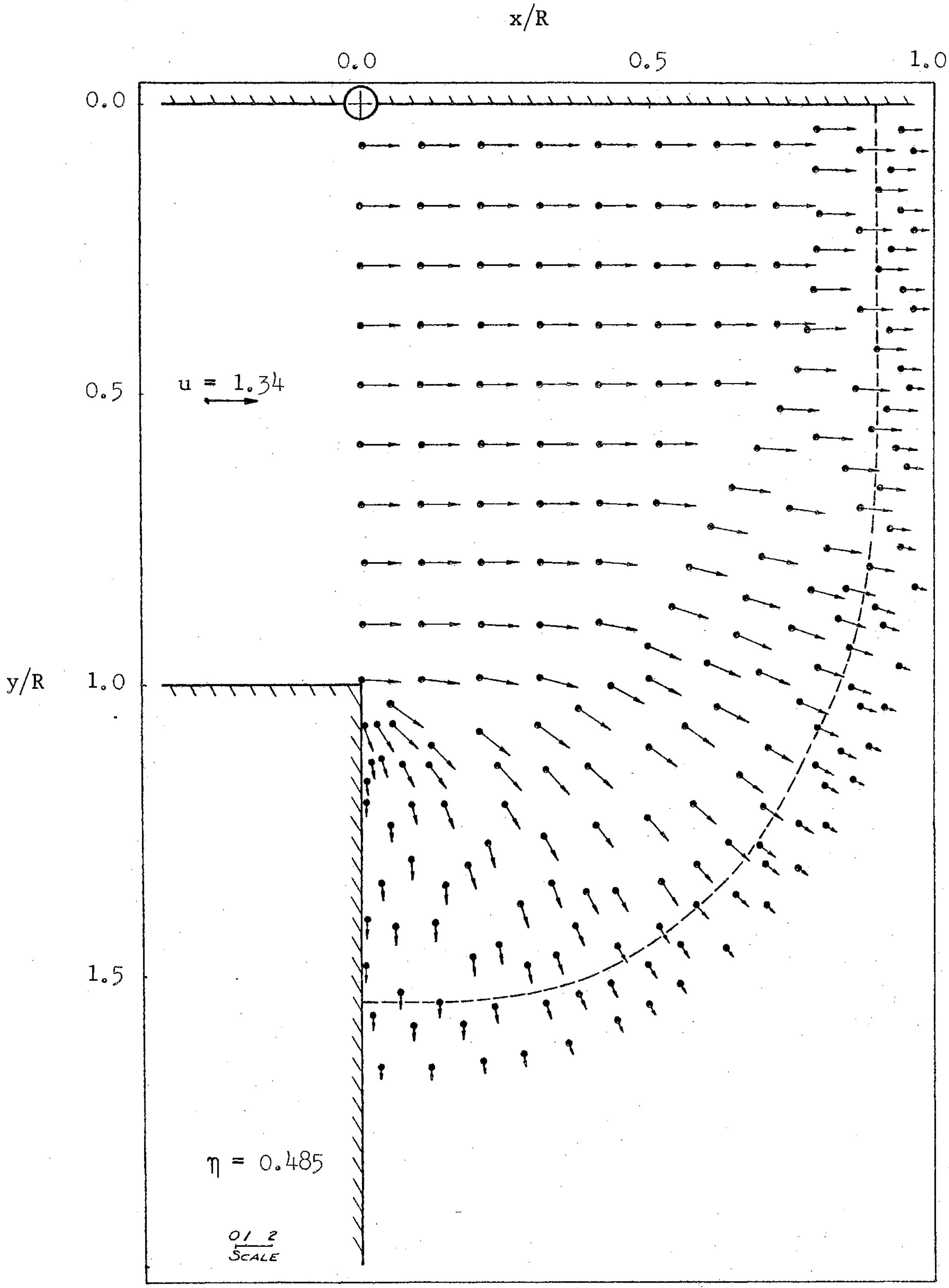

Figure 25. Particle Vector Field for the Still-Plane Geometry. Initial Shock Pressure Ratio 4.0.

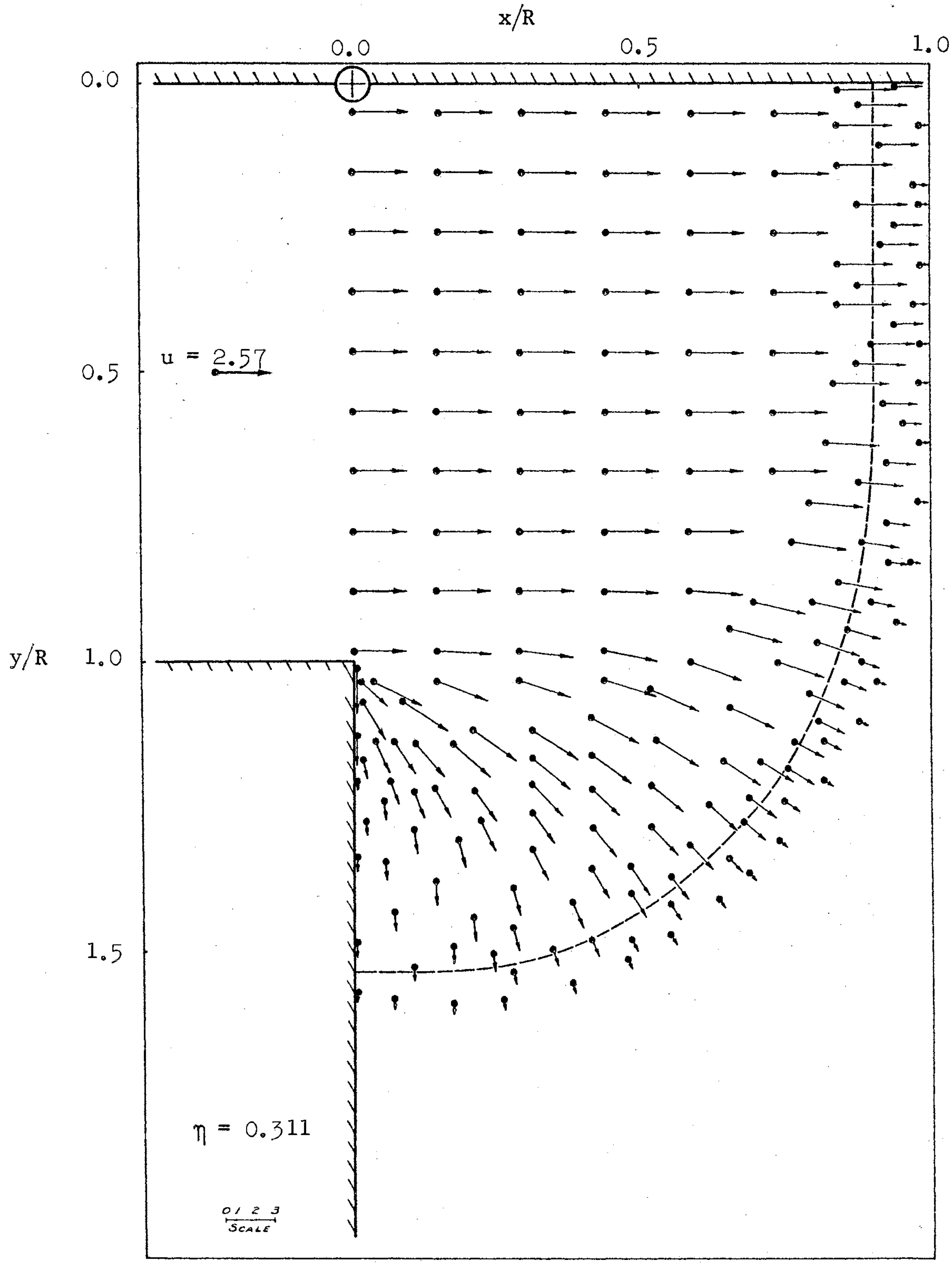

Figure 26. Particle Vector Field for the Still-Plane Geometry. Initial Shock Pressure Ratio 10.0.

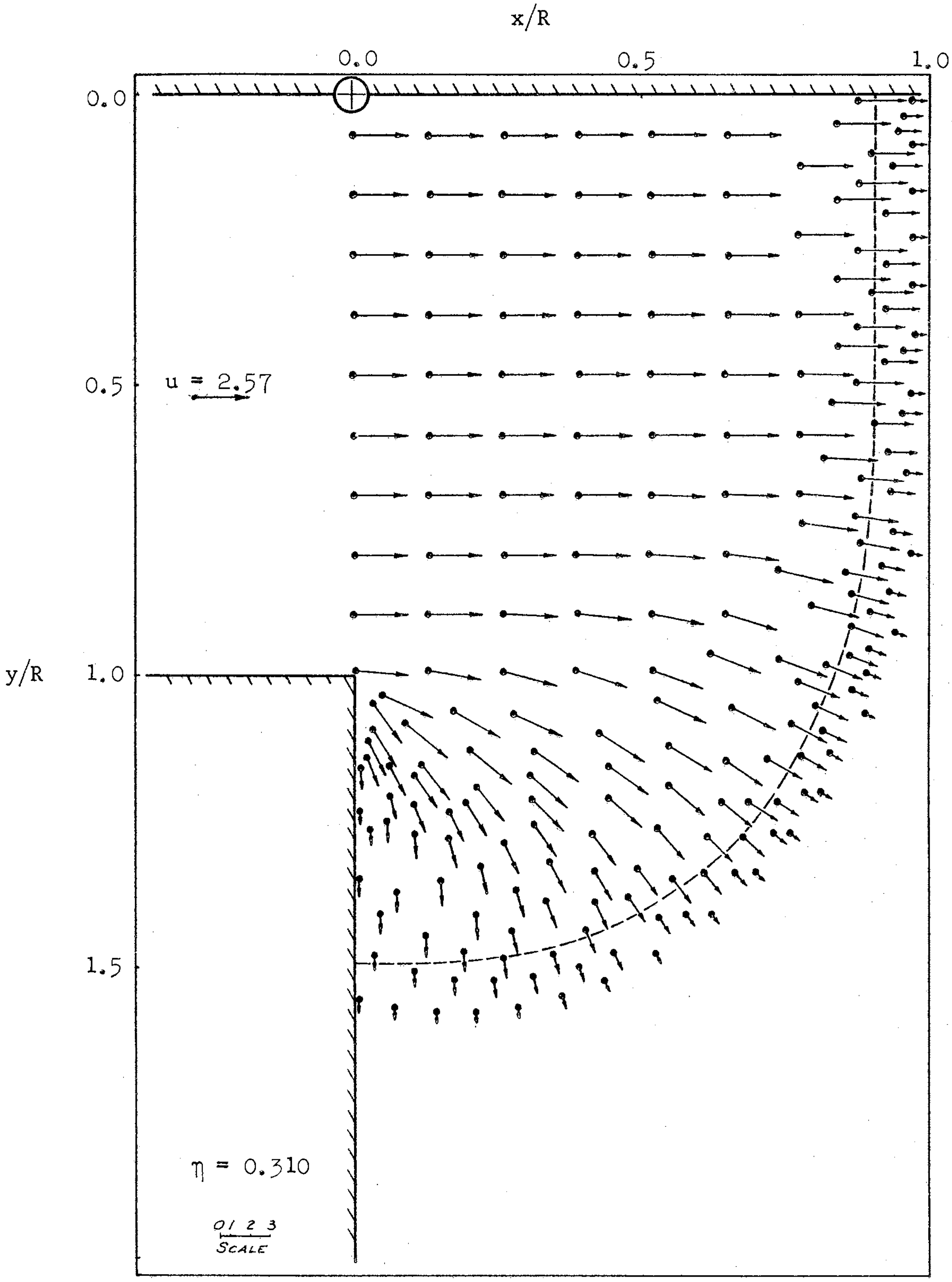

Figure 27. Particle Vector Field for the Still-Axisymmetric Geometry. Initial Shock Pressure Ratio 10.0.

numbers of 2.0 and 5.0 in the two cases. The initial conditions are given in Table II where the subscripts are defined according to Figure 21 on page 54 .

TABLE II

INITIAL CONDITIONS FOR CROSSFLOWING PROBLEMS

Properties	$M_1 = 2.0$	$M_1 = 5.0$
k	1.4	1.4
p_1	1.0	1.0
ρ_1	1.0	1.0
u_1	0.0	0.0
v_1	2.37	5.92
p_{o1}*	29.5	29.5
p_2	10.0	10.0
ρ_2	3.81	3.81
u_2	2.57	2.57
v_2	0.0	0.0
p_{o2}	7.8	529.10
σ_o	0.50	0.50
ω	1.345	1.345

The characteristic length used to determine the η values was the channel width W (Figure 21), and the number of net spaces N was 29. Constant velocity modulus and constant pressure line figures are given in Appendix A with a plot of η versus Time Plane Number for each set

*Subscript o denotes stagnation condition.

of initial conditions. The approximate shock position is defined by a dashed line in the same manner as for the still-medium problems.

The Mach 2 and 5 crossflows give two qualitatively different conditions for the crossflow stream with an initial shock pressure ratio of 10.0. This can be seen by considering values of p_{o2}/p_{o1}, the ratio of stagnation pressure of the shock tube flow to that of the main stream. For the Mach 5.0 stream the ratio is 0.056, and for the Mach 2.0 stream it is 3.76. For a stagnation pressure ratio p_{o2}/p_{o1} less than unity the flow energy of the crossflowing stream is greater than that of the shock stream; and, therefore, the crossflow stream would tend to dominate the flow from the shock channel. The Mach 5 flow represents the crossflow domination condition. For a stagnation pressure ratio p_{o2}/p_{o1} greater than unity the comparative energies of the two streams are reversed and the shock channel flow dominates the crossflow, as in the Mach 2.0 condition.

In considering both of these conditions, it is well to note that the primary concern is to establish whether or not this arrangement of a shock emerging into a crossflow can represent a blast wave interacting with a flying body.

The results of the crossflow domination of the Mach 5.0 stream is considered first. From the constant pressure figures in Appendix A, it is seen that the shock emerging into a high energy stream appears to seek a fixed location a short distance upstream of shock channel. The fluid location along the vertical wall $(x/W = 0.0)$ is found by examining the pressure distributions along the exit plane $(x/W = 0.0)$ of the shock channel for various times. Such a plot is given in Figure 28, and the fixed shock position is at $y/W = -0.67$. The expansion along the downstream wall at $y/W = 0.50$ is also seen to be steady. The approximate shock position history in Figure 29 gives some understanding of the propagation of the shock while the particle vector field in Figure 30 gives an insight to the particle flow. The approximate shock shape and movement of Figure 29 seems to compare well qualitatively with the corresponding hydraulic waves in the water table photographs in Plate IV. It appears in the latter photographs that the hydraulic waves have also reached a fixed position a short distance upstream. From the water table pictures, it appears that the moving hydraulic wave has become a fixed curved wave at a distance x/W along the centerline of 1.5. To investigate the possibility that a uniform portion of the shock exists, the pressure distributions along the y/W lines of 0.0 and 0.5 were considered. From the extrapolation of the envelope of the pressure distribution curves, no common pressure values seem to exist for the two y/W locations at a common distance x. By considering the water table photographs, the extrapolated envelope appears to have extended beyond the position at which the shock becomes fixed. It appears, therefore, that for the condition where the crossflow stream possesses a greater energy than the shock stream there is no apparent way to obtain a uniform blast wave simulation.

For the case in which the shock stream dominates the phenomenon (i.e., crossflow of Mach 2), it is observed that the shock wave emerges from the channel and propagates upstream at a fairly constant rate along the vertical wall. This would be expected since the total energy behind the shock is greater than that of the crossflow stream. The progress of the shock along the wall may be seen by considering the pressure distribution in Figure 33 for various times along the exit

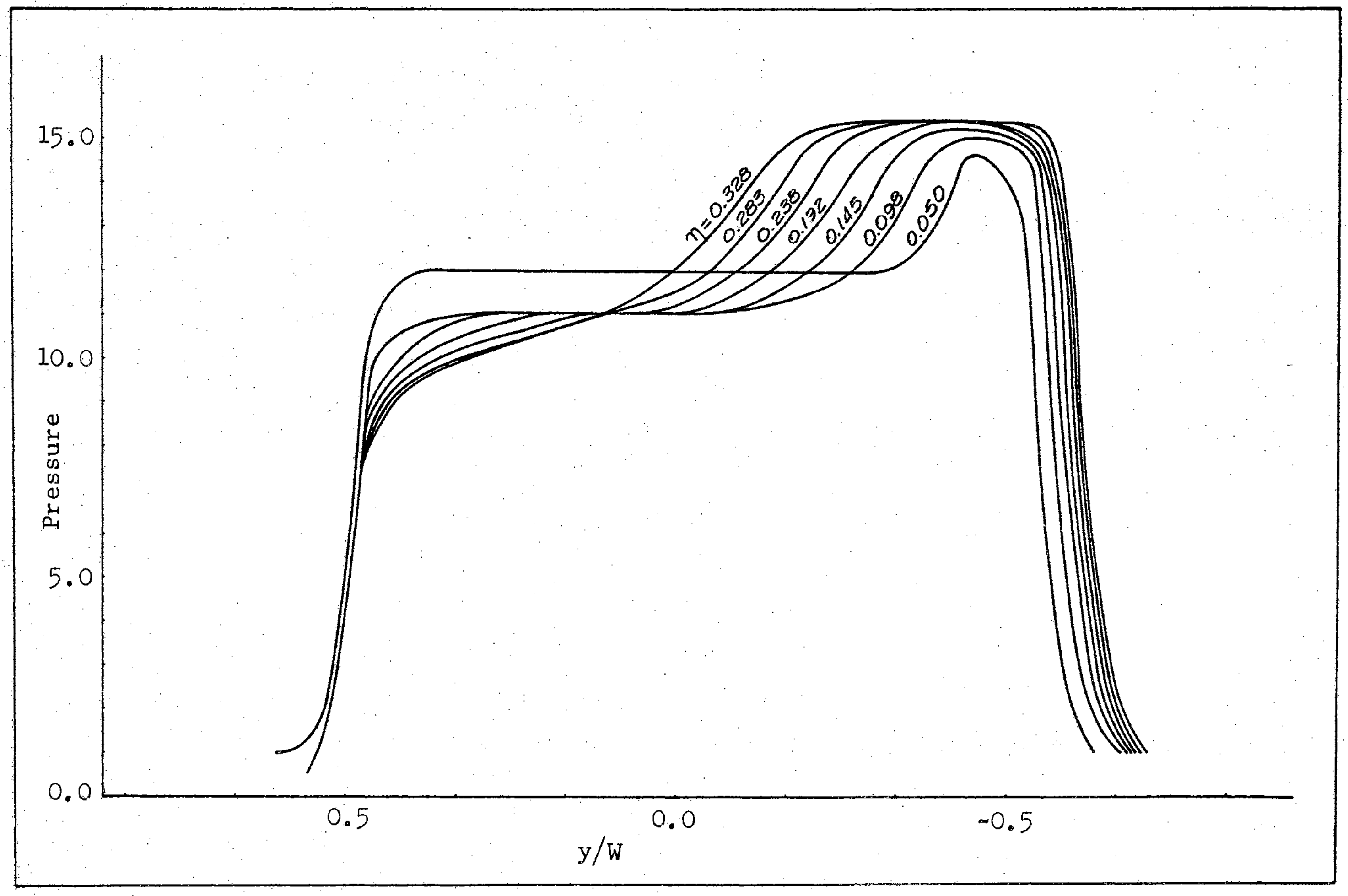

Figure 28. Exit Plane Pressure Distributions for a Mach 5 Crossflow.

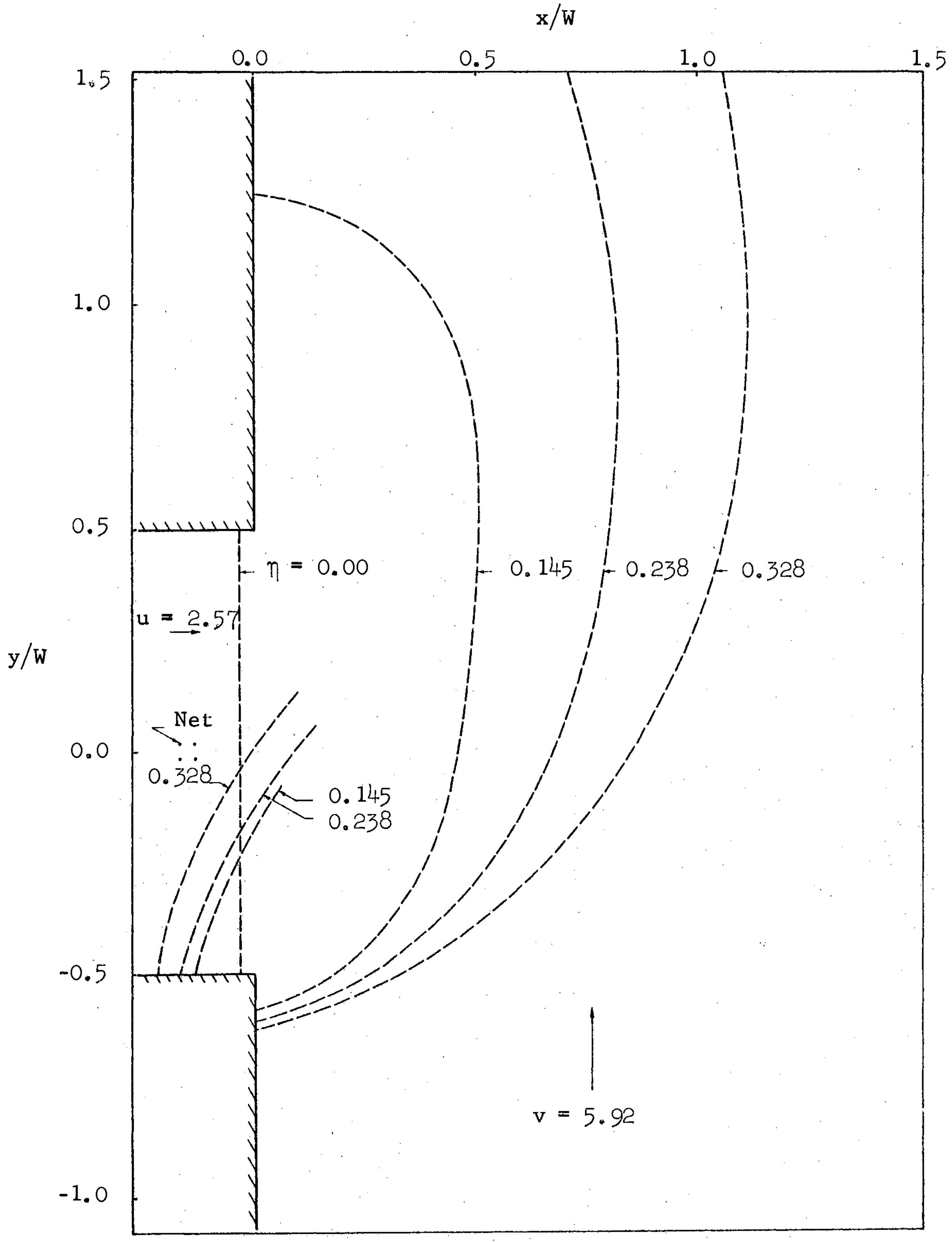

Figure 29. Shock Positions at Different Times for a Mach 5 Crossflow.

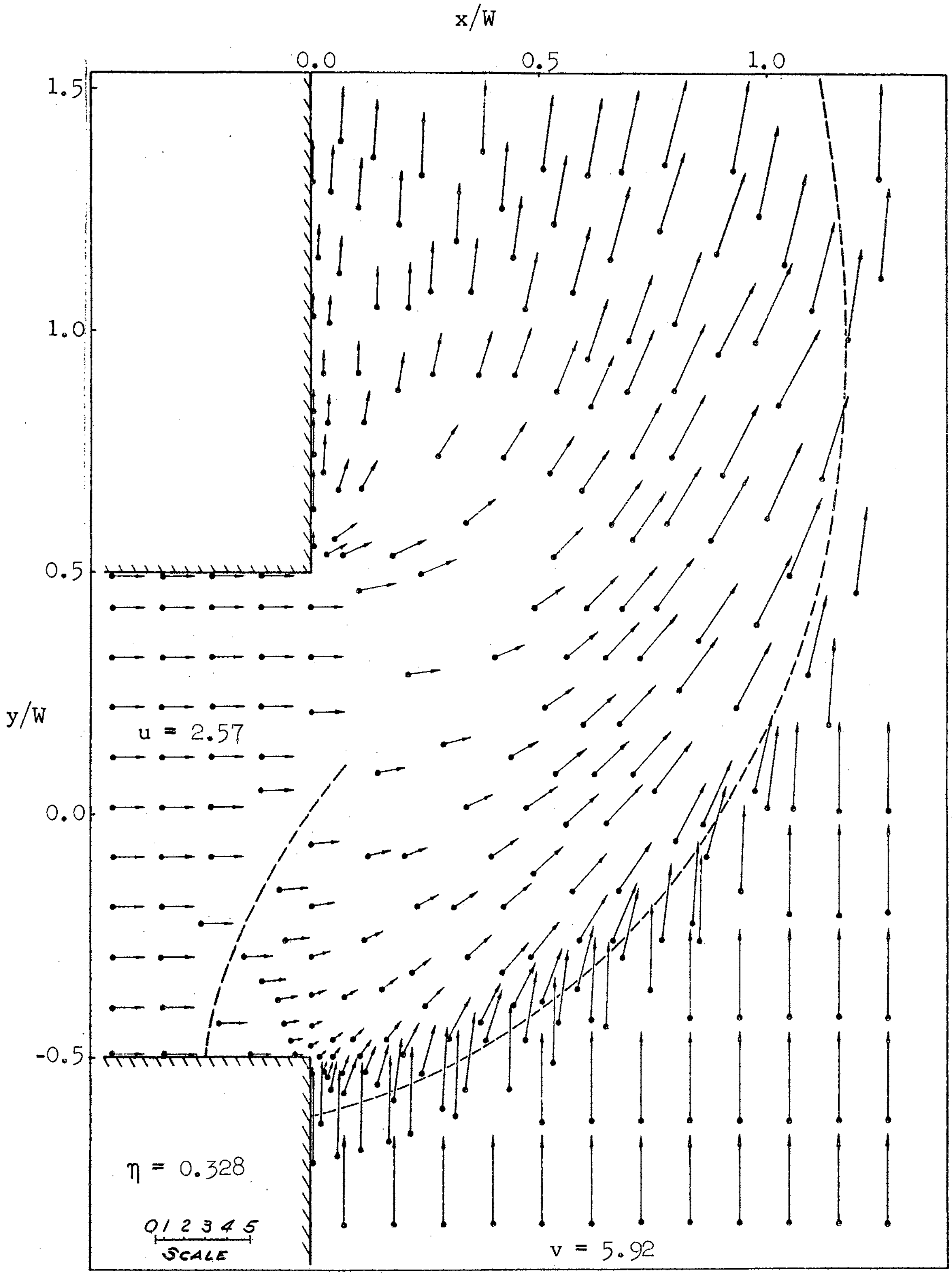

Figure 30. Particle Vector Field for a Mach 5 Crossflow.

PLATE IV

A HYDRAULIC BORE (SHOCK PRESSURE RATIO OF 10.0)
EMERGING FROM A SHOCK CHANNEL INTO A
CROSSFLOWING MEDIUM (MACH 5 FLOW)

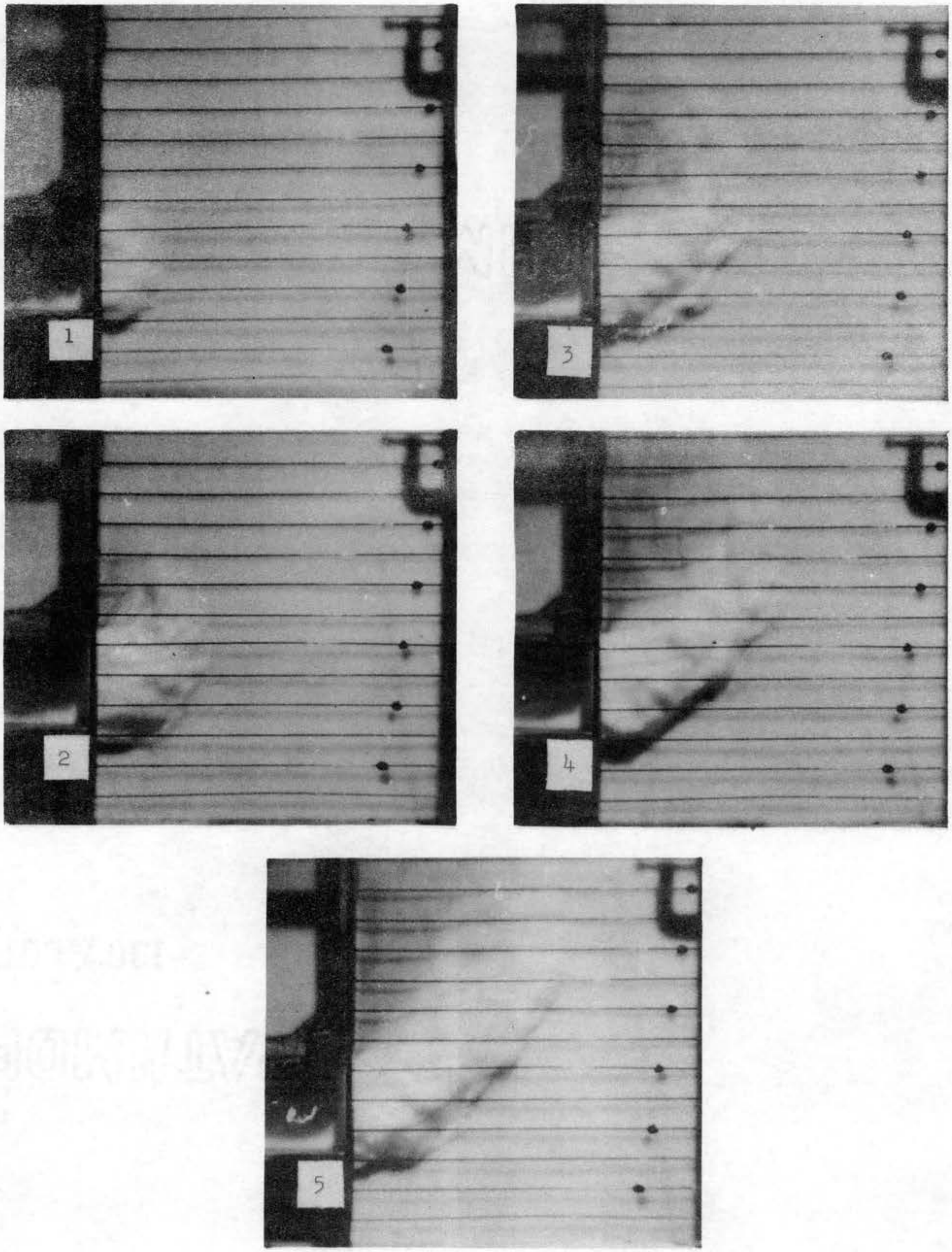
1
3
2
4
5

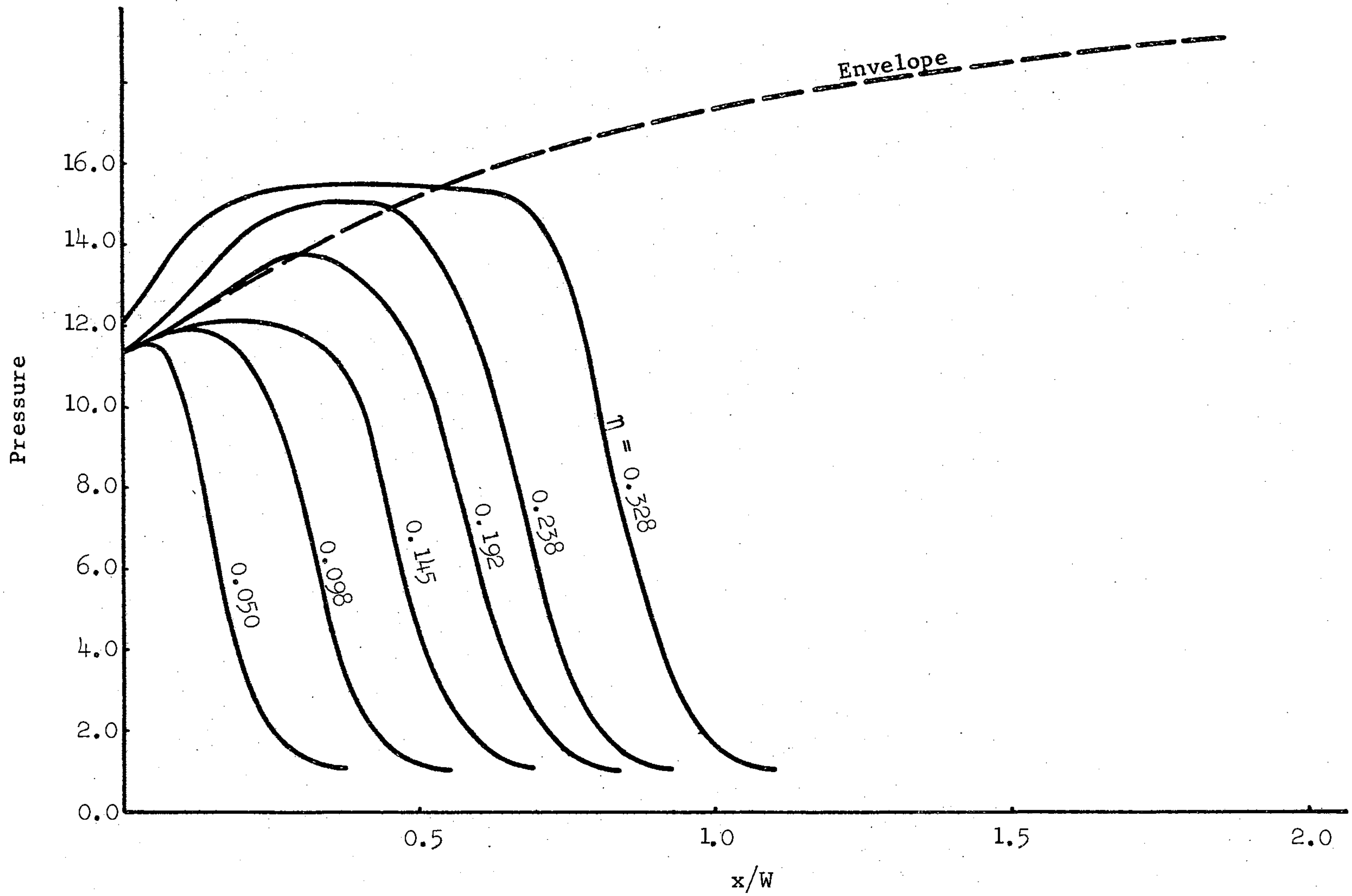

Figure 31. Pressure Distributions Along y/W = 0.0 in Mach 5 Crossflow.

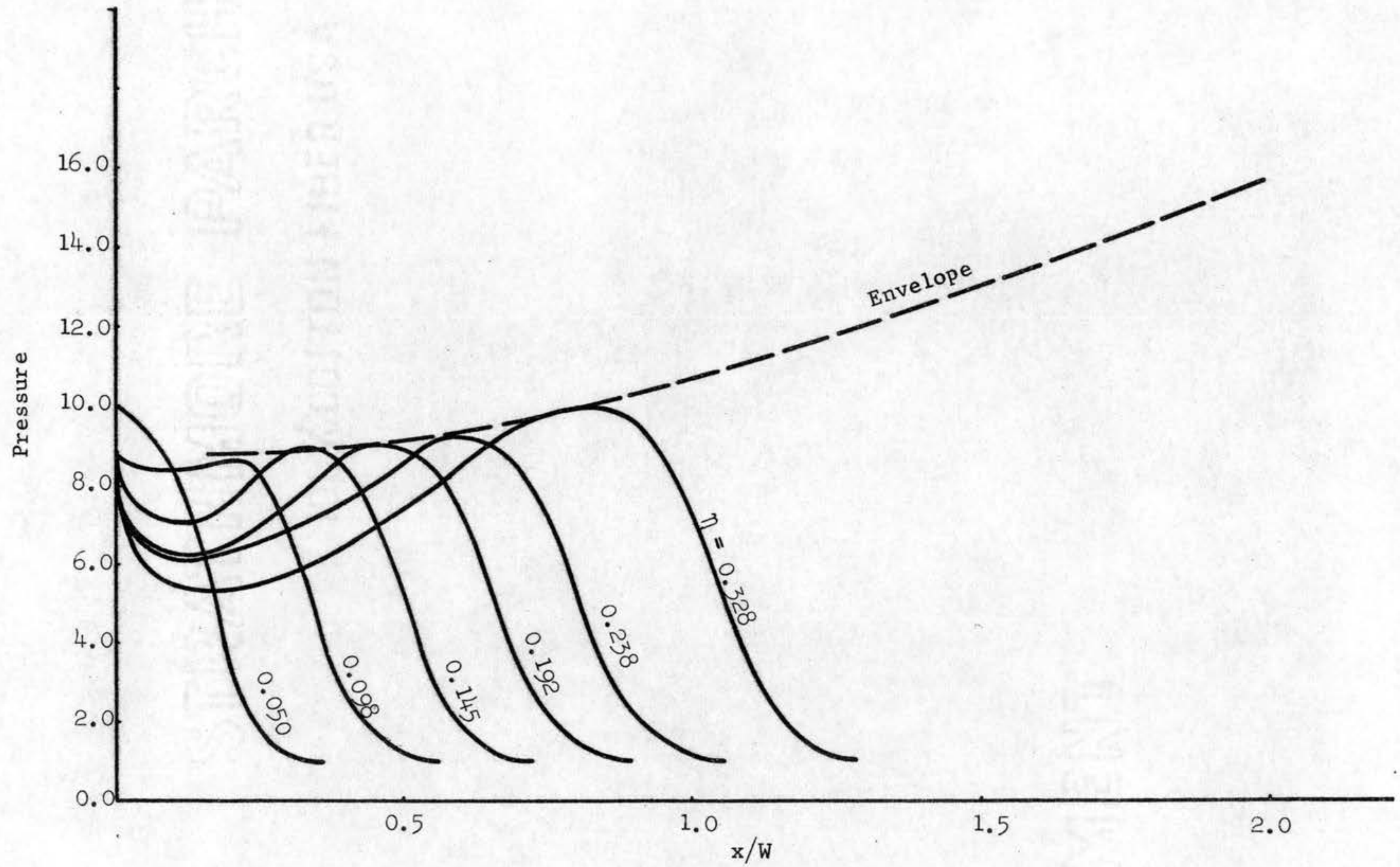

Figure 32. Pressure Distributions Along y/W = 0.5 in Mach 5 Crossflow.

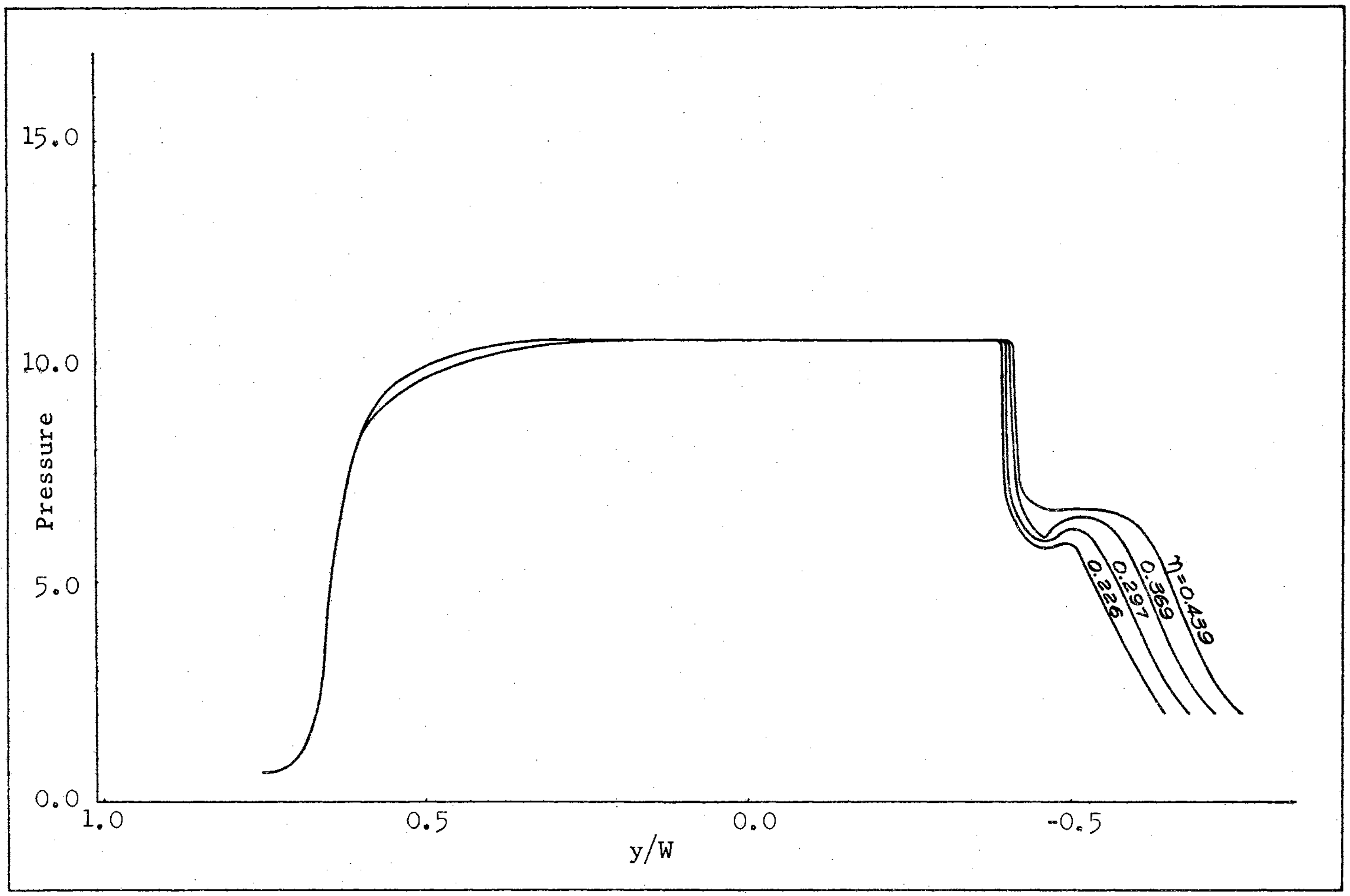

Figure 33. Exit Plane Pressure Distributions for a Mach 2 Crossflow.

plane of the shock channel (i.e., $x/W = 0.0$). The approximate shock locations for various times are given in Figure 34 and provide a better understanding of the shock shape as the shock emerges into a Mach 2 crossflow. The particle vector field in Figure 35 may also aid in understanding the flow field behind the shock. It can be seen that some particles do move upstream. The shock shapes and propagation direction seem to compare qualitatively with the corresponding hydraulic waves in Plate V. The hydraulic waves are seen to propagate faster normal to the stream than the corresponding $M = 5$ condition but not as fast downstream. These results should be expected since the energy behind shock is greater than the energy of the stream. Since the wave does propagate well into the crossflow, it seems worthwhile to check the conditions along the shock for possible blast testing simulation. From the hydraulic wave pictures it appears that a fairly uniform wave exists downstream of a line through the center of the shock channel. Therefore, the pressure distributions on the y/W lines of 0, 0.5, and 1.0 (Figures 36, 37, and 38) for different times are given to compare the shock progress along these lines. By extrapolating the envelope of the pressure distribution on these curves and comparing them (Figure 39), at an x/W value of 2.0 the y/W lines of 0.0 and 0.5 have approximately the same peak pressure value; but this does not give the time at which the shock reaches this x/W point on the two y/W lines. By considering the plot of constant pressure lines on a time versus x/W diagram for the same two y/W positions (Figures 40 and 41), the rate at which the pressure wave moves in the x/W direction is seen to be fairly uniform; and, by comparing the diagrams for the two y/W positions, the velocities of the pressure waves along the two lines are approximately the

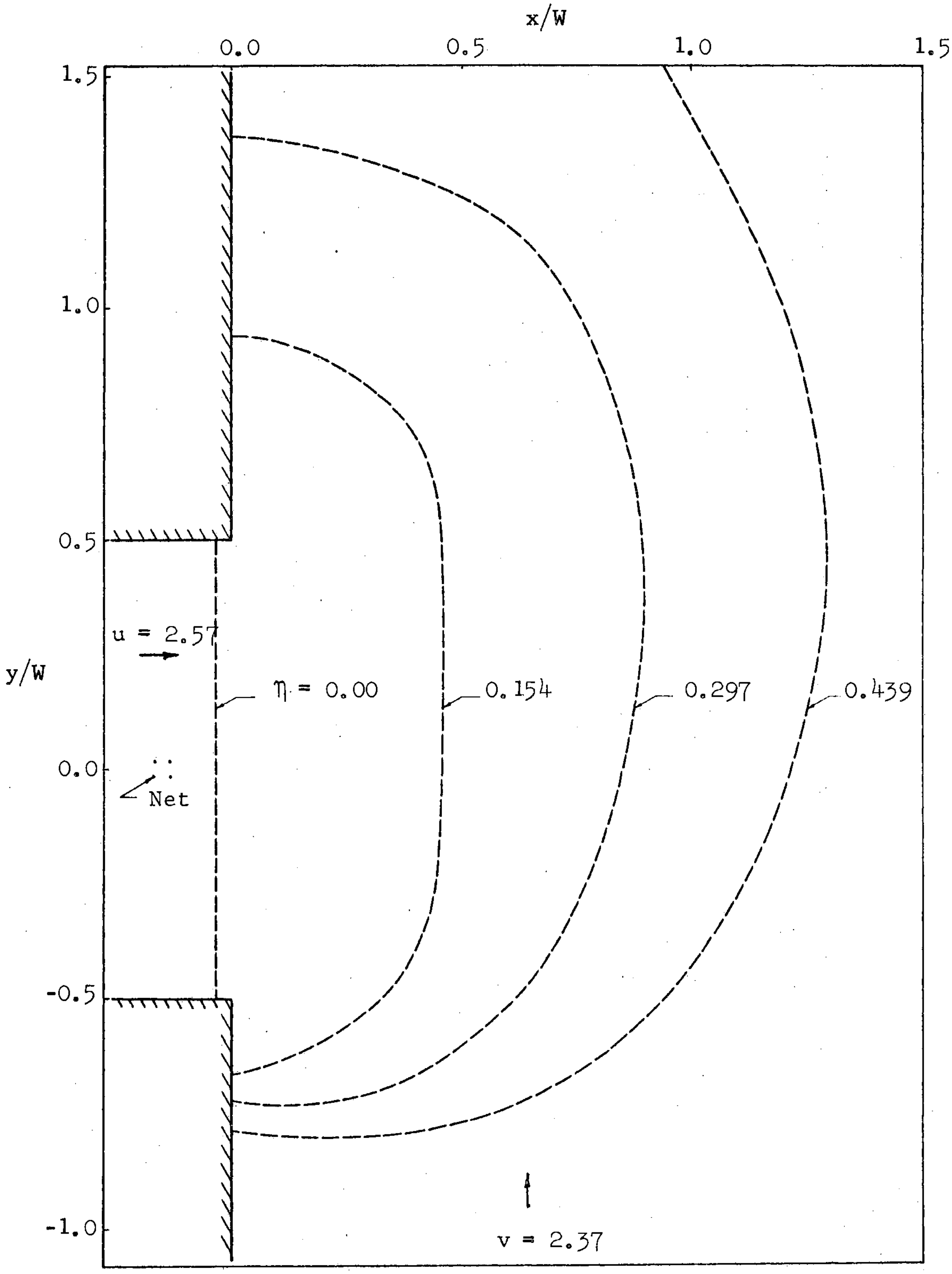

Figure 34. Shock Positions at Different Times for a Mach 2 Crossflow.

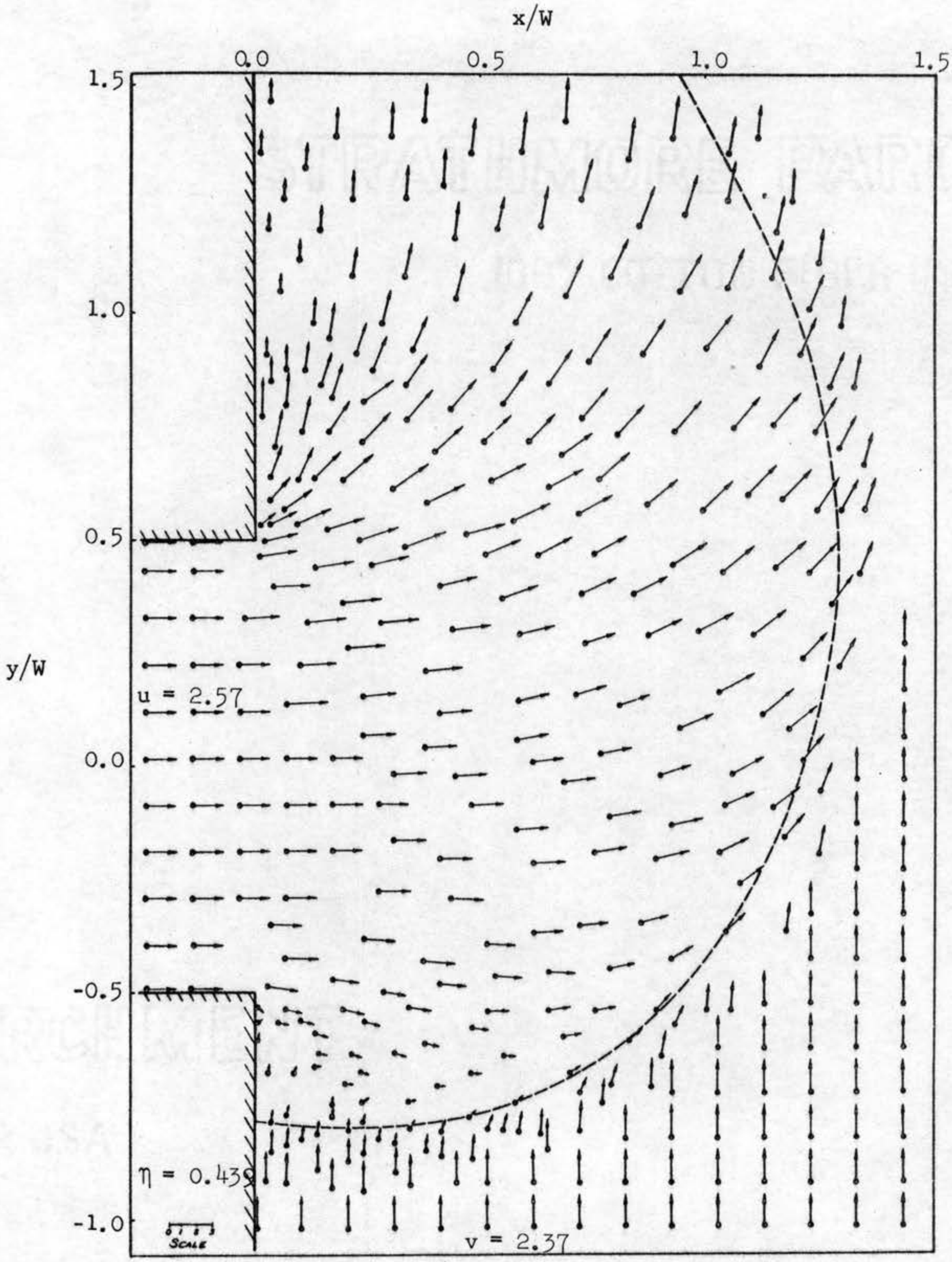

Figure 35. Particle Vector Field for a Mach 2 Crossflow.

PLATE V

A HYDRAULIC BORE (SHOCK PRESSURE RATIO OF 10.0)
EMERGING FROM A SHOCK CHANNEL INTO A
CROSSFLOWING MEDIUM (MACH 2 FLOW)

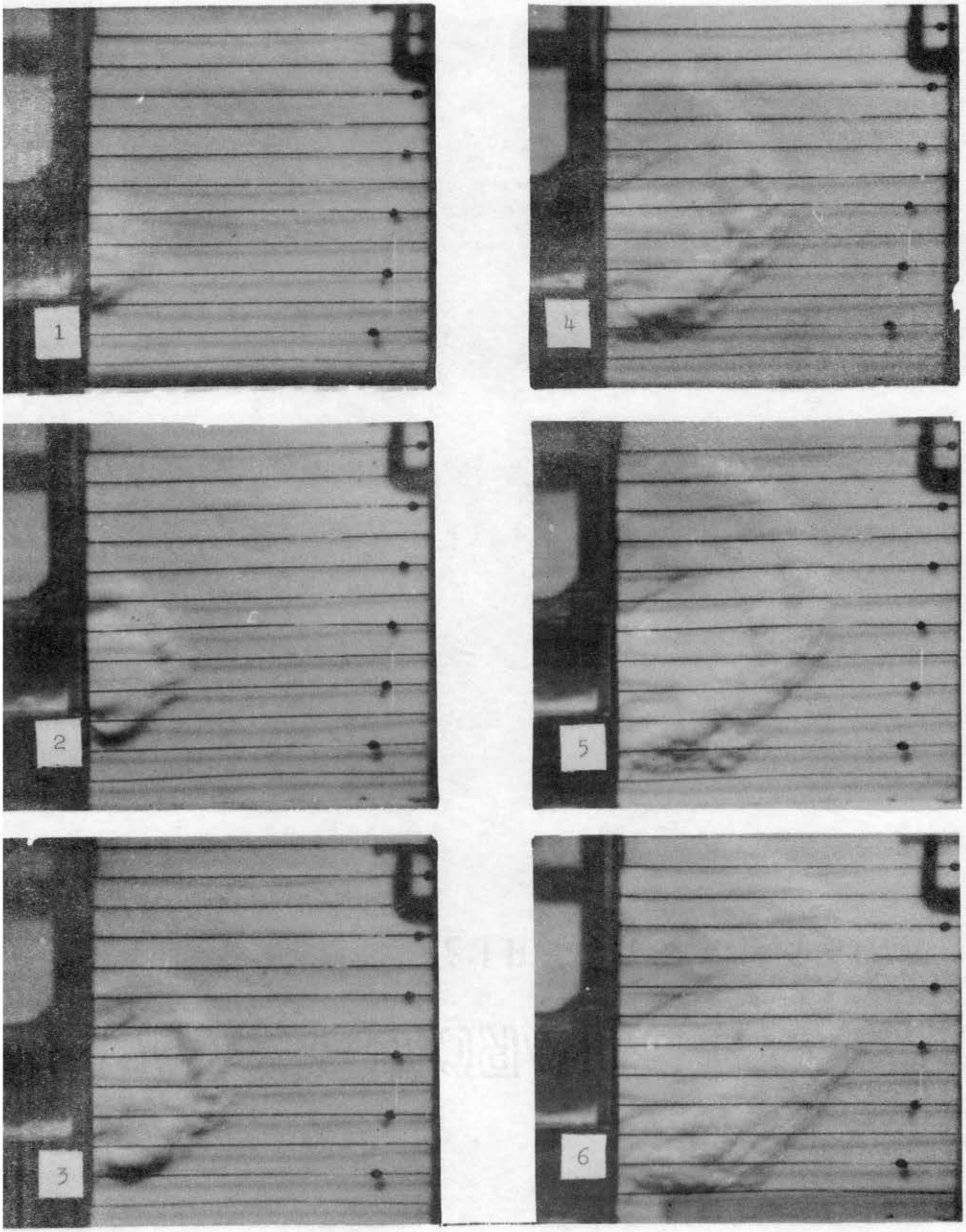
1
2
3
4
5
6

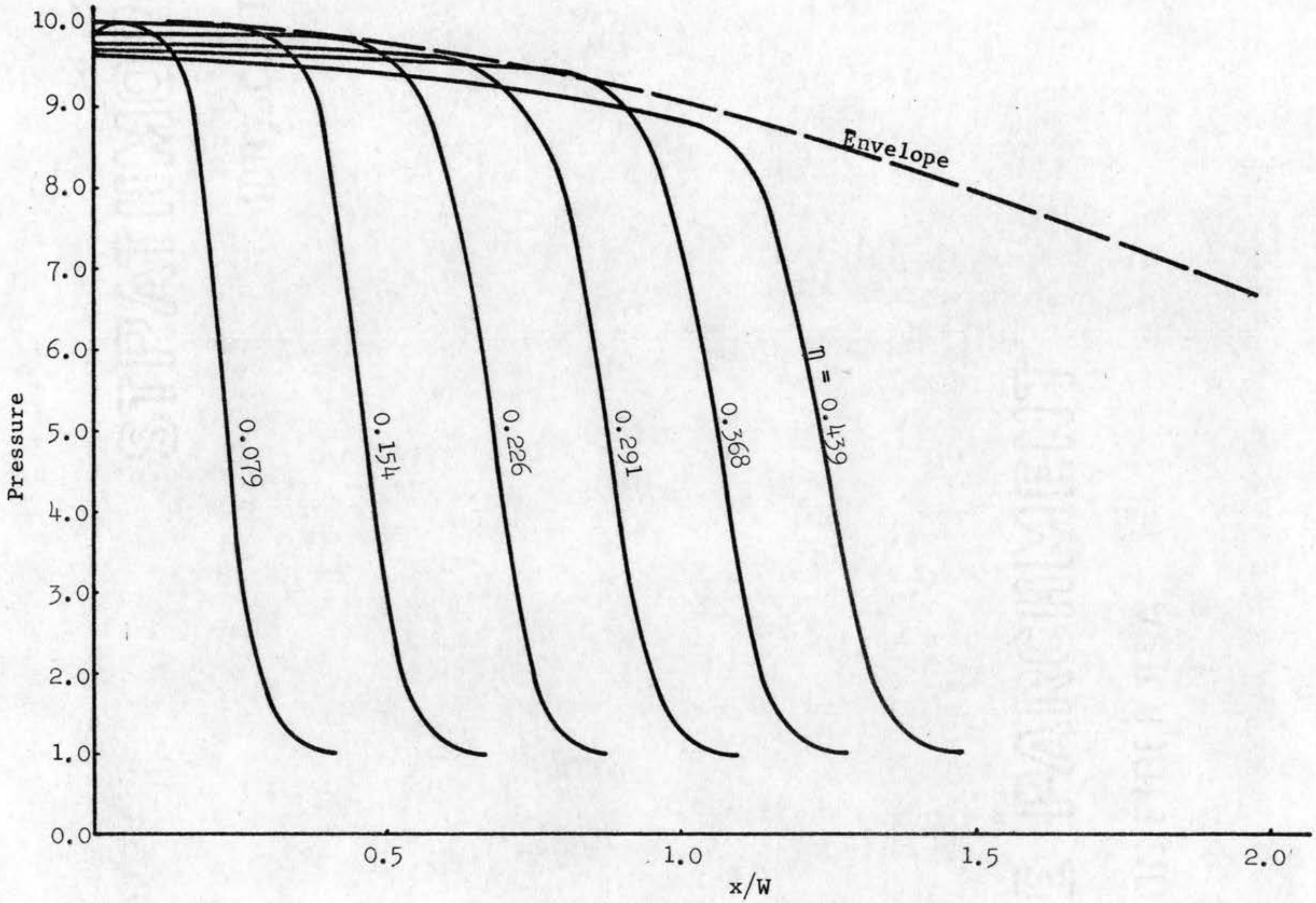

Figure 36. Pressure Distributions Along y/W = 0.0 in Mach 2 Crossflow.

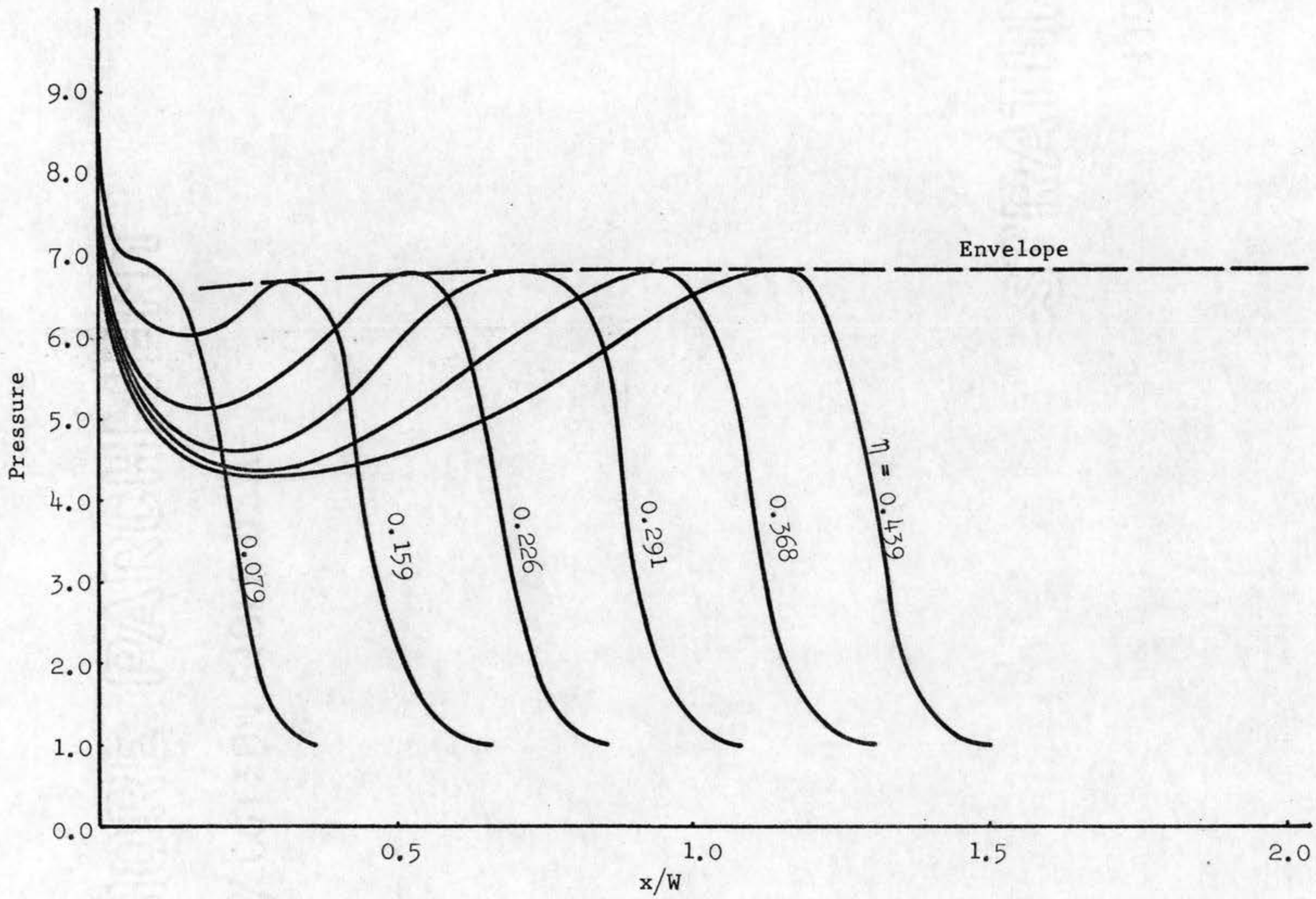

Figure 37. Pressure Distributions Along y/W = 0.5 in Mach 2 Crossflow.

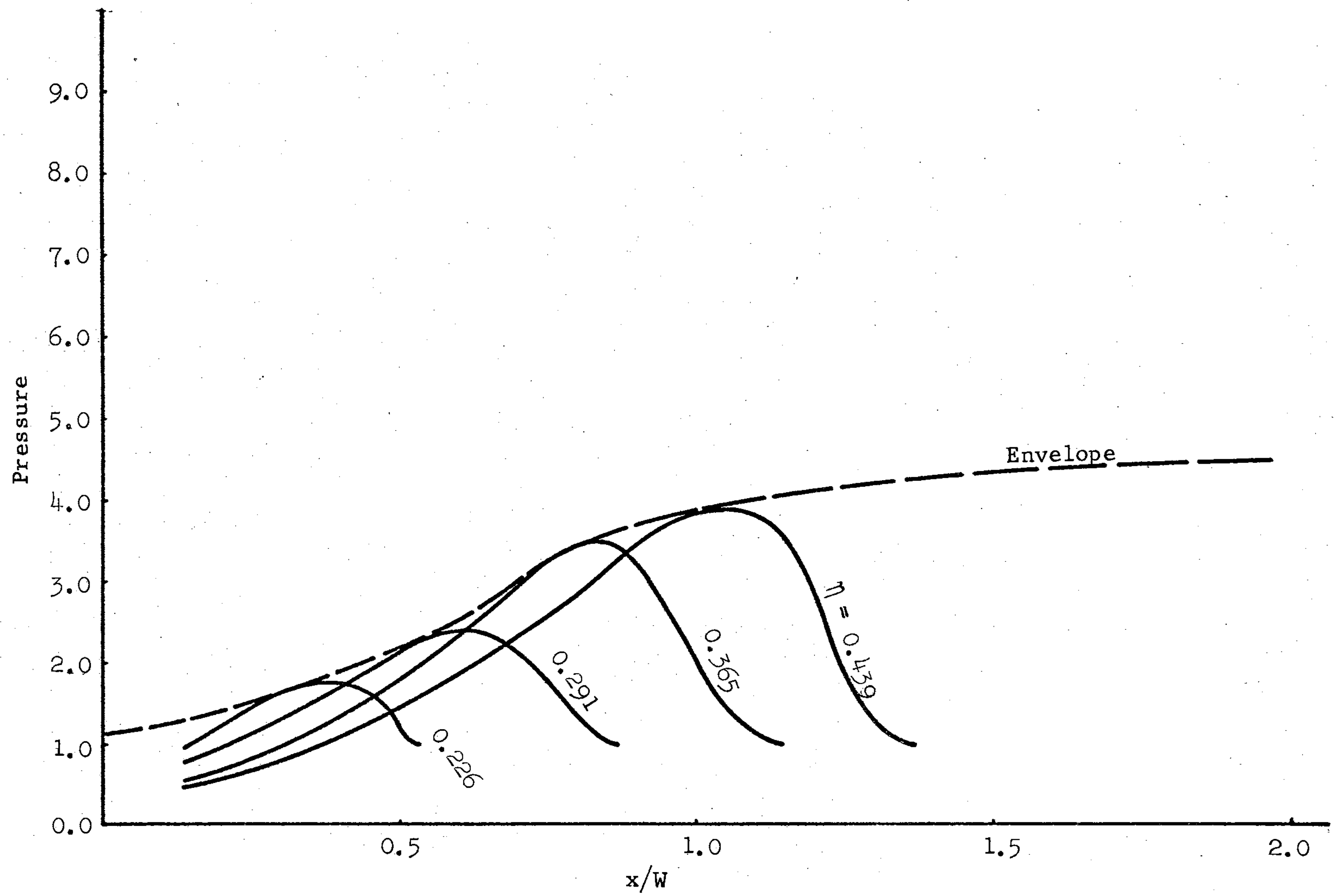

Figure 38. Pressure Distributions Along y/W = 1.0 in Mach 2 Crossflow.

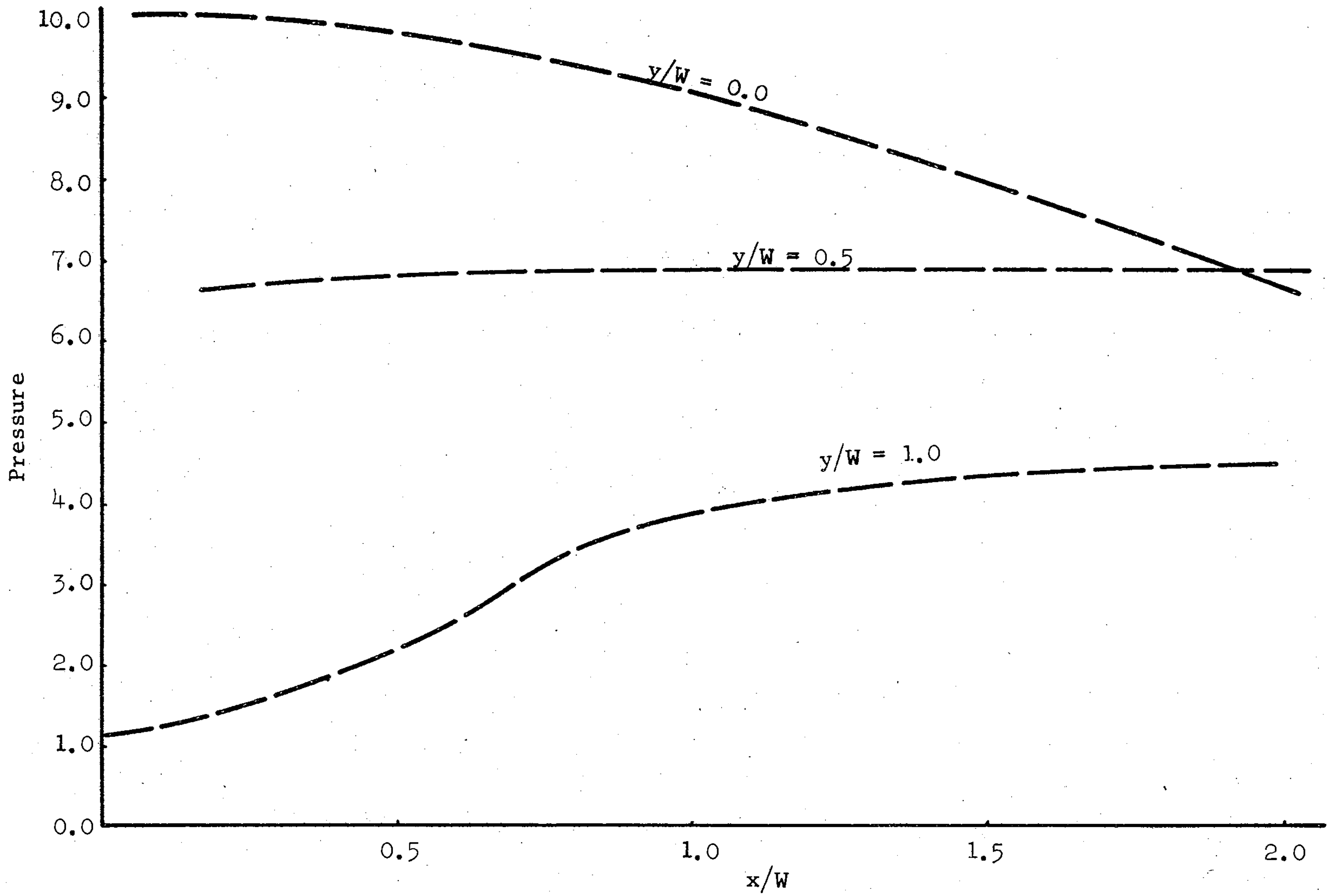

Figure 39. Envelopes of Pressure Distributions in Mach 2 Crossflow.

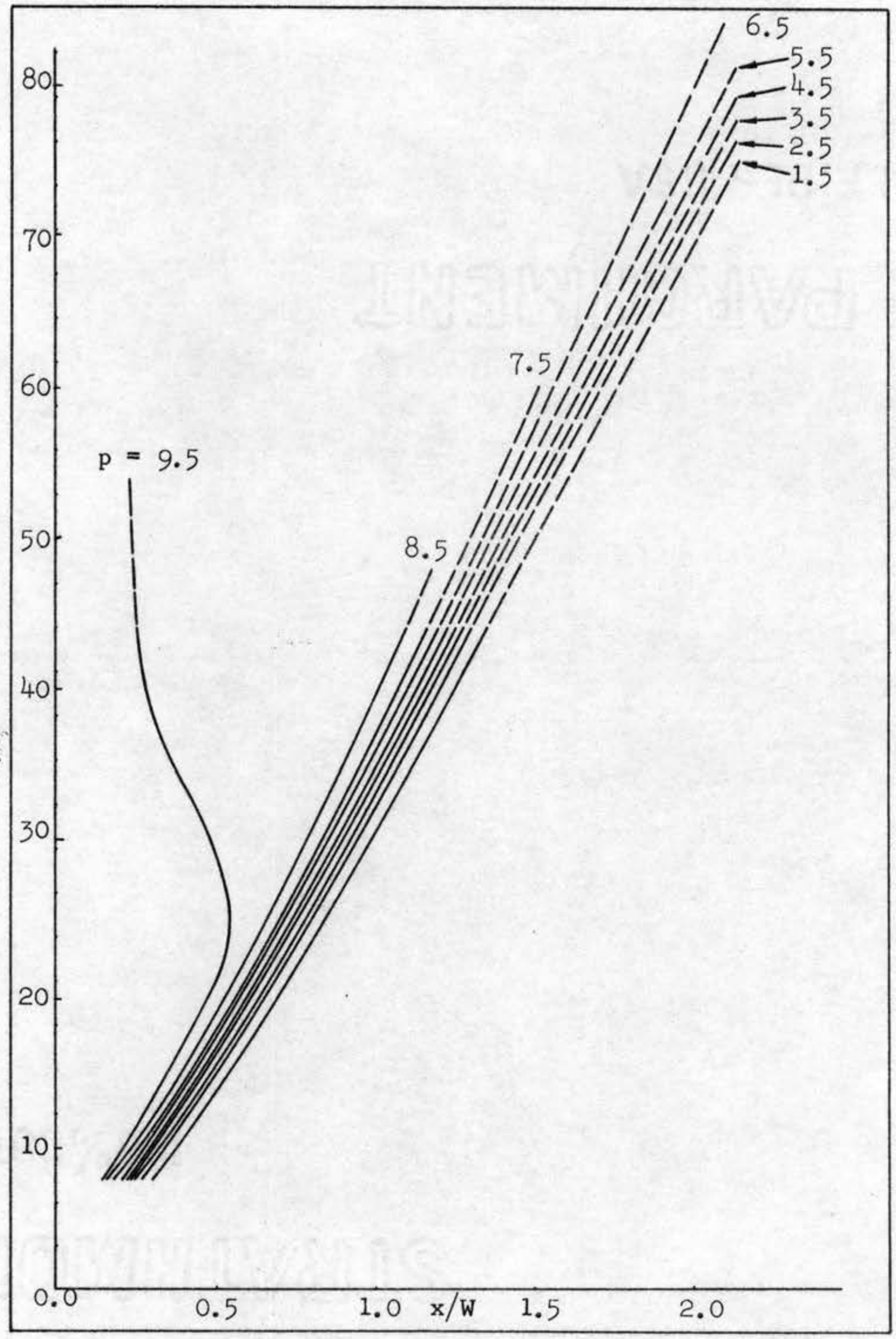

Figure 40. η versus x/W for Constant Pressure Lines Along y/W = 0.0. Mach 2 Crossflow.

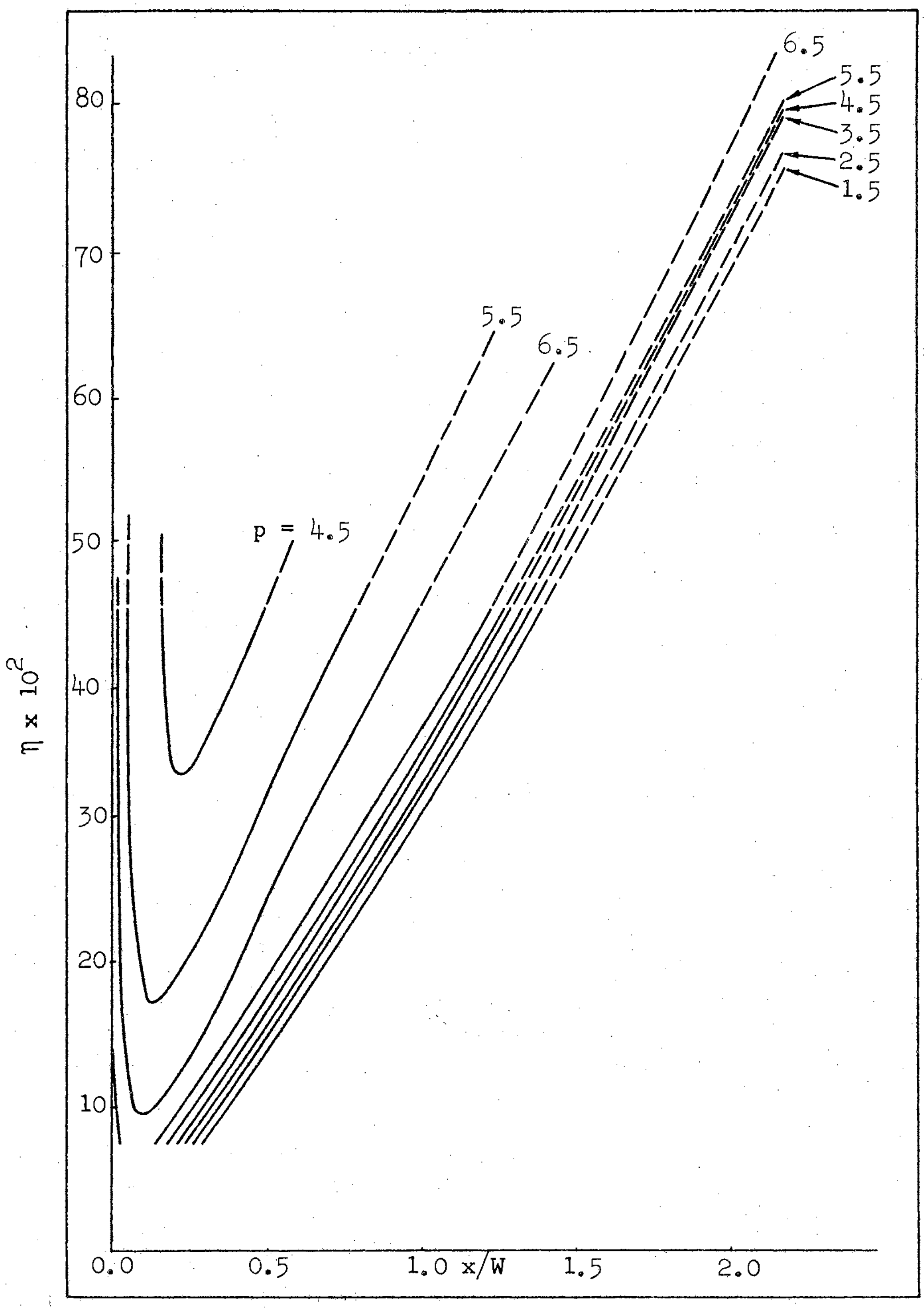

Figure 41. η Versus x/W for Constant Pressure Lines Along y/W = 0.5. Mach 2 Crossflow.

same. Again considering that the hydraulic wave moved far into the stream, the constant pressure lines are extrapolated. The extrapolated values indicate that the shock would reach the $x/W = 2$ position at approximately the same time for both y/W planes. From the discussion thus far, a portion of the shock wave appears to be fairly uniform. For blast simulation the pressure history at a point must also be considered. In Figures 42 and 43 the pressure histories at a number of locations along the two y/W lines are shown and indicate that the pressure history at a point tends to be similar to that expected for a blast wave.

From the above discussion of the two crossflow conditions, it appears that the blast simulation arrangement of a shock tube firing into a crossflowing stream may be possible within some definite limits. There seems to be no possible way of simulating a blast if the stagnation pressure of the crossflow stream is greater than that of the shock stream. For the case where the shock stream dominates the crossflow, there appears to be a given x/W position for which a portion of the shock is uniform and may be expected to give a reasonable blast simulation.

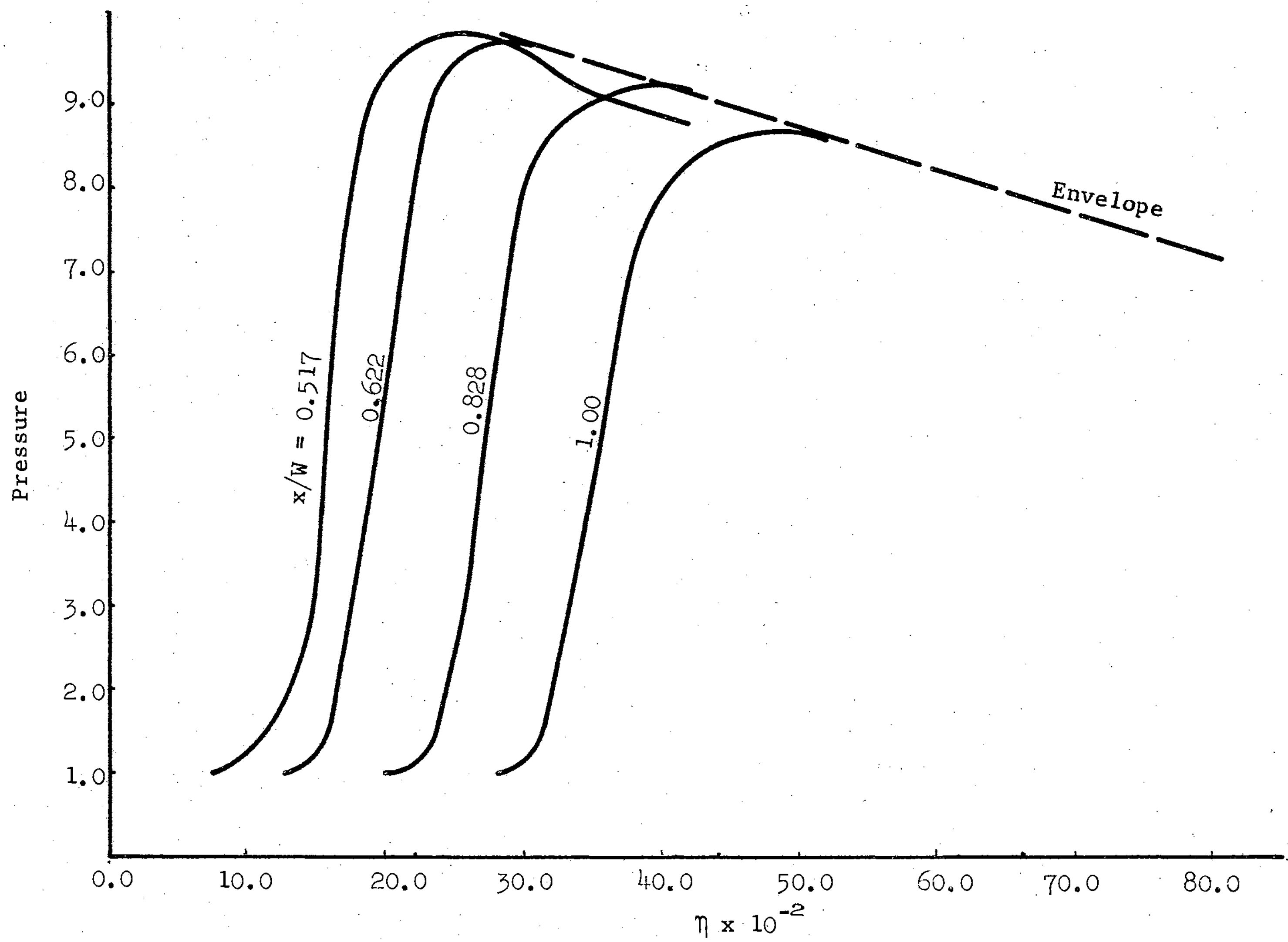

Figure 42. Pressure Time Curves on y/W = 0.0 for Mach 2 Crossflow.

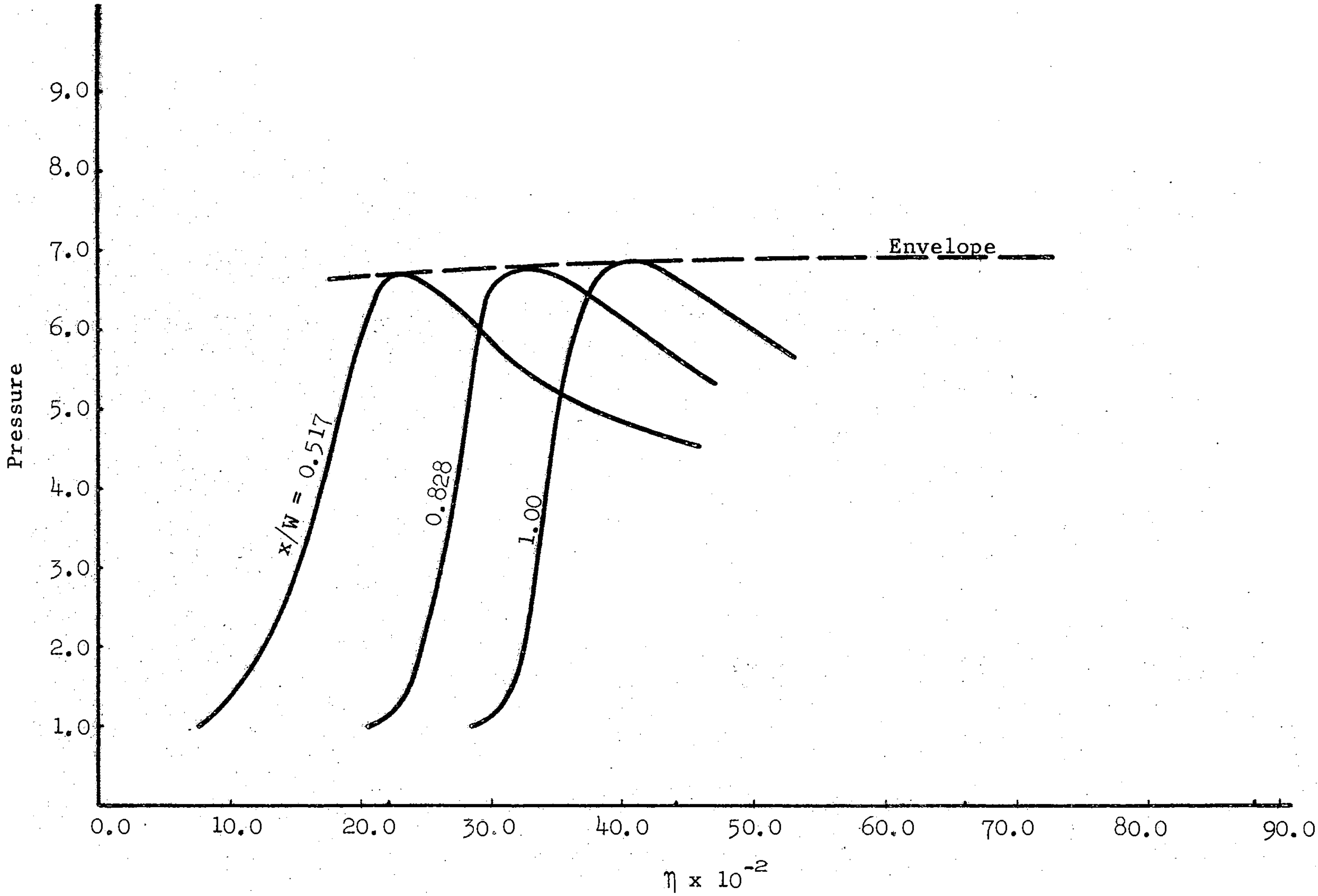

Figure 43. Pressure Time Curves on y/W = 0.5 for Mach 2 Crossflow.

CHAPTER VI

CONCLUSIONS AND RECOMMENDATIONS

Conclusions

There are two primary conclusions that may be made from this study. The first conclusion pertains to the numerical technique used to obtain the solutions for the various problems given in this study, and the second concerns the applicability of the shock tube - wind tunnel arrangement for blast simulation.

By considering the results given, the difference technique, described in Chapter IV, has been used very satisfactorily for a complex nonlinear interaction problem. There were two types of transient interactions considered: the interaction of a shock wave with a crossflowing stream, and the interaction of two supersonic streams. To the author's knowledge, no similar application has been made for such a difference technique, and no other technique is available for this problem.

From the results given in Chapter V, the conditions were established for which the shock tube - wind tunnel combination would simulate a blast. The results indicated that only for a stagnation pressure ratio (i.e., shock stream to crossflow stream) greater than unity is a blast simulation possible. For the stagnation pressure ratio greater than unity, there exists a given location at which a portion of the shock is approximately uniform and may be used for blast simulation.

Recommendations for Future Work

Three recommendations are given below for future investigation of problems connected with shock propagation from openings.

A double diaphragm shock tube has been constructed by a co-worker, Mr. Glen Lazalier, to be used as a blast producing device. Using the blast tube, an experimental study of shock propagation from both rectangular and axisymmetric openings into a still medium could be compared with the numerical results presented in this thesis.

The results presented for the two crossflow cases demonstrated the effect on given shock of a change in the crossflow condition. An additional study to determine the effect of various strength (p_2/p_1) shock waves on a given crossflow condition may be valuable and helpful in determining test conditions for an experimental investigation. It would also be helpful to obtain results for the conditions given in this thesis at greater times to establish better the shock simulation conditions and the flow fields.

It has been conjectured by Lee [26] that the contact discontinuity follows the shock closely for a strong shock. If this were true, the region directly behind the shock might be too small for desirable testing. Therefore, additional work should be done to define the flow field between the shock and contact discontinuity as they emerge from a shock tube. In connection with this work there is a need to develop a numerical technique in which a contact discontinuity is acceptably represented. In most difference schemes this type of discontinuity is too greatly diffused to define contact surface loactions.

The suggestions presented above are considered to be very important by the author. These additional studies would help to establish additional conditions for the experimentalist to use in conducting blast simulation tests.

SELECTED BIBLIOGRAPHY

1. Pierce, D., "Simulation of Blast Waves in a Supersonic Wind Tunnel," Royal Aircraft Establishment Tech. Note Aero. 2665, January 1960.

2. Merritt, D. L., and P. M. Aronson, "Study of Blast-Bow Wave Interactions in a Wind Tunnel," AIAA Paper 65-5, January 1965.

3. Von Neumann, J., "Oblique Reflection of Shocks," John von Neumann Collected Works, Vol. VI, New York: MacMillan, 1963, p. 238.

4. Lighthill, M. J., "The Diffraction of Blast I," Proc. Roy. Soc., Series A, Vol. 198, 1949, p. 454.

5. Lighthill, M. J., "The Diffraction of Blast II," Proc. Roy. Soc., Series A, Vol. 200, 1950, pp. 554.

6. Parks, E. K., "Supersonic Flow in a Shock Tube of Divergent Cross-Section," UTIA Report 18, May 1952.

7. Ting, L., and H. F. Ludloff, "Aerodynamics of Blasts," J. Aero. Sci., Vol. 19, 1952, p. 317.

8. Chester, W., "The Propagation of Shock Waves in a Channel of Non-Uniform Width," Quart. J. Mech. and Applied Math., Vol. VI, Pt. 4, 1953, p. 440.

9. Chester, W., "The Diffraction and Reflection of Shock Waves," Quart. J. Mech. and Applied Math., Vol. VII, Pt. 1, 1954, p. 57.

10. Chester, W., "The Quasi-Cylindrical Shock Tube," Phil. Mag. (7), Vol. 45, 1954, p. 1293.

11. Laporte, O., "On the Interaction of a Shock With a Constriction," Los Alamos Scientific Laboratory Report, LA-1740, 1955.

12. Whitham, G. B., "On the Propagation of Weak Shock Waves," J. Fluid Mech., Vol. 1, 1956, p. 290.

13. Chisnell, R. F., "The Motion of a Shock Wave in a Channel, With Applications to Cylindrical and Spherical Shock Waves," J. Fluid Mech., Vol. 2, 1957, p. 286.

14. Ting, L., "Diffraction of Disturbances Around a Convex Right Corner With Applications in Acoustics and Wing-Body Interference," J. Aero. Sci., Vol. 24, 1957, p. 821.

15. Whitham, G. B., "A New Approach to Problems of Shock Dynamics, Part I, Two-dimensional Problems," J. Fluid Mech., Vol. 2, 1957, p. 145.

16. Whitham, G. B., "On the Propagation of Shock Waves Through Regions of Non-uniform Area or Flow," J. Fluid Mech., Vol. 4, 1958, p. 337.

17. Sternberg, J., "Triple-Shock-Wave Intersections," The Physics of Fluids, Vol. 2, 1959, p. 179.

18. Whitham, G. B., "A New Approach to Problems of Shock Dynamics, Part II, Three-Dimensional Problems," J. Fluid Mech., Vol. 5, 1959, p. 369.

19. Bezhanov, K. A., "On the Theory of Diffraction of Shock Waves," PMM, Vol. 24, Pt. 4, 1960, p. 718.

20. Bryson, A. E., and R. W. F. Gross, "Diffraction of Strong Shock by Cones, Cylinders, and Spheres," J. Fluid Mech., Vol. 10, 1961, p. 1.

21. Filippov, I. G., "On the Theory of Diffraction of Weak Shock Waves Round Contours of Arbitrary Shape," PMM, Vol. 27, Pt. 1, 1963, p. 73.

22. Smyrl, J. L., "The Impact of a Shock-Wave on a Thin Two-dimensional Aerofoil Moving at Supersonic Speeds," J. Fluid Mech., Vol. 15, 1963, p. 223.

23. Miles, J. W., "Notes on the Diffraction of Blasts by Flying Vehicles," Aerospace Corp. Report TDR-269(4230-30)-1, August 1963.

24. Pack, D. C., "The Reflexion and Diffraction of Shock Waves," J. Fluid Mech., Vol. 15, 1963, p. 549.

25. Wolff, W. S., "Transient Flow Field Analysis Around a Conical Body Exposed to a Blast Wave," Lockheed Corp. Report LMSC No. 4-70-64-1, 1964.

26. Lee, J. D., "Some Aspects of Flight Through a Nuclear Blast and Its Laboratory Simulation," Sandia Corp. Report SC-RR-64-1781 Aerodynamics, 1965.

27. Von Neumann, J., and R. D. Richtmyer, "A Method for the Numerical Calculation of Hydrodynamic Shocks," J. Appl. Physics, Vol. 21, 1950, p. 232.

28. Courant, R., E. Isaacson, and M. Rees, "On the Solution of Nonlinear Hyperbolic Differential Equations by Finite Differences," Comm. Pur and Appl. Math., Vol. V, 1952, p. 243.

29. Lax, P., "On Discontinuous Initial Value Problems for Nonlinear Equations and Finite Difference Schemes," LAMS-1332, 1953.

30. Fox, L., Numerical Solution of Ordinary and Partial Differential Equations, Addison Wesley, Reading, Massachusetts, 1962.

31. Ludford, G., H. Polachek, and R. J. Seeger, "On Unsteady Flow of Compressible Viscous Fluids," J. Appl. Physics, Vol. 24, No. 4, 1953.

32. Lax, P., "Weak Solutions of Nonlinear Hyperbolic Equations and Their Numerical Computation," Comm. Pure and Appl. Math., Vol. VII, 1954, p. 159.

33. Ludloff, H. F., and M. B. Friedman, "Aerodynamics of Blasts - Diffraction of Blast Around Finite Corners," J. Aero. Sci., Vol. 22, 1955, p. 27.

34. Ludloff, H. F., and M. B. Friedman, "Difference Solution of Shock Diffraction Problem," J. Aero. Sci., Vol. 22, 1955, p. 139.

35. Payne, R. B., "A Numerical Method for a Converging Cylindrical Shock," J. Fluid Mech., Vol. II, 1957, p. 185.

36. Godunov, S. K., "A Difference Method for the Numerical Calculation of Discontinuous Solutions of Hydrodynamic Equations," Mathematicheskii Sbornik, Vol. 47, No. 3, 1959, p. 271.

37. Lax, P., and B. Wendroff, "Systems of Conservation Laws," Comm. Pure and Appl. Math, Vol. XIII, 1960, p. 217.

38. Rusanov, V. V., "The Calculation of the Interaction of Non-Stationary Shock Waves and Obstacles," National Research Council of Canada Library, Ottowa, Canada, Tech. Translation 1027 by D. A. Sinclair, 1962. Translated From: Zhurnal Vychislitelnoi Fiziki, (Akademiya Nauk, SSSR 1, Vol. 1, No. 2, 1961, p. 267.

39. Makino, R. C., "A Method for Computing the Interaction of Two Spherical Blast Waves," BRL Memo 1462, 1963.

40. Harlow, F. H., "The Particle-In-Cell Method for Numerical Solution of Problems in Fluid Dynamics," Proc. Symposia In Applied Math., Vol. XV, 1963, p. 269.

41. Crocco, L., "Solving Numerically the Navier-Stokes Equations," General Electric Document No. 63SD891, 1964.

42. Burstein, S. Z., "Numerical Methods in Multidimensional Shocked Flows," AIAA, Vol. 2, No. 12, 1964, p. 2111.

43. Bohachevsky, I. O., E. L. Rubin, and R. E. Mates, "A Direct Method for Computation of Nonequilibrium Flows With Detached Shock Waves," AIAA Paper 65-24, 1965.

44. Bingham, G. J., and T. E. Davidson, "Investigation of Simulation of Shock-Shock Interaction in Hypersonic Gasdynamic Test Facility," Wright-Patterson Air Force Base Tech. Report FDL-TDR-64-9, 1964.

45. Ames Research Staff, "Equations, Tables, and Charts for Compressible Flow," NACA Report 1135, 1953.

46. Jeffery, A., and T. Taniuti, Non-Linear Wave Propagation, Academic Press, New York, 1964.

47. Courant, R., and D. Hilbert, Methods of Mathematical Physics, Vol. 2, Interscience, New York, 1962.

48. Godunov, S. K., "The Problem of a Generalized Solution in the Theory of Quasilinear Equations and in Gas Dynamics," Russian Mathematical Surveys, Vol. 17, No. 3, 1962, p. 145.

49. Lax, P., "Hyperbolic Systems of Conservation Laws II," Comm. Pure and Appl. Math., 1957, p. 537.

50. Hopf, E., "The Partial Differential Equation $U_t + UU_x = \mu U_{xx}$," Comm. Pure and Appl. Math., Vol. 3, 1950, p. 201.

51. Godunov, S. K., "On the Concept of Generalized Solution," Soviet Mathematics, Vol. 134, 1964, p. 1194.

52. Oleninik, O. A., "Construction of a Generalized Solution of the Cauchy Problem for a Quasi-Linear Equation of First Order by the Introduction of Vanishing Viscosity," American Mathematical Society Translations, Vol. 33, Series 2, 1963, p. 277.

53. Douglis, Avron, "The Continuous Dependence of Generalized Solutions of Nonlinear Partial Differential Equations Upon Initial Data," Comm. Pure And Appl. Math., Vol. 14, 1961, p. 267.

54. Shapiro, A. H., The Thermodynamics of Compressible Fluid Flow, Vol. I, Ronald, New York, 1953.

55. Liepmann, H. W., and A. Roshko, Elements of Gasdynamics, John Wiley and Sons, Inc., New York, 1957.

APPENDIX A

PLOTTED COMPUTER RESULTS

The results from both the still and crossflow computer programs are presented in this appendix as field graphs. The still program results are given for constant pressure and constant velocity modulus lines. For each initial pressure condition, the results are presented as a set containing an η versus time plane number graph with constant pressure line and constant velocity modulus line plots. The crossflow results are presented similarly with the addition of a constant density line graph at the end of each set of results. The results for the different initial conditions are presented in the following order:

Still Problem Results

1. Plane Geometry - Shock Pressure Ratio 4.0
2. Plane Geometry - Shock Pressure Ratio 10.0
3. Axisymmetric Geometry - Shock Pressure Ratio 10.0

Crossflow Problem Results

1. Mach 5.0 Crossflow.
2. Mach 2.0 Crossflow.

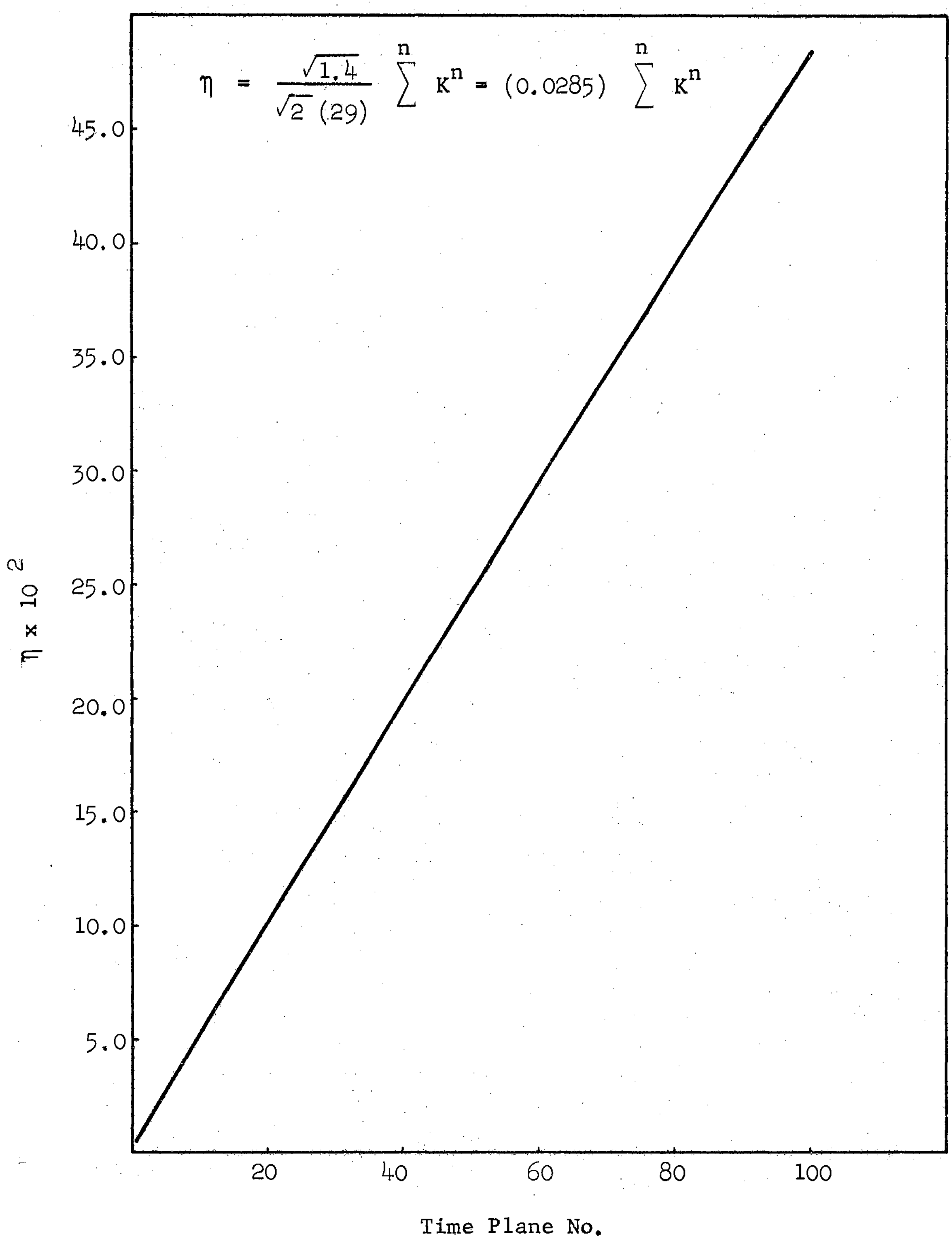

Figure 44. η Versus Time Plane Number for Still-Plane Geometry. Initial Shock Pressure Ratio - 4.0.

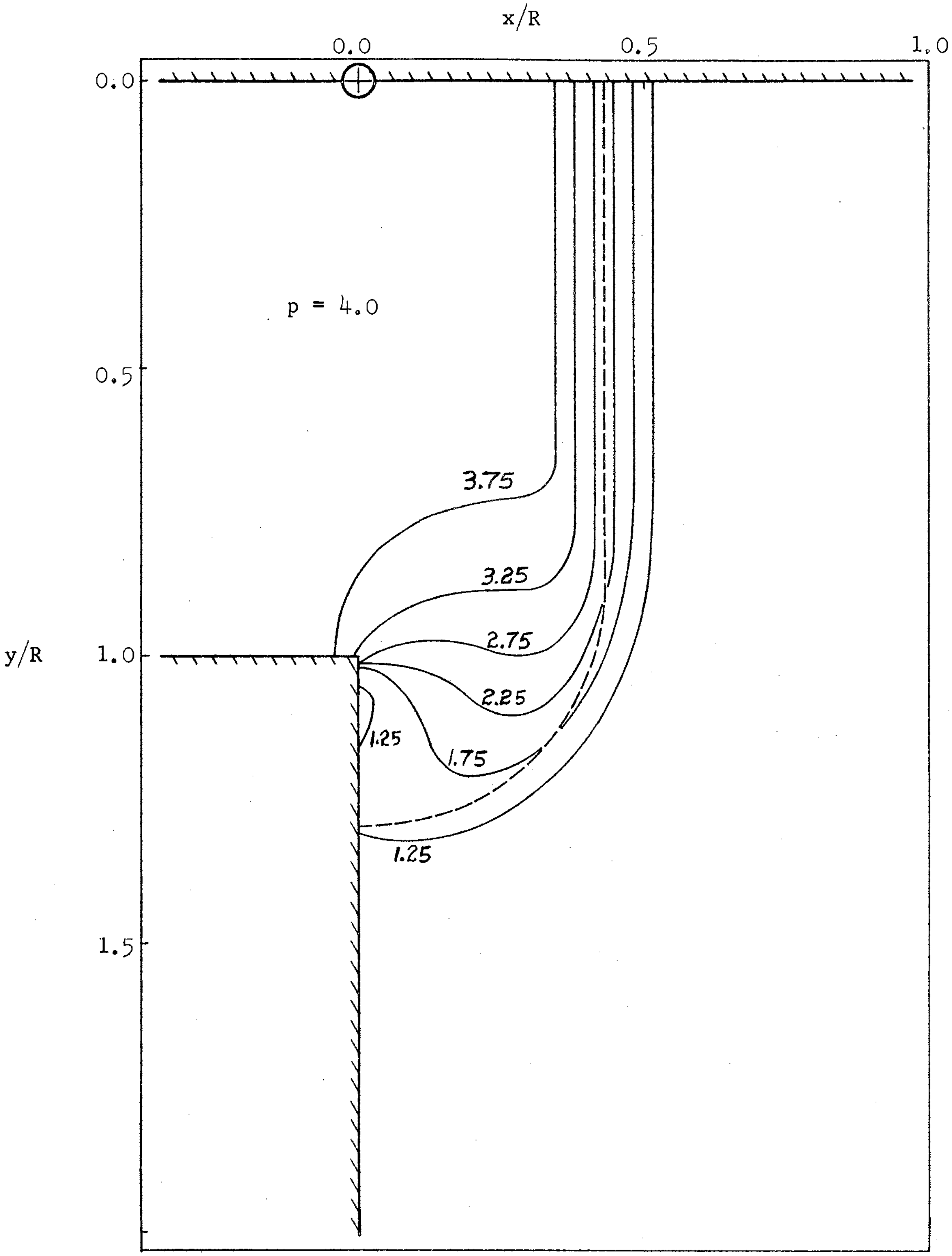

Figure 45. Constant Pressure Lines for $\eta = 0.247$ in Plane Geometry. Initial Shock Pressure Ratio - 4.0.

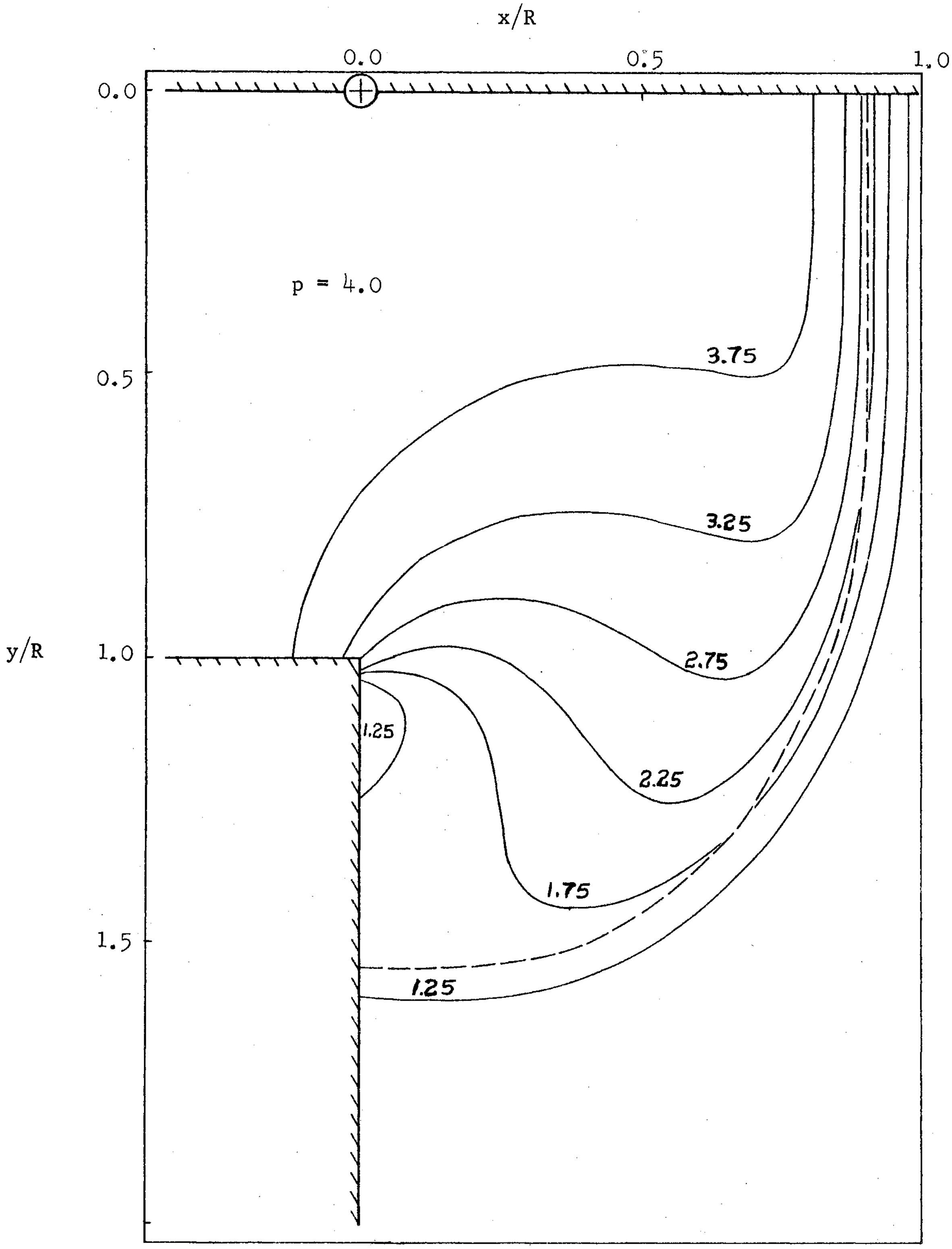

Figure 46. Constant Pressure Lines for η = 0.485 in Plane Geometry. Initial Shock Pressure Ratio - 4.0.

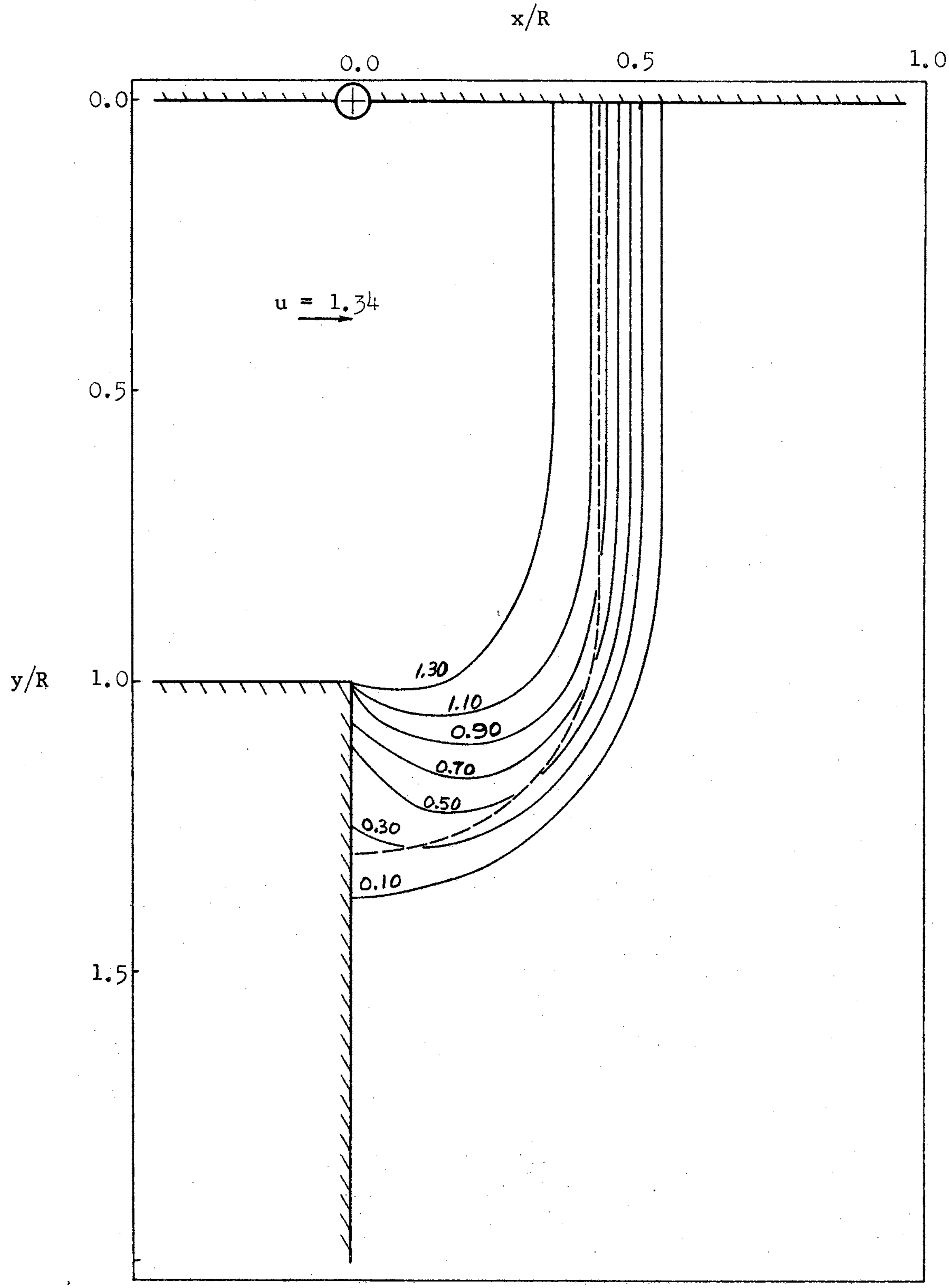

Figure 47. Constant Velocity Modulus Lines for η = 0.247 in Plane Geometry. Initial Shock Pressure Ratio - 4.0.

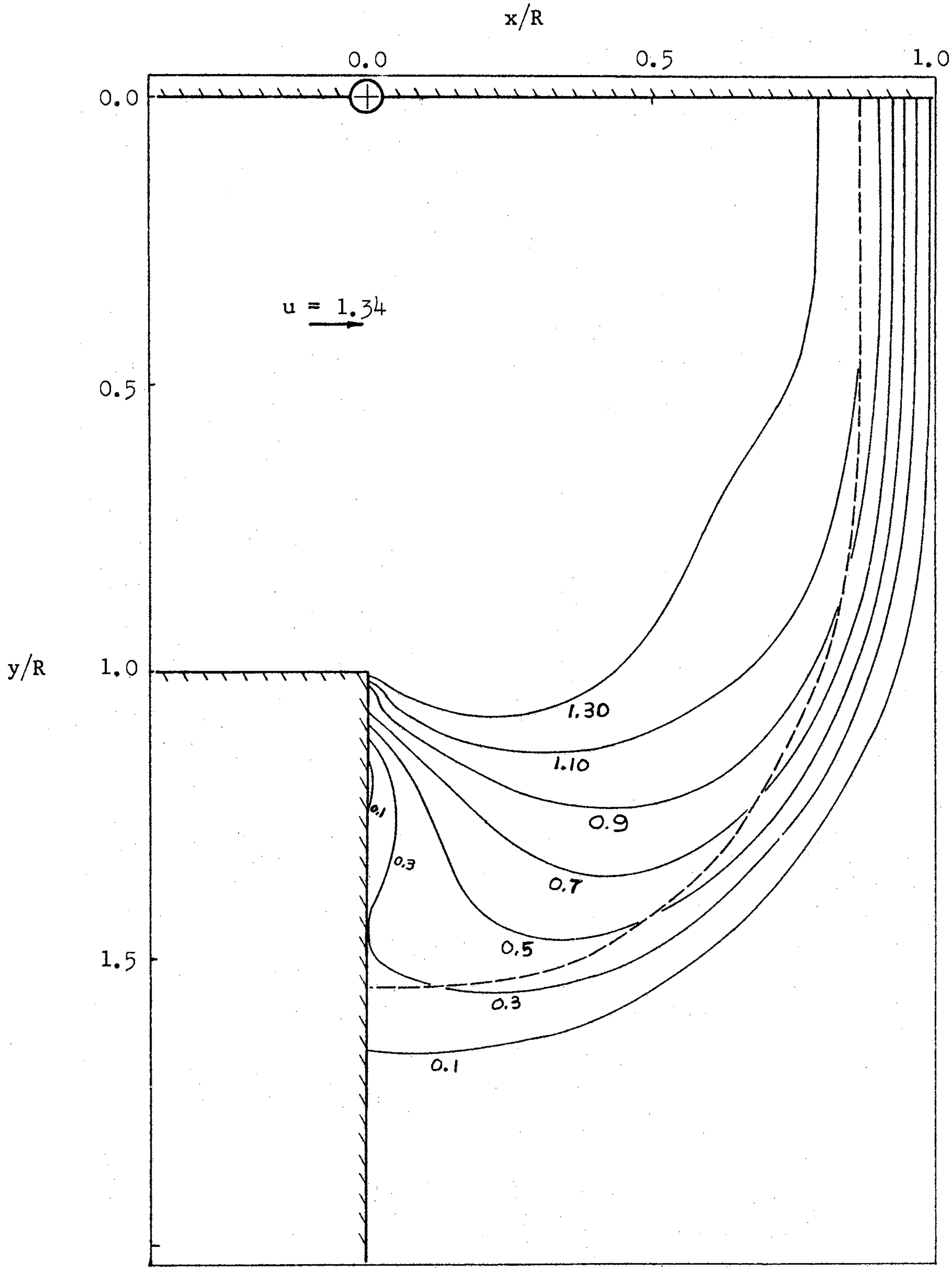

Figure 48. Constant Velocity Modulus Lines for η = 0.485 in Plane Geometry. Initial Shock Pressure Ratio - 4.0.

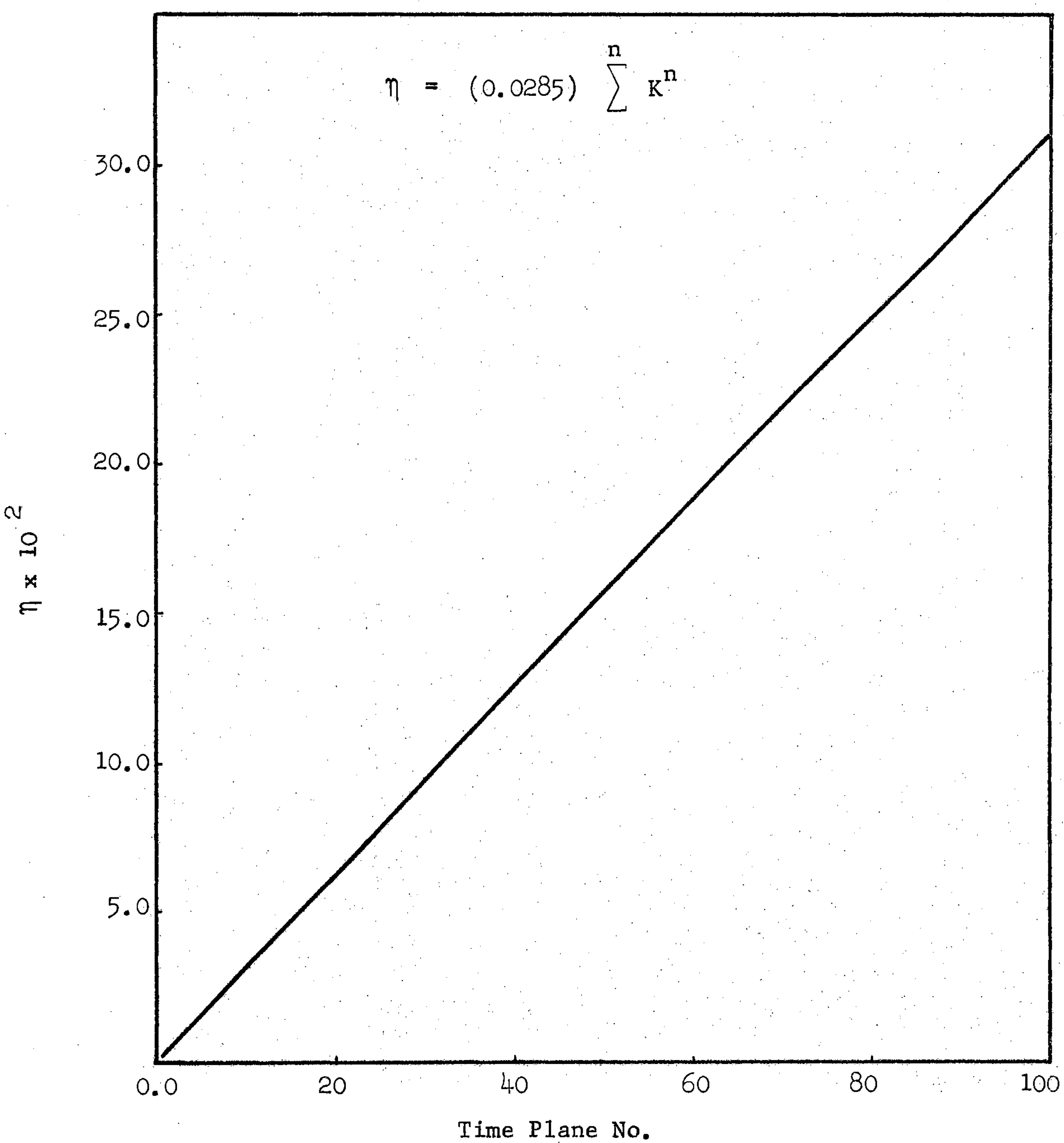

Figure 49. η Versus Time Plane Number for Still-Plane Geometry. Initial Shock Pressure Ratio - 10.0.

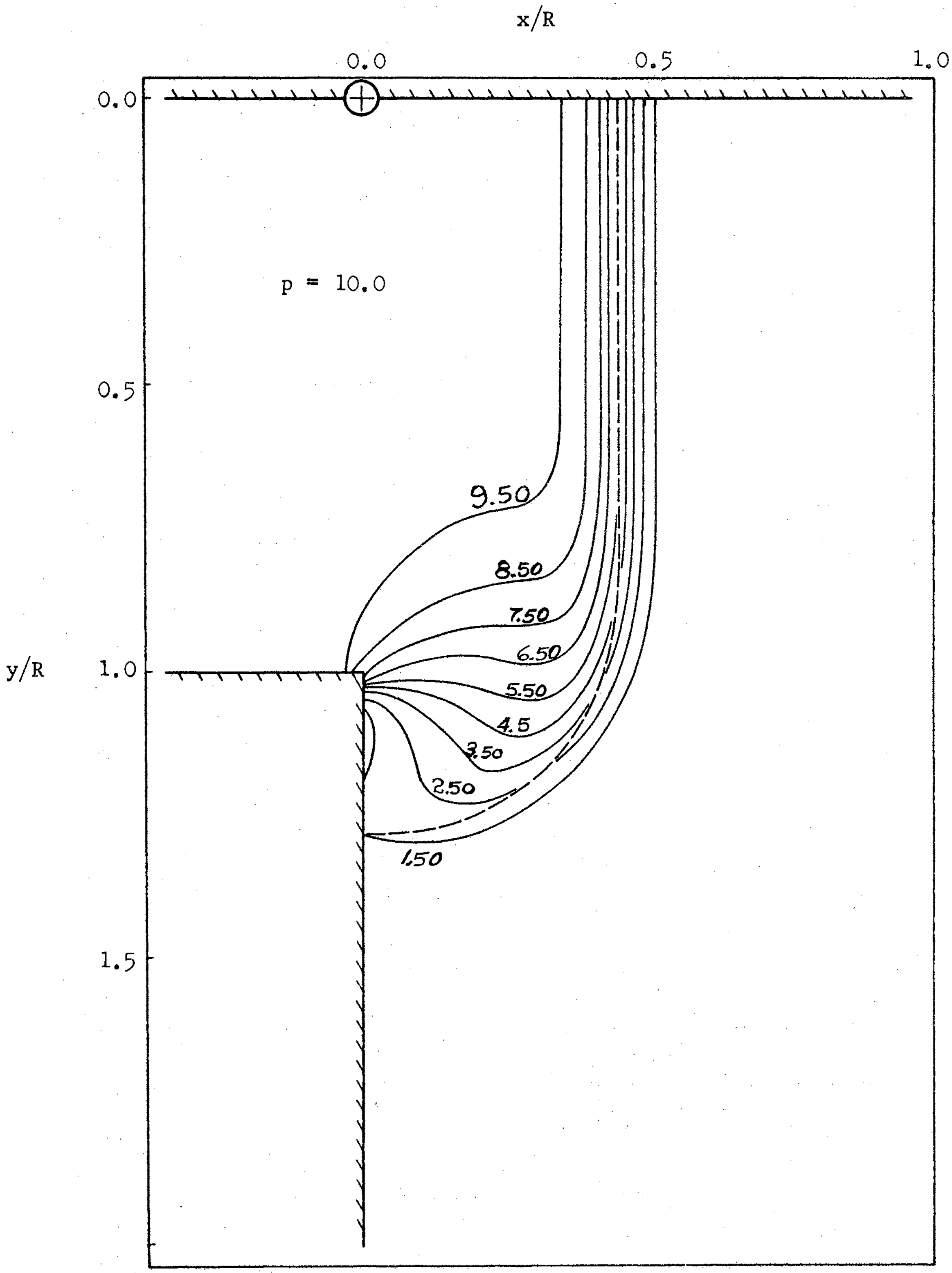

Figure 50. Constant Pressure Lines for η = 0.157 in Plane Geometry. Initial Shock Pressure Ratio - 10.0.

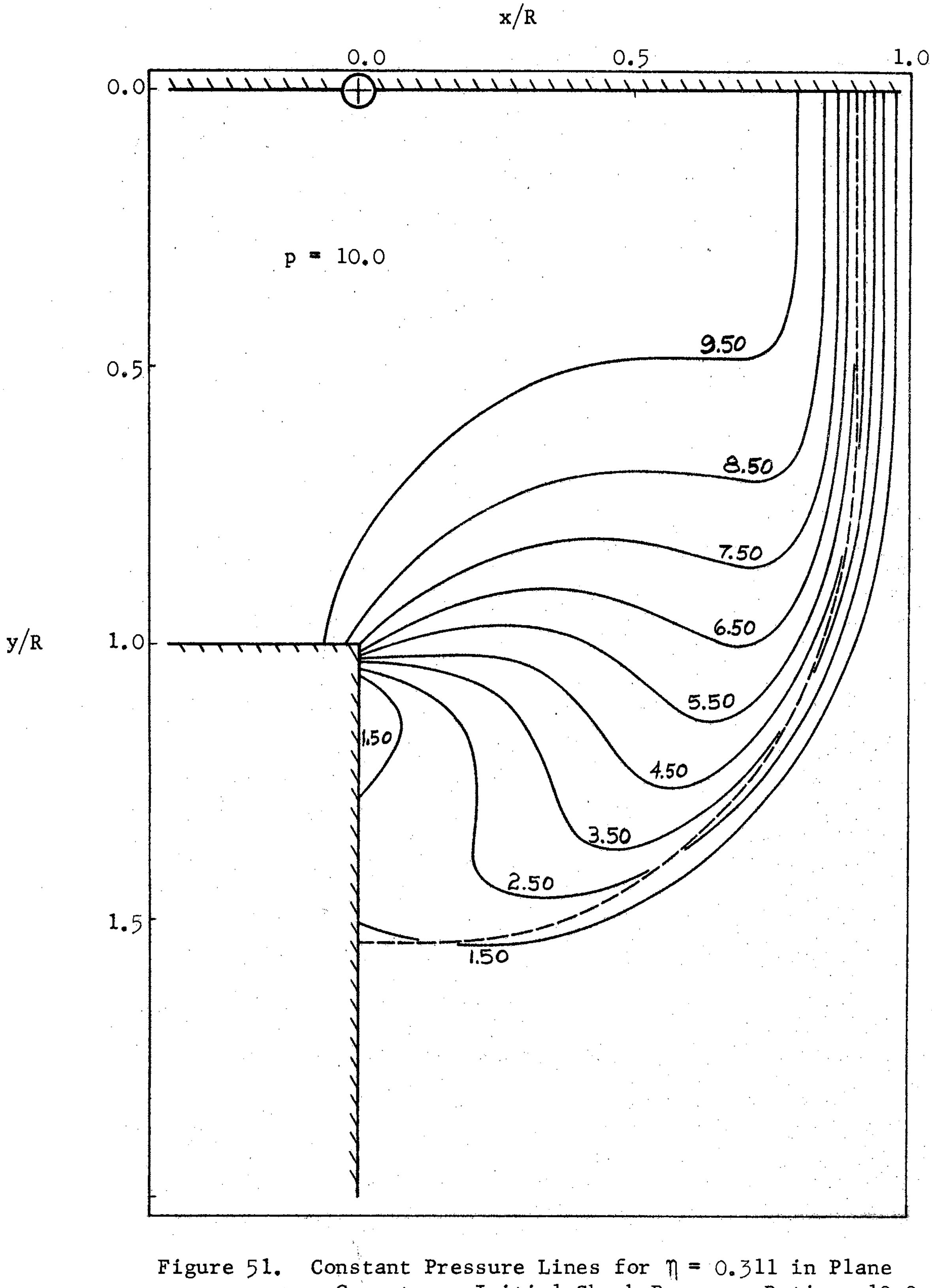

Figure 51. Constant Pressure Lines for η = 0.311 in Plane Geometry. Initial Shock Pressure Ratio - 10.0.

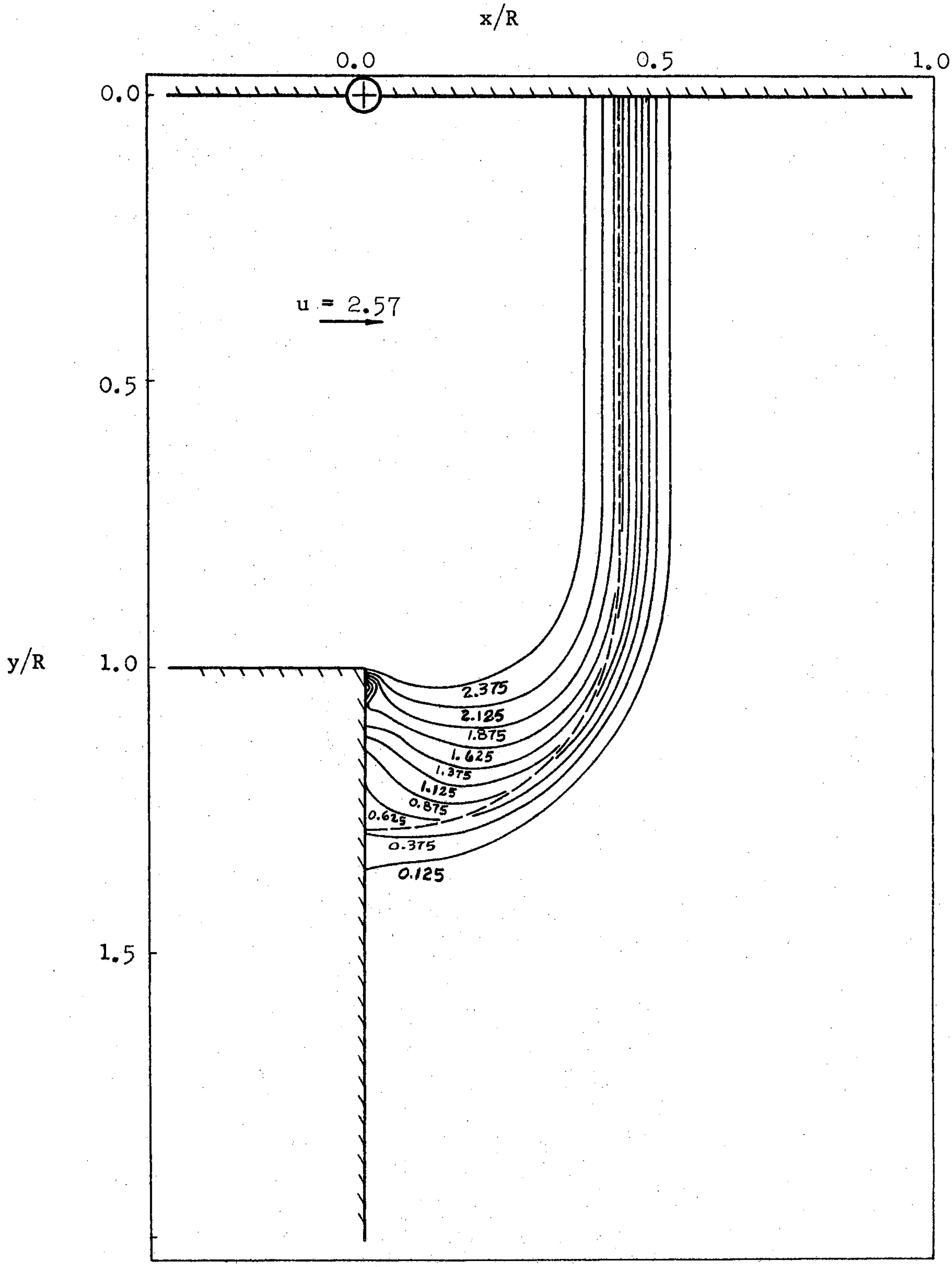

Figure 52. Constant Velocity Modulus Lines for $\eta = 0.157$ in Plane Geometry. Initial Shock Pressure Ratio - 10.0.

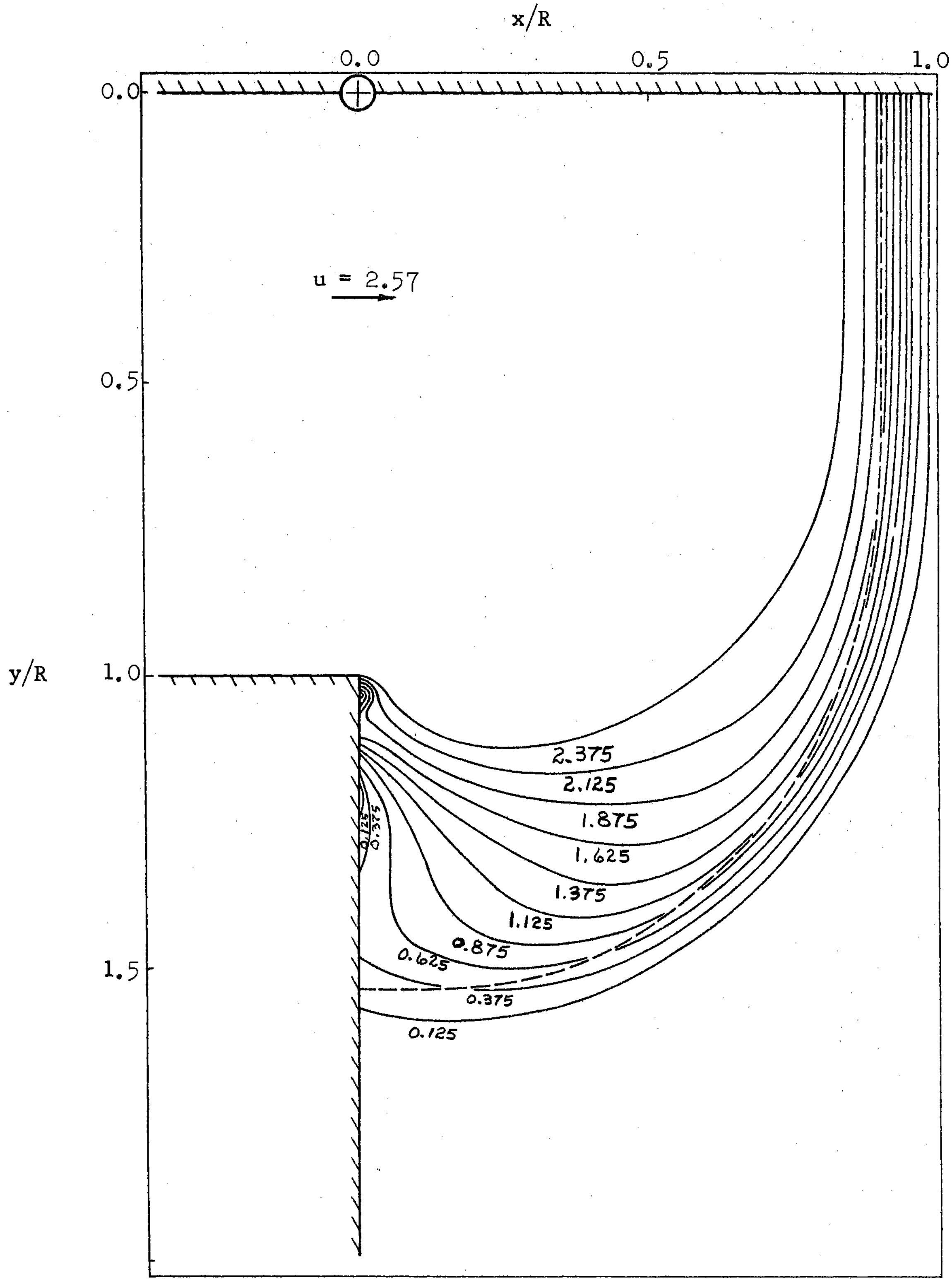

Figure 53. Constant Velocity Modulus Lines for η = 0.311 in Plane Geometry. Initial Shock Pressure Ratio - 10.0.

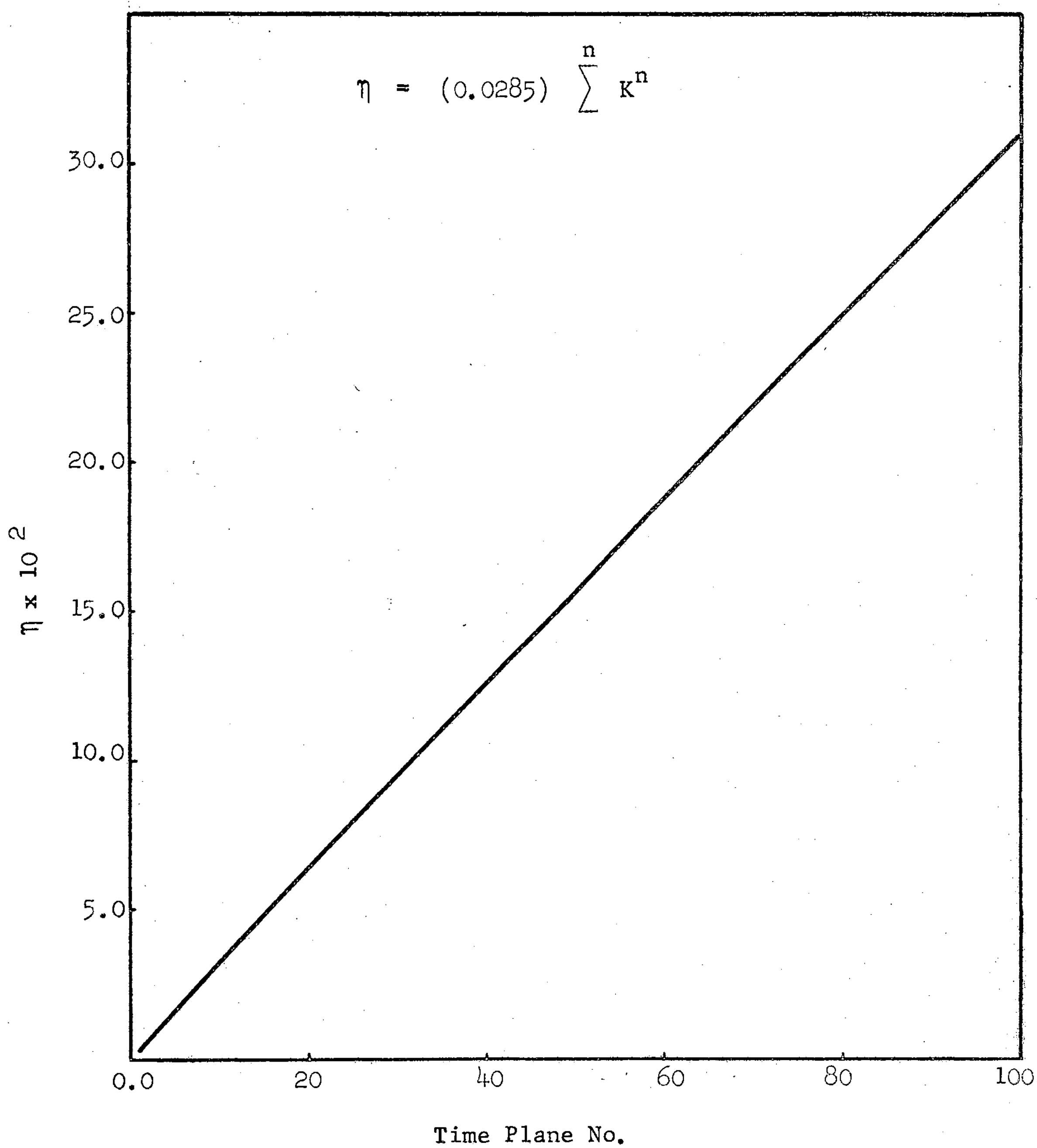

Figure 54. η Versus Time Plane Number for Axisymmetric Geometry. Initial Shock Pressure Ratio - 10.0.

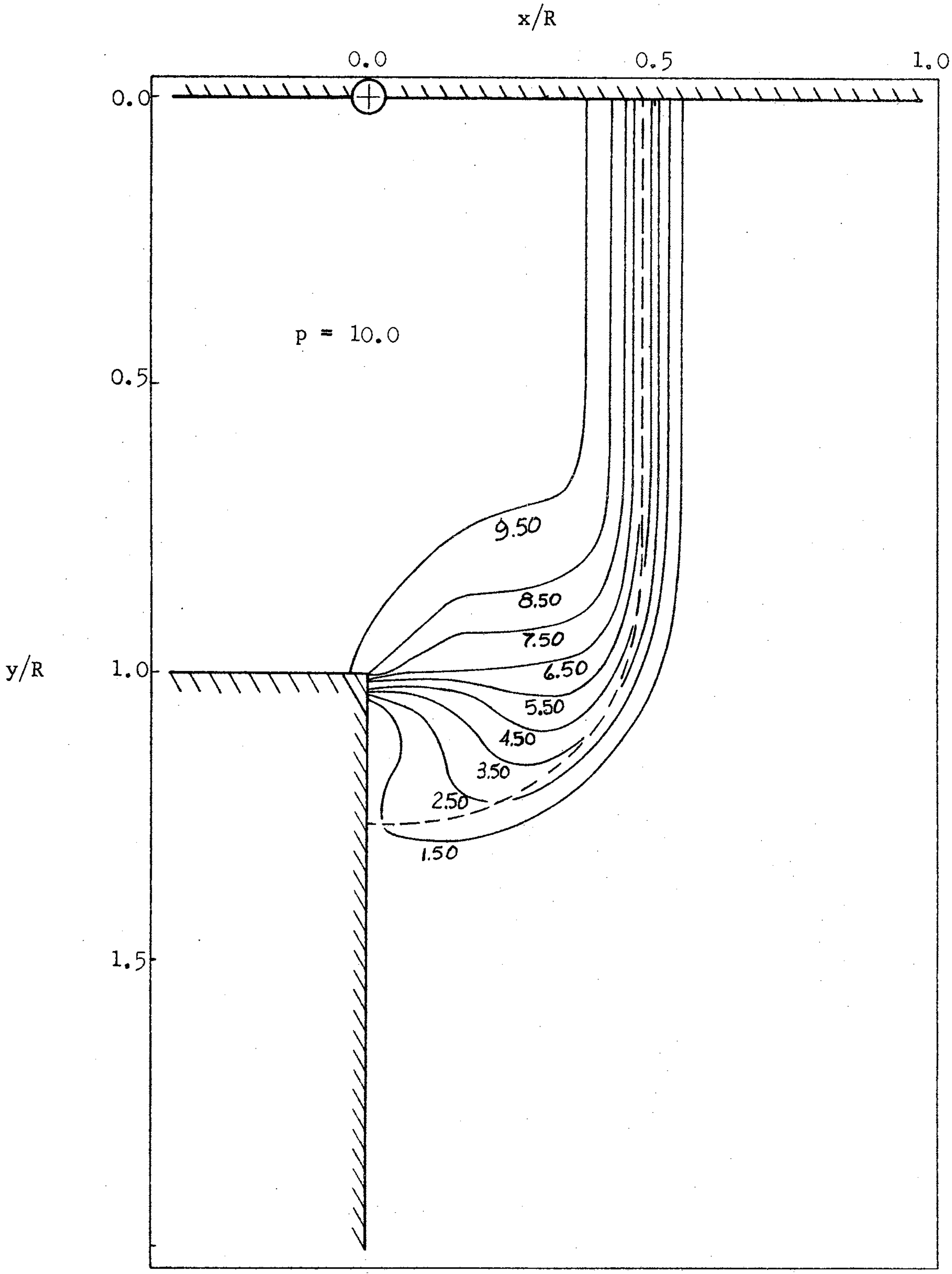

Figure 55. Constant Pressure Lines for $\eta = 0.157$ in Axisymmetric Geometry. Initial Shock Pressure Ratio - 10.0.

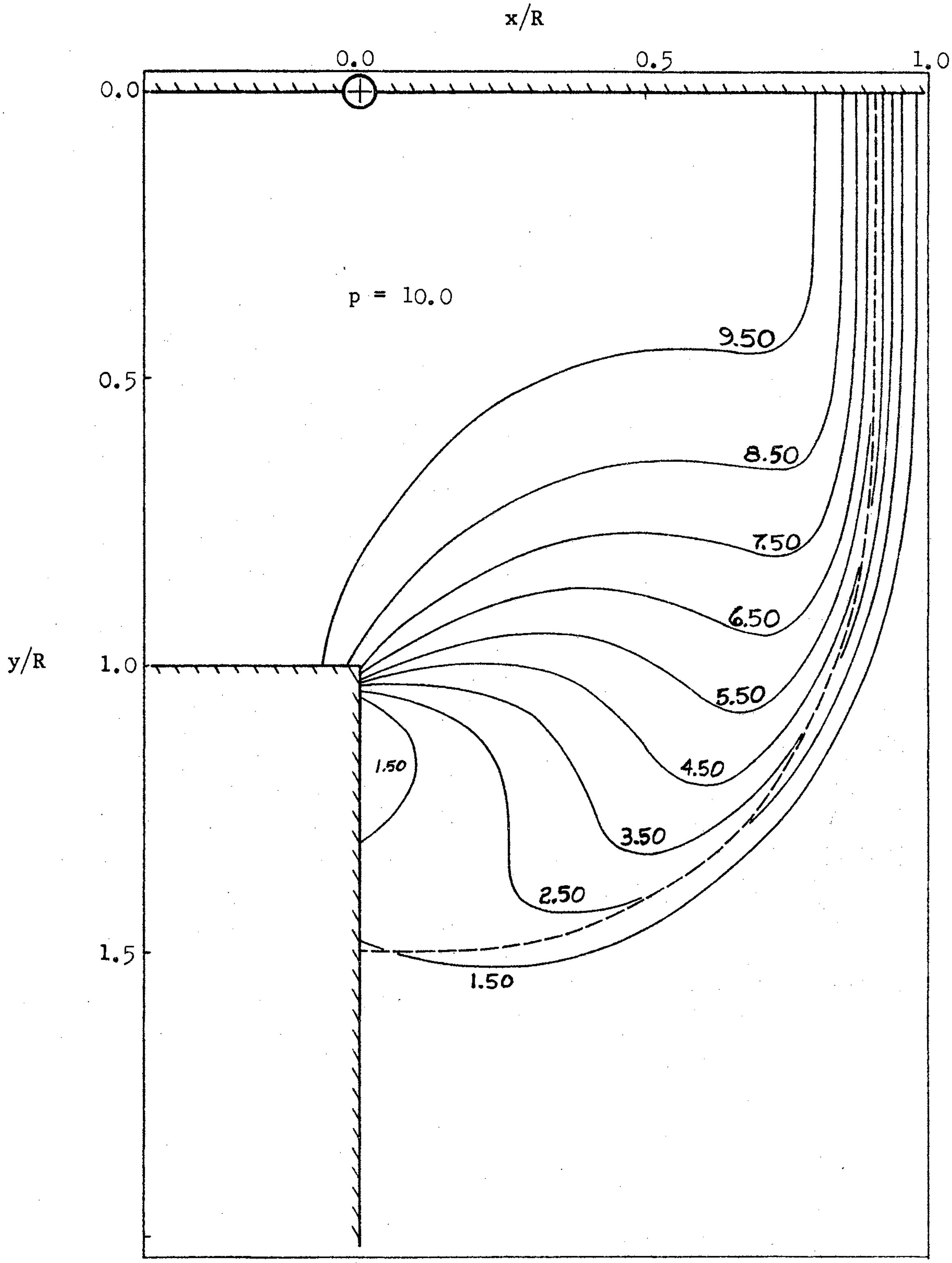

Figure 56. Constant Pressure Lines for η = 0.310 in Axisymmetric Geometry. Initial Shock Pressure Ratio - 10.0.

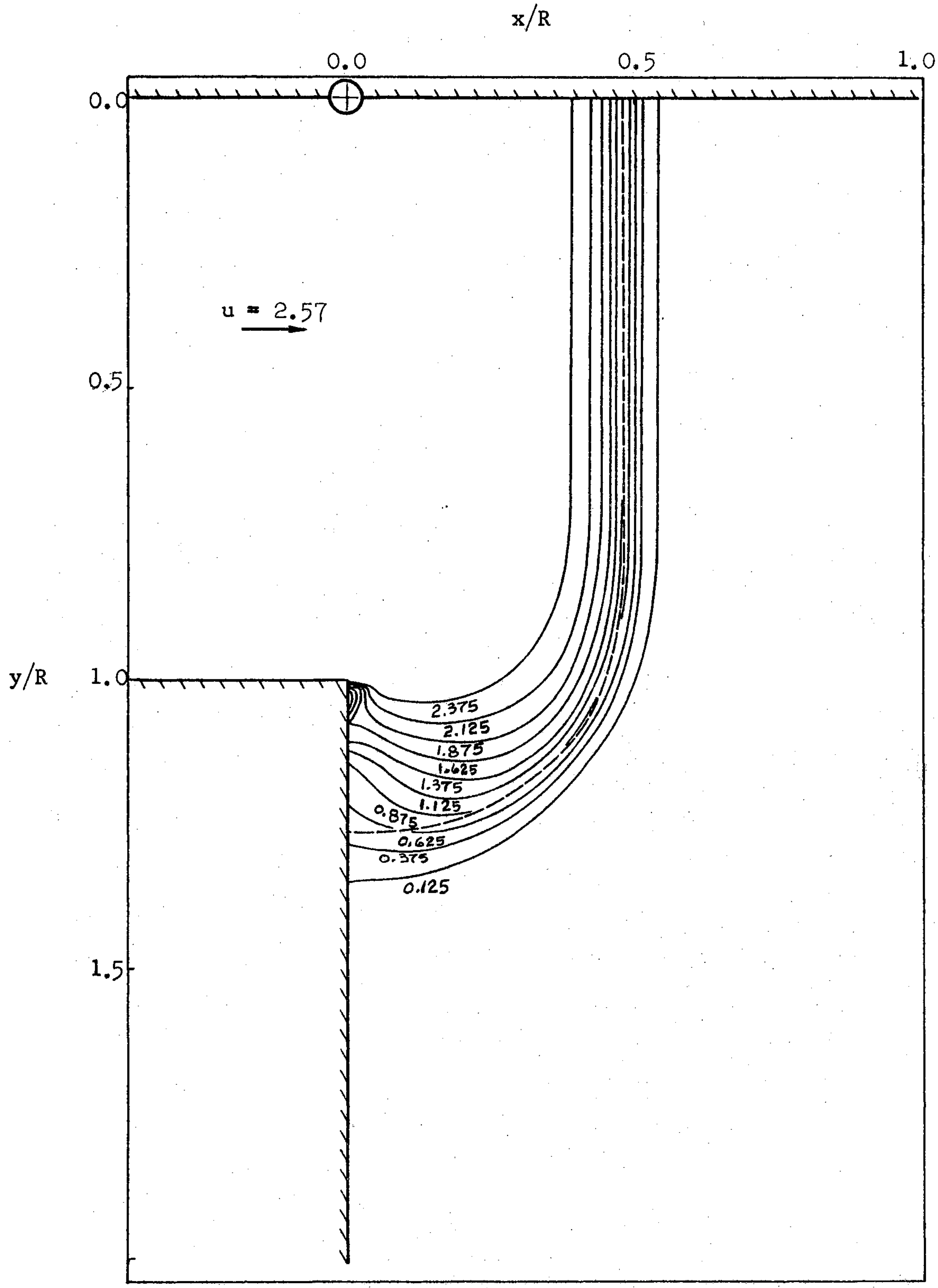

Figure 57. Constant Velocity Modulus Lines for $\eta = 0.157$ in Axisymmetric Geometry. Initial Shock Pressure Ratio - 10.0.

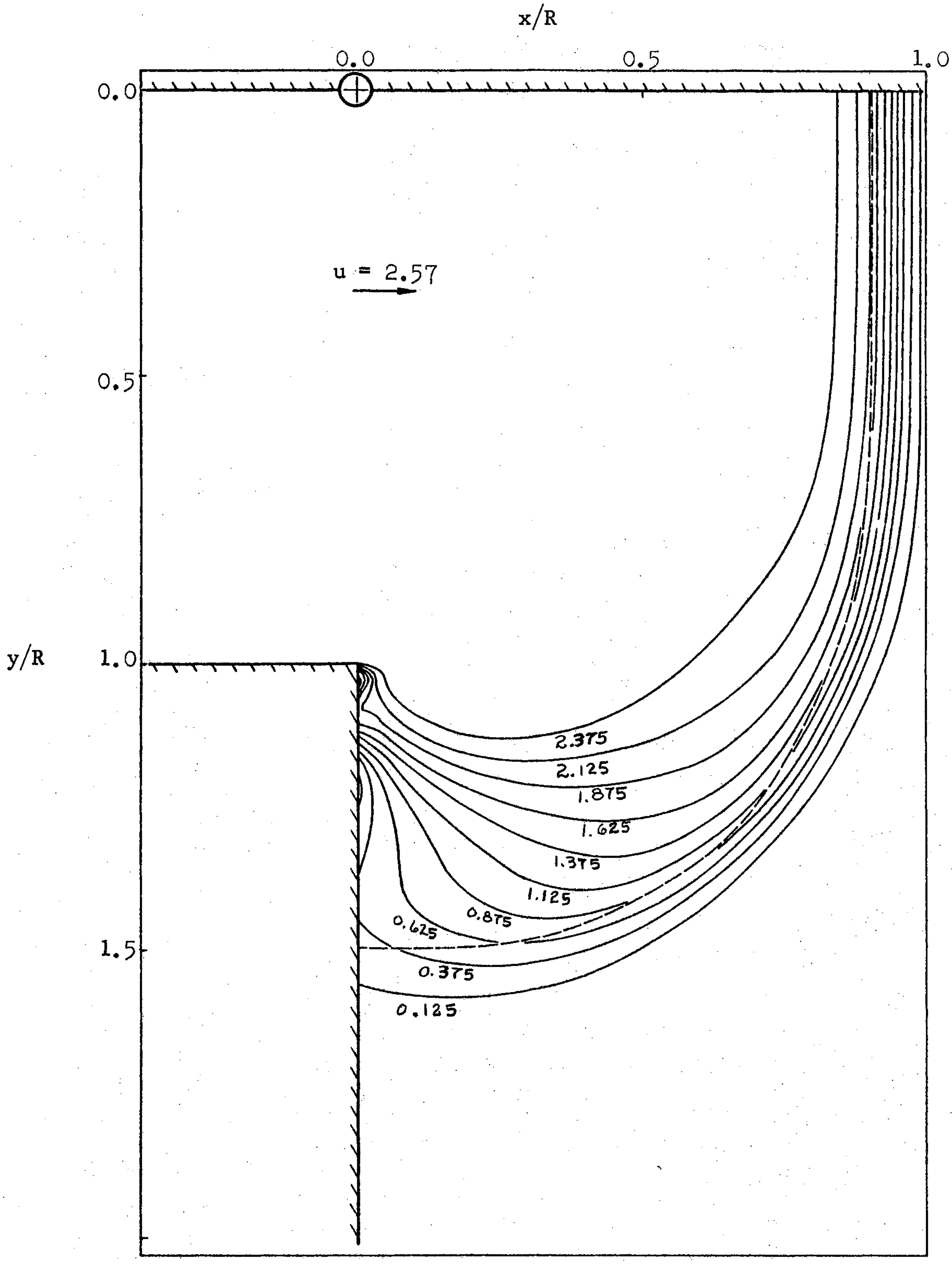

Figure 58. Constant Velocity Modulus Lines for η = 0.310 in Axisymmetric Geometry. Initial Shock Pressure Ratio - 10.0.

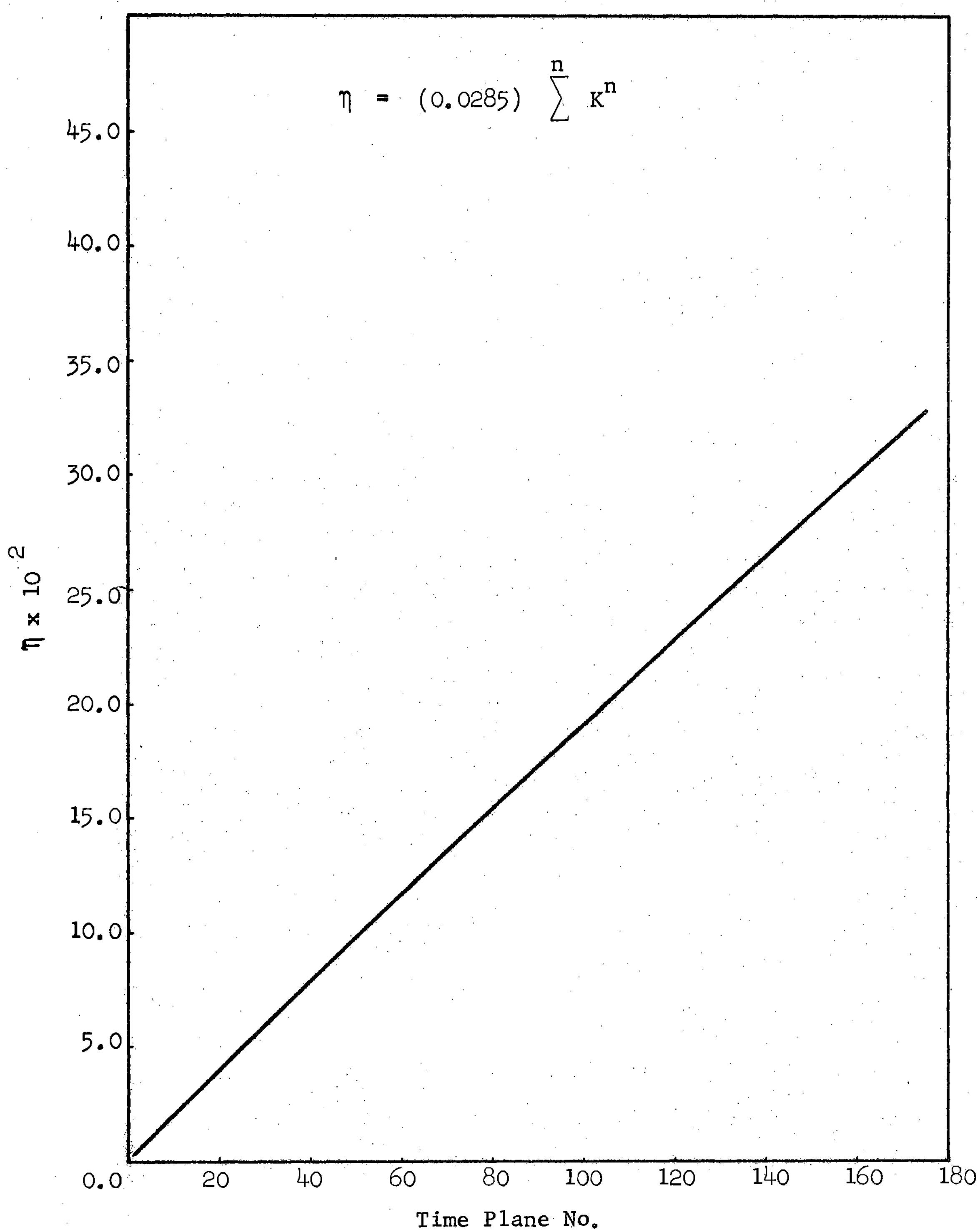

Figure 59. η Versus Time Plane Number for Mach 5.0 Crossflow.

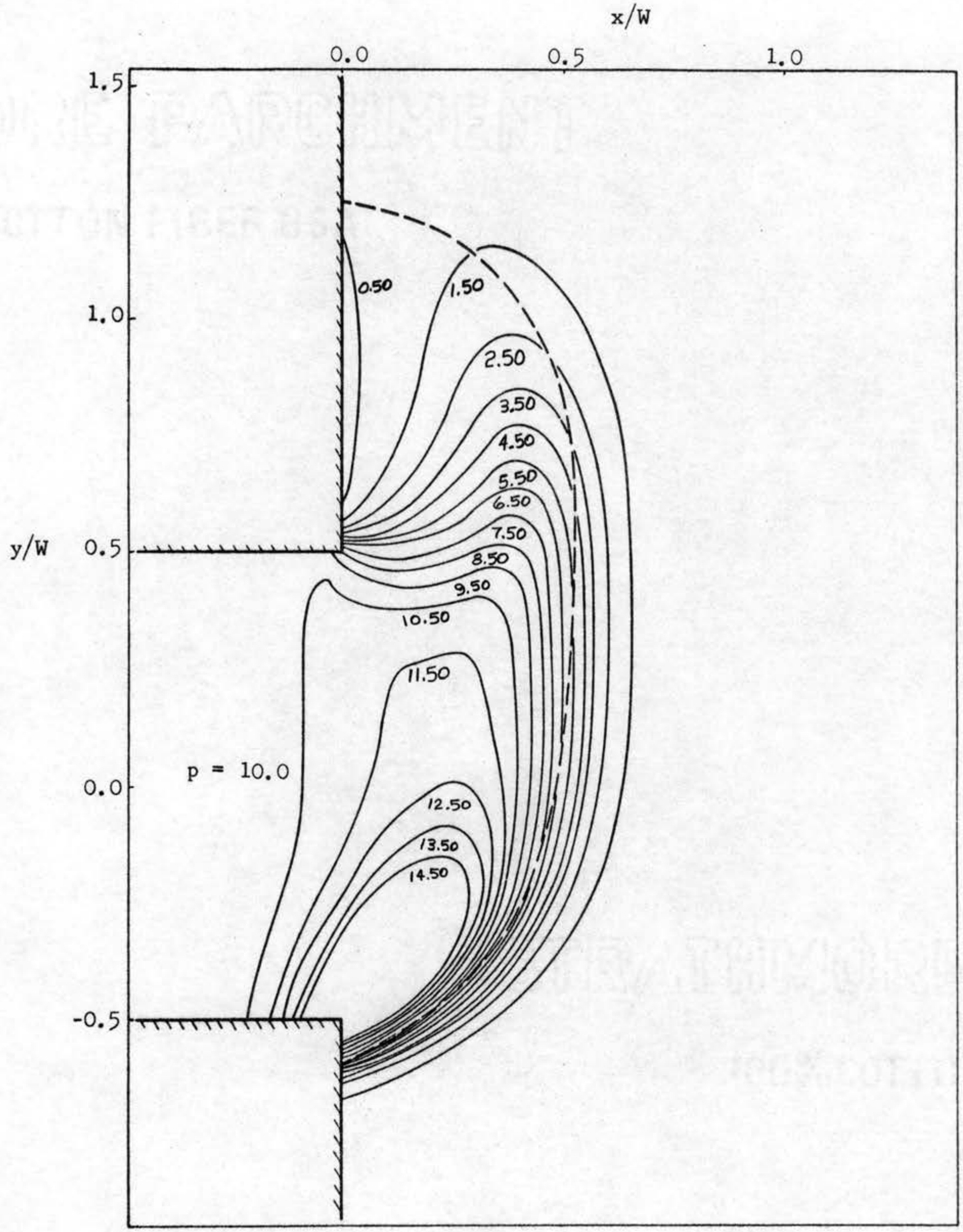

Figure 60. Constant Pressure Lines for $\eta = 0.145$ in Mach 5.0 Crossflow.

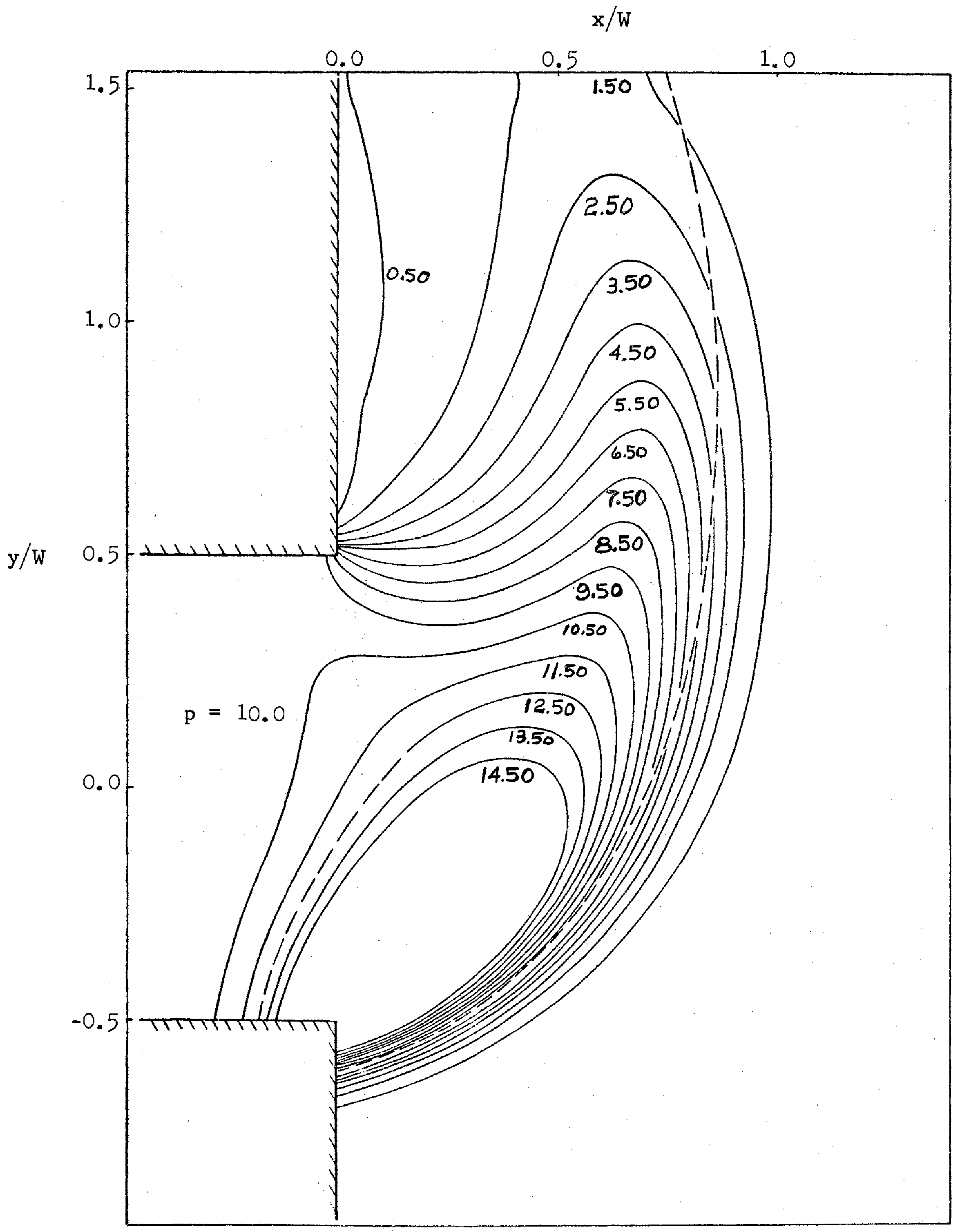

Figure 61. Constant Pressure Lines for $\eta = 0.238$ in Mach 5.0 Crossflow.

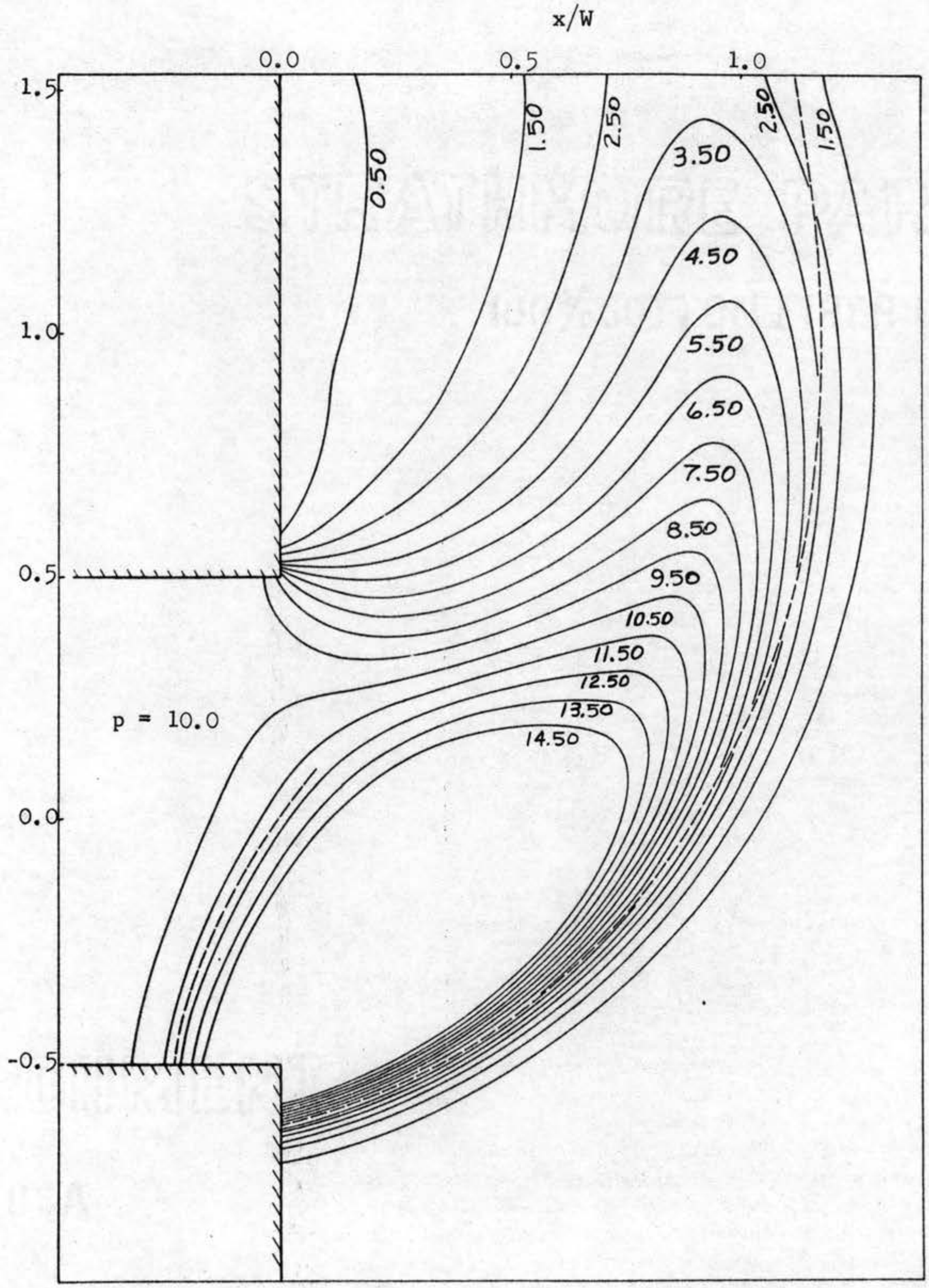

Figure 62. Constant Pressure Lines for η = 0.328 in Mach 5.0 Crossflow.

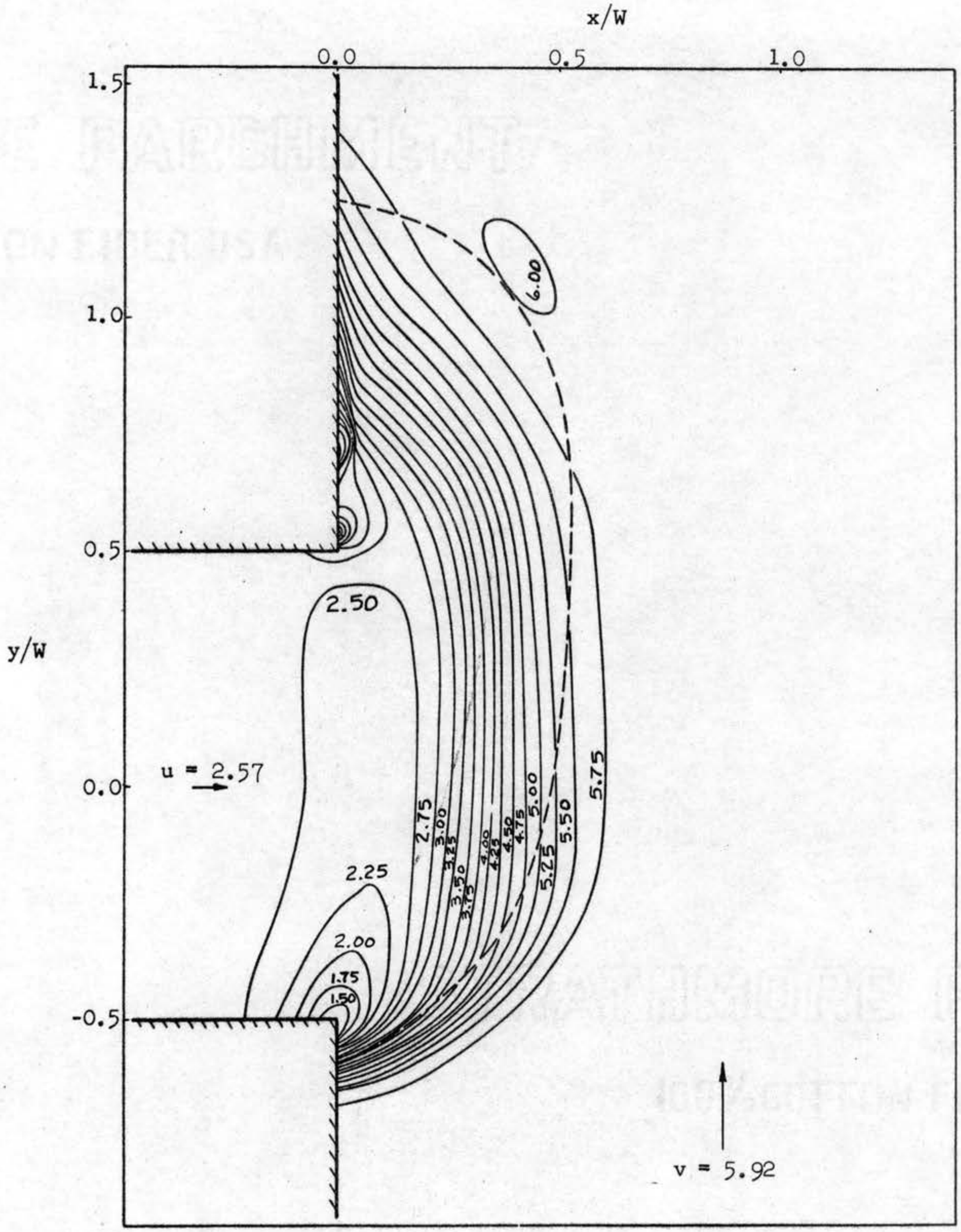

Figure 63. Constant Velocity Modulus Lines for $\eta = 0.145$ in Mach 5.0 Crossflow.

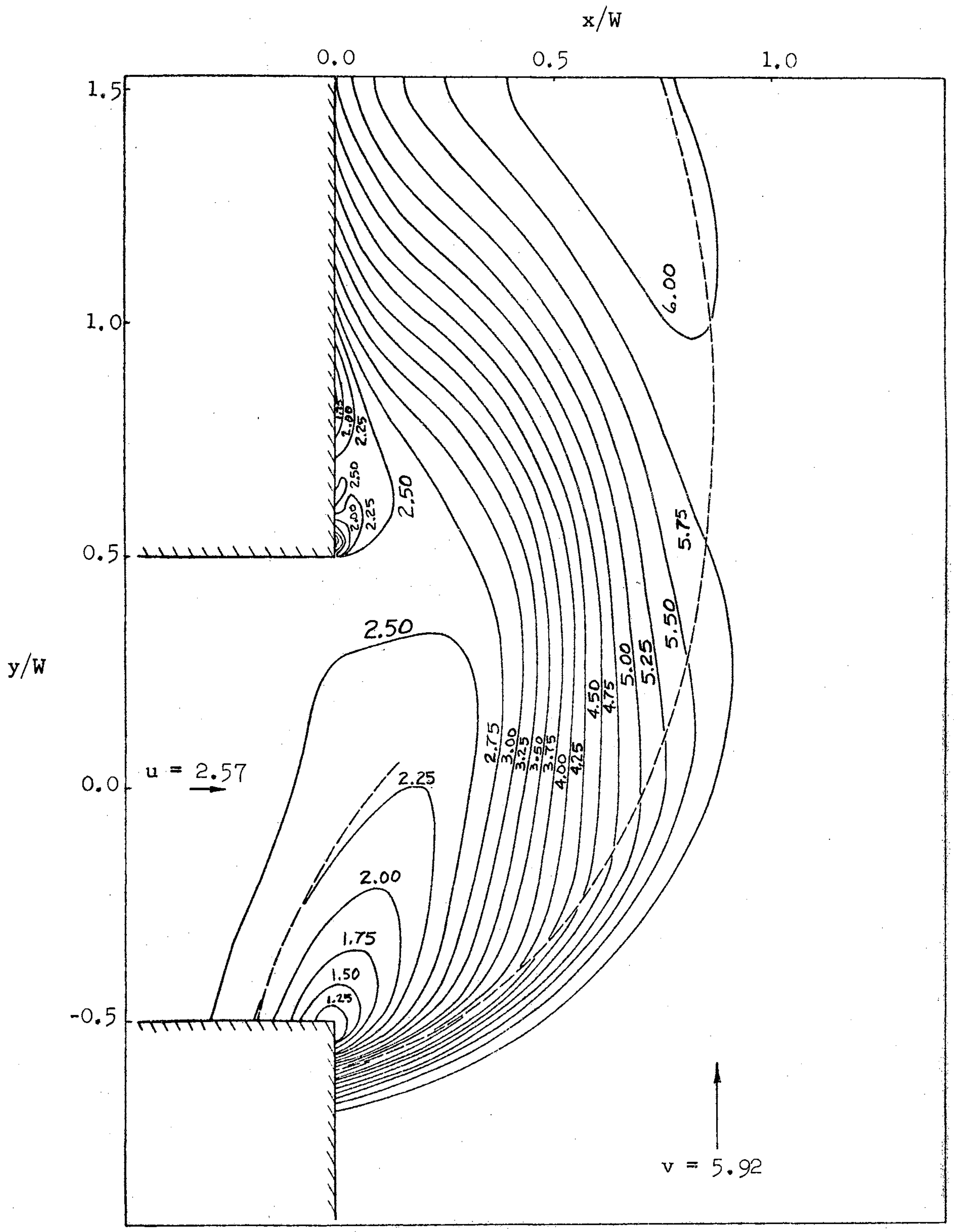

Figure 64. Constant Velocity Modulus Lines for $\eta = 0.238$ in Mach 5.0 Crossflow.

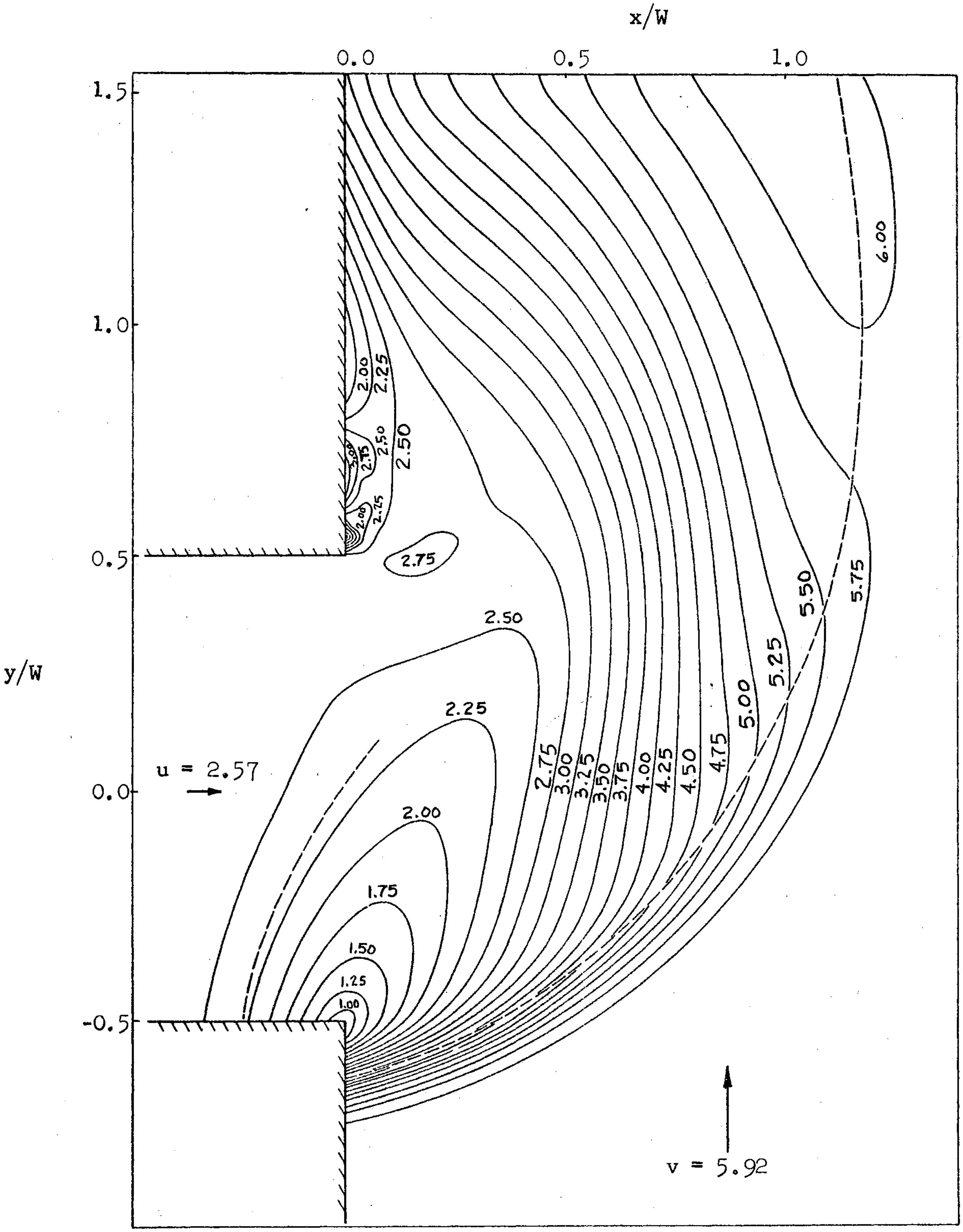

Figure 65. Constant Velocity Modulus Lines for η = 0.328 in Mach 5.0 Crossflow.

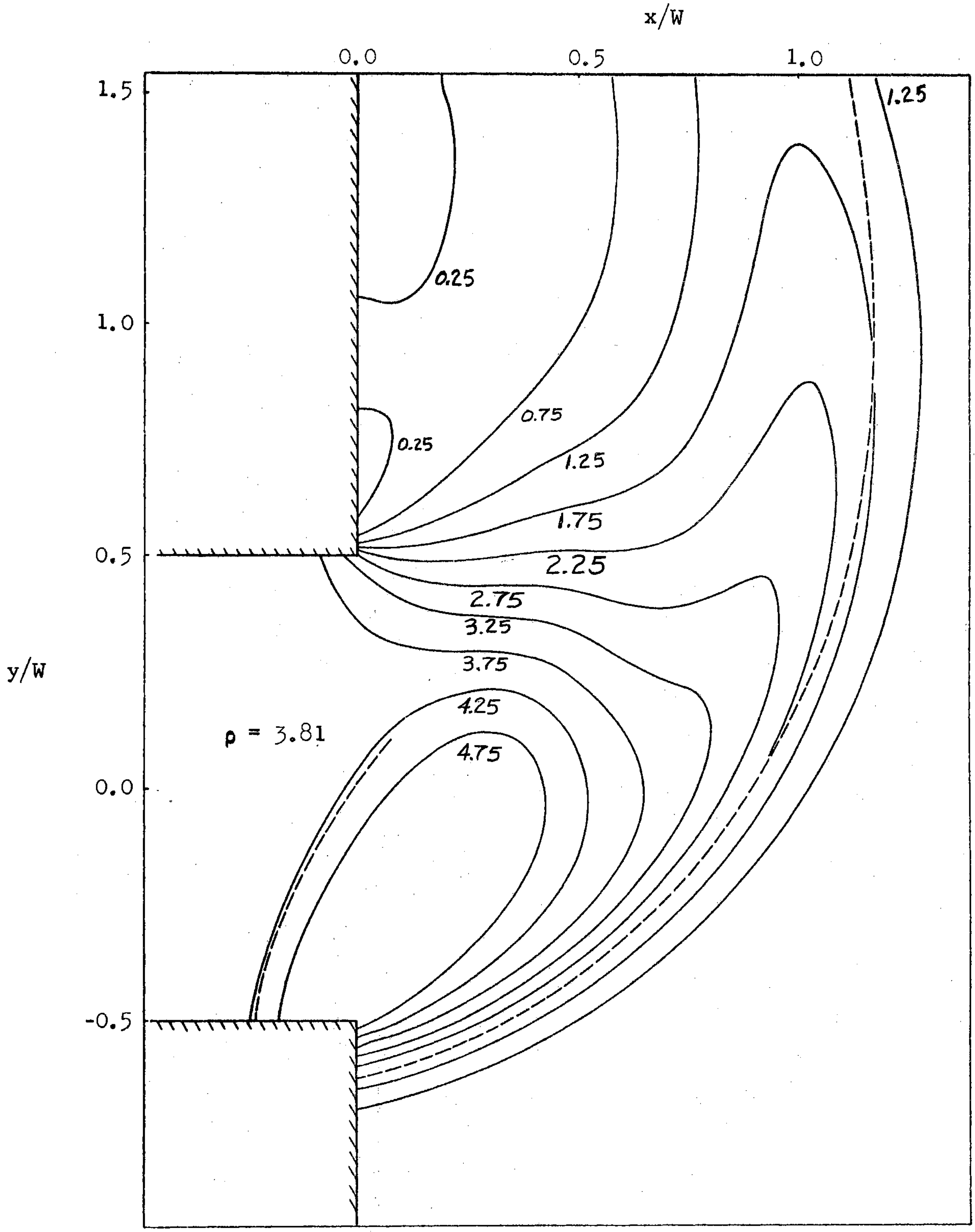

Figure 66. Constant Density Lines for $\eta = 0.328$ in Mach 5.0 Crossflow.

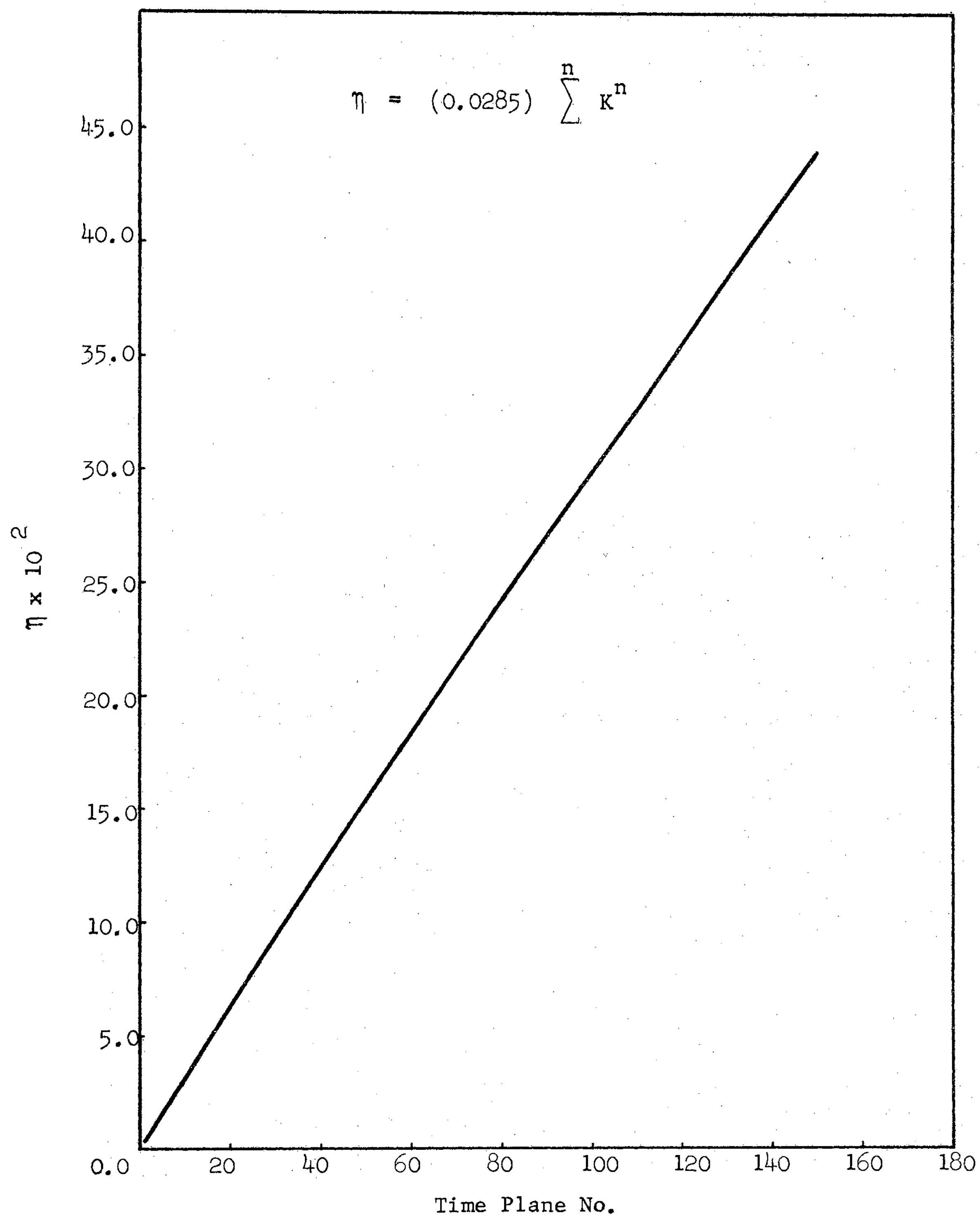

Figure 67. η Versus Time Plane Number for Mach 2.0 Crossflow.

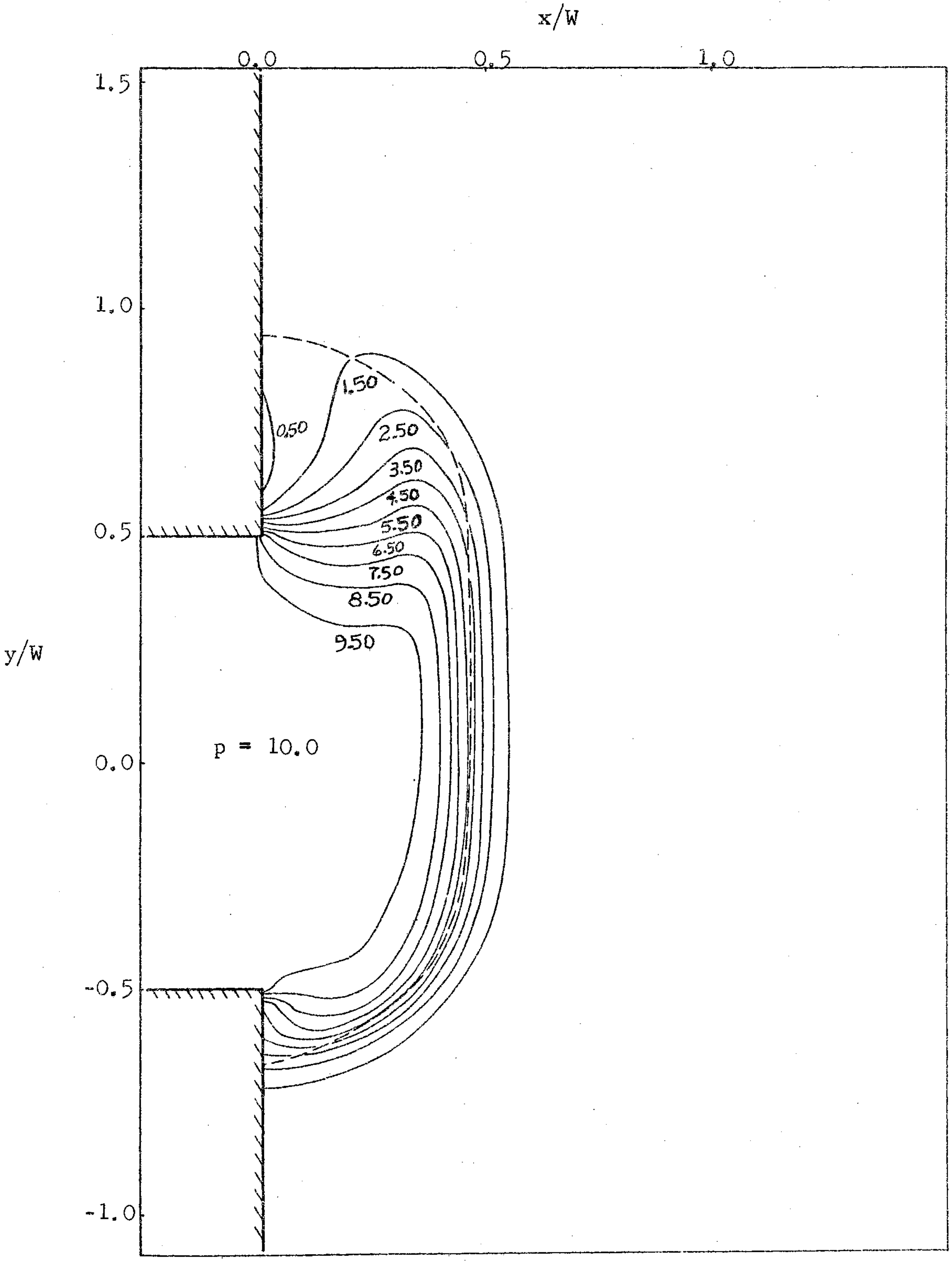

Figure 68. Constant Pressure Lines for $\eta = 0.154$ in Mach 2.0 Crossflow.

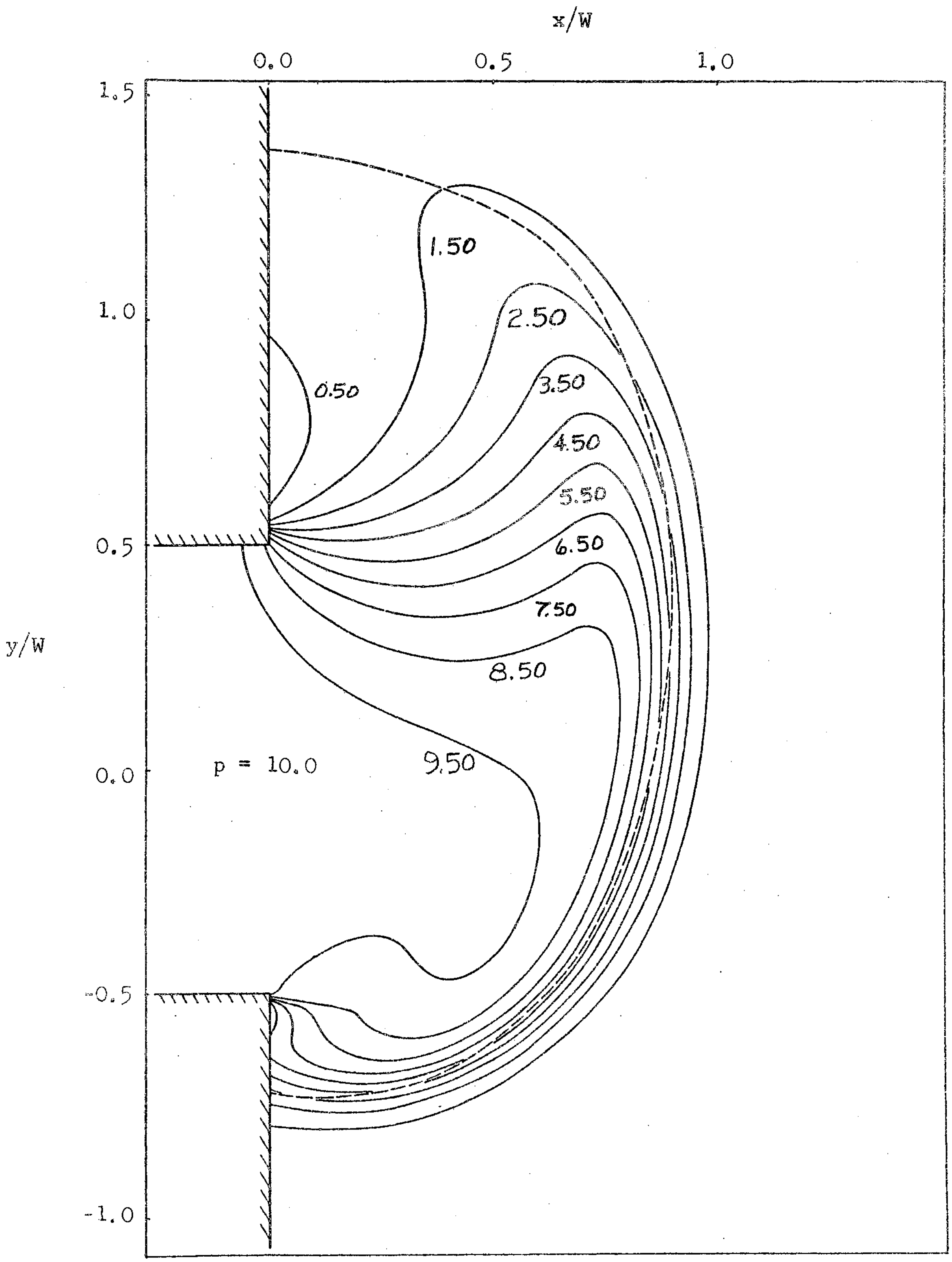

Figure 69. Constant Pressure Lines for η = 0.297 in Mach 2.0 Crossflow.

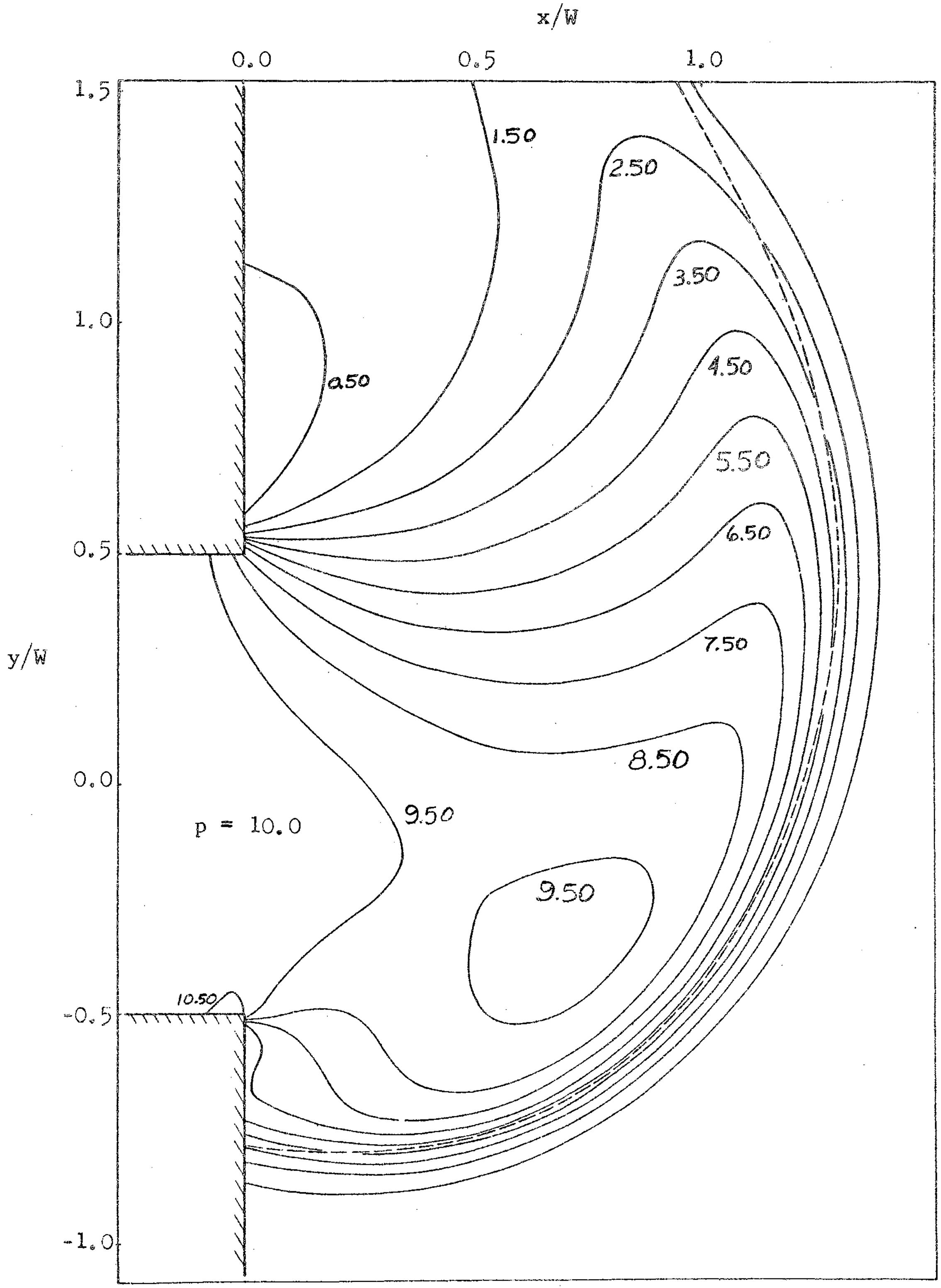

Figure 70. Constant Pressure Lines for $\eta = 0.439$ in Mach 2.0 Crossflow.

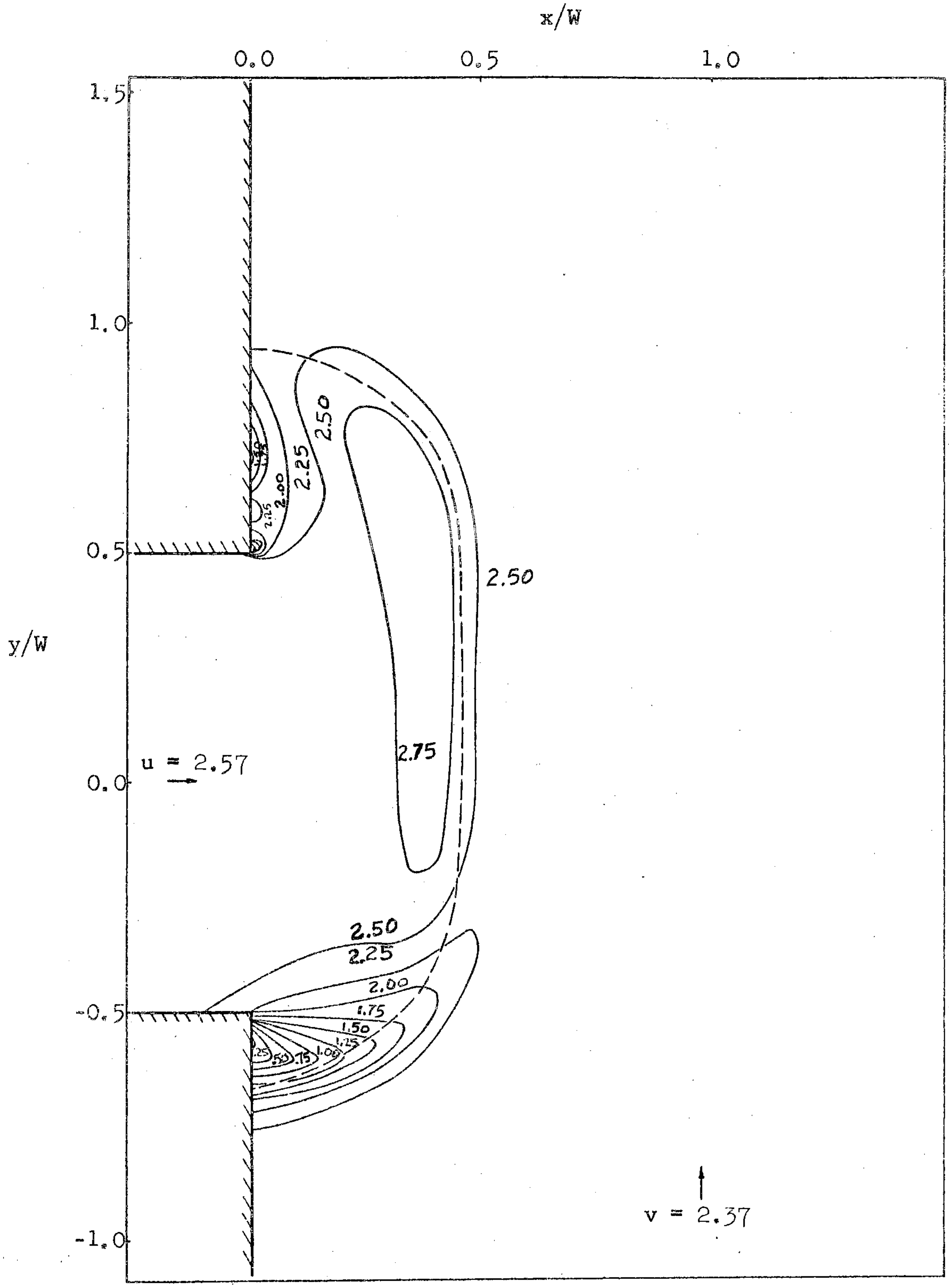

Figure 71. Constant Velocity Modulus Lines for $\eta = 1.54$ in Mach 2.0 Crossflow.

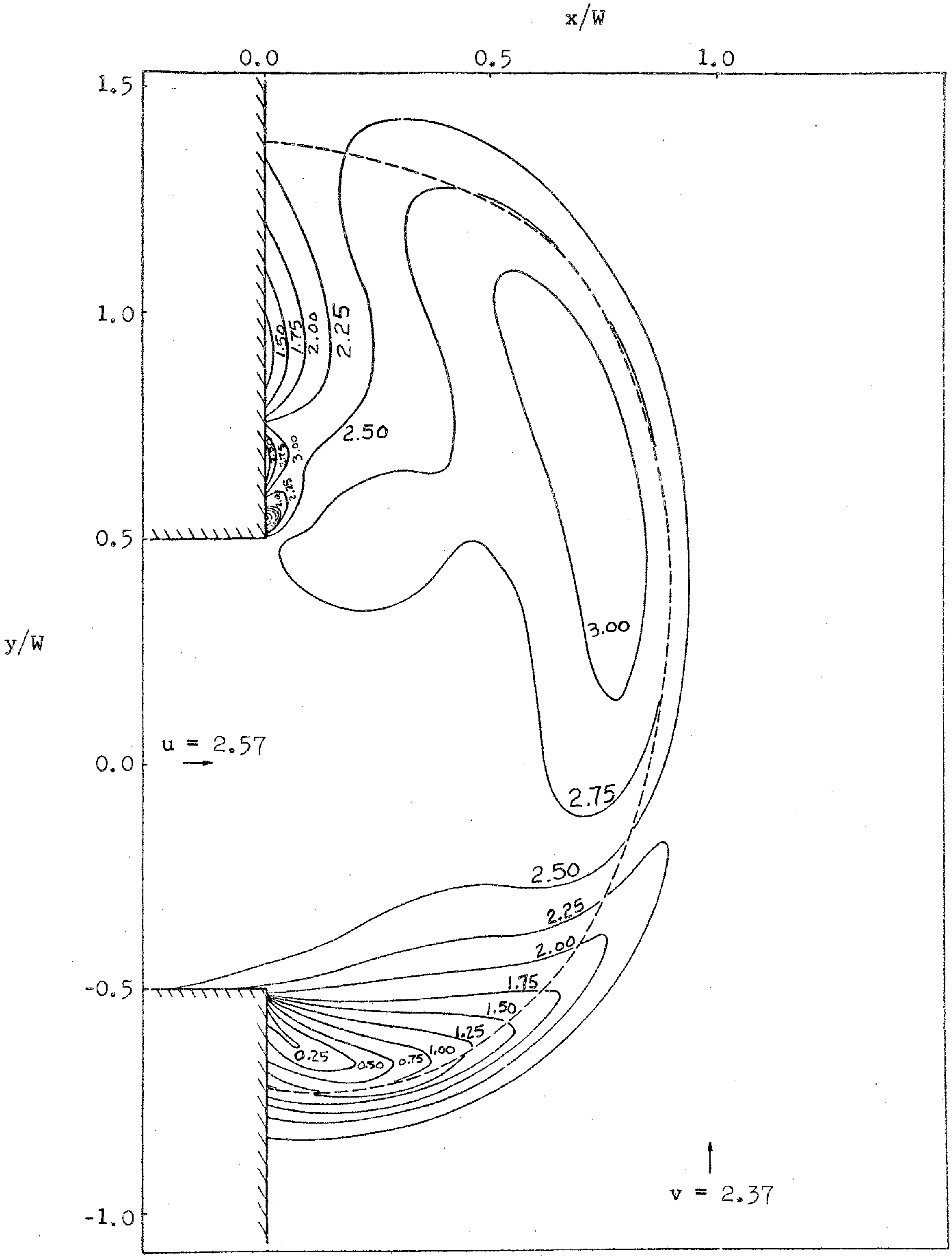

Figure 72. Constant Velocity Modulus Lines for $\eta = 0.297$ in Mach 2.0 Crossflow.

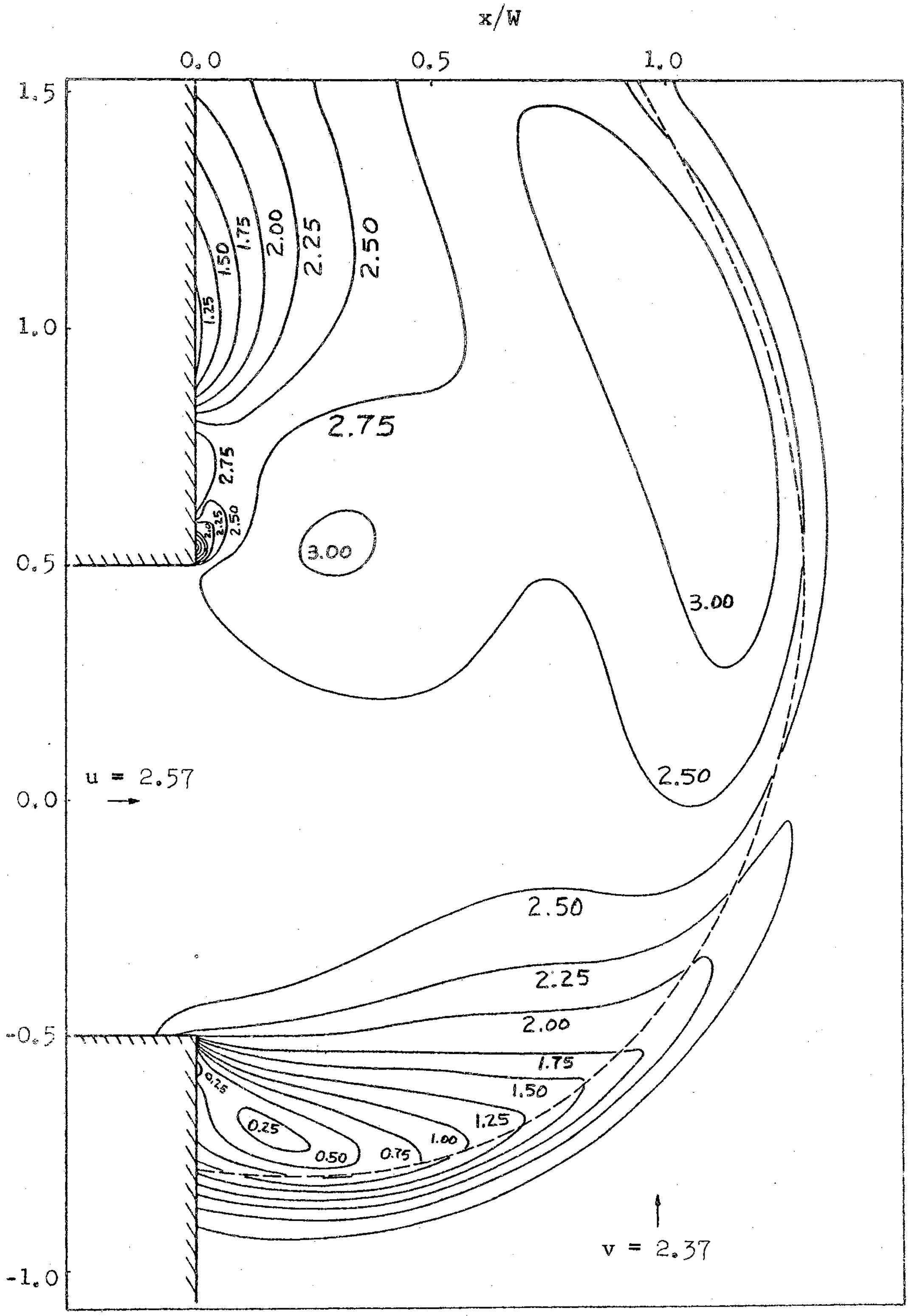

Figure 73. Constant Velocity Modulus Lines for $\eta = 0.439$ in Mach 2.0 Crossflow.

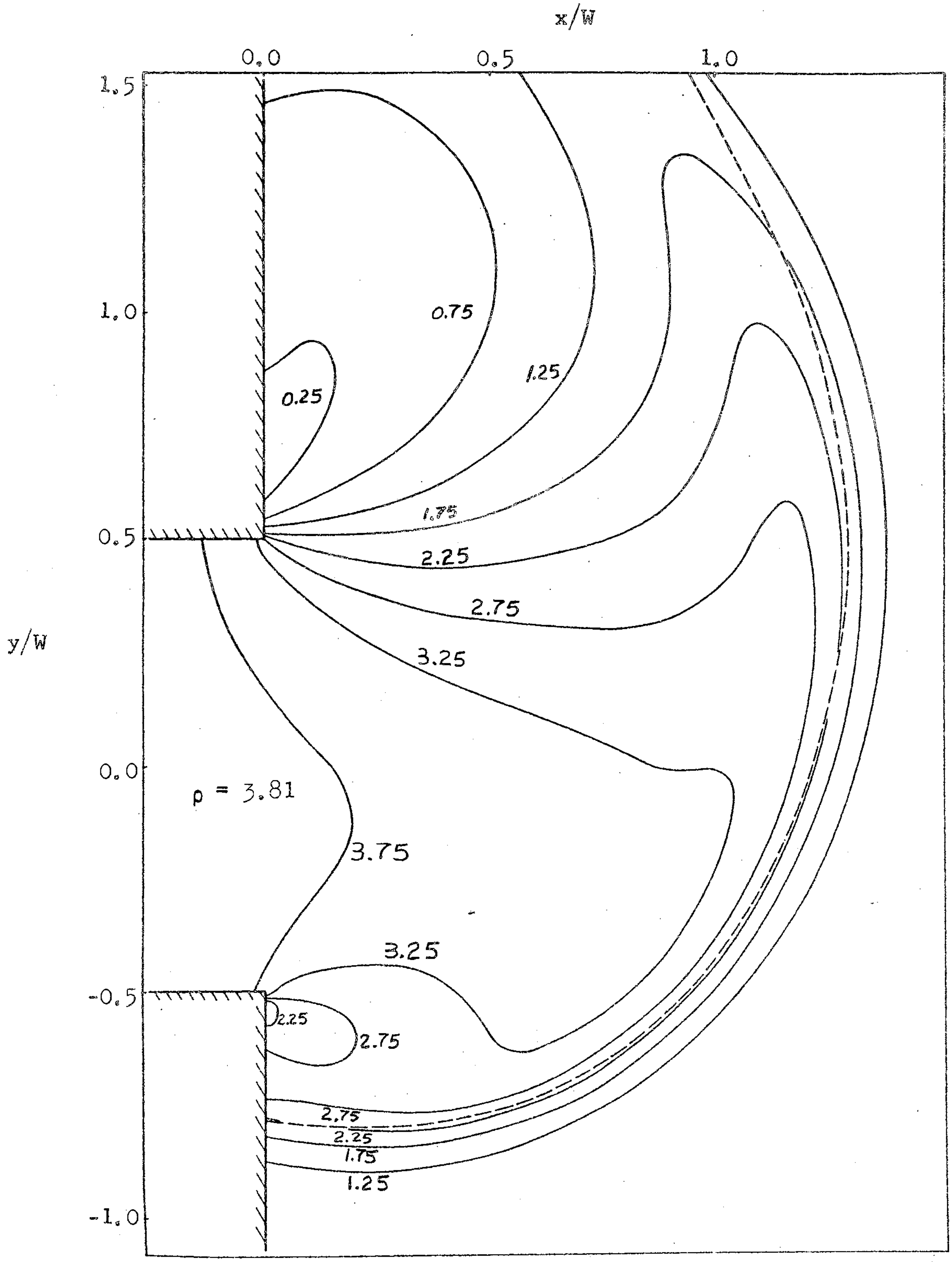

Figure 74. Constant Density Lines for η = 0.439 in Mach 2.0 Crossflow.

APPENDIX B

DERIVATION OF THE CONSERVATION FLOW EQUATIONS

The general flow equations are the continuity, momentum, and energy. The equations are derived using vector notation in conservation form. The conservation of quantities through a control volume γ, which is fixed in space, is considered. The control volume is enclosed by a surface σ on which a unit normal $\bar{n}$ is defined as positive in an outward direction. The figure below is used for the derivation of the flow equations.

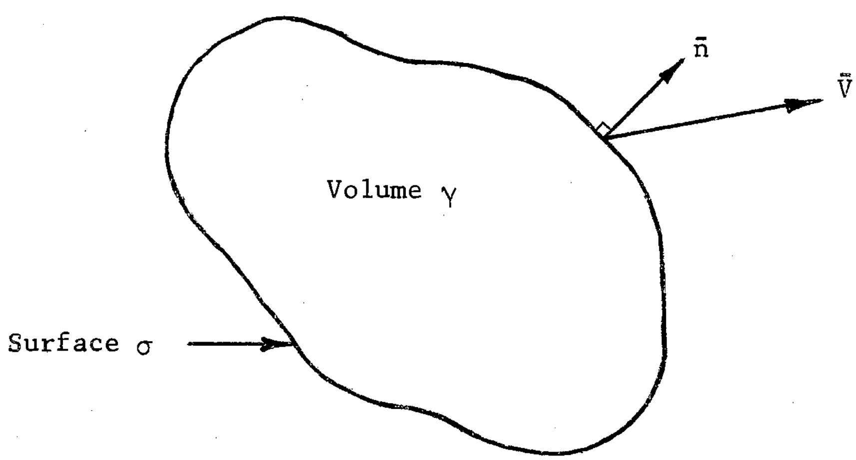

Continuity Equation

The continuity equation expresses the conservation of mass for a fluid flowing through the volume γ. The mass balance for γ may be expressed in the form

[Net flux of mass crossing σ] = [Rate of change of mass in γ].

The conservation form of the continuity equations is the familiar equation

$$\frac{\partial \rho}{\partial t} + \nabla \cdot (\rho \bar{V}) = 0 , \tag{B-1}$$

which is derived in many books [54], [55].

Momentum Equation

The momentum equation, which describes the conservation of momentum, may be expressed as

[Net force acting on the fluid in γ] =

[Rate of change of momentum of the fluid in γ] +

[Flux of momentum crossing σ] (B-2)

Only the force due to pressure acting on σ is considered (i.e., the viscous and body forces are neglected). The total force acting on σ is

$$- \int_{\sigma} p \, d\bar{\sigma} , \tag{B-3}$$

with $d\bar{\sigma} = \bar{n} d\sigma$.

The total momentum contained in γ is

$$\int_{\gamma} \rho \bar{V} d\gamma ,$$

and the rate of change of this momentum is

$$\frac{\partial}{\partial t} \int_{\gamma} \rho \bar{V} d\gamma . \tag{B-4}$$

The total flux of momentum crossing σ is

$$\int_\sigma \rho[\bar{V}\bar{V}] \circ d\bar{\sigma} \tag{B-5}$$

where $[\bar{V}\bar{V}]$ is defined as the dyadic product of two vectors $\bar{V}$. Substitution of (B-3), (B-4), and (B-5) into (B-2) gives

$$-\int_\sigma p\, d\bar{\sigma} = \frac{\partial}{\partial t}\int_\gamma \rho\bar{V}d\gamma + \int_\sigma \rho[\bar{V}\bar{V}] \cdot d\bar{\sigma} .$$

The divergence theorum applied to the surface integral gives

$$-\int_\gamma \nabla p\, d\gamma = \int_\gamma \frac{\partial(\rho\bar{V})}{\partial t} d\gamma + \int_\gamma \nabla \cdot (\rho[\bar{V}\bar{V}])d\gamma$$

or

$$\int_\gamma \left\{ \frac{\partial(\rho\bar{V})}{\partial t} + \nabla \cdot \rho[\bar{V}\bar{V}] + \nabla P \right\} d\gamma = 0 .$$

This integral vanishes for an arbitrary volume; therefore, the integrand also vanishes,

$$\frac{\partial(\rho\bar{V})}{\partial t} + \nabla \cdot \rho[\bar{V}\bar{V}] + \nabla p = 0 . \tag{B-6}$$

Equation (B-6) is the conservation form of the momentum equation.

Energy Equation

The energy equation derived considers the conservation of energy in γ under the following conditions:

1. Gravity and viscous forces are neglected.
2. There is no heat addition to the fluid in γ.
3. The only work is the "flow work".
4. The fluid obeys the ideal gas equation of state.

The energy of a fluid particle per unit volume is noted as e and defined as the sum of the internal energy and kinetic energy,

$$e = \rho\epsilon + \frac{\rho|\bar{V}|^2}{2} .$$

Using the ideal gas equation of state $(p/\rho = RT)$ and the internal energy relation $(\epsilon = C_v T)$, the fluid energy is expressed as

$$e = \frac{pC_v}{R} + \frac{1}{2}\rho|\bar{V}|^2 ,$$

or

$$e = \frac{p}{k - 1} + \frac{1}{2}\rho|\bar{V}|^2 , \tag{B-7}$$

where k is the specific heat ratio (C_p/C_v). The conservation of the fluid energy per unit volume is

$$[\text{Net energy of the fluid crossing } \sigma] + [\text{Rate of "flow work" at } \sigma] = [\text{Rate of change of the fluid energy in } \gamma]. \tag{B-8}$$

The net energy crossing σ is

$$\int_\sigma e\bar{V} \cdot d\bar{\sigma} . \tag{B-9}$$

The rate of "flow work" per unit volume acting on σ is

$$\int_\sigma p\bar{V} \cdot d\bar{\sigma} . \tag{B-10}$$

The energy contained in the total volume γ is

$$\int_\gamma e d\gamma$$

and the rate of change of this energy is

$$- \frac{\partial}{\partial t} \int_\gamma e d\gamma . \qquad \text{(B-11)}$$

This rate is negative due to the defined direction of $\bar{n}$. Substitution of (B-9), (B-10), and (B-11) into (B-8) gives

$$\int_\sigma e\bar{V} \cdot d\bar{\sigma} + \int_\sigma p\bar{V} \cdot d\bar{\sigma} = - \frac{\partial}{\partial t} \int_\gamma e d\gamma ,$$

The divergence theorum applied to the surface integrals gives

$$\int_\gamma \frac{\partial e}{\partial t} d\gamma + \int_\gamma \nabla \cdot (e\bar{V}) d\gamma + \int_\gamma \nabla \cdot (p\bar{V}) d\gamma = 0$$

or

$$\int_\gamma \left\{ \frac{\partial e}{\partial t} + \nabla \cdot [(e + p)\bar{V}] \right\} d\gamma = 0 .$$

Since the integral vanishes for an arbitrary volume, the integrand also vanishes to

$$\frac{\partial e}{\partial t} + \nabla \cdot [(e + p)\bar{V}] = 0 \qquad \text{(B-12)}$$

which is the conservation form of the energy equation.

The Conservation Equations

The system of conservation equations may be summarized:

1. Continuity,

$$\frac{\partial \rho}{\partial t} + \nabla \cdot (\rho\bar{V}) = 0 ; \qquad \text{(B-1)}$$

2. Momentum,

$$\frac{\partial(\rho\bar{V})}{\partial t} + \nabla \cdot \rho[\bar{V}\bar{V}] + \nabla p = 0 ; \qquad \text{(B-6)}$$

3. Energy,

$$\frac{\partial e}{\partial t} + \nabla \cdot [(e + p)\bar{V}] = 0 . \tag{B-12}$$

APPENDIX C

METHOD OF NONDIMENSIONALIZING DEPENDENT VARIABLES

The properties on both sides of a normal shock wave which propagates to the right are:

p_2				p_1 (Pressure)
ρ_2	$\xrightarrow{U_2}$	$\xrightarrow{U_s}$	$\xrightarrow{U_1}$	ρ_1 (Density)
T_2				T_1 (Temperature)
$C_2 = \sqrt{k \dfrac{p_2}{\rho_2}}$				$C_1 = \sqrt{k \dfrac{p_1}{\rho_1}}$

where U_s = shock velocity,

C = speed of sound,

k = specific heat ratio.

The properties of the gas are made dimensionless with respect to the properties in front of the shock (i.e., state 1). The velocities U_1, U_2, and U_s are made dimensionless with respect to the quantity $\sqrt{p_1 / \rho_1}$. The new state defined in front of the shock by x and behind as y gives the dimensionless properties on either side of a moving shock.

p_y $\quad U_y \longrightarrow \quad \Big| \; D \longrightarrow \quad U_x \longrightarrow \quad$ p_x

ρ_y $\qquad\qquad\qquad\qquad\qquad\qquad\qquad\qquad\qquad\qquad$ ρ_x

T_y $\qquad\qquad\qquad\qquad\qquad\qquad\qquad\qquad\qquad\qquad$ T_x

$$C_y = \sqrt{k \frac{p_y}{\rho_y}} \qquad\qquad\qquad C_x = \sqrt{k \frac{p_x}{\rho_x}}$$

where

$$p_y = \frac{p_2}{p_1} \qquad\qquad U_y = \frac{U_2}{\sqrt{p_1/\rho_1}}$$

$$p_x = \frac{p_1}{p_1} = 1.0 \qquad\qquad D = \frac{U_s}{\sqrt{p_1/\rho_1}}$$

$$\rho_y = \frac{\rho_2}{\rho_1} \qquad\qquad U_x = \frac{U_1}{\sqrt{p_1/\rho_1}}$$

$$\rho_x = \frac{\rho_1}{\rho_1} = 1.0 \qquad\qquad C_x = \sqrt{k}$$

$$T_y = \frac{T_2}{T_1}$$

$$T_x = \frac{T_1}{T_1} = 1.0$$

A transformation made to a coordinate system relative to the shock gives (let V denote velocity quantities in the transformed system)

p_y $\qquad\qquad\qquad\qquad\qquad\qquad\qquad\qquad\qquad\qquad$ p_x

ρ_y $\quad \xleftarrow{V_y = D - U_y} \quad \Big| \quad \xleftarrow{V_x = D - U_x} \quad$ ρ_x

T_y $\qquad\qquad\qquad\qquad\qquad\qquad\qquad\qquad\qquad\qquad$ T_x

C_y $\qquad\qquad\qquad\qquad\qquad\qquad\qquad\qquad\qquad\qquad$ C_x.

The static properties in state x have a value of 1.0. In the y state the static properties have the value of the property ratio across a normal stationary shock wave.

APPENDIX D

DERIVATION OF THE DIFFERENCE EQUATION FOR A FIELD POINT (m,ℓ)

The difference equation corresponding to the partial differential equation

$$\frac{\partial f}{\partial t} + \frac{\partial F^x}{\partial x} + \frac{\partial F^y}{\partial y} = \frac{\partial}{\partial x}\left[A(x,y,t)\ \frac{\partial f}{\partial x}\right] + \frac{\partial}{\partial y}\left[B(x,y,t)\ \frac{\partial f}{\partial y}\right]$$

is obtained by using a forward difference for the time derivative and a central difference on the space derivatives. The time derivative is, then, defined in difference form as

$$\frac{\partial f}{\partial t} = \frac{f^{n+1}_{m,\ell} - f^{n}_{m,\ell}}{\tau}.$$

The central difference for the first order space derivatives is defined over a double net space, $2h_1$, and is in the form

$$\frac{\partial F^x}{\partial x} = \frac{\left(F^x_{m+1,\ell} - F^x_{m-1,\ell}\right)^n}{2h_1}$$

and

$$\frac{\partial F^y}{\partial y} = \frac{\left(F^y_{m,\ell+1} - F^y_{m,\ell-1}\right)^n}{2h_1}.$$

The second order space derivatives are also defined by a central difference over a double net space, $2h_1$, and are given as

$$\frac{\partial}{\partial x}\left[A(x,y,t)\,\frac{\partial f}{\partial x}\right] = \frac{1}{h_1}\left[\,A^n_{m+\frac{1}{2},\ell}\left(\frac{\partial f}{\partial x}\right)^n_{m+\frac{1}{2},\ell} - A^n_{m-\frac{1}{2},\ell}\left(\frac{\partial f}{\partial y}\right)^n_{m-\frac{1}{2},\ell}\,\right] =$$

$$\frac{1}{h_1{}^2}\left[\,A^n_{m+\frac{1}{2},\ell}\left(f_{m+1,\ell} - f_{m,\ell}\right)^n - A^n_{m-1,\ell}\left(f_{m,\ell} - f_{m-1,\ell}\right)^n\,\right]$$

and

$$\frac{\partial}{\partial y}\left[B(x,y,t)\,\frac{\partial f}{\partial y}\right] = \frac{1}{h_1{}^2}\left[B^n_{m,\ell+1}\left(f_{m,\ell+1} - f_{m,\ell}\right)^n - B^n_{m,\ell-1}\left(f_{m,\ell} - f_{m,\ell-1}\right)^n\right].$$

With the above difference definitions, the difference equation has the form

$$\frac{f^{n+1}_{m,\ell} - f^n_{m,\ell}}{\tau} + \frac{\left(F^x_{m+1,\ell} - F^x_{m-1,\ell}\right)^n}{2h_1} + \frac{\left(F^y_{m,\ell+1} - F^y_{m,\ell-1}\right)^n}{2h_1} =$$

$$\frac{1}{h_1{}^2}\left[A^n_{m+\frac{1}{2},\ell}\left(f_{m+1,\ell} - f_{m,\ell}\right)^n - A^n_{m-\frac{1}{2},\ell}\left(f_{m,\ell} - f_{m-1,\ell}\right)^n\right] +$$

$$\frac{1}{h_1{}^2}\left[B^n_{m,\ell+\frac{1}{2}}\left(f_{m,\ell+1} - f_{m,\ell}\right) - B^n_{m,\ell-\frac{1}{2}}\left(f_{m,\ell} - f_{m,\ell-1}\right)^n\,\right]$$

or

$$f^{n+1}_{m,\ell} = f^n_{m,\ell} - \frac{K_1}{2}\left[F^x_{m+1,\ell} - F^x_{m-1,\ell} + F^y_{m,\ell+1} - F^y_{m,\ell-1}\right]^n +$$

$$\frac{\tau}{h_1{}^2}\left[A^n_{m+\frac{1}{2},\ell}\left(f_{m+1,\ell} - f_{m,\ell}\right)^n - A^n_{m-\frac{1}{2},\ell}\left(f_{m,\ell} - f_{m-1,\ell}\right)^n +\right.$$

$$\left.B^n_{m,\ell+\frac{1}{2}}\left(f_{m,\ell+1} - f_{m,\ell}\right)^n - B^n_{m,\ell-\frac{1}{2}}\left(f_{m,\ell} - f_{m,\ell-1}\right)^n\,\right].$$

From Appendix E, the coefficients $A^n_{m,\ell}$ and $B^n_{m,\ell}$ are defined, in the development of the stability condition, as

$$A^n_{m,\ell} = \frac{h_1^2 \alpha^n_{m,\ell}}{2\tau}$$

and

$$B^n_{m,\ell} = \frac{h_1^2 \beta^n_{m,\ell}}{2\tau} .$$

With these definitions applied to the difference equation, the final form of the difference equation for a plane geometry is

$$f^{n+1}_{m,\ell} = f^n_{m,\ell} - \frac{K_1}{2}\left[F^x_{m+1,\ell} - F^x_{m-1,\ell} + F^y_{m,\ell+1} - F^y_{m,\ell-1}\right]^n +$$

$$\frac{1}{2}\left[\alpha^n_{m+\frac{1}{2},\ell}\left(f_{m+1,\ell} - f_{m,\ell}\right)^n - \alpha^n_{m-\frac{1}{2},\ell}\left(f_{m,\ell} - f_{m-1,\ell}\right)^n + \right.$$

$$\left.\beta^n_{m,\ell+\frac{1}{2}}\left(f_{m,\ell+1} - f_{m,\ell}\right)^n - \beta^n_{m,\ell-\frac{1}{2}}\left(f_{m,\ell} - f_{m,\ell-1}\right)^n\right] \tag{D-1}$$

For axisymmetric geometry, the partial differential equation

$$\frac{\partial f}{\partial t} + \frac{\partial F^z}{\partial z} + \frac{\partial F^r}{\partial r} + \psi = \frac{\partial}{\partial z}\left[C(z,r,t)\,\frac{\partial f}{\partial z}\right] + \frac{\partial}{\partial r}\left[D(z,r,t)\,\frac{\partial f}{\partial r}\right]$$

is represented by a difference equation which uses the same difference-derivative and coefficient definitions as are used above for the plane geometry. The additional term ψ is defined at the point (m,ℓ) for the time n (i.e., $\psi^n_{m,\ell}$). Therefore, the difference equation for an axisymmetric geometry is

$$f_{m,\ell}^{n+1} = f_{m,\ell}^{n} - \frac{K_1}{2}\left[F_{m+1,\ell}^{z} - F_{m-1,\ell}^{z} + F_{m,\ell+1}^{r} - F_{m,\ell-1}^{r}\right]^{n} - \psi_{m,\ell}^{n} +$$

$$\frac{1}{2}\left[\alpha_{m+\frac{1}{2},\ell}^{n}\left(f_{m+1,\ell} - f_{m,\ell}\right)^{n} - \alpha_{m-\frac{1}{2},\ell}^{n}\left(f_{m,\ell} - f_{m-1,\ell}\right)^{n} + \right.$$

$$\left. \beta_{m,\ell+\frac{1}{2}}^{n}\left(f_{m,\ell+1} - f_{m,\ell}\right)^{n} - \beta_{m,\ell-\frac{1}{2}}^{n}\left(f_{m,\ell} - f_{m,\ell-1}\right)^{n} \right]. \tag{D-2}$$

Because a square net is used, the stability development gives

$$\alpha_{m,\ell}^{n} = \beta_{m,\ell}^{n} .$$

This simplification is used to record the equations in the text.

APPENDIX E

STABILITY STUDY OF THE DIFFERENCE EQUATIONS

The difference equations derived in Appendix E are nonlinear equations for which no general method has been developed to determine stability. The common approach to a stability study of nonlinear equations is to linearize the equations and use the methods for stability analysis of linear equations, namely, determine the effect on the solution of small changes in the coefficients [30, p. 223]. Therefore, a stability study for the plane geometry is made by linearizing the general field equation and applying the Fourier stability technique, as outlined by Rusanov [38].

The general field equation (D-1) for the plane geometry (from Appendix D)

$$f^{n+1}_{m,\ell} = f^{n}_{m,\ell} - \frac{K_1}{2}\left[F^{x}_{m+1,\ell} - F^{x}_{m-1,\ell} + F^{y}_{m,\ell+1} - F^{y}_{m,\ell-1}\right]^{n} +$$

$$\frac{\tau}{h_1^{2}}\left[A^{n}_{m+\frac{1}{2},\ell}\left(f_{m+1,\ell} - f_{m,\ell}\right)^{n} - A^{n}_{m-\frac{1}{2},\ell}\left(f_{m,\ell} - f_{m-1,\ell}\right)^{n} +\right.$$

$$\left.B^{n}_{m,\ell+1}\left(f_{m,\ell+1} - f_{m,\ell}\right)^{n} - B^{n}_{m,\ell-1}\left(f_{m,\ell} - f_{m,\ell-1}\right)\right] \tag{E-1}$$

is linearized by assuming all dependent variables (ρ, u, v, e, p) depend on a function $\varphi^{n}_{m,\ell}$ at a point and by referring the coefficients of the variations of $\varphi^{n}_{m,\ell}$ to one point. If $\delta\varphi^{n}_{m,\ell}$ denotes the variation of $\varphi^n_{m,\ell}$, equation (E-1) becomes

$$\frac{df}{d\varphi}\,\delta\varphi^{n+1}_{m,\ell} = \frac{df}{d\varphi}\,\delta\varphi^{n}_{m,\ell} - \frac{K_1}{2}\left[\frac{dF^x}{d\varphi}\left(\delta\varphi_{m+1,\ell} - \delta\varphi_{m-1,\ell}\right)^n + \frac{dF^y}{d\varphi}\left(\delta\varphi_{m,\ell+1} - \delta\varphi_{m,\ell-1}\right)^n\right] + \frac{\alpha}{2}\frac{df}{d\varphi}\left(\delta\varphi_{m+1,\ell} - 2\delta\varphi_{m,\ell} + \delta\varphi_{m-1,\ell}\right)^n + \frac{\beta}{2}\frac{df}{d\varphi}\left(\delta\varphi_{m,\ell+1} - 2\delta\varphi_{m,\ell} + \delta\varphi_{m,\ell-1}\right)^n \tag{E-2}$$

where

$$\frac{\alpha^n_{m,\ell}}{2} = \frac{\tau\, A^n_{m,\ell}}{h_1^2}$$

and

$$\frac{\beta^n_{m,\ell}}{2} = \frac{\tau\, B^n_{m,\ell}}{h_1^2}\ .$$

A stability criterion may now be obtained for the linearized equation (E-2) by using the Fourier technique. The technique considers the propagation effect of a set of errors at time zero, which on the initial plane are represented by a Fourier series. The series is finite and the number of terms is equal to the number of net points in the initial plane. The propagation effect of a single term with an initial error $\delta\varphi^o_{o,o}$ which is represented by

$$\delta\varphi^n_{m,\ell} = \xi^n\, e^{i(\psi_1 m + \psi_2 \ell)}\ \delta\varphi^o_{o,o}\ ,$$

may be considered if ψ_1 and ψ_2 are any real numbers. The propagated error $\delta\varphi^n_{m,\ell}$ must be bounded for equation (E-1) to be stable; therefore, the condition

$$|\xi| \leq 1$$

must be satisfied. Applying the relation for $\delta\varphi^n_{m,\ell}$ to equation (E-2) gives

$$\frac{df}{d\varphi}(\xi - 1) + i K_1 \left[\frac{dF^x}{d\varphi} \sin \psi_1 + \frac{dF^y}{d\varphi} \sin \psi_2 \right] +$$

$$2 \left[\alpha \sin^2 \left(\frac{\psi_1}{2}\right) + \beta \sin^2 \left(\frac{\psi_2}{2}\right)\right] \frac{df}{d\varphi} = 0 . \qquad \text{(E-3)}$$

With the definitions of f, F^x and F^y in Equation (E-3), four equations are developed and solved simultaneously to give an equation for ξ in the form

$$\zeta \left[\zeta^2 + c^2 K_1^{\,2} (\sin^2 \psi_1 + \sin^2 \psi_2)\right] = 0 \qquad \text{(E-4)}$$

where

$$\zeta = \xi - 1 + iK_1 (u \sin \psi_1 + v \sin \psi_2) + 2\left[\alpha \sin^2 \left(\frac{\psi_1}{2}\right) + \beta \sin^2 \left(\frac{\psi_2}{2}\right)\right]$$

c = speed of sound.

Solving equation (E-4) for the roots of ξ gives

$$\xi_s = 1 - 2 \left[\alpha \sin^2 \left(\frac{\psi_1}{2}\right) + \beta \sin^2 \left(\frac{\psi_2}{2}\right)\right] -$$

$$iK_1 \left[u \sin \psi_1 + v \sin \psi_2 + sc \sqrt{\sin^2 \psi_1 + \sin^2 \psi_2}\right] \qquad \text{(E-5)}$$

where s may have the values -1, 0, and 1.

The roots of ξ_s for $\psi_1 = \psi_2 = \pi$ reduce to

$$\xi_s = 1 - 2(\alpha + \beta) .$$

Substitution of the relation into the condition

$$|\xi| \leq 1$$

gives

$$0 \leq \alpha + \beta \leq 1 \tag{E-6}$$

where

$$|\xi| = \pm\sqrt{[1 - 2(\alpha + \beta)]^2}$$

$$= \pm [1 - 2(\alpha + \beta)] \ .$$

When considering the roots of ξ_s for small values of ψ_1 and ψ_2, equation (E-5) becomes

$$\xi_s = 1 - \frac{1}{2} (\alpha \psi_1^2 + \beta \psi_2^2) - iK_1 \left[u\psi_1 + v\psi_2 + sc\sqrt{\psi_1^2 + \psi_2^2}\right].$$

Substitution of the relation into the condition

$$1 - |\xi|^2 \geq 0$$

gives

$$\alpha\psi_1^2 + \beta\psi_2^2 - K_1^2 \left[u\psi_1 + v\psi_2 + sc\sqrt{\psi_1^2 + \psi_2^2}\right]^2 \geq 0 \ .$$

This inequality may be put in the form

$$\alpha \cos^2 \theta + \beta \sin^2 \theta \geq \frac{\sigma^2}{2}$$

with

$$\cos\theta = \frac{\psi_1}{\sqrt{\psi_1^2 + \psi_2^2}} ,$$

$$\sin\theta = \frac{\psi_2}{\sqrt{\psi_2^2 + \psi_1^2}}$$

and

$$\begin{aligned}\sigma &= K(u \cos\theta + v \sin\theta + sc)\\ &= K(w + c) \qquad\qquad \text{(Courant Number).}\end{aligned}$$

If the net spacing is square, the "dissipative" terms should have an equal effect in the x and y directions; therefore, the "dissipative" coefficients are taken to be equal (i.e., $\alpha = \beta$). With this condition, the inequality becomes

$$\alpha \geq \frac{\sigma^2}{2} . \tag{E-7}$$

The two conditions (E-6) and (E-7) give

$$\sigma^2 \leq 2\alpha \leq 1$$

as the bounds on the "dissipative" coefficients for which stability will exist. If α is defined to be the straight line

$$\alpha = \frac{\omega\sigma}{2}$$

where ω is a parameter, the condition $|\xi| \leq 1$ is satisfied for all ψ_1 and ψ_2 if the condition

$$\sigma \leq \omega \leq \frac{1}{\sigma}$$

is satisfied. This is the stability criterion specified by Rusanov and stated in the text of Chapter IV.

APPENDIX F

DERIVATION OF THE DIFFERENCE EQUATIONS FOR BOUNDARIES

The boundary difference equations may be derived from the general field difference equation by using a reflection principle. For flow along a wall, the equations must insure that no steep gradients perpendicular to the wall exist due to the addition of the "dissipative" terms. The difference equation for a point representing a solid boundary will first be derived for the plane geometry and then extended to the axisymmetric geometry. Also, the difference equation will be derived for an axis point for the axisymmetric geometry.

For the plane geometry, the general field equation is

$$f^{n+1}_{m,\ell} = f^{n}_{m,\ell} - \frac{K_1}{2}\left[F^x_{m+1,\ell} - F^x_{m-1,\ell} + F^y_{m,\ell+1} - F^y_{m,\ell-1}\right]^n +$$

$$\frac{1}{2}\left[\Phi_{m+\frac{1}{2},\ell} - \Phi_{m-\frac{1}{2},\ell} + \Phi_{m,\ell+\frac{1}{2}} - \Phi_{m,\ell-\frac{1}{2}}\right] . \qquad \text{(F-1)}$$

The reflection principle may be applied to a wall parallel to the x axis by constructing a line of virtual points within the wall. The point (m,ℓ) is considered on such a wall with flow above.

The conservation variables are defined at the virtual point $(m,\ell-1)$ by the reflection rule

$$\rho_{m,\ell+1} = \rho_{m,\ell-1} ; \qquad v_{m,\ell+1} = - v_{m,\ell-1}$$

$$u_{m,\ell+1} = u_{m,\ell-1} ; \qquad e_{m,\ell+1} = e_{m,\ell-1} .$$

Also, to insure that the effect perpendicular to the wall of the "dissipative" mechanism is eliminated, the terms $\Phi_{m,\ell+1}$ and $\Phi_{m,\ell-1}$ which are the difference terms that approximate the derivative

$$\frac{\partial}{\partial y}\left[B \frac{\partial f}{\partial y} \right]$$

are removed from the field equation. With the above change in Equation (F-1), the boundary difference equation for flow along a wall parallel to the x axis is

$$f^{n+1}_{m,\ell} = f^{n}_{m,\ell} - \frac{K_1}{2}\left[F^x_{m+1,\ell} - F^x_{m-1,\ell}\right]^n \mp K_1 \left[F^y_{m,\ell\pm1}\right]^n +$$

$$\frac{1}{2}\left[\Phi_{m+\frac{1}{2},\ell} - \Phi_{m-\frac{1}{2},\ell}\right]$$

where the sign convention is the same as that used in the text.

For flow along a wall that is parallel to the y axis, the reflection rule for the density and energy variables is the same, but the role of the velocity variables is interchanged. Therefore, the reflection rule is now

$$\rho_{m+1,\ell} = \rho_{m-1,\ell} ; \qquad v_{m+1,\ell} = v_{m-1,\ell}$$

$$u_{m+1,\ell} = - u_{m-1,\ell} ; \qquad e_{m+1,\ell} = e_{m-1,\ell}$$

for a point (m,ℓ). The $\Phi_{m+\frac{1}{2},\ell}$ and $\Phi_{m-\frac{1}{2},\ell}$ terms, which correspond to the derivative

$$\frac{\partial}{\partial x}\left[A \frac{\partial f}{\partial x} \right],$$

are neglected to remove the "dissipative" effect perpendicular to the wall. With application of these conditions to (F-1), the difference equation for flow along a wall parallel to the y axis is

$$f^{n+1}_{m,\ell} = f^{n}_{m,\ell} \mp K_1 \left[F^{x}_{m\pm 1,\ell} \right]^n - \frac{K_1}{2}\left[F^{y}_{m,\ell+1} - F^{y}_{m,\ell-1}\right]^n +$$

$$\frac{1}{2}\left[\Phi_{m,\ell+\frac{1}{2}} - \Phi_{m,\ell-\frac{1}{2}}\right].$$

The reflection principle and condition on the "dissipative" terms may also be applied to the axisymmetric geometry field equation

$$f^{n+1}_{m,\ell} = f^{n}_{m,\ell} - \frac{K_1}{2}\left[F^{z}_{m+1,\ell} - F^{z}_{m-1,\ell} + F^{r}_{m,\ell+1} - F^{r}_{m,\ell-1}\right]^n - \tau\, \psi^{n}_{m,\ell} +$$

$$\frac{1}{2}\left[\Phi_{m+\frac{1}{2},\ell} - \Phi_{m-\frac{1}{2},\ell} + \Phi_{m,\ell+\frac{1}{2}} - \Phi_{m,\ell-\frac{1}{2}}\right] \qquad \text{(F-2)}$$

to obtain the difference equations for boundary points. In a manner similar to that used for the plane geometry, the difference equation for points on a wall parallel to the z axis is

$$f^{n+1}_{m,\ell} = f^{n}_{m,\ell} - \frac{K_1}{2}\left[F^{z}_{m+1,\ell} - F^{z}_{m-1,\ell} \right]^n \mp K_1 \left[F^{r}_{m,\ell\pm 1} \right]^n -$$

$$\tau\, \psi^{n}_{m,\ell} + \frac{1}{2}\left[\Phi_{m+\frac{1}{2},\ell} - \Phi_{m-\frac{1}{2},\ell}\right]$$

and on a wall parallel to the r axis is

$$f^{n+1}_{m,\ell} = f^{n}_{m,\ell} \mp K_1 \left[F^{z}_{m\pm1,\ell} \right]^{n} - \frac{K_1}{2} \left[F^{r}_{m+1,\ell} - F^{r}_{m-1,\ell} \right]^{n} -$$

$$\tau\, \psi^{n}_{m,\ell} + \frac{1}{2} \left[\Phi_{m,\ell+\frac{1}{2}} - \Phi_{m,\ell-\frac{1}{2}} \right] .$$

For the axis of symmetry, only the reflection principle is applied to the field equation (F-2), because shock waves may impinge on the axis. The difference equation for an axis of symmetry at $r = 0$ is

$$f^{n+1}_{m,o} = f^{n}_{m,o} - \frac{K_1}{2} \left[F^{z}_{m+1,o} - F^{z}_{m-1,o} \right]^{n} - K_1 \left[F^{r}_{m,1} \right] - \tau\, \hat{\psi}^{n}_{m,o} +$$

$$\frac{1}{2} \left[\Phi_{m+\frac{1}{2},o} - \Phi_{m-\frac{1}{2},o} + 2\Phi_{m,\frac{1}{2}} \right] .$$

The element v/r in the term $\hat{\psi}^{n}_{m,o}$ is approximated by its value at $(m,1)$ because of its indeterminacy at $r = 0$.

APPENDIX G

INITIAL CONDITIONS FOR THE CENTER OF A MOVING SHOCK WAVE

In the finite difference calculation of a moving shock wave, the wave has an initial thickness of two mesh spaces.

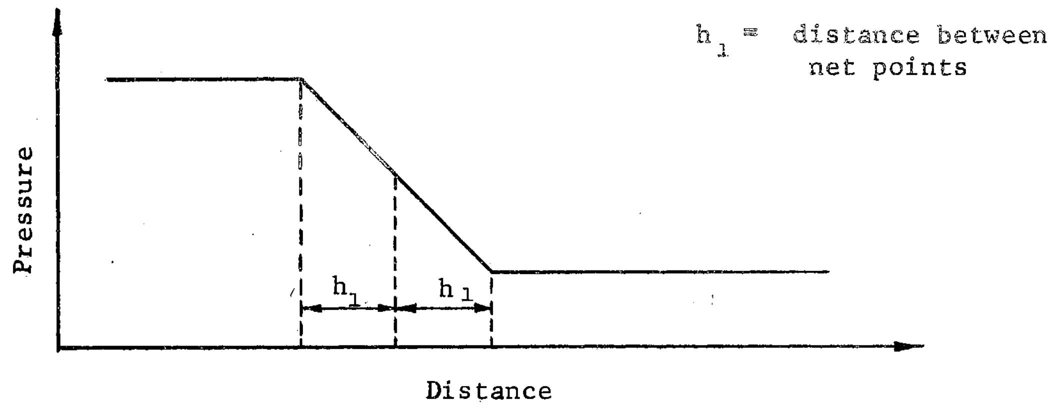

The pressure at the shock center is calculated as the arithmetic mean of the pressure in front of and behind the wave. Various ways of determining the remaining properties at the shock center have been investigated, but only one method has proved satisfactory. This method is described below.

The basic parameters on both sides of a shock wave propagating into a still medium are assumed to be known.

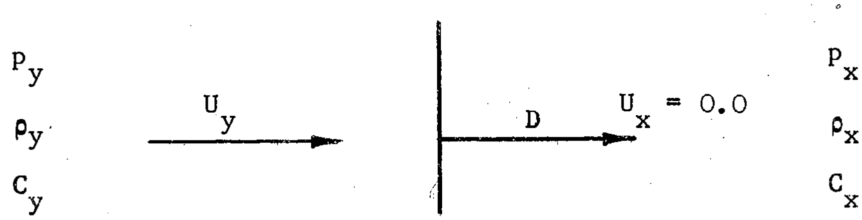

The properties at the center of the shock wave are evaluated by assuming the shock is divided into two shock waves (I and II).

Shock I

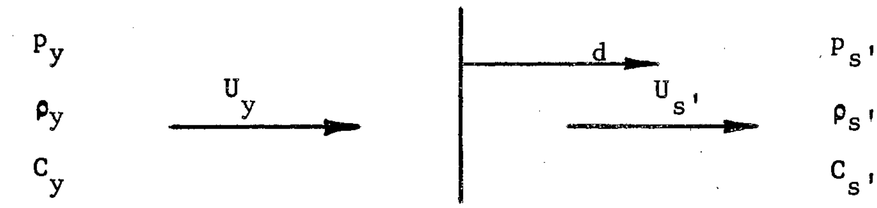

Shock II

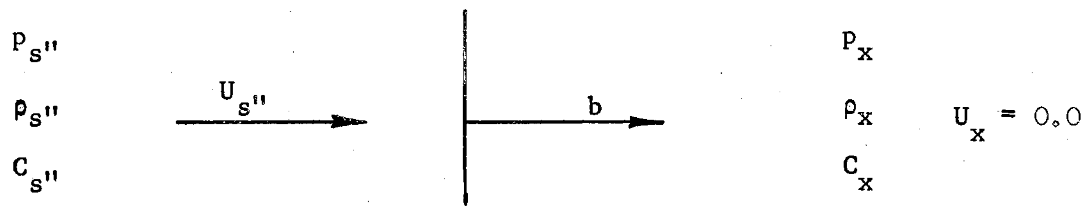

The pressures $p_{s'}$ and $p_{s''}$ are given by

$$p_{s'} = p_{s''} = \frac{(p_y + p_x)}{2.0} .$$

The two shock waves are now transformed to a coordinate system relative to the respective shock wave.

Shock I

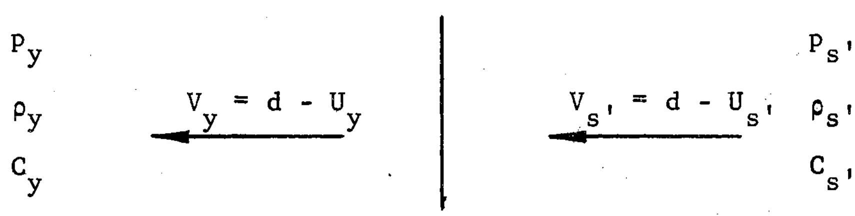

Shock II

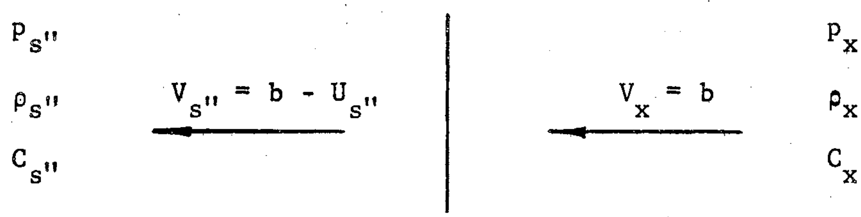

Tables (NACA 1135) may be used to obtain the values of density and temperature in states s' and s". Also found in the tables are the Mach number values M_{V_x}, $M_{V_{s'}}$, M_{V_y}, and $M_{V_{s''}}$. The particle velocity $U_{s'}$ is found from

$$U_{s'} = d - V_{s'}$$

where $d = V_y + U_y = M_{V_y} C_y + U_y$

$$V_{s'} = M_{V_{s'}} C_{s'}$$

and the particle velocity $U_{s''}$ is

$$U_{s''} = b - V_{s''}$$

where $b = V_x = M_{V_x} C_x$

$$V_{s''} = M_{V_{s''}} C_{s''} \quad .$$

The properties at the shock center are the average of the properties in states s' and s".

$$p_s = (p_x + p_y)/2$$

$$\rho_s = (\rho_{s'} + \rho_{s''})/2$$

$$U_s = (U_{s'} + U_{s''})/2$$

The s values are the initial conditions at the shock center. This method is shown on the temperature-entropy diagram below.

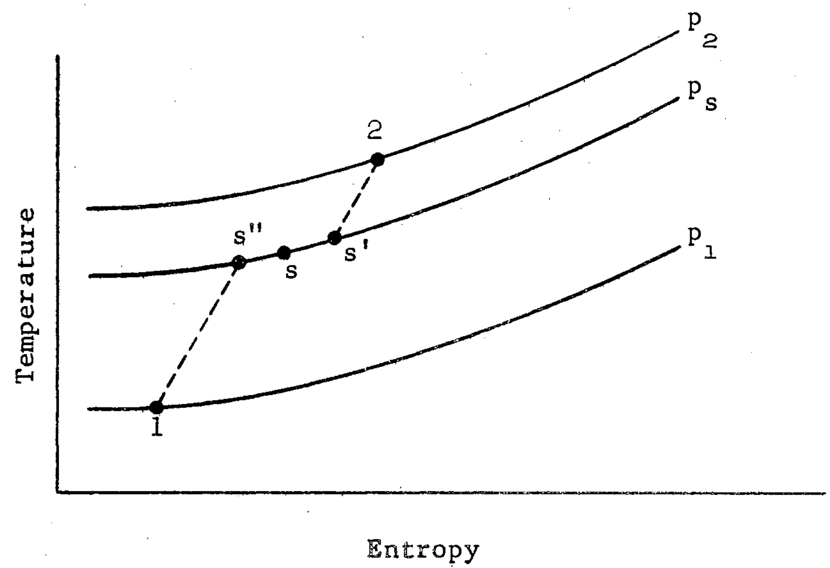

The following numerical example may be helpful in understanding the method for obtaining the initial shock center properties. Consider a plane shock propagating into a still medium. From compressible flow Table [45], the conditions for a shock of strength $p_y/p_x = 4.0$ is

$p_y = 4.00$	$U_y = 1.34 \longrightarrow$	$D = 2.24 \longrightarrow$	$p_x = 1.0$
$\rho_y = 2.50$			$\rho_x = 1.0$
$C_y = 1.50$			$C_x = \sqrt{k} = 1.18$

where the values are dimensionless according to the method of Appendix C. For shocks I and II in a coordinate system relative to the shock the properties are found from the flow tables.

Shock I

$p_y = 4.00$	$\longleftarrow V_y = ?$	$\longleftarrow V_{s'} = ?$	$p_{s'} = 2.5$
$\rho_y = 2.50$			$\rho_{s'} = ?$
$C_y = 1.50$			$C_{s'} = ?$

For a pressure ratio of

$$\frac{p_y}{p_{s'}} = \frac{4.00}{2.5} = 1.6$$

the compressible flow tables give

$$\frac{\rho_y}{\rho_{s'}} = 1.39, \qquad M_{V_y} = 0.82, \qquad M_{V_{s'}} = 1.23.$$

Therefore, the unknown quantities are determined, giving

$$\rho_{s'} = 1.79,$$

$$V_y = M_{V_y} \qquad C_y = 1.23$$

$$C_{s'} = 1.40$$

$$V_{s'} = M_{V_{s'}} \cdot C_{s'} = 1.72.$$

Similarly for Shock II the properties become

Shock II

$p_{s''} = 2.5$ | $p_x = 1.0$

$\rho_{s''} = 1.88$ $\quad \xleftarrow{V_{s''} = .95}$ | $\xleftarrow{V_x = 1.79}$ $\quad \rho_x = 1.0$

$C_{s''} = 1.37$ | $C_x = 1.18$.

Transforming Shock I and II to a coordinate system relative to state x gives for Shock I

$p_y = 4.00$ | $p_{s'} = 2.5$

$\rho_y = 2.50$ $\quad \xrightarrow{U_y = 1.34}$ | $\xrightarrow{d = ?}$ $\quad \xrightarrow{U_{s'} = ?}$ $\quad \rho_{s'} = 1.79$

$C_y = 1.50$ | $C_{s'} = 1.40$,

where the velocities d and $U_{s'}$ are

$$d = V_y + U_y$$

$$= 1.23 + 1.34 = 2.57$$

and

$$U_{s'} = d - V_{s'}$$

$$= 2.57 - 1.72 = 0.85$$

and for Shock II gives

$$\begin{array}{lcc|ccl} p_{s''} = 2.50 & & & & & p_x = 1.0 \\ \rho_{s''} = 1.88 & \xrightarrow{U_{s''} = 0.83} & & \xrightarrow{b = 1.79} & \xrightarrow{U_x = 0.0} & \rho_x = 1.0 \\ C_{s''} = 1.37 & & & & & C_x = 1.18 \,. \end{array}$$

The properties for the state s are then given to be

$$p_s = p_{s'} = p_{s''} = 2.5$$

$$\rho_s = \frac{(\rho_{s'} + \rho_{s''})}{2} = 1.84$$

$$U_s = \frac{(U_{s'} + U_{s''})}{2} = 0.84 \,.$$

APPENDIX H

COMPUTER PROGRAMS FOR STILL AND CROSSFLOW SOLUTIONS

In the following sections complete listings of the programs for both the still and crossflow problems are presented in Fortran IV notation for use on a CDC 3600 computer. Definitions for quantities called as input and for those received as output are given before each listing.

The geometry of the still case was divided into three spaces

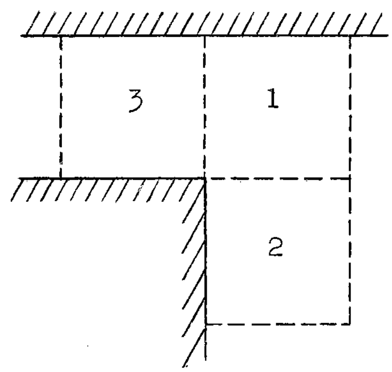

and the crossflow geometry was divided into four spaces.

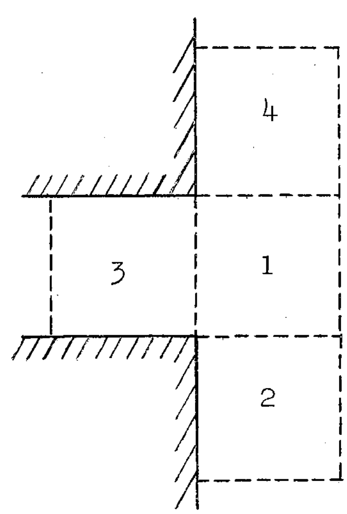

The spaces 1, and 2 for the still solution and spaces 1, 2, and 4 for the crossflow solution represent the field in front of the initial shock which is located along the right most column of net points in space 3. The remaining points of space 3 represent the uniform field behind the shock.

Both programs are designed to initialize the entire flow field, compute the unknown quantities for the following time plane, interpolate constant property lines, and print the coordinates of the constant property lines. Also, a technique in both programs allows the entire field for a given time plane to be stored on a designated tape which may be used at a later date as input conditions to compute field values for subsequent time increments.

Still Solution Computer Program

Before presenting the program listing, the following input and output variables are defined.

(1) JUMP = a number which is defined to indicate the source of input data. (For JUMP = 1.0 only card input is used and calculations begin at the first time plane. JUMP = 2.0 denotes use of storage tape and card input for calculations of subsequent time planes.)

(2) DP = density for the field in front of the shock.

(3) DN = density of the field behind the shock.

(4) UP = x- or z-velocity in front of the shock for the respective plane or axisymmetric geometry.

(5) UN = x- or z-velocity behind the shock.

(6) VP = y- or r-velocity in front of the shock for the respective plane or axisymmetric geometry.

(7) VN = y- or r-velocity behind the shock.

(8) PP = pressure in front of the shock.

(9) PN = pressure behind the shock.

(10) DS = density at shock center.

(11) US = x- or z-velocity at shock center.

(12) VS = y- or r-velocity at shock center.

(13) PS = pressure at shock center.

(14) VAR = number of time increments to be computed before a set of output data is recorded. This number is also used to determine the number of subsequent time increments to be computed for storage tape input.

(15) Z = a number to denote type of geometry (Z = 0.0 refers to a plane geometry and Z = 1.0 to an axisymmetric).

(16) GAM = specific heat ratio.

(17) SIG = Courant number (σ), used for the stability condition.

(18) OMEG = the stability parameter ω.

(19) TMAX = the number of time increments to be computed for an input number for JUMP = 1.0, and the number of time increments that has been computed for JUMP = 2.0. TMAX as an output number is the total number of time increments computed.

(20) M = the number of the storage tape unit and is a fixed point number. A value of this variable is read out on the last line of output and should correspond to the input value.

(21) L = a number assigned to a scratch tape for use during computation.

(22) CONST = the maximum value of the quantity (w + c) for JUMP = 1.0 and for JUMP = 2.0 the value is given by the output from the previous computation run.

(23) PPCH = the difference in pressure between two constant pressure lines.

(24) PVCH = the difference in velocity between two constant velocity lines.

(25) TIME = an input value only for JUMP = 2.0 and is the next time to be computed. This value is given on the last line of output data from the previous run. The value of TIME read out in statement 226 corresponds to time number for the given output data.

(26) N = the space number.

(27) CAP = the quantity K.

(28) AXY = an assigned coordinate for a constant pressure value.

(29) PA = an interpolated coordinate for a constant pressure value.

(30) AAY = an assigned coordinate for a constant velocity value.

(31) XAA = an interpolated coordinate for a constant velocity value.

(32) DIR = a value of the sine of the angle between the velocity vector and the x direction.

All quantities defined above must be defined by a decimal value except items (20) and (21). The program listing is given on page 160.

Program for the Crossflow Solution

With the exception of the following quantities, the definitions given in the first section of this appendix are valid in the program of the crossflow solution.

PROGRAM LISTING OF THE STILL SOLUTION

```
      PROGRAM STILL
C     MAIN PROGRAM--STILL--TWO DIMENSION AND AXISYMMETRIC
      INTEGER X
      DIMENSION DFD(30,30),DFDA(30,30),DYO(30),DXO(30),UFD(30,30),UFDA(3
     10,30),UYO(30),UXO(30),VFD(30,30),VFDA(30,30),VYO(30),VXO(30),EFD(3
     20,30),EFDA(30,30),EYO(30),EXO(30)
    1 FORMAT(8F10.5)
    3 FORMAT(4F10.5,2I3,F10.5)
    5 FORMAT(10H TIME NO= ,F10.5,9HSPACE NO=,I4,6HCAPA= ,F10.5,3HZ= ,F10
     1.5)
  101 FORMAT(    13H   PRESSURE= ,F10.5,16H    VEL MODULUS= ,F10.5)
  103 FORMAT(    46H    Y            X            Y            X        SINE)
  107 FORMAT(1X,10HINPUT DATA)
  105 FORMAT(    I3)
  109 FORMAT(1X,7H TMAX= ,F10.5,1X,4H M= ,I3,1X,8H CONS= ,F10.5,1X,7H TI
     1ME= ,F10.5)
  100 READ(1,105)JUMP
      IF (EOF,1) 555,557
  557 READ(1,1)DP,DN,UP,UN,VP,VN,PP,PN
      READ(1,1)DS,US,VS,PS,VAR,Z
      READ(1,3)GAM,SIG,OMEG,TMAX,M,L,CONST
      READ(1,1)PPCH,PVCH
      ID=30
      GO TO(548,550),JUMP
  550 READ(1,1)TIME
      REWIND L
      DO 568 N=1,3
      READ(M)((DFD(I,K),UFD(I,K),VFD(I,K),EFD(I,K),I=1,ID),K=1,ID)
      GO TO(568,570,572),N
  570 DO 562 K=1,ID
      DXO(K)=DFD(1,K)
      UXO(K)=UFD(1,K)
      VXO(K)=VFD(1,K)
  562 EXO(K)=EFD(1,K)
      GO TO 568
  572 DO 564 K=1,ID
      DYO(K)=DFD(K,ID)
      UYO(K)=UFD(K,ID)
      VYO(K)=VFD(K,ID)
  564 EYO(K)=EFD(K,ID)
      GO TO 568
  568 WRITE(L)((DFD(I,K),UFD(I,K),VFD(I,K),EFD(I,K),I=1,ID),K=1,ID)
      REWIND L
      REWIND M
      DO 566 N=1,3
      WRITE(L)((DFD(I,K),UFD(I,K),VFD(I,K),EFD(I,K),I=1,ID),K=1,ID)
      READ(M)((DFD(I,K),UFD(I,K),VFD(I,K),EFD(I,K),I=1,ID),K=1,ID)
  566 CONTINUE
      REWIND L
      DELT =TMAX+VAR
      TMAX=2.0*VAR +TMAX
      GO TO 553
  548 DELT=VAR
  553 X=ID-1
      GO TO(556,558),JUMP
  556 PP=DP*(UP*UP+VP*VP)/2.0+PP/(GAM-1.0)
```

PROGRAM LISTING OF THE STILL SOLUTION (Continued)

```
      EN=DN*(UN*UN+VN*VN)/2.0+PN/(GAM-1.0)
      ES=DS*(US*US+VS*VS)/2.0+PS/(GAM-1.0)
      DO 2I=1,ID
      DYO(I)=DS
      UYO(I)=US
      VYO(I)=VS
      EYO(I)=ES
      DXO(I)=DP
      UXO(I)=UP
      VXO(I)=VP
    2 EXO(I)=EP
      REWIND M
      REWIND L
 2002 DO 2000J=1,3
      GO TO(208,208,210),J
  208 DO10I=1,ID
      DO 10 K=1,ID
      DFD(I,K)=DP
      UFD(I,K)=UP
      VFD(I,K)=VP
   10 EFD(I,K)=EP
      GO TO 2000
  210 DO 14I=1,ID
      DFD(I,ID)=DS
      UFD(I,ID)=US
      VFD(I,ID)=VS
      EFD(I,ID)=ES
      DO 14K=1,X
      DFD(I,K)=DN
      UFD(I,K)=UN
      VFD(I,K)=VN
   14 EFD(I,K)=EN
 2000 WRITE(M)((DFD(I,K),UFD(I,K),VFD(I,K),EFD(I,K),I=1,ID),K=1,ID)
      TIME=1.0
  558 REWIND M
      AFIX=0.0
   16 DO 2004N=1,3
      READ (M)((DFD(I,K),UFD(I,K),VFD(I,K),EFD(I,K),I=1,ID),K=1,ID)
      CAP=SIG/CONST
      GO TO(214,216,218),N
  214 CALL FIELD(DFDA(1,1),UFDA(1,1),VFDA(1,1),EFDA(1,1),CAP,OMEG,GAM,DF
     1D(1,1),DYO(1)   ,DFD(1,2),DFD(2,1),DYO(1),UFD(1,1),UYO(1)   ,UFD(1,2
     2),UFD(2,1),UYO(1),VFD(1,1),VYO(1)   ,VFD(1,2),VFD(2,1),VYO(1),EFD(1
     3,1),EYO(1)   ,EFD(1,2),EFD(2,1),EYO(1),3,1,Z)
      CALL FIELD(DFDA(ID,1),UFDA(ID,1),VFDA(ID,1),EFDA(ID,1),CAP,OMEG,GA
     2M,DFD(ID,1),DFD(X,1),DFD(ID,2),DXO(1),DYO(ID),UFD(ID,1),UFD(X,1),U
     3FD(ID,2),UXO(1),UYO(ID),VFD(ID,1),VFD(X,1),VFD(ID,2),VXO(1),VYO(ID
     4),EFD(ID,1),EFD(X,1),EFD(ID,2),EXO(1),EYO(ID),1,ID,Z)
      DO 18I=2,X
      CALL FIELD(DFDA(I,1),UFDA(I,1),VFDA(I,1),EFDA(I,1),CAP,OMEG,GAM,DF
     1D(I,1),DFD(I-1,1),DFD(I,2),DFD(I+1,1),DYO(I),UFD(I,1),UFD(I-1,1),U
     2FD(I,2),UFD(I+1,1),UYO(I),VFD(I,1),VFD(I-1,1),VFD(I,2),VFD(I+1,1),
     3VYO(I),EFD(I,1),EFD(I-1,1),EFD(I,2),EFD(I+1,1),EYO(I),1,I,Z)
      CALL FIELD(DFDA(ID,I),UFDA(ID,I),VFDA(ID,I),EFDA(ID,I),CAP,OMEG,GA
     2M,DFD(ID,I),DFD(X,I),DFD(ID,I+1),DXO(I),DFD(ID,I-1),UFD(ID,I),UFD(
     3X,I),UFD(ID,I+1),UXO(I),UFD(ID,I-1),VFD(ID,I),VFD(X,I),VFD(ID,I+1)
```

PROGRAM LISTING OF THE STILL SOLUTION (Continued)

```
     4,VXO(I),VFD(ID,I-1),EFD(ID,I),EFD(X,I),EFD(ID,I+1),EXO(I),EFD(ID,I
     5-1),1,ID,Z)
      GO TO 37
   18 CONTINUE
      GO TO 212
   37 CALL FIELD(DFDA(1,I),UFDA(1,I),VFDA(1,I),EFDA(1,I),CAP,OMEG,GAM,DF
     2D(1,I),DFD(1,I),DFD(1,I+1),DFD(2,I),DFD(1,I-1),UFD(1,I),UFD(1,I),U
     3FD(1,I+1),UFD(2,I),UFD(1,I-1),VFD(1,I),VFD(1,I),VFD(1,I+1),VFD(2,I
     4),VFD(1,I-1),EFD(1,I),EFD(1,I),EFD(1,I+1),EFD(2,I),EFD(1,I-1),3,1,
     5Z)
      GO TO (18,32,44),N
  216 NO=ID+1
      CALL FIELD(DFDA(1,1),UFDA(1,1),VFDA(1,1),EFDA(1,1),CAP,OMEG,GAM,DF
     1D(1,1),DXO(1),DFD(1,2),DFD(2,1),DFD(1,1),UFD(1,1),UXO(1),UFD(1,2),
     2UFD(2,1),UFD(1,1),VFD(1,1),VXO(1),VFD(1,2),VFD(2,1),VFD(1,1),EFD(1
     3,1),EXO(1),EFD(1,2),EFD(2,1),EFD(1,1),2,NO,Z)
      DO 32I=2,X
   95 NO=ID+I
      CALL FIELD(DFDA(I,1),UFDA(I,1),VFDA(I,1),EFDA(I,1),CAP,OMEG,GAM,DF
     1D(I,1),DFD(I-1,1),DFD(I,2),DFD(I+1,1),DFD(I,1),UFD(I,1),UFD(I-1,1)
     2,UFD(I,2),UFD(I+1,1),UFD(I,1),VFD(I,1),VFD(I-1,1),VFD(I,2),VFD(I+1
     3,1),VFD(I,1),EFD(I,1),EFD(I-1,1),EFD(I,2),EFD(I+1,1),EFD(I,1),2,NO
     4,Z)
      NO=ID+1
   32 CALL FIELD(DFDA(1,I),UFDA(1,I),VFDA(1,I),EFDA(1,I),CAP,OMEG,GAM,DF
     1D(1,I),DXO(I),DFD(1,I+1),DFD(2,I),DFD(1,I-1),UFD(1,I),UXO(I),UFD(1
     2,I+1),UFD(2,I),UFD(1,I-1),VFD(1,I),VXO(I),VFD(1,I+1),VFD(2,I),VFD(
     31,I-1),EFD(1,I),EXO(I),EFD(1,I+1),EFD(2,I),EFD(1,I-1),1,NO,Z)
      GO TO 212
  218 CALL FIELD(DFDA(1,ID),UFDA(1,ID),VFDA(1,ID),EFDA(1,ID),CAP,OMEG,GA
     2M,DFD(1,ID),DFD(1,ID),DYO(1),DFD(2,ID),DFD(1,X),UFD(1,ID),UFD(1,ID
     3),UYO(1),UFD(2,ID),UFD(1,X),VFD(1,ID),VFD(1,ID),VYO(1),VFD(2,ID),V
     4FD(1,X),EFD(1,ID),EFD(1,ID),EYO(1),EFD(2,ID),EFD(1,X),3,1,Z)
      CALL FIELD(DFDA(ID,ID),UFDA(ID,ID),VFDA(ID,ID),EFDA(ID,ID),CAP,OME
     1G,GAM,DFD(ID,ID),DFD(X,ID),DYO(ID),DFD(ID,ID),DFD(ID,X),UFD(ID,ID)
     2,UFD(X,ID),UYO(ID),UFD(ID,ID),UFD(ID,X),VFD(ID,ID),VFD(X,ID),VYO(I
     3D),VFD(ID,ID),VFD(ID,X),EFD(ID,ID),EFD(X,ID),EYO(ID),EFD(ID,ID),EF
     4D(ID,X),4,ID,Z)
      DO 44I=2,X
      CALL FIELD(DFDA(ID,I),UFDA(ID,I),VFDA(ID,I),EFDA(ID,I),CAP,OMEG,GA
     1M,DFD(ID,I),DFD(X,I),DFD(ID,I+1),DFD(ID,I),DFD(ID,I-1),UFD(ID,I),U
     2FD(X,I),UFD(ID,I+1),UFD(ID,I),UFD(ID,I-1),VFD(ID,I),VFD(X,I),VFD(I
     3D,I+1),VFD(ID,I),VFD(ID,I-1),EFD(ID,I),EFD(X,I),EFD(ID,I+1),EFD(ID
     4,I),EFD(ID,I-1),4,ID,Z)
      GO TO 37
   44 CALL FIELD(DFDA(I,ID),UFDA(I,ID),VFDA(I,ID),EFDA(I,ID),CAP,OMEG,GA
     2M,DFD(I,ID),DFD(I-1,ID),DYO(I),DFD(I+1,ID),DFD(I,X),UFD(I,ID),UFD(
     3I-1,ID),UYO(I),UFD(I+1,ID),UFD(I,X),VFD(I,ID),VFD(I-1,ID),VYO(I),V
     4FD(I+1,ID),VFD(I,X),EFD(I,ID),EFD(I-1,ID),EYO(I),EFD(I+1,ID),EFD(I
     5,X),1,I,Z)
  212 JJ=2
      DO 24I=2,X
      DO 23K=2,X
      GO TO(542,540),JJ
  540 GO TO(300,302,300),N
  300 NO=I
```

PROGRAM LISTING OF THE STILL SOLUTION (Continued)

```
      GO TO 544
  302 NO=I+ID
 544  CALL FIELD(DFDA(I,K),UFDA(I,K),VFDA(I,K),EFDA(I,K),CAP,OMEG,GAM,DF
     1D(I,K),DFD(I-1,K),DFD(I,K+1),DFD(I+1,K),UFD(I,K-1),UFD(I,K),UFD(I-
     21,K),UFD(I,K+1),UFD(I+1,K),UFD(I,K-1),VFD(I,K),VFD(I-1,K),VFD(I,K+
     31),VFD(I+1,K),VFD(I,K-1),EFD(I,K),EFD(I-1,K),EFD(I,K+1),EFD(I+1,K)
     4,EFD(I,K-1),1,NO,Z)
  542 IF(DFDA(I,K).NE.DFDA(I,K-1))GO TO 538
      IF(UFDA(I,K).NE.UFDA(I,K-1))GO TO 538
      IF(VFDA(I,K).NE.VFDA(I,K-1))GO TO 538
      IF(EFDA(I,K).NE.EFDA(I,K-1))GO TO 538
      KIN = K
      DO 546 KY=KIN,X
      DFDA(I,KY)=DFD(I,KY)
      UFDA(I,KY)=UFD(I,KY)
      VFDA(I,KY)=VFD(I,KY)
 546  EFDA(I,KY)=EFD(I,KY)
      GO TO 24
  538 JJ=2
 23   CONTINUE
   24 CONTINUE
      DO 89 I=1,ID
      GO TO (80,80,82),N
   80 DFDA(I,ID)=DFD(I,ID)
      UFDA(I,ID)=UFD(I,ID)
      VFDA(I,ID)=VFD(I,ID)
      EFDA(I,ID)=EFD(I,ID)
      GO TO (89,81,82),N
   81 DFDA(ID,I)=DFD(ID,I)
      UFDA(ID,I)=UFD(ID,I)
      VFDA(ID,I)=VFD(ID,I)
      EFDA(ID,I)=EFD(ID,I)
      GO TO 89
   82 DFDA(I,1)=DFD(I,1)
      UFDA(I,1 )=UFD(I,1 )
      VFDA(I,1 )=VFD(I,1 )
      EFDA(I,1 )=EFD(I,1 )
       GO TO 89
   89 CONTINUE
      GO TO (220,222,224),N
  220 DO 30I=1,ID
      DXO(I)=DFD(ID,I)
      DYO(I)=DFD(I,1)
      UXO(I)=UFD(ID,I)
      UYO(I)=UFD(I,1)
      VXO(I)=VFD(ID,I)
      VYO(I)=VFD(I,1)
      EXO(I)=EFD(ID,I)
   30 EYO(I)=EFD(I,1)
      GO TO 226
  222 DO 38I=1,ID
      DXO(I)=DFDA(1,I)
      UXO(I)=UFDA(1,I)
      VXO(I)=VFDA(1,I)
   38 EXO(I)=EFDA(1,I)
      GO TO 226
```

PROGRAM LISTING OF THE STILL SOLUTION (Continued)

```
  224 DO 50I=1,ID
      DYO(I)=DFDA(I,ID)
      UYO(I)=UFDA(I,ID)
      VYO(I)=VFDA(I,ID)
   50 EYO(I)=EFDA(I,ID)
  226 WRITE(3,5)TIME,N,CAP,Z
      FIXMX=0.0
      DO 28I=1,ID
      DO 28K=1,ID
      UFD(I,K)=SQRTF(UFDA(I,K)*UFDA(I,K)+VFDA(I,K)*VFDA(I,K))
      DFD(I,K)=VFDA(I,K)/UFD(I,K)
      EFD(I,K)=(GAM-1.0)*(EFDA(I,K)-DFDA(I,K)*UFD(I,K)*UFD(I,K)/2.0)
      SS=SQRTF(GAM*EFD(I,K)/DFDA(I,K))
      VFD(I,K)=UFD(I,K)/SS
      SS=SS+UFD(I,K)
      IF(SS.LE.FIXMX)GO TO 28
      FIXMX=SS
   28 CONTINUE
      IF(FIXMX.LE.AFIX)GO TO 10000
      AFIX=FIXMX
10000 IF(TIME.NE.DELT) GO TO 2004
      PPV=PP+PPCH/2.0
      VPV=PVCH/2.0
      PA =XAA=AXY=AAY=0.0
  106 WRITE(3,101)PPV,VPV
      WRITE(3,103)
      DO112I=1,ID
      DO104K=1,ID
      DO116J=1,2
      IF(PPV.GT.PN)GO TO 132
      GO TO (118,120),J
  118 IF(K.EQ.1)GO TO 132
      A=EFD(I,K)
      B=EFD(I,K-1)
      GO TO 124
  120 IF(K.EQ.1)GO TO 132
      A=EFD(K,I)
      B=EFD(K-1,I)
      GO TO 124
  124 IF(A.GT.PPV)GO TO 122
      IF(B.GT.PPV)GO TO 126
      GO TO 132
  122 IF(B.GT.PPV)GO TO 132
  126 AXX=K
      AXY=I
      AX=K-1
      PA=AX+(AXX-AX)*(PPV-B)/(A-B)
  132 IF(VPV.GT.UN)GO TO 114
      GO TO (134,136),J
  134 IF(K.EQ.1)GO TO 114
      AA=UFD(I,K)
      BB=UFD(I,K-1)
      CC=VFDA(I,K)
      DD=VFDA(I,K-1)
      GO TO 138
  136 IF(K.EQ.1)GO TO 114
```

PROGRAM LISTING OF THE STILL SOLUTION (Continued)

```
      AA=UFD(K,I)
      BB=UFD(K-1,I)
      CC=VFDA(K,I)
      DD=VFDA(K-1,I)
  138 IF(AA.GT.VPV)GO TO 140
      IF(BB.GT.VPV)GO TO 142
      GO TO 114
  140 IF(BB.GT.VPV)GO TO 114
  142 AAX=K
      AAY=I
      XA=K-1
      XAA=XA+(AAX-XA)*(VPV-BB)/(AA-BB)
      UU=DD+(XAA-XA)*(CC-DD)/(AAX-XA)
      DIR=UU/VPV
  114 IF(PA.NE.0.0)GO TO 148
      IF(XAA.NE.0.0)GO TO 148
      GO TO 116
  148 GO TO (150,152),J
  150 WRITE(3,1)AXY,PA,AAY,XAA,DIR
      GO TO 154
  152 WRITE(3,1)PA,AXY,XAA,AAY,DIR
  154 PA=0.0
      XAA=0.0
  116 CONTINUE
  104 CONTINUE
  112 CONTINUE
      VPV=VPV+PVCH
      PPV=PPV+PPCH
  156 IF(VPV.LE.UN)GO TO 106
      IF(PPV.LE.PN)GO TO 106
 2004 WRITE(L)((DFDA(I,K),UFDA(I,K),VFDA(I,K),EFDA(I,K),I=1,ID),K=1,ID)
      IF(TIME.GT.TMAX)GO TO56
      IF(TIME.NE.DELT)GO TO 56
      DELT=DELT+VAR
   56 TIME=TIME+1.0
      IF(M.GT.L)GO TO 62
   60 M=I
      L=M-1
      GO TO 64
   62 L=M
      M=L-1
   64 REWIND L
      REWIND M
      CONST=AFIX
      IF(TIME.GT.TMAX)GO TO554
      AFIX=0.0
      GO TO 16
  554 WRITE(3,107)
      WRITE(3,109)TMAX,M,CONST,TIME
      GO TO 100
  555 CONTINUE
      END
```

PROGRAM LISTING OF THE STILL SOLUTION (Continued)

```
      SUBROUTINE FIELD(D1B,U1B,V1B,E1B,CAPA,OMEGA,SPHT,D1,D2,D3,D4,D5,U1
     1,U2,U3,U4,U5,V1,V2,V3,V4,V5,E1,E2,E3,E4,E5,K,NO,Z)
      Y=NO
      T1=U1*U1+V1*V1
      T2=U2*U2+V2*V2
      T3=U3*U3+V3*V3
      T4=U4*U4+V4*V4
      T5=U5*U5+V5*V5
      P1=(SPHT-1.0)*(E1-D1*T1/2.0)
      P2=(SPHT-1.0)*(E2-D2*T2/2.0)
      P3=(SPHT-1.0)*(E3-D3*T3/2.0)
      P4=(SPHT-1.0)*(E4-D4*T4/2.0)
      P5=(SPHT-1.0)*(E5-D5*T5/2.0)
      T1=SQRTF(SPHT*P1/D1)+SQRTF(T1)
      T2=SQRTF(SPHT*P2/D2)+SQRTF(T2)
      T3=SQRTF(SPHT*P3/D3)+SQRTF(T3)
      T4=SQRTF(SPHT*P4/D4)+SQRTF(T4)
      T5=SQRTF(SPHT*P5/D5)+SQRTF(T5)
      GO TO(301,302,312,302),K
  312 IF(Z.NE.1.0)GO TO 302
  301 R=2.0
      GO TO 303
  302 R=4.0
  303 GO TO(304,305,306,307),K
  304 A=1.0
      B=1.0
      C=1.0
      D=1.0
      E=1.0
      F=1.0
      G=1.0
      H=1.0
      GO TO308
  305 A=1.0
      B=0.0
      C=1.0
      D=0.0
      E=1.0
      F=2.0
      G=1.0
      H=0.0
      GO TO 308
  306 A=0.0
      B=1.0
      IF(Z.NE.1.0)GO TO 313
      C=2.0
      Y=1.0
      V1=V4
      GO TO 314
  313 C=0.0
  314 D=1.0
      E=0.0
      F=1.0
      G=2.0
      H=1.0
      GO TO 308
```

PROGRAM LISTING OF THE STILL SOLUTION (Continued)

```
307 A=0.0
    B=1.0
    C=0.0
    D=1.0
    E=2.0
    F=1.0
    G=0.0
    H=1.0
308 IF(Z.NE.1.0)GO TO 315
    E=-E
    G=-G
315 SUM=1.0-OMEGA*CAPA*(T1/8.+(A*T2+B*T3+C*T4+D*T5)/8.0)
     D1B=D1*SUM+OMEGA*CAPA*(A*T2*D2+B*T3*D3+C*T4*D4+D*T5*D5+(A*D2+B*D3+
    1C*D4+D*D5)*T1)/8.0-CAPA*(E*D2*V2+F*D3*U3-G*D4*V4-H*D5*U5)/2.82842-
    2CAPA*Z*V1*D1/(Y*1.414214)
     U1B=(D1*U1*SUM+OMEGA*CAPA*(A*T2*D2*U2+B*T3*D3*U3+C*T4*D4*U4+D*T5*D
    15*U5+(A*D2*U2+B*D3*U3+C*D4*U4+D*D5*U5)*T1)/8.0-CAPA*(E*D2*U2*V2+F*
    2(P3+D3*U3*U3)-G*D4*U4*V4-H*(P5+D5*U5*U5))/2.82842-CAPA*V1*D1*U1*Z/
    3(Y*1.414214))/D1B
     V1B=(D1*V1*SUM+OMEGA*CAPA*(A*T2*D2*V2+B*T3*D3*V3+C*T4*D4*V4+D*T5*D
    15*V5+(A*D2*V2+B*D3*V3+C*D4*V4+D*D5*V5)*T1)/8.0-CAPA*(E*(P2+D2*V2*V
    22)+F*D3*V3*U3-G*(P4+D4*V4*V4)-H*D5*V5*U5)/2.82842-CAPA*V1*D1*V1*Z/
    3(Y*1.414214))/D1B
     E1B=E1*SUM+OMEGA*CAPA*(A*T2*E2+B*T3*E3+C*T4*E4+D*T5*E5+(A*E2+B*E3+
    1C*E4+D*E5)*T1)/8.0-CAPA*(E*(E2+P2)*V2+F*(E3+P3)*U3-G*(E4+P4)*V4-H*
    2(E5+P5)*U5)/2.82842-CAPA*Z*V1*(E1+P1)/(Y*1.414214)
     GO TO(309,310,311,311),K
310 U1B=U1
    GO TO 309
311 V1B=0.0
309 RETURN
    END
```

(1) PDCH = the difference in density between two constant density lines.

(2) PPM = the pressure of the maximum constant pressure line.

(3) PVM = the velocity of the maximum constant velocity line.

(4) PDM = the density of the maximum constant density line.

(5) ADY = an assigned coordinate for a constant density line.

(6) DDX = an interpolated coordinate for a constant density line.

All of the above quantities are defined in decimal notation. The program is given on page 169 in Fortran IV notation.

PROGRAM LISTING OF THE CROSSFLOW SOLUTION

```
      PROGRAM CROSS
C     MAIN PROGRAM--CROSSFLOW DIFFRACTION
      INTEGER X
      INTEGER Y
      DIMENSION DFD(30,50),DFDA(30,50),DYO(30),DXO(50),UFD(30,50),UFDA(3
     10,50),UYO(30),UXO(50),VFD(30,50),VFDA(30,50),VYO(30),VXO(50),EFD(3
     20,50),EFDA(30,50),EYO(30),EXO(50),DZO(50),UZO(50),VZO(50),EZO(50)
    1 FORMAT(8F10.5)
    3 FORMAT(4F10.5,2I3,F10.5)
    5 FORMAT(10H TIME NO= ,F10.5,9HSPACE NO=,I4,6HCAPA= ,F10.5)
  101 FORMAT   (13H   PRESSURE= ,F10.5,16H   VEL MODULUS= ,F10.5,12H   D
     1ENSITY= ,F10.5)
  103 FORMAT   (65H   Y          X          Y          X        SINE
     1 Y       X)
  105 FORMAT(   I3)
  107 FORMAT(1X,10HINPUT DATA)
  109 FORMAT(1X,7H TMAX= ,F10.5,1X,4H M= ,I3,1X,7H CONS= ,F10.5,1X,7H TI
     1ME= ,F10.5)
  100 READ(1,105)JUMP
      IF(EOF,1)555,557
  557 READ(1,1)DP,DN,UP,UN,VP,VN,PP,PN
      READ(1,1)DS,US,VS,PS,VAR
      READ(1,3)GAM,SIG,OMEG,TMAX,M,L,CONST
      READ(1,1)PPCH,PVCH,PDCH,PPM,PVM,PDM
      ID=30
      KD=50
      GO TO(548,550),JUMP
  550 READ(1,1)TIME
      REWIND L
      DO 568 N=1,4
      READ(M)((DFD(I,K),UFD(I,K),VFD(I,K),EFD(I,K),I=1,ID),K=1,KD)
      GO TO(568,570,572,574),N
  570 DO 562 K=1,KD
      DXO(K)=DFD(1,K)
      UXO(K)=UFD(1,K)
      VXO(K)=VFD(1,K)
  562 EXO(K)=EFD(1,K)
      GO TO 568
  572 DO 564 I=1,ID
      DYO(I)=DFD(I,KD)
      UYO(I)=UFD(I,KD)
      VYO(I)=VFD(I,KD)
  564 EYO(I)=EFD(I,KD)
      GO TO 568
  574 DO 576 K=1,KD
      DZO(K)=DFD(ID,K)
      UZO(K)=UFD(ID,K)
      VZO(K)=VFD(ID,K)
  576 EZO(K)=EFD(ID,K)
      GO TO 568
  568 WRITE(L)((DFD(I,K),UFD(I,K),VFD(I,K),EFD(I,K),I=1,ID),K=1,KD)
      REWIND L
      REWIND M
      DELT =TMAX+VAR
      TMAX=2.0*VAR +TMAX
      GO TO 553
```

PROGRAM LISTING OF THE CROSSFLOW SOLUTION (Continued)

```
 548 DELT=VAR
 553 X=ID-1
     Y=KD-1
     GOTO(556,558),JUMP
 556 EP=DP*(UP*UP+VP*VP)/2.0+PP/(GAM-1.0)
     EN=DN*(UN*UN+VN*VN)/2.0+PN/(GAM-1.0)
     ES=DS*(US*US+VS*VS)/2.0+PS/(GAM-1.0)
     DO 2I=1,ID
     DYO(I)=DS
     UYO(I)=US
     VYO(I)=VS
   2 EYO(I)=ES
     DO 400I=1,KD
     DXO(I)=DP
     UXO(I)=UP
     VXO(I)=VP
     EXO(I)=EP
     DZO(I)=DP
     UZO(I)=UP
     VZO(I)=VP
 400 EZO(I)=EP
     REWIND M
     REWIND L
2002 DO 2000J=1,4
     GO TO(208,208,210,208),J
 208 DO10I=1,ID
     DO 10 K=1,KD
     DFD(I,K)=DP
     UFD(I,K)=UP
     VFD(I,K)=VP
  10 EFD(I,K)=EP
     GO TO 2000
 210 DO 14I=1,ID
     DFD(I,KD)=DS
     UFD(I,KD)=US
     VFD(I,KD)=VS
     EFD(I,KD)=ES
     DO 14K=1,Y
     DFD(I,K)=DN
     UFD(I,K)=UN
     VFD(I,K)=VN
  14 EFD(I,K)=EN
2000 WRITE(M)((DFD(I,K),UFD(I,K),VFD(I,K),EFD(I,K),I=1,ID),K=1,KD)
     TIME=1.0
 558 REWIND M
     AFIX=0.0
  16 DO 2004N=1,4
     READ (M)((DFD(I,K),UFD(I,K),VFD(I,K),EFD(I,K),I=1,ID),K=1,KD)
     CAP=SIG/CONST
     GO TO(214,216,218,228),N
 214 CALL FIELD(DFDA(1,1),UFDA(1,1),VFDA(1,1),EFDA(1,1),CAP,OMEG,GAM,DF
    1D(1,1),DZO(1)   ,DFD(1,2),DFD(2,1),DYO(1),UFD(1,1),UZO(1)   ,UFD(1,2
    2),UFD(2,1),UYO(1),VFD(1,1),VZO(1)   ,VFD(1,2),VFD(2,1),VYO(1),EFD(1
    3,1),EZO(1)   ,EFD(1,2),EFD(2,1),EYO(1),1)
     CALL FIELD(DFDA(ID,1),UFDA(ID,1),VFDA(ID,1),EFDA(ID,1),CAP,OMEG,GA
    2M,DFD(ID,1),DFD(X,1),DFD(ID,2),DXO(1),DYO(ID),UFD(ID,1),UFD(X,1),U
```

PROGRAM LISTING OF THE CROSSFLOW SOLUTION (Continued)

```
   3FD(ID,2),UXO(1),UYO(ID),VFD(ID,1),VFD(X,1),VFD(ID,2),VXO(1),VYO(ID
   4),EFD(ID,1),EFD(X,1),EFD(ID,2),EXO(1),EYO(ID),1)
    DO 18I=2,X
    CALL FIELD(DFDA(I,1),UFDA(I,1),VFDA(I,1),EFDA(I,1),CAP,OMEG,GAM,DF
   1D(I,1),DFD(I-1,1),DFD(I,2),DFD(I+1,1),DYO(I),UFD(I,1),UFD(I-1,1),U
   2FD(I,2),UFD(I+1,1),UYO(I),VFD(I,1),VFD(I-1,1),VFD(I,2),VFD(I+1,1),
   3VYO(I),EFD(I,1),EFD(I-1,1),EFD(I,2),EFD(I+1,1),EYO(I),1)
 18 CONTINUE
    DO 402I=2,Y
    CALL FIELD(DFDA(ID,I),UFDA(ID,I),VFDA(ID,I),EFDA(ID,I),CAP,OMEG,GA
   2M,DFD(ID,I),DFD(X,I),DFD(ID,I+1),DXO(I),DFD(ID,I-1),UFD(ID,I),UFD(
   3X,I),UFD(ID,I+1),UXO(I),UFD(ID,I-1),VFD(ID,I),VFD(X,I),VFD(ID,I+1)
   4,VXO(I),VFD(ID,I-1),EFD(ID,I),EFD(X,I),EFD(ID,I+1),EXO(I),EFD(ID,I
   5-1),1)
    CALL FIELD(DFDA(1,I),UFDA(1,I),VFDA(1,I),EFDA(1,I),CAP,OMEG,GAM,DF
   1D(1,I),DZO(I),DFD(1,I+1),DFD(2,I),DFD(1,I-1),UFD(1,I),UZO(I),UFD(1
   2,I+1),UFD(2,I),UFD(1,I-1),VFD(1,I),VZO(I),VFD(1,I+1),VFD(2,I),VFD(
   31,I-1),EFD(1,I),EZO(I),EFD(1,I+1),EFD(2,I),EFD(1,I-1),1)
402 CONTINUE
    GO TO 212
 37 CALL FIELD(DFDA(1,I),UFDA(1,I),VFDA(1,I),EFDA(1,I),CAP,OMEG,GAM,DF
   2D(1,I),DFD(1,I),DFD(1,I+1),DFD(2,I),DFD(1,I-1),UFD(1,I),UFD(1,I),U
   3FD(1,I+1),UFD(2,I),UFD(1,I-1),VFD(1,I),VFD(1,I),VFD(1,I+1),VFD(2,I
   4),VFD(1,I-1),EFD(1,I),EFD(1,I),EFD(1,I+1),EFD(2,I),EFD(1,I-1),3)
    GO TO (18,32,44,90),N
216 CALL FIELD(DFDA(1,1),UFDA(1,1),VFDA(1,1),EFDA(1,1),CAP,OMEG,GAM,DF
   1D(1,1),DXO(1),DFD(1,2),DFD(2,1),DFD(1,1),UFD(1,1),UXO(1),UFD(1,2),
   2UFD(2,1),UFD(1,1),VFD(1,1),VXO(1),VFD(1,2),VFD(2,1),VFD(1,1),EFD(1
   3,1),EXO(1),EFD(1,2),EFD(2,1),EFD(1,1),2)
    DO 32I=2,X
    GO TO 95
 32 CONTINUE
    DO 406I=2,Y
406 CALL FIELD(DFDA(1,I),UFDA(1,I),VFDA(1,I),EFDA(1,I),CAP,OMEG,GAM,DF
   1D(1,I),DXO(I),DFD(1,I+1),DFD(2,I),DFD(1,I-1),UFD(1,I),UXO(I),UFD(1
   2,I+1),UFD(2,I),UFD(1,I-1),VFD(1,I),VXO(I),VFD(1,I+1),VFD(2,I),VFD(
   31,I-1),EFD(1,I),EXO(I),EFD(1,I+1),EFD(2,I),EFD(1,I-1),1)
    GO TO 212
 95 CALL FIELD(DFDA(I,1),UFDA(I,1),VFDA(I,1),EFDA(I,1),CAP,OMEG,GAM,DF
   1D(I,1),DFD(I-1,1),DFD(I,2),DFD(I+1,1),DFD(I,1),UFD(I,1),UFD(I-1,1)
   2,UFD(I,2),UFD(I+1,1),UFD(I,1),VFD(I,1),VFD(I-1,1),VFD(I,2),VFD(I+1
   3,1),VFD(I,1),EFD(I,1),EFD(I-1,1),EFD(I,2),EFD(I+1,1),EFD(I,1),2)
    GO TO(18,32,44,408),N
228 CALL FIELD(DFDA(ID,1),UFDA(ID,1),VFDA(ID,1),EFDA(ID,1),CAP,OMEG,GA
   1M,DFD(ID,1),DFD(ID-1,1),DFD(ID,2),DZO(1),DFD(ID,1),UFD(ID,1),UFD(I
   2D-1,1),UFD(ID,2),UZO(1),UFD(ID,1),VFD(ID,1),VFD(ID-1,1),VFD(ID,2),
   3VZO(1),VFD(ID,1),EFD(ID,1),EFD(ID-1,1),EFD(ID,2),EZO(1),EFD(ID,1),
   42)
    DO 90 I=2,Y
 90 CALL FIELD(DFDA(ID,I),UFDA(ID,I),VFDA(ID,I),EFDA(ID,I),CAP,OMEG,GA
   1M,DFD(ID,I),DFD(ID-1,I),DFD(ID,I+1),DZO(I),DFD(ID,I-1),UFD(ID,I),U
   2FD(ID-1,I),UFD(ID,I+1),UZO(I),UFD(ID,I-1),VFD(ID,I),VFD(ID-1,I),VF
   3D(ID,I+1),VZO(I),VFD(ID,I-1),EFD(ID,I),EFD(ID-1,I),EFD(ID,I+1),EZO
   4(I),EFD(ID,I-1),1)
    DO 408 I=2,X
    GO TO 95
```

PROGRAM LISTING OF THE CROSSFLOW SOLUTION (Continued)

```
408 CONTINUE
    GO TO 212
218 CALL FIELD(DFDA(1,KD),UFDA(1,KD),VFDA(1,KD),EFDA(1,KD),CAP,OMEG,GA
   2M,DFD(1,KD),DFD(1,KD),DYO(1),DFD(2,KD),DFD(1,Y),UFD(1,KD),UFD(1,KD
   3),UYO(1),UFD(2,KD),UFD(1,Y),VFD(1,KD),VFD(1,KD),VYO(1),VFD(2,KD),V
   4FD(1,Y),EFD(1,KD),EFD(1,KD),EYO(1),EFD(2,KD),EFD(1,Y),3)
    CALL FIELD(DFDA(ID,KD),UFDA(ID,KD),VFDA(ID,KD),EFDA(ID,KD),CAP,OME
   1G,GAM,DFD(ID,KD),DFD(X,KD),DYO(ID),DFD(ID,KD),DFD(ID,Y),UFD(ID,KD)
   2,UFD(X,KD),UYO(ID),UFD(ID,KD),UFD(ID,Y),VFD(ID,KD),VFD(X,KD),VYO(I
   3D),VFD(ID,KD),VFD(ID,Y),EFD(ID,KD),EFD(X,KD),EYO(ID),EFD(ID,KD),EF
   4D(ID,Y),4)
    DO 44I=2,Y
    CALL FIELD(DFDA(ID,I),UFDA(ID,I),VFDA(ID,I),EFDA(ID,I),CAP,OMEG,GA
   1M,DFD(ID,I),DFD(X,I),DFD(ID,I+1),DFD(ID,I),DFD(ID,I-1),UFD(ID,I),U
   2FD(X,I),UFD(ID,I+1),UFD(ID,I),UFD(ID,I-1),VFD(ID,I),VFD(X,I),VFD(I
   3D,I+1),VFD(ID,I),VFD(ID,I-1),EFD(ID,I),EFD(X,I),EFD(ID,I+1),EFD(ID
   4,I),EFD(ID,I-1),4)
    GO TO 37
 44 CONTINUE
    DO 404I=2,X
404 CALL FIELD(DFDA(I,KD),UFDA(I,KD),VFDA(I,KD),EFDA(I,KD),CAP,OMEG,GA
   2M,DFD(I,KD),DFD(I-1,KD),DYO(I),DFD(I+1,KD),DFD(I,Y),UFD(I,KD),UFD(
   3I-1,KD),UYO(I),UFD(I+1,KD),UFD(I,Y),VFD(I,KD),VFD(I-1,KD),VYO(I),V
   4FD(I+1,KD),VFD(I,Y),EFD(I,KD),EFD(I-1,KD),EYO(I),EFD(I+1,KD),EFD(I
   5,Y),1)
212 JJ=2
    DO 24I=2,X
    DO 23K=2,Y
540 CALL FIELD(DFDA(I,K),UFDA(I,K),VFDA(I,K),EFDA(I,K),CAP,OMEG,GAM,DF
   1D(I,K),DFD(I-1,K),DFD(I,K+1),DFD(I+1,K),DFD(I,K-1),UFD(I,K),UFD(I-
   21,K),UFD(I,K+1),UFD(I+1,K),UFD(I,K-1),VFD(I,K),VFD(I-1,K),VFD(I,K+
   31),VFD(I+1,K),VFD(I,K-1),EFD(I,K),EFD(I-1,K),EFD(I,K+1),EFD(I+1,K)
   4,EFD(I,K-1),1)
23  CONTINUE
 24 CONTINUE
    GO TO (80,80,82,80),N
 80 DO 89I=1,ID
    DFDA(I,KD)=DFD(I,Y )
    UFDA(I,KD)=UFD(I,Y )
    VFDA(I,KD)=VFD(I,Y )
 89 EFDA(I,KD)=EFD(I,Y )
    GO TO (416,81,82,92),N
 81 DO 410I=1,Y
    DFDA(ID,I)=DFD(X ,I)
    UFDA(ID,I)=UFD(X ,I)
    VFDA(ID,I)=VFD(X ,I)
410 EFDA(ID,I)=EFD(X ,I)
    GO TO 416
 82 DO 412I=1,ID
    DFDA(I,1)=DFD(I,2)
    UFDA(I,1 )=UFD(I,2 )
    VFDA(I,1 )=VFD(I,2 )
412 EFDA(I,1 )=EFD(I,2 )
    GO TO 416
 92 DO 414I=1,Y
    DFDA(1,I)=DFD(2,I)
```

PROGRAM LISTING OF THE CROSSFLOW SOLUTION (Continued)

```
      UFDA(1,I)=UFD(2,I)
      VFDA(1,I)=VFD(2,I)
  414 EFDA(1,I)=EFD(2,I)
  416 GO TO (220,222,224,232),N
  220 DO 30I=1,KD
      DZO(I)=DFD(1,I)
      DXO(I)=DFD(ID,I)
      UZO(I)=UFD(1,I)
      UXO(I)=UFD(ID,I)
      VZO(I)=VFD(1,I)
      VXO(I)=VFD(ID,I)
      EZO(I)=EFD(1,I)
   30 EXO(I)=EFD(ID,I)
      DO 418I=1,ID
      DYO(I)=DFD(I,1)
      UYO(I)=UFD(I,1)
      VYO(I)=VFD(I,1)
  418 EYO(I)=EFD(I,1)
      GO TO 226
  222 DO 38I=1,KD
      DXO(I)=DFDA(1,I)
      UXO(I)=UFDA(1,I)
      VXO(I)=VFDA(1,I)
   38 EXO(I)=EFDA(1,I)
      GO TO 226
  232 DO 230 I=1,KD
      DZO(I)=DFDA(ID,I)
      UZO(I)=UFDA(ID,I)
      VZO(I)=VFDA(ID,I)
  230 EZO(I)=EFDA(ID,I)
      GO TO 226
  224 DO 50I=1,ID
      DYO(I)=DFDA(I,KD)
      UYO(I)=UFDA(I,KD)
      VYO(I)=VFDA(I,KD)
   50 EYO(I)=EFDA(I,KD)
  226 WRITE(3,5)TIME,N,CAP
      FIXMX=0.0
      DO 28I=1,ID
      DO 28K=1,KD
      UFD(I,K)=SQRTF(UFDA(I,K)*UFDA(I,K)+VFDA(I,K)*VFDA(I,K))
      EFD(I,K)=(GAM-1.0)*(EFDA(I,K)-DFDA(I,K)*UFD(I,K)*UFD(I,K)/2.0)
      IF(EFD(I,K).GE.0.0) GO TO 302
      SS = 0.0
      GO TO 304
 302  SS=SQRTF(GAM*EFD(I,K)/DFDA(I,K))
 304  SS=SS+UFD(I,K)
      IF(SS.LE.FIXMX)GO TO 28
      FIXMX=SS
   28 CONTINUE
      IF(FIXMX.LE.AFIX)GO TO 10000
      AFIX=FIXMX
10000 IF(TIME.NE.DELT) GO TO 2004
      PPV=-0.5
      VPV=PVCH
      DPV=-0.25
```

PROGRAM LISTING OF THE CROSSFLOW SOLUTION (Continued)

```
    PXA=VVX=DDX=APY=AVY= ADY=DIR=0.0
106 WRITE(3,101) PPV,VPV,DPV
    WRITE (3,103)
    DO112 I=1,ID
    DO104 K=1,KD
    DO116 J=1,2
    IF(PPV.GT.PPM)GO TO 132
    GO TO (118,120),J
118 IF(K.EQ.1  )GO TO 132
    A=EFD(I,K)
    B=EFD(I,K-1)
    GO TO 124
120 IF(I.EQ.1  )GO TO 132
    A=EFD(I,K)
    B=EFD(I-1,K)
    GO TO 124
124 IF(A.GT.PPV)GO TO 122
    IF(B.GT.PPV)GO TO 126
    GO TO 132
122 IF(B.GT.PPV)GO TO 132
126 GO TO (500,502),J
500 APX=K
    APY=I
    AX=K-1
    GO TO 504
502 APX=I
    APY=K
    AX=I-1
504 PXA=AX+(APX-AX)*(PPV-B)/(A-B)
132 IF(VPV.GT.PVM)GO TO 114
    GO TO (134,136),J
134 IF(K.EQ.1  )GO TO 114
    AA=UFD(I,K)
    BB=UFD(I,K-1)
    CC=VFDA(I,K)
    DD=VFDA(I,K-1)
    GO TO 138
136 IF(I.EQ.1  )GO TO 114
    AA=UFD(I,K)
    BB=UFD(I-1,K)
    CC=VFDA(I,K)
    DD=VFDA(I-1,K)
138 IF(AA.GT.VPV)GO TO 140
    IF(BB.GT.VPV)GO TO 142
    GO TO 114
140 IF(BB.GT.VPV)GO TO 114
142 GO TO (506,508),J
506 AVX=K
    AVY=I
    VX=K-1
    GO TO 510
508 AVX=I
    AVY=K
    VX=I-1
510 VVX=VX+(AVX-VX)*(VPV-BB)/(AA-BB)
    DD=DD+(VVX-VX)*(CC-DD)/(AVX-VX)
```

PROGRAM LISTING OF THE CROSSFLOW SOLUTION (Continued)

```
      DIR=UU/VPV
 114  IF(DPV.GT.PDM)GO TO 522
      GO TO (512,514),J
 512  IF(K.EQ.1   )GO TO 522
      A=DFDA(I,K)
      B=DFDA(I,K-1)
      GO TO 516
 514  IF(I.EQ.1   )GO TO 522
      A=DFDA(I,K)
      B=DFDA(I-1,K)
 516  IF(A.GT.DPV)GO TO 518
      IF(B.GT.DPV)GO TO 520
      GO TO 522
 518  IF(B.GT.DPV)GO TO 522
 520  GO TO (524,526),J
 524  ADX=K
      ADY=I
      DX=K-1
      GO TO 528
 526  ADX=I
      ADY=K
      DX=I-1
 528  DDX=DX+(ADX-DX)*(DPV-B)/(A-B)
 522  IF(PXA.NE.0.0)GO TO 530
      IF(VVX.NE.0.0)GO TO 530
      IF(DDX.NE.0.0)GO TO 530
      GO TO 116
 530  GO TO (532,534),J
 532  WRITE(3,1)APY,PXA,AVY,VVX,DIR,ADY,DDX
      GO TO 536
 534  WRITE(3,1)PXA,APY,VVX,AVY,DIR,DDX,ADY
 536  PXA=0.0
      VVX=0.0
      DDX=0.0
 116  CONTINUE
 104  CONTINUE
 112  CONTINUE
      VPV=VPV+PVCH
      PPV=PPV+PPCH
      DPV=DPV+PDCH
      IF(VPV.LE.PVM)GO TO 106
      IF(PPV.LE.PPM)GO TO 106
      IF(DPV.LE.PDM)GO TO 106
2004  WRITE(L)((DFDA(I,K),UFDA(I,K),VFDA(I,K),EFDA(I,K),I=1,ID),K=1,KD)
      IF(TIME.GT.TMAX)GO TO56
      IF(TIME.NE.DELT)GO TO 56
      DELT=DELT+VAR
  56  TIME=TIME+1.0
      IF(M.GT.L)GO TO 62
  60  M=L
      L=M-1
      GO TO 64
  62  L=M
      M=L-1
  64  REWIND L
      REWIND M
```

PROGRAM LISTING OF THE CROSSFLOW SOLUTION (Continued)

```
      CONST=AFIX
      IF(TIME.GT.TMAX)GO TO554
      AFIX=0.0
      GO TO 16
  554 WRITE(3,107)
      WRITE(3,109)TMAX,M,CONST,TIME
      GO TO 100
  555 CONTINUE
      END
```

PROGRAM LISTING OF THE CROSSFLOW SOLUTION (Continued)

```
      SUBROUTINE FIELD(D1B,U1B,V1B,E1B,CAPA,OMEGA,SPHT,D1,D2,D3,D4,D5,U1
     1,U2,U3,U4,U5,V1,V2,V3,V4,V5,E1,E2,E3,E4,E5,K)
      T1=U1*U1+V1*V1
      T2=U2*U2+V2*V2
      T3=U3*U3+V3*V3
      T4=U4*U4+V4*V4
      T5=U5*U5+V5*V5
      P1=(SPHT-1.0)*(E1-D1*T1/2.0)
      P2=(SPHT-1.0)*(E2-D2*T2/2.0)
      P3=(SPHT-1.0)*(E3-D3*T3/2.0)
      P4=(SPHT-1.0)*(E4-D4*T4/2.0)
      P5=(SPHT-1.0)*(E5-D5*T5/2.0)
      IF(P1.LT.0.0) GO TO 312
      T1=SQRTF(SPHT*P1/D1)+SQRTF(T1)
312   IF(P2.LT.0.0) GO TO 313
      T2=SQRTF(SPHT*P2/D2)+SQRTF(T2)
313   IF(P3.LT.0.0) GO TO 314
      T3=SQRTF(SPHT*P3/D3)+SQRTF(T3)
314   IF(P4.LT.0.0) GO TO 315
      T4=SQRTF(SPHT*P4/D4)+SQRTF(T4)
315   IF(P5.LT.0.0) GO TO 316
      T5=SQRTF(SPHT*P5/D5)+SQRTF(T5)
  316 CONTINUE
      GO TO(301,302,302,302),K
  301 R=2.0
      GO TO303
  302 R=4.0
  303 GO TO(304,305,306,307),K
  304 A=1.0
      B=1.0
      C=1.0
      D=1.0
      E=1.0
      F=1.0
      G=1.0
      H=1.0
      GO TO308
  305 A=1.0
      B=0.0
      C=1.0
      D=0.0
      E=1.0
      F=2.0
      G=1.0
      H=0.0
      GO TO 308
  306 A=0.0
      B=1.0
      C=0.0
      D=1.0
      E=0.0
      F=1.0
      G=2.0
      H=1.0
      GO TO 308
  307 A=0.0
```

PROGRAM LISTING OF THE CROSSFLOW SOLUTION (Continued)

```
      B=1.0
      C=0.0
      D=1.0
      E=2.0
      F=1.0
      G=0.0
      H=1.0
  308 SUM=1.0-OMEGA*CAPA*(T1/H+(A*T2+B*T3+C*T4+D*T5)/8.0)
      D1B=D1*SUM+OMEGA*CAPA*(A*T2*D2+B*T3*D3+C*T4*D4+D*T5*D5+(A*D2+B*D3+
     1C*D4+D*D5)*T1)/8.0-CAPA*(E*D2*V2+F*D3*U3-G*D4*V4-H*D5*U5)/2.82842
      U1B=(D1*U1*SUM+OMEGA*CAPA*(A*T2*D2*U2+B*T3*D3*U3+C*T4*D4*U4+D*T5*D
     15*U5+(A*D2*U2+B*D3*U3+C*D4*U4+D*D5*U5)*T1)/8.0-CAPA*(E*D2*U2*V2+F*
     2(P3+D3*U3*U3)-G*D4*U4*V4-H*(P5+D5*U5*U5))/2.82842)/D1B
      V1B=(D1*V1*SUM+OMEGA*CAPA*(A*T2*D2*V2+B*T3*D3*V3+C*T4*D4*V4+D*T5*D
     15*V5+(A*D2*V2+B*D3*V3+C*D4*V4+D*D5*V5)*T1)/8.0-CAPA*(E*(P2+D2*V2*V
     22)+F*D3*V3*U3-G*(P4+D4*V4*V4)-H*D5*V5*U5)/2.82842)/D1B
      E1B=E1*SUM+OMEGA*CAPA*(A*T2*E2+B*T3*E3+C*T4*E4+D*T5*E5+(A*E2+B*E3+
     1C*E4+D*E5)*T1)/8.0-CAPA*(E*(E2+P2)*V2+F*(E3+P3)*U3-G*(E4+P4)*V4-H*
     2(E5+P5)*U5)/2.82842
      GO TO(309,310,311,311),K
  310 U1B=U1
      GO TO 309
  311 V1B=V1
  309 RETURN
      END
```

VITA

Lynn Dolan Tyler

Candidate for the Degree of

Doctor of Philosophy

Thesis: NUMERICAL SOLUTIONS OF THE FLOW FIELD PRODUCED BY A PLANE SHOCK WAVE EMERGING INTO A CROSSFLOW

Major Field: Mechanical Engineering (Aerospace)

Biographical:

Personal Data: Born in Coffeyville, Kansas, October 28, 1935, the son of Dolan A. and Eleanor Marie Tyler.

Education: Attended grade school in Coffeyville, Kansas; graduated from Will Rogers High School, Tulsa, Oklahoma in 1953; received the Bachelor of Science in Mechanical Engineering from the University of Tulsa, Tulsa Oklahoma in May, 1961; received the Master of Science degree from Oklahoma State University in June, 1962; completed requirements for the Doctor of Philosophy degree in May, 1965.

Experience: Laboratory instructor at the University of Tulsa, Tulsa, Oklahoma, during the school years 1959 and 1960; engineer with Williams Bros. Company, Tulsa, Oklahoma, in the summer of 1960; temporary engineering employee of Cities Service Research Company, Tulsa, Oklahoma, during the summers of 1961 and 1962; graduate assistant in Mechanical Engineering of Oklahoma State University, Stillwater, Oklahoma, for spring semester 1962 and fall semester through summer 1964, also served on the faculty at the rank of Instructor for the academic year 1964-65.

Professional Organizations: The author is a member of the professional organizations: American Institute of Aeronautics and Astronautics, and American Society of Engineering Education.